The Kinetic and Chemical Mechanisms of Human Cytochrome P450 17A1

By

Eric Gonzalez

Dissertation

Submitted to the Faculty of the

Graduate School of Vanderbilt University

in partial fulfillment of the requirements

for the degree of

DOCTOR OF PHILOSOPHY

in

Biochemistry

May 2017

Nashville, Tennessee

Approved By:

F. Peter Guengerich, PhD

Martin Egli, PhD

Charles R. Sanders, PhD

Claus Schneider, PhD

Daniel Liebler, PhD

To my beloved wife, Amy, thank you for taking this journey with me

y

A mis padres, Tomas y Juana, por su amor, apoyo y oraciones

ACKNOWLEDGMENTS

I would first like to recognize Dr. Guengerich for his constant support throughout my tenure in his lab. He is a great role model, and I am confident that the training I've received has equipped me to be a proficient scientist. I am eternally grateful for his encouragement and guidance.

I would also like to acknowledge all the fellow dogs that I had the pleasure of getting to know during my time in the lab. There are too many to name each one individually, but I want everyone to know that you all made this arduous undertaking an enjoyable venture. I'm very appreciative of all the discussions that were essential as I progressed through my project. I would like to acknowledge Dr. Francis Yoshimoto, with whom I collaborated with on a portion of my dissertation work. I must also acknowledge Lindsay Folkman, Leslie Nagy, and Thanh Phan for keeping the lab stocked with enzymes and reagents, and also Kathy Trisler for help with manuscript preparation.

I also wish to thank my dissertation committee members: Dr. Martin Egli, Dr. Daniel Liebler, Dr. Claus Schneider, and Dr. Charles R. Sanders. The guidance and input I received was instrumental in keeping me on track with my project.

I would also like to thank the IMSD program and Dr. Linda Sealy and Dr. Roger Chalkley for their mentorship. Their support was essential for my success during the first year in grad school.

Lastly, I wish to acknowledge the funding support from the NIEHS T32 training grant (T32 ES007028) and grants awarded to Dr. Guengerich (R01 GM103937 and R37 CA090426).

TABLE OF CONTENTS

LIST OF FIGURES

LIST OF TABLES

ABBREVIATIONS

P450	cytochrome P450
kDa	kilodalton
NADPH	nicotinamide adenine dinucleotide phosphate, reduced
POR	NADPH cytochrome P450 Reductase
FAD	flavin adenine dinucleotide
FMN	flavin mononucleotide
Adx	adrenodoxin
ADR	adrenodoxin reductase
b_5	microsomal cytochrome b_5
bp	basepair
mRNA	messenger ribonucleic acid
Preg	pregnenolone
Prog	progesterone
17α-OHpreg	17α-hydroxypregnenolone
17α-OHprog	17α-hydroxyprogesterone
DHEA	dehydroepiandrosterone
Andro	androstenedione
11-DOC	11-deoxycorticosterone
CRPC	castration resistant prostate cancer
16α-OHprog	16α-hydroxypregnenolone
PTM	posttranslational modification
NMR	nuclear magnetic resonance
LC-MS	liquid chromatography-mass spectrometry
HRMS	high resolution mass spectrometry
PhIO	iodosylbenzene

CHAPTER 1

1. Introduction

1.1 Enzymes

Chemical reactions provide the foundation for all life. However, the typical rates for most of the essential reactions needed to support life are too slow under spontaneous processes. To this end, Nature has developed biological catalysts, called enzymes, which facilitate the chemical reactions at the accelerated rates needed to sustain life. Carbonic anhydrase is one example of these vital enzymes in humans and other organisms, catalyzing the interconversion of carbon dioxide and water to bicarbonate and protons.

$$CO_2 + H_2O \leftrightarrows H^+ + HCO_3^-$$

At near physiological conditions, the rates for the spontaneous hydration of carbon dioxide and dehydration of carbonic acid are ~0.15 s^{-1} and ~0.019 s^{-1}, respectively [1], which carbonic anhydrase accelerates to 1 x 10^6 s^{-1} and 6 x 10^5 s^{-1}, respectively [2]. Catalysis of these reactions is critical for maintenance of acid-base equilibrium in tissues and bodily export of carbon dioxide. The necessity of the function of this enzyme is apparent given that its loss results in osteoporosis, renal tubular acidosis, and cerebral calcification [3].

The value of enzymes for mankind is not limited to biological activities, as their power is also harnessed for commercial purposes. Enzymes are used for the manufacture of many consumer staples such as cheese, alcohol, and bread. Cheese is comprised of coagulated milk proteins (casein), whereby a mixture of enzymes produced in the stomach of ruminant (multi-chambered) mammals, termed rennet, are used for the curdling process. Additionally, many types of alcoholic beverages and bread are produced by harnessing the power of sugar fermentation enzymes in yeast, which produce ethanol and

CO_2. Indeed, Wilhelm Kühne coined the term enzyme while studying yeast extracts, which is derived from the medieval Greek word “enzymos,” referring to the process of leavening bread [4].

1.1.1 Mechanistic Enzymology

Investigation of mechanistic enzymology is a primary focus in this thesis work. Through exploitation of the advancing technology, studies on enzyme-mediated reaction mechanisms began in the late nineteenth century. One of the founding principles in mechanistic enzymology was the “lock and key” model, first proposed by Emil Fischer in 1894 [5]. Fischer used this metaphor to describe the intricate and requisite interaction(s) between an enzyme and its substrate(s) following observations of sugar substrate specificity by various fermentation yeasts [6]. The notion was later extended to the important theory of the formation of an enzyme-substrate complex [7], which was essential for the derivation of rate equations that mathematically and accurately describe the enzyme kinetics. Building upon a model developed by Victor Henri in 1903, Leonor Michaelis and Maud Leonora Menten established a fundamental mathematical model that showed the direct proportionality between the rate of an enzyme catalyzed reaction and the enzyme-substrate complex, which is known as the Michaelis-Menten equation [8]. Kenneth Johnson stated “Nearly a century after the original publication, the work of Michaelis and Menten stands up to the most critical scrutiny of informed hindsight” [9].

In 1925 Briggs and Haldane further substantiated the work by Michaelis and Menten by rederiving their equation and postulating that the concentration of the enzyme-substrate complex is constant, i.e. the steady-state approximation [10]. Attempts have been made to simplify the previously complex non-linear regression analysis by using linear transformations of the Michaelis-Menten equation. A double reciprocal equation developed by Lineweaver and Burk [11] gained considerable popularity and use, despite its deficiencies when including low substrate concentrations in the analysis. Alternatively, the Eadie-Hofstee plot [12] uses a non-inverse linear transform of the Michaelis-Menten equation that more accurately estimates the kinetic parameters, albeit the error analysis is more

arduous. Fortunately, the computing power of contemporary computers facilitates non-linear regression analysis, making linear regression transformations of the Michaelis-Menten equation unnecessary. Kenneth Johnson and his company (KinTek) have developed a dynamic simulation program, KinTek Explorer® [13,14], that eliminates the need for simplifying assumptions and permits the simultaneous fitting of multiple (and variable) experiments to a specified kinetic model developed by the user. The utility of the KinTek Explorer global fitting ability will be demonstrated in the kinetic modeling discussed in this dissertation, *vide infra*.

1.2 Cytochrome P450

Cytochrome P450 (P450) proteins are heme thiolate oxidase enzymes that are ubiquitous throughout life. Currently, the P450 superfamily has over 41,000 named genomic sequences, which are found within all the kingdoms, as well as viruses [drnelson.uthsc.edu/cytochromeP450.html, 15]. These ~50 kDa enzymes have a heme prosthetic group attached to a cysteine residue, which is in the only known conserved amino acid region found within all the P450s [16]. The heme moiety in P450s gives them their characteristic spectroscopic properties and conspicuously contributed to their naming. Tsueno Omura and Ryo Sato were the first to characterize these enzymes and christened them cytochrome P450, derived from "pigment 450," consequent of the typical peak at 450 nm that is observed in the difference absorbance spectrum of the reduced, CO-bound enzyme [17-19].

P450s, as a group, are versatile enzymes with a broad range of substrates that are able to catalyze various reactions, including mixed-function oxidations, reductions, rearrangements, and others (Figure 1.1) [20]. The archetypal reaction catalyzed by P450 enzymes is a monooxygenation with the following stoichiometry (RH is the substrate):

$$RH + NADPH + O_2 + H^+ \rightarrow ROH + NADP^+ + H_2O$$

A typical hydroxylation reaction cycle is comprised of several steps that are outlined in Figure 1.2. The reaction generally begins with the ferric form of the heme moiety, which is normally coordinated with a

distal water molecule. The cycle commences with substrate binding, which usually displaces the water but does not itself coordinate with iron, and is followed by a single electron reduction. Molecular oxygen is then able to bind to the iron, giving a ferrous dioxygen complex, prior to a second reduction. The resulting peroxo species can then be protonated, forming a ferric hydroperoxide. A dehydration step then generates the acclaimed perferryl species known as “Compound I” that is ascribed for the substrate chemistry in most of the P450 reactions. The fleeting intermediate species proceeds to abstract the alkane hydrogen, resulting in a carbon radical. Radical recombination ensues to yield the ferric heme and a hydroxylated product that is released in the final step of the cycle. Experimental procedures have been developed to assess the kinetic rates for most of individual reaction steps in search of rate-limiting steps, including the characterization of the transient Compound I species as reported by Rittle and Green [21].

The reaction cycle discussed above requires two reducing equivalents (electrons) that are extricated from a reduced nicotinamide adenine dinucleotide phosphate (NADPH) molecule. Electron transport from NADPH to the P450 heme is facilitated by associated redox partners, which differ depending on the localization of the P450 within the cell. Microsomal P450s, which are localized to the endoplasmic reticulum, receive the electrons from NADPH-cytochrome P450 reductase (POR). The reductase facilitates the stepwise transfer of electrons using flavin adenine dinucleotide (FAD) and flavin mononucleotide (FMN) prosthetic groups. The POR FAD prosthetic group accepts a hydride ion from NADPH and consecutively transfers single electrons to the FMN, which in turn transfers the electrons to the P450 as it receives them. Alternatively, mitochondrial and some bacterial P450s have two redox partners, adrenodoxin (Adx) and adrenodoxin reductase (ADR). The pair functions in a manner that parallels POR, where ADR is the FAD component that accepts the two electrons from NADPH, but Adx contains an iron-sulfur cluster as opposed to an FMN cofactor. Additionally, microsomal cytochrome b_5 (b_5) can sometimes be used as a redox partner for certain microsomal P450 reactions.

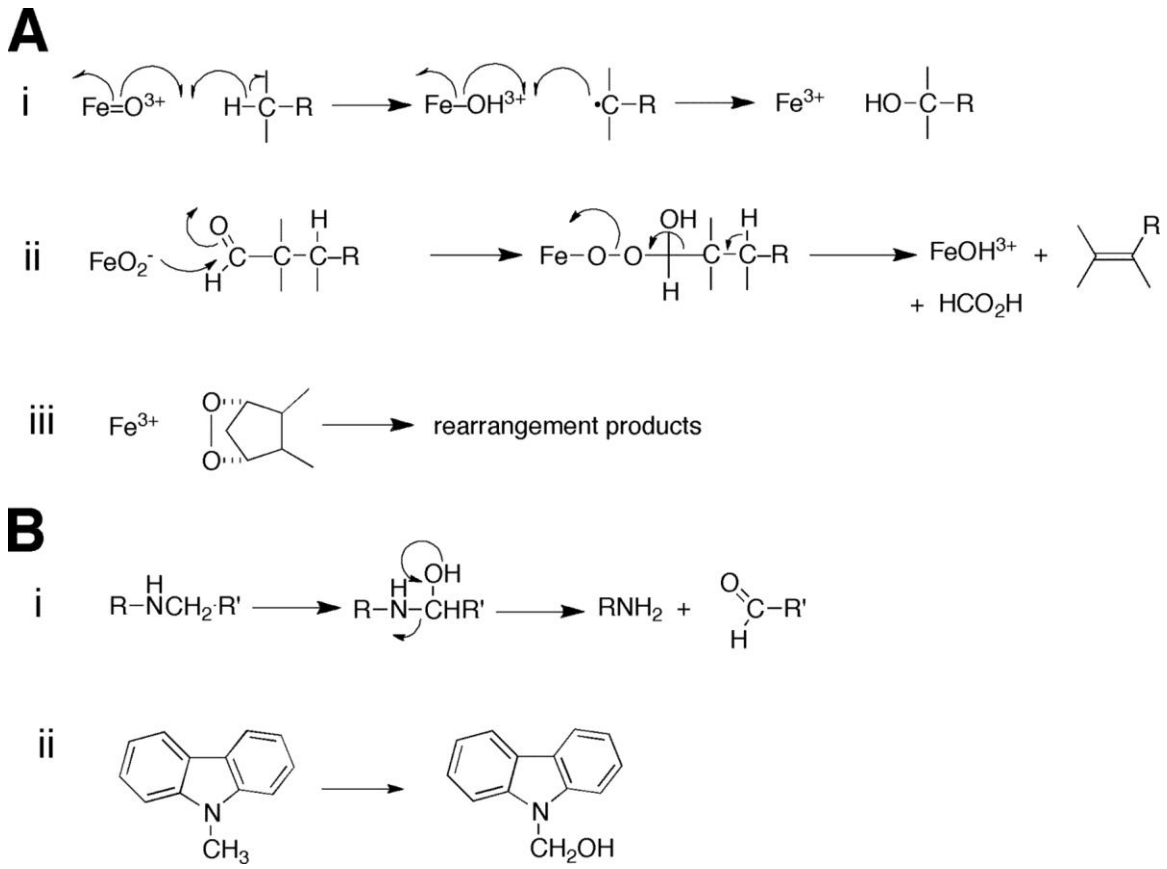

Figure 1.1 Reactions catalyzed by P450 enzymes [20]

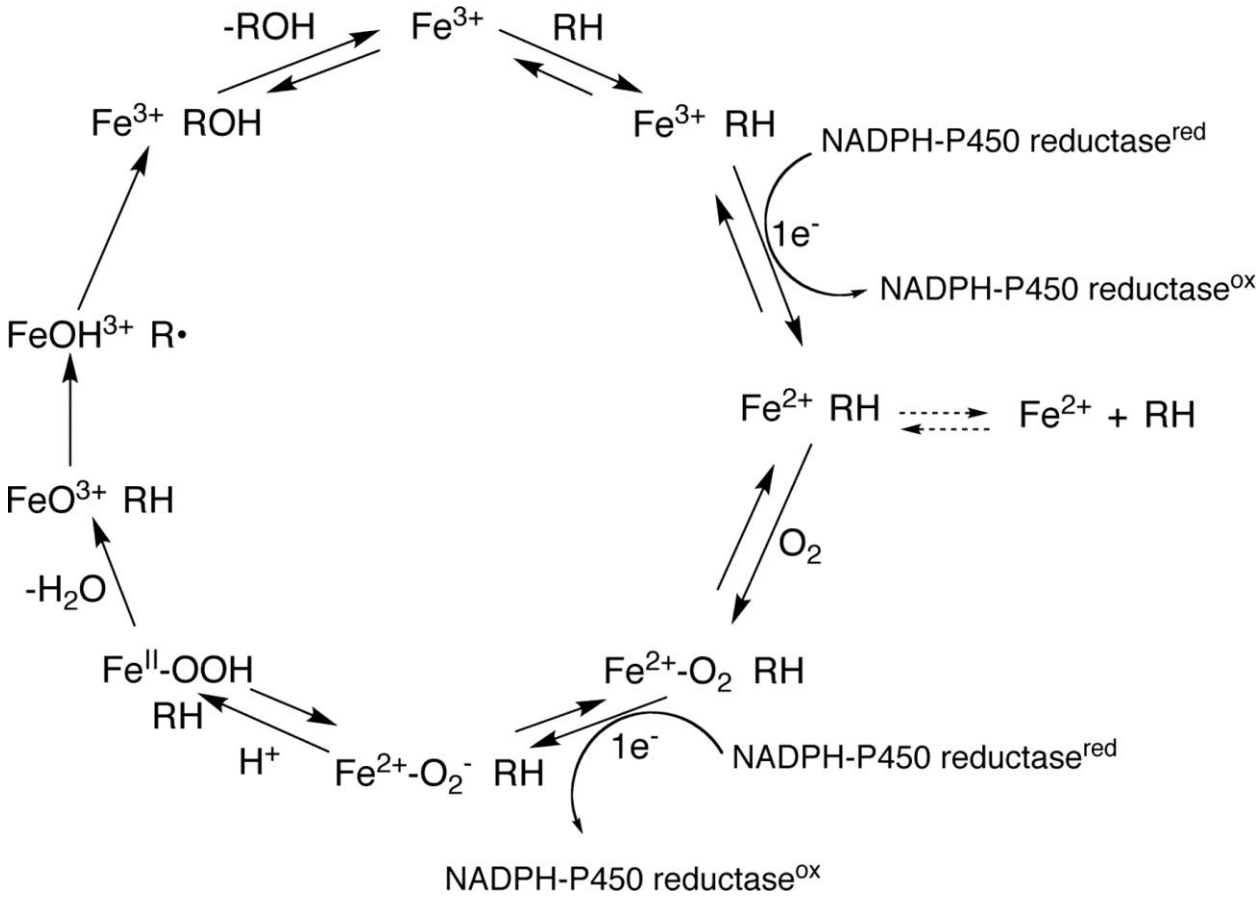

Figure 1.2 Catalytic cycle for a typical P450-mediated hydroxylation reaction [22]

Considering the magnitude of P450s that have been, and continue to be, identified through sequencing studies, it became necessary to develop a standard naming system to distinguish between the enzymes [23]. P450 enzymes are classified into families based on an amino acid sequence identity at >40% (denoted by an initial identification number), while >55% sequence identity is required to be placed in the same subfamily (denoted by a successive capital letter). For example, P450 17A1 is classified into family 17, subfamily A, and the final number, 1, designates the individual P450 in the group.

The earliest reported P450 structures were generated using soluble bacterial P450s. Poulos et al. first crystallized P450 101A1, also known as $P450_{cam}$, in complex with camphor (its substrate) in 1985 at 2.6 Å resolution, and later improved the resolution to 1.63 Å [24,25]. To date, a Protein Data Bank query for "cytochrome P450" yields over 800 results [rscb.org, 26]. Despite the differences in sequence identity, cellular localization, and function, a conserved overall fold is observed in the reported P450 structures. The secondary structure of P450 enzymes has also shown consistency with 13 α-helices (A, B, B', and C–L) and five β-sheets (β1–β5) [27]. Another structural feature shared by eukaryotic microsomal P450s is the N-terminal polypeptide chain, which serves solely as a membrane anchor to the endoplasmic reticulum. The membrane anchor is frequently removed to improve heterologous expression efficiency without loss of catalytic activity.

1.3 Human P450 Enzymes

The Human Genome Project revealed that humans have 57 P450-encoding genes. Human P450s have been studied extensively, generating a great deal of knowledge about the functions of these enzymes. In addition to the nomenclature classification based on sequence identity (*vide supra*), human P450s can also be categorized based on their substrate class, as shown in Table 1-1. It should also be clarified that the grouping based on substrate class is rather arbitrary, in considering that several P450s

can be placed under more than one substrate class. For example, human P450 3A4 is a classical xenobiotic metabolizing enzyme, but it is also functions in the metabolism of steroids [28,29].

The general role(s) of P450 enzymes are viewed in two categories: (1) they are substrate specific and have essential biological functions or (2) they are promiscuous and serve to protect the organism [30]. Characterization of the human P450s that catalyze vital physiological reactions, such as those needed for sterol and vitamin metabolism, has been facilitated through association with heritable metabolic diseases [31]. Some of the diseases that have been linked with defects in human P450 genes are listed in Table 1-2. Conversely, P450s that metabolize xenobiotics, e.g. ingested natural products, environmental pollutants, and therapeutic drugs, are not typically associated with important physiological consequences of endogenous substrate chemistry. The significance of this second group is to safeguard against accumulation of potentially harmful agents, but this function is sometimes problematic in regards to medicine. P450s are currently credited for the metabolism of ~75% of "small molecule" drugs processed by enzymes [32]. In this regard, ~90% of P450 mediated metabolism is attributed to a small group of P450s, including 1A2, 2C9, 2C19, 2D6, and 3A4 [30]. P450 3A4 is perhaps the most renowned P450 involved in drug oxidation, considering that it accounts for almost half of the medicinal drug clearance [33]. A primary reason for the large contribution by P450 3A4 is due to the high levels of expression in the intestine and liver. Needless to say, the xenobiotic metabolizing P450s have been studied extensively, and their reactions are taken into account in the development of new drugs.

Table 1-1 P450 Classification by substrate class [32]

Sterols	Xenobiotics	Fatty acids	Eicosanoids	Vitamins	Unknown
1B1	1A1	2J2	4F2	2R1	2A7
7A1	1A2	2U1	4F3	24A1	2S1
7B1	2A6	4A11	4F8	26A1	2W1
8B1	2A13	4B1	5A1	26B1	4A22
11A1	2B6	4F11	8A1	26C1	4X1
11B1	2C8	4F12		27B1	4Z1
11B2	2C9	4F22		27C1	20A1
17A1	2C18	4V2			
19A1	2C19				
21A2	2D6				
27A1	2E1				
39A1	2F1				
46A1	3A4				
51A1	3A5				
	3A7				
	3A43				

Table 1-2 Some diseases associated with defects in *CYP* genes [32]

Gene	Disorder
CYP1B1	Primary congenital glaucoma (buphthalmos)
CYP2R1	Rickets
CYP4A	Defects in salt metabolism, water balance leading to arterial hypertension
CYP4F22	Ichthyosis
CYP4V2	Bietti's crystalline dystrophy
CYP5A1, 8A1	Defects leading to clotting and inflammatory disorders, coronary artery disease, and pulmonary hypertension
CYP7A1	Hypercholesterolemia
CYP7B1	Severe hyperoxysterolemia and neonatal liver disease
CYP11A1	Lipoid adrenal hyperplasia; occasional congenital adrenal hyperplasia (CAH)
CYP11B1	Occasional CAH
CYP11B2	Corticosterone methyl oxidase deficiency type I, or type II; occasional CAH
CYP11B1, 11B2	Chimeric enzymes causing glucocorticoid- remediable aldosteronism; occasional CAH
CYP17A1	Mineralocorticoid excess syndromes, glucocorticoid and sex hormone deficiencies; association with increased risk of prostate cancer and benign prostatic hypertrophy; occasional CAH
CYP19A1	Loss of function: virilization of females, hypervirilization of males, occasional CAH; gain of function: gynecomastia in young males
CYP21A2	> 90% of all CAH
CYP24A1 [a]	Hypervitaminosis D
CYP27A1	Cerebrotendinous xanthomatosis
CYP27B1	Vitamin D-dependent rickets type I
CYP46A1 [a]	Learning disability

[a] Evidence of disease in animal models but not yet in clinical studies

1.4 Human Steroid Biosynthesis

Several P450 enzymes contribute to the production of human steroids, as listed in Table 1. The steroid biosynthetic pathway illustrated in Figure 1.3 shows the sequence in which the P450s take part, in coordination with two hydroxysteroid dehydrogenase enzymes (3β- and 17β-) and 5α-reductase. The illustration also provides a categorized view of the prominent natural human steroids in five groups: progestogens, mineralocorticoids, glucocorticoids, androgens, and estrogens. The first group of steroids is the progestogens, whose production begins with P450 11A1, also known as the cholesterol side-chain cleavage enzyme or P450scc (scc: side-chain cleavage), as it catalyzes the conversion of cholesterol to pregnenolone (Preg). 3β-Hydroxysteroid dehydrogenase can transform Preg to progesterone (Prog) by oxidizing the 3-hydroxy group to a ketone while simultaneously isomerizing the 5,6-double bond to the 4,5 position. P450 17A1 is the next enzyme in the pathway and mediates key bifurcations in steroid production that lead to mineralocorticoids, glucocorticoids, and sex hormones (androgens and estrogens). P450 17A1 is a dual function enzyme that catalyzes the hydroxylation of carbon-17 on Preg and Prog to yield 17α-hydroxy steroids, 17α-hydroxypregnenolone (17α-OHpreg) and 17α-hydroxyprogesterone (17α-OHprog), and in turn uses them as substrates in a “desmolase” or “lyase” reaction that generates dehydroepiandrosterone (DHEA) and androstenedione (Andro), respectively. An alternate course for Prog and 17-OHprog leads to aldosterone and cortisol synthesis, respectively, through oxidation reactions from P450s 21A2, 11B1, and 11B2. The androgens produced by the P450 17A1 17,20-lyase function lead to the synthesis of testosterone via hydroxysteroid dehydrogenase activity. The pathway ultimately terminates with P450 19A1, commonly referred to as aromatase, which generates estrogens from Andro and testosterone. The vitality of the steroid metabolizing P450 enzymes is apparent, given the physiological relevance of their products. At the crux of pathway lies P450 17A1, the enzyme of focus in this dissertation work.

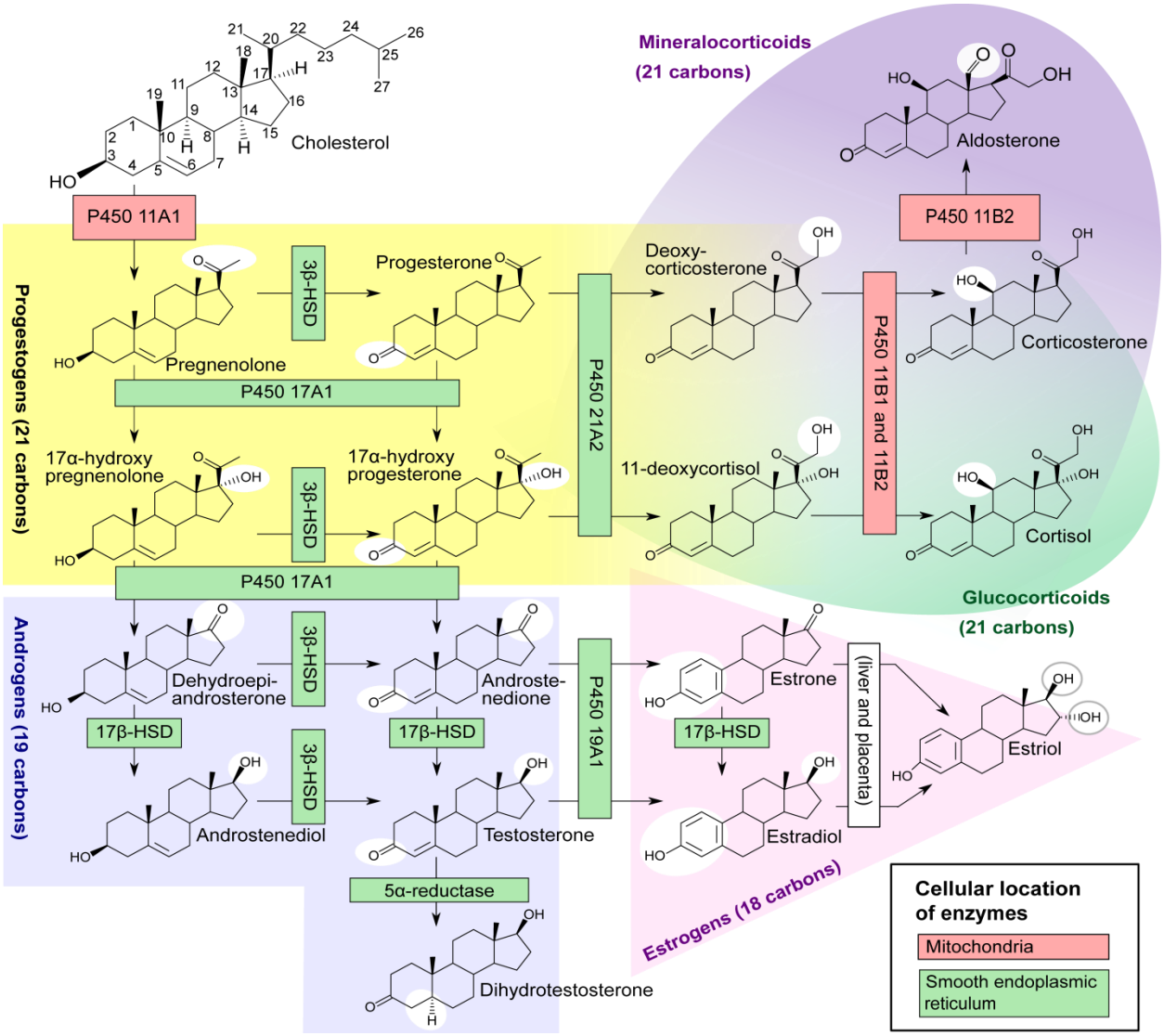

Figure 1.3 The steroid biosynthetic pathway [adapted from 34]

1.5 Human Cytochrome P450 17A1

Homo sapiens P450 17A1 is encoded by a single gene, *CYP17A1*, located on chromosome 10q24.32 [35]. The gene consists of eight exons that are transcribed to a 1895 bp mRNA sequence, which is further translated to a 508 amino acid protein at 57 kDa. The primary sites of expression are the gonads and the adrenal glands. P450 17A1 is abundant in the Leydig cells of the testis and theca cells of the ovaries, whereas in adrenal tissue it is localized in the zona fasciculata and zona reticularis. Notably, P450 17A1 protein has also been observed in fetal human nervous tissue and adult adipose tissue, and its enzymatic activity has been detected in adipose cells and tissue preparations from fetal kidney, thymus, and spleen [36-38].

1.5.1 Substrates and Catalytic Activity

As discussed above, the dual functionality of P450 17A1 is indispensable in the steroid biosynthetic pathway; however, the enzyme possesses additional catalytic abilities, presented in Figure 1.4. The primary major catalytic activity by P450 17A1 is the hydroxylation of Preg and Prog (21-carbon steroids) to yield 17-OHpreg and 17-OHprog. Alternatively, hydroxylation of carbon-16 is also observed with Prog, producing 16α-hydroxyprogesterone (16α-OHprog) at a 1:4 ratio in comparison with 17-OHprog [39]. Trace amounts (~1% of products) of 11-DOC from 21-hydroxylation activity is a third reported Prog hydroxylation reaction mediated by P450 17A1 [40]. The second major catalytic activity by P450 17A1 is the 17,20-lyase chemistry, a carbon-carbon bond cleavage reaction that generates 19-carbon steroids and acetic acid. As such, P450 17A1 produces DHEA and Andro from 17-OHpreg and 17-OHprog, respectively. However, the desmolase activity with 17-OHprog as the substrate is reportedly much lower than when 17-OHpreg is used, indicating that human sex hormone production likely proceeds mainly through the pregnenolone steroids [41]. Bypass of the 17α-hydroxy intermediate for 17,20-lyase catalysis has been exhibited with Preg as a substrate yielding androstadienol, 15,16-

androstadien-3*β*-ol [42]. Further adding to the gamut of P450 17A1 chemistry, novel catalytic products have been identified in these studies, which are reviewed in Chapter 2.

The hydroxylation reactions catalyzed by human P450 17A1 are deemed to proceed through the typical hydroxylation cycle, *vide supra*, that is supported by the Compound I iron oxygen species (FeO^{3+}). The 17,20-lyase reaction, however, has been subject the subject of deliberation. The speculative issue is whether the active oxidant is a ferric peroxide (FeO_2^-), an early intermediate after oxygen addition, or Compound I. Akhtar and his associates have investigated the issue and concluded that the ferric peroxide is involved in the reaction [43]. P450 19A1 is another steroidogenic enzyme that catalyzes a carbon-carbon bond cleavage reaction whose mechanism was reported to be ferric peroxide-mediated [44]. However, reanalysis of the chemistry using current technologies revealed that P450 19A1 operates via the Compound I active iron species in catalyzing the reaction [45]. Following the revision to the chemical mechanism of P450 19A1, the P450 17A1 17,20-lyase reaction has been reexamined, and the results are presented in Chapter 2.

1.5.2 Posttranslational Modification

One of the most prevalent modes of protein/enzyme (in)activation is through posttranslational modification (PTM). P450s are not an exception, and phosphorylation of P450 7A1, one of the steroid metabolizing variants, was proposed to be a posttranslational regulatory factor early in the P450 research field [46,47]. Furthermore, *in vivo* phosphorylation of several human xenobiotic metabolizing P450s has been detected through proteomic methods, although the relevance has yet to be clarified [48]. In regard to human P450 17A1, serine phosphorylation has been reported to enhance 17,20-lyase rates without altering hydroxylation activity [49,50]. Likewise, dephosphorylation diminishes the desmolase activity [51]. Alternatively, human b_5 is another selective 17,20-lyase enhancer but in combination with phosphorylation the stimulation was not additive, leading to the conclusion that the stimulation by either factor is exclusive [52].

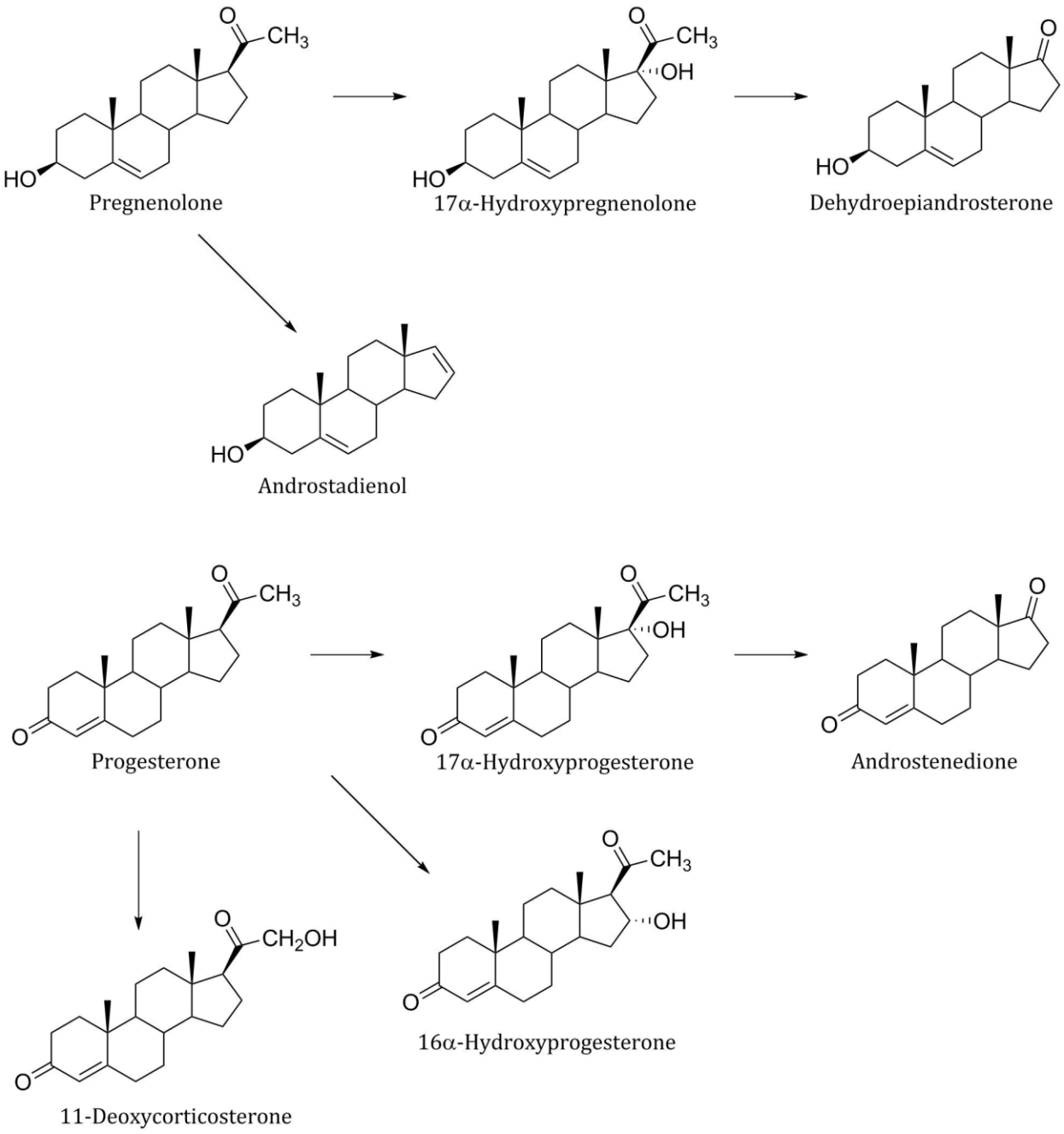

Figure 1.4 Human P450 17A1 Catalyzed Reactions

1.5.3 Cytochrome b_5 Stimulation of the 17,20-Lyase Reaction

Selective stimulation of the P450 17A1 17,20-lyase reaction by human b_5 is a well-established phenomenon. Prompted by studies revealing a discrepancy in the desmolase catalytic ability of purified enzyme and human tissue homogenates, Katagiri et al. investigated the influence of b_5 on recombinant P450 17A1 activity [53]. They showed that b_5 enhanced the P450 17A1 C-C cleavage reactions with 17-OHpreg and 17-OHprog by 13- and 10-fold, respectively, in comparison to only 2-fold for the 17-hydroxylation of Preg, while stimulation of 17-OHprog and 16-OHprog production was relatively weak (see Figures 1.5 and 1.6). The mechanism for the b_5-mediated stimulation has remained enigmatic. Hildebrant and Estabrook reported the first account of a b_5-supported P450 reaction, in which they postulated b_5 as the second electron donor in the oxidation of ethylmorphine in liver microsomes [54]. Although POR is the redox competent in P450 3A4-catalyzed testosterone oxidation, the reaction is 90% faster when b_5 is present [55]. Notably, the mechanism of b_5 in the P450 17A1 17,20-lyase reaction does not involve electron transfer. Lee-Robichaud et al. reported that redox-deficient Mn-substituted b_5 is able to stimulate the 17,20-lyase activity [56]. Furthermore, apo-b_5, a form completely devoid of the heme cofactor, showed no difference when compared to holo-b_5 [57]. The results are compelling and establish the precedent that b_5 functions through an allosteric mechanism, a role first reported by Morgan and Coon [58]. An alternative theory is that apo-b_5 scavenges heme that has liberated from the P450 enzyme in the reaction mixture [59], but a contradictory study found that not enough free heme is present to suffice the b_5 stimulation and it is unlikely to transfer in the time scale of the enzyme assay [60]. Interestingly, the function of b_5 allostery has been ascribed to alter the kinetics of electron transfer [61]. The stimulatory effect of b_5 in P450 17A1 reactions is a continual focus in this work. Chapter 2 includes interesting results using b_5 and oxygen surrogates in support of the 17,20-lyase reaction, while a focus of Chapter 3 is the influence of b_5 on individual reaction steps.

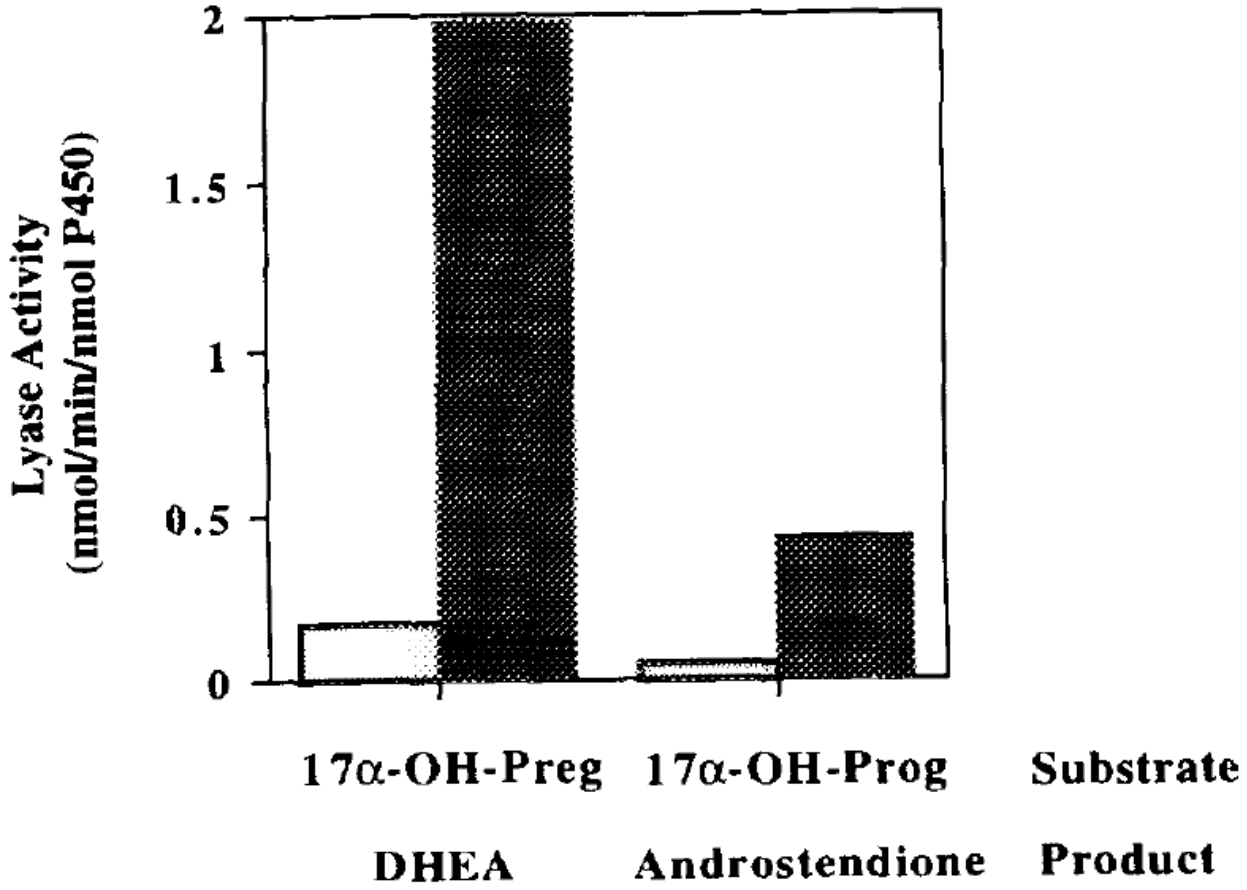

Figure 1.5 b_5 stimulation of the P450 17A1 17,20-lyase reaction [53]

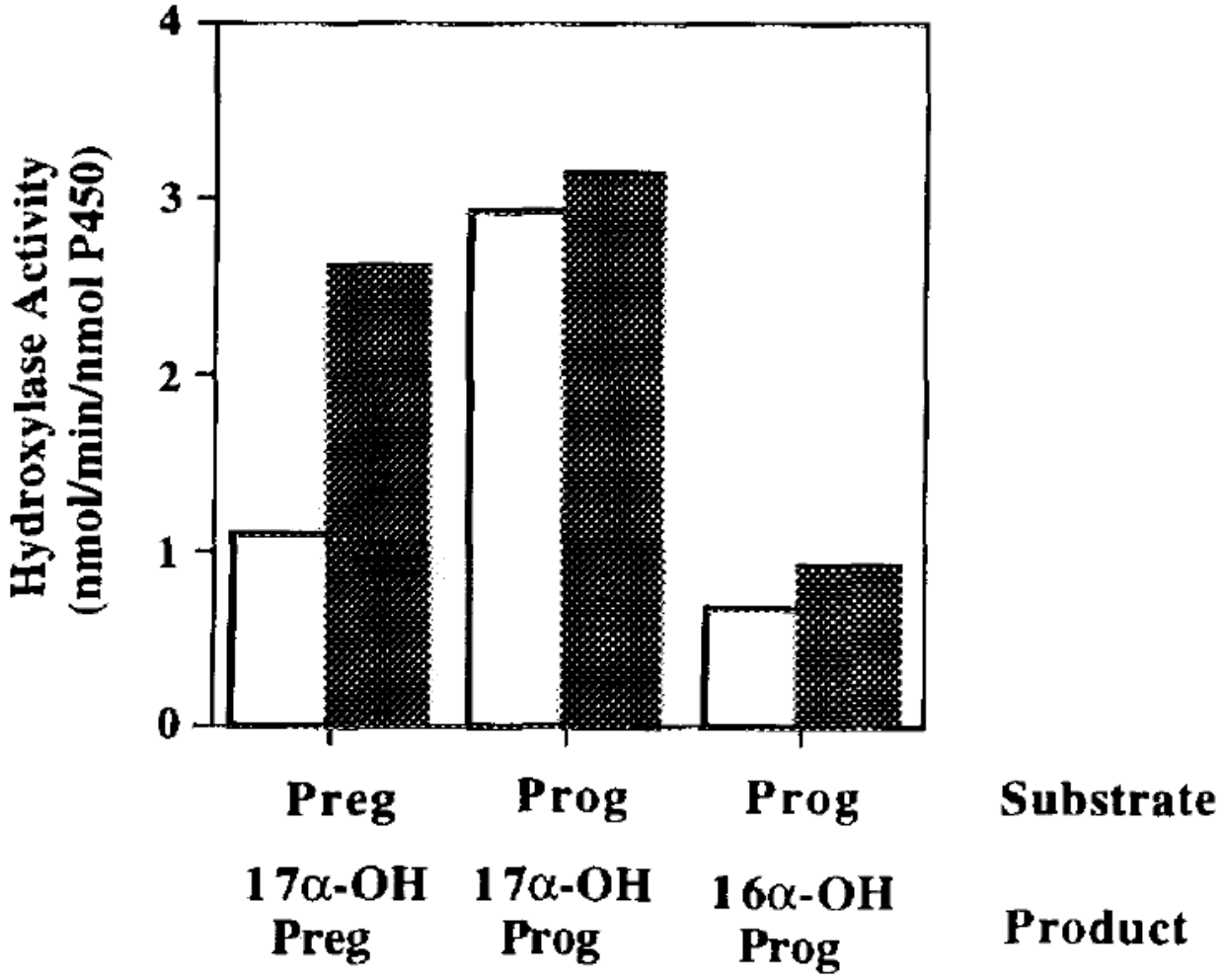

Figure 1.6 b_5 stimulation of the P450 17A1 hydroxylation reactions [53]

1.5.4 Structural Analyses

The first crystal structures of human P450 17A1 were solved and reported by DeVore and Scott [62]. The enzymes were crystallized in complex with the inhibitors abiraterone (Figure 1.7) and galeterone, both of which have a steroidal backbone with either a pyridine or benzimidazole group, respectively, attached at the carbon-17 atom. The structures exhibited the typical P450 fold and both inhibitors formed the expected heme iron-nitrogen bond. The authors also note the presence of empty space in the substrate pocket with the bound inhibitors, despite the fact they are larger than natural ligands. More recently, human P450 17A1, with a A105L mutation, has been co-crystalized with substrates bound [63]. The mutation was deemed structurally inconsequential, and the substrate orientations and bonding characteristics were similar to that with abiraterone. Interestingly, void space was again observed in the substrate pocket. The observation of unoccupied space in the active site provides a rationale for the unexpected, novel product synthesis detailed in Chapter 2.

Considering the significant effect on the 17,20-lyase reaction, structural analysis of human P450 17A1 in complex with b_5 has been a subject of great interest. For some time now, it has been known that mutation of arginine residues at positions 347 and 358 in P450 17A1 diminishes the 17,20-lyase function in humans [64]. Mutagenesis studies using recombinant enzymes revealed that cationic residues at these positions are essential for catalysis of the desmolase reaction [56,65]. Peng and colleagues demonstrated a direct interaction between P450 17A1 and b_5 at these amino acid residues using crosslinking experiments [66]. Structural nuclear magnetic resonance (NMR) analysis of human P450 17A1 in solution with b_5 have yielded consistent results, in which the b_5 interaction with P450 17A1 arginine residues 347 and 358 was corroborated [67]. However, the findings were also puzzling in that the binding interactions with both b_5 and POR were mapped to the same region of P450 17A1. Considering that b_5 does not transfer electrons, and therefore POR must provide both reducing equivalents for each catalytic cycle, the exchange between the two proteins is perplexing.

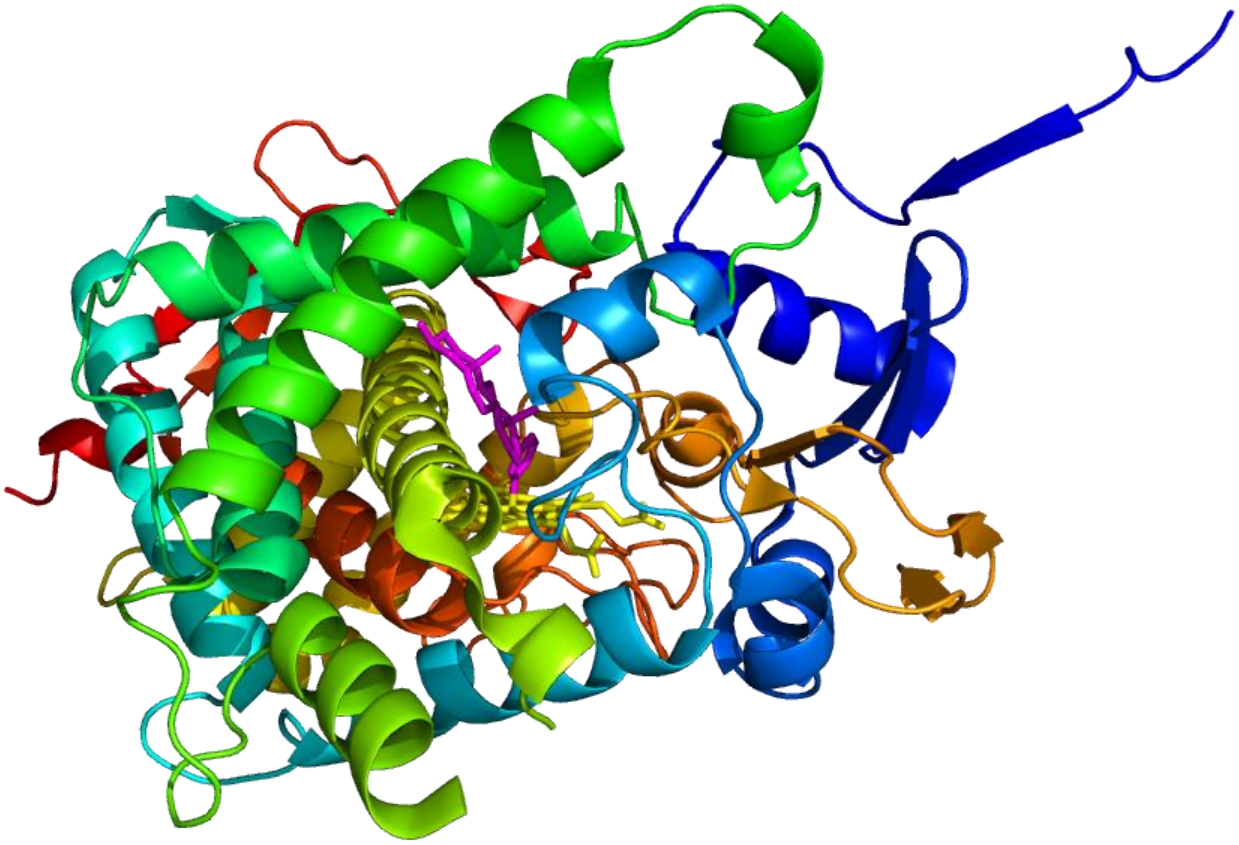

Figure 1.7 Human P450 17A1 Structure [PDB 3RUK]

1.5.5 Human P450 17A1 Related Diseases

P450 17A1 is consequential to human physiology and disease due to its central role in steroid biosynthesis. DeVore and Scott have tabulated numerous genetic variants identified in the clinic with their associated effect on the enzymatic activity and structural context [62]. The scope of genetic lesions includes missense mutations, deletions, duplications, and premature stop codons. In some cases, the missense mutation leads to a moderate decrease in catalytic activity, while others completely inactivate the enzyme with only a single amino acid change. Diminished 17α-hydroxylation and 17,20-lyase catalysis results in cortisol and sex hormone deficiency, stemming from the deficit in 17α-hydroxy steroids, with concomitant mineralocorticoid accretion. The excess 11-deoxycorticosterone (11-DOC) causes sodium retention, hypertension, hypokalemia, suppressed plasma renin activity, and suppressed aldosterone production [68]. When remedied with glucocorticoid therapy, 11-DOC synthesis is suppressed, while plasma renin activity and aldosterone concentrations normalize [69]. Additionally, the lack of androgens and estrogens results in sexual infantilism, pubertal failure, and infertility. As such, females with this disorder appear phenotypically normal, while males lack or have incomplete genitalia, a syndrome known as male pseudohermaphroditism. Remarkably, some missense mutations in P450 17A1 lead to isolated 17,20-lyase deficiency with normal 17α-hydroxylase activity, i.e. R347H, R358Q, and E305G [64,70]. The first two amino acid differences disrupt the associations with the redox partners while the second alters the 17-OHpreg binding [70,71].

Bearing in mind that human P450 17A1 is responsible for androgen synthesis, it is considered an important factor in sex hormone responsive cancers, e.g. prostate cancer. The current standard remedy for prostate cancer is androgen deprivation therapy through excision of the androgen producing tissues (castration). Unfortunately, the procedure does not always resolve the affliction, and relapse usually occurs in what is known as castration-resistant prostate cancer (CRPC). In some cases, CPRC develops from mutations of the androgen receptor. Conversely, CRPC tumors have shown the ability to generate

androgens *de novo*, and therapy with P450 17A1 inhibitors provides a selective pressure for cells expressing high levels of the enzyme [72].

1.5.6 Inhibitors

Inhibition of human P450 17A1 has become a major goal for prostate cancer therapy, and presumably the remedy is useful for other steroid-responsive maladies (e.g. breast and endometrial cancer). Five of the small molecule inhibitors that have been used/tested in prostate cancer therapy are shown in Figure 1.7. The earliest attempt at preventing androgen synthesis by means biosynthetic inhibition was the "off label" use of ketoconazole. Ketoconazole is a broad spectrum P450 inhibitor, which is primarily prescribed to treat fungal infections. Studies in 1985 using microsomal preparations revealed the aptitude of the drug for 17,20-lyase inhibition [73]. Although the drug does inhibit human P450 17A1, it obstructs general steroid production by indiscriminately impeding P450 11A1, 21A2, 11B1, and 19A1 function [74,75], as well as the drug-metabolizing P450s such as P450 3A4. Ketoconazole is no longer used for the treatment of prostate cancer, but its trial is noteworthy for establishing the foundation of steroidogenic inhibition in prostate cancer therapy.

In 2011 the U.S. Food and Drug Administration approved abiraterone acetate, the pro-drug for abiraterone, as a treatment for CRPC [76]. Abiraterone is a selective P450 17A1 inhibitor, albeit with a steroidal core structure and a D-ring attached pyridine. The molecule falls short as an optimal therapy in that it inhibits the 17α-hydroxylation reaction in addition to the 17,20-lyase function. Consequently, adjuvant prednisone or dexamethasone (synthetic glucocorticoids) is required to counteract the cortisol deficit and associated elevated 11-DOC issues observed with complete P450 17A1 deficiency, *vide supra*. Glucocorticoid therapy, however, cannot be endured indefinitely, and activation of a mutant androgen receptor has been observed with prednisone [77]. Presumably, a reaction specific inhibitor that is exclusive to 17,20-lyase catalysis would prevent the adverse effects caused by glucocorticoid shortage.

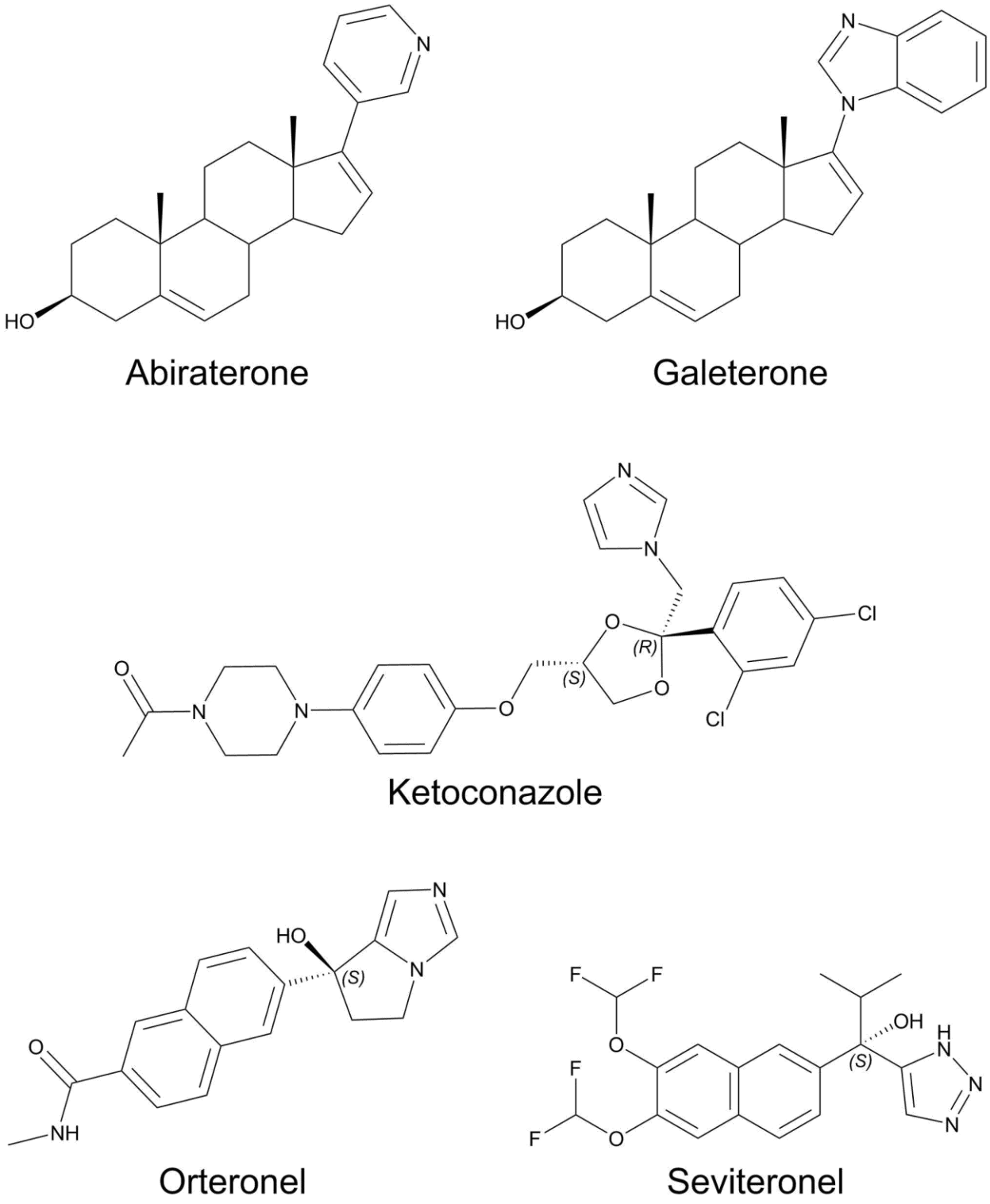

Figure 1.8 Human P450 17A1 Inhibitors

Pharmaceutical industry efforts have generated several reaction selective-inhibitors. Orteronel (TAK-700) is a non-steroidal P450 17A1 inhibitor brought to Phase III clinical trials for metastatic CRPC. The drug was developed through structure-activity relationship studies with the cleavage reaction [78,79]. 17,20-Lyase selectivity over 17α-hydroxylation was five-fold for half-maximal inhibitory concentrations (IC_{50}) [80]. In contrast, reviews on the topic indicate that the *in vivo* selectivity and resulting side effects are not better than those of abiraterone [77,81,82]. In 2014 Takeda discontinued the orteronel development initiative, reporting that the therapy did not improve overall survival nor did it have a clinical profile that was better than currently available therapies [83]. Human P450 17A1 inhibition by orteronel has been reevaluated in this work, including comparisons of the two enantiomers (Chapter 3).

Other P450 17A1 selective inhibitors currently in clinical trials include galeterone (TOK-001) and seviteronel (VT-464). In addition to inhibition of P450 17A1, galeterone is an androgen receptor antagonist [84,85]. Seviteronel is a non-steroidal, desmolase selective inhibitor that has a reported 17α-hydroxylase:17,20-lyase IC_{50} ratio of ~10 [86]. For further reading on these two molecules, see references 77,82,87,88.

1.5.7 Processivity

P450 17A1 is one of the multi-step, sequential reaction P450s, a group that includes both xenobiotic and endogenous substrate metabolizing enzymes. Interestingly, five of the P450s involved in steroid biosynthesis belong to this special group, and remarkably four of them complete their reaction sequences with a C-C bond scission reaction. P450s 11A1 and 11B2 catalyze a three-step processes that generates Preg and aldosterone from cholesterol and 11-DOC, respectively. P450 19A1 is another three-step enzyme but is unique in that it aromatizes and deformylates its substrate in the final step. As stated above, P450 17A1 is a dual function enzyme that sequentially catalyzes 17α-hydroxylation and 17,20-lyase reactions. The issue of processivity refers to the capacity of the enzyme to catalyze the sequential

reactions in a processive or distributive manner. In a processive mechanism, the intermediate products remain in the enzyme during the multi-step process resulting in final product synthesis. Alternatively, in a distributive sequence the intermediate products dissociate from the enzyme and must rebind before the next round of catalysis is possible. Processivity studies have suggested that steroidogenic P450s employ both mechanisms. Bovine P450 11B2 has been reported to catalyze the hydroxylation of carbons 11 and 18 of 11-DOC and corticosterone, respectively, prior to a final oxidation of 18-hydroxycorticosterone to yield aldosterone as a final product in a processive fashion [89]. Remarkably, co-incubation with P450 11A1 has been reported to disrupt the processivity of P450 11B2 by promoting the dissociation of the intermediate product, corticosterone. On the other hand, human P450 19A1 follows a distributive mechanism in the production of estrogens from androgens [22].

While the processivity of human P450 17A1 has not been ascertained, investigations using P450 17A1 enzymes from other species have generated conflicting results. Guinea pig P450 17A1 was reported to follow a processive mechanism through the sequential hydroxylation and cleavage reactions on the progesterone series substrates [90]. Studies with the bovine enzyme suggested a primarily distributive mechanism, with only 20% of the Preg metabolized to DHEA processively [91]. The bovine enzyme was more distributive with Prog as the substrate, with a 10-fold larger dissociation rate for 17-OHprog over 17-OHpreg. Guinea pig P450 17A1 utilizes both Preg and Prog substrates, while bovine P450 17A1, like the human enzyme, preferentially uses Preg [53]. In view of the known stimulatory effect human b_5 has on the 17,20-lyase reaction, the allosteric interaction may make human P450 17A1 a processive enzyme. Chapter 3 presents a model that has been developed describing the processivity of human P450 17A1 in association with b_5.

1.6 Research Aims

The central goal of this project is to better describe the mechanisms by which human P450 17A1 catalyzes the 17α-hydroxylase and 17,20-lyase reactions, with the view that the results will support the initiative to develop therapeutically effective, reaction selective inhibitors.

The first step in all biochemical studies is the procurement of the protein of interest. Fortunately, heterologous expression of human P450 17A1 and its purification was established more than 20 years ago [92,93].

1.6.1 Evaluate the Chemical Mechanism of the 17,20-Lyase Reaction

Presumably, a better grasp of the 17,20-lyase reaction would facilitate the development of reaction-selective human P450 17A1 inhibitors. One theory that has garnered considerable support is that ferric peroxide (FeO_2^-) is the active iron-oxygen species in human P450 17A1 that facilitates the carbon-carbon bond cleavage reaction. The use of several methods to evaluate this issue, the first of which is isotopic labelling of enzyme products with oxygen-18, is reviewed in Chapter 2. The current dogma is that FeO_2^- is a nucleophilic species that incorporates an ^{18}O atom into the 17,20-lyase acetic acid product, whereas as the electrophilic FeO^{3+} does not. Assays using pig testis microsomes have generated ^{18}O labeled acetate as a product, supporting the ferric peroxide mechanism [43,94]. As an alternative method, enzyme incubations were conducted with oxygen surrogates that discriminate between the two species. Based on previous reports, the Compound I and ferric peroxide active iron species can be generated with either iodosylbenzene or hydrogen peroxide, respectively. It is possible to misinterpret the hydrogen peroxide results, given that the ferric peroxide species can form Compound I. However, iodosylbenzene is capable of transferring only a single oxygen atom, thereby designating the reacting species for product(s) generated as Compound I. LC-MS and NMR studies were also conducted to characterize some novel and unexpected chemistry. Taken together, the results from these analyses will better clarify the reaction intermediates for 17,20-lyase catalysis by human P450 17A1.

1.6.2 Evaluation of the Processivity of Human P450 17A1 and the Effect of Cytochrome b_5

Reaction-selective inhibition of human P450 17A1 is more likely if the enzyme catalyzes the sequential reactions through a distributive mechanism. Varying degrees of processivity have been reported for P450 17A1 from other animals [90,91,95], but an analysis of human P450 17A1 using purified enzymes has not been reported. One concept for evaluation is whether the b_5 enhances the 17,20-lyase reaction by allosterically inducing a processive enzyme-desmolase substrate conformation. Steady-state catalytic analyses were first conducted to understand the catalytic efficiency of the enzyme with the different substrates. In order to assess the effect of b_5 on individual reaction steps, a series of pre-steady-state techniques were employed. Processivity of human P450 17A1 was also investigated using pulse-chase assays, which follow the conversion of radiolabeled substrates. Chapter 3 concludes with a kinetic model, for the human P450 17A1 mechanism, developed using global data fitting software, i.e. KinTek Explorer®.

Chapter 2

2. Chemical Mechanism of the 17,20-lyase Reaction and New Hydroxylation Products

2.1 Introduction

P450 enzymes catalyze oxidations of more chemicals than any other group of proteins [96]. The list of reactions includes aliphatic and aromatic hydroxylations, heteroatom oxidations, epoxidations, and reactions involving both ring formation and cleavage [97-99]. Many P450 reactions are important in the biosynthesis and degradation of steroids and sterols [68,99], including several critical C–C bond cleavage reactions, i.e. those catalyzed by P450s 11A1, 17A1 (Figure 1.4), 19A1, and 51A1 [32,100].

The mechanisms of the C–C cleavage reactions have been the subject of considerable interest and debate. One of the questions with P450s 17A1, 19A1, and 51A1 has been whether the active oxidant is a ferric peroxide (FeO_2^-), which is an early intermediate following oxygen addition to the iron (Figure 2.1, step 4) or the FeO^{3+} species (Figure 2.1, step 6), often referred to as Compound I [99,101,102]. With P450s 17A1 and 19A1, a variety of approaches has been applied, including theoretical calculations, biomimetic models, spectroscopy, substrate atom labeling, and kinetics [44,94,103-121].

These C–C bond cleavage reactions are complex, and many of the results are ambiguous; also, a "mixed" mechanism would not be discerned in many of these experiments. One powerful approach originally used by Akhtar and co-workers [94,117-120] analyzes the actual reaction and can provide discrimination between the nucleophilic FeO_2^- and electrophilic FeO^{3+} reactions (Figure 2.1), based on the incorporation of ^{18}O label from O_2 into the carboxylic acid products (Figure 2.2) [100]. However, these experiments are complicated due to the ubiquitous presence of formic acid (P450 19A1 and 51A1 reactions) and acetic acid (P450 17A1) in laboratory settings. Thus, the data from such experiments are interpreted with the most confidence when the steroid substrates are labeled with ^2H or ^{13}C isotopes to facilitate analysis [44,45]. Even then, the mass spectrometry results can be problematic, particularly if a

shift of only one atomic mass unit is introduced and isotopologues derived from ^{18}O incorporation are not discriminated from molecules containing natural abundance ^{13}C atoms [45].

The incorporation of one atom of ^{18}O label from O_2 into formic acid (Figure 2.2 A) had been considered one of the most critical pieces of evidence in support of an FeO_2^- mechanism for P450 19A1 [44,105,122]. Because of the importance of this evidence in the existing dogma, Yoshimoto and Guengerich re-examined this experiment using several technical improvements including the following: (i) purified recombinant P450 19A1; (ii) a new diazo reagent with a pyridine nitrogen to facilitate positive ionization for liquid chromatography-mass spectrometry (LC-MS); and (iii) the use of high resolution mass spectrometry (HRMS) [45]. The results for P450 19A1 unambiguously ruled out incorporation of an ^{18}O label from $^{18}O_2$ into formic acid by distinguishing ^2H from ^{13}C isotope composition and are only consistent with an FeO^{3+} mechanism for P450 19A1 [45].

Because of the impact of the new studies [45], the ^{18}O experiments with P450 17A1 [94,117-120] were repeated using the newer methodologies. Although the ^{18}O labeling results could be interpreted as support of an FeO_2^- mechanism for human P450 17A1, at least three possible FeO^{3+} mechanisms are still consistent with the data (Figure 2.2 B, C, and F). Artificial oxygen surrogates that might distinguish among mechanisms were also employed, i.e. iodosylbenzene, a single oxygen atom donor, and H_2O_2. Finally, kinetic solvent isotope effects for the reactions were measured, in light of inconsistencies in the field [113,123]. The evidence now suggests that an FeO^{3+} mechanism is likely, at least in part, for the 17α,20-lyase reaction, and the enzyme also demonstrated the ability to catalyze additional 6β- and 16-hydroxylation reactions.

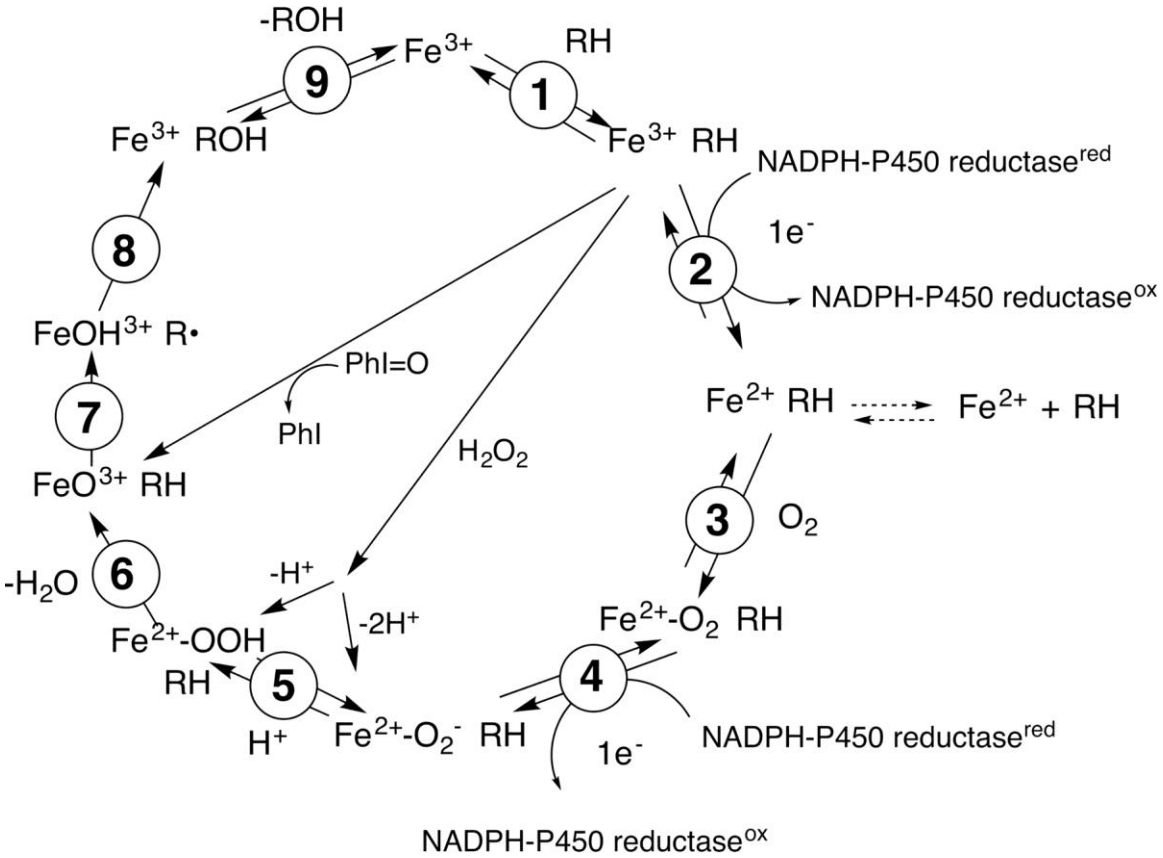

Figure 2.1 Classic P450 cycle with paths for oxygen surrogates [99]

Paths for oxygen surrogates (PhI=O, H_2O_2) are also included. Note the FeO_2^- (ferric peroxide) and FeO^{3+} (compound I) forms discussed in the text. In the literature there exists different nomenclature for the same iron intermediates in this P450 catalytic cycle (*i.e.* $Fe^{III}O_2^-$, $Fe^{III}O_2H$, $Fe^{IV}O^+$, and $Fe^{IV}OH$) [124,125]. For clarity throughout the text, compound I is referred to interchangeably with FeO^{3+}, and ferric peroxide is referred to interchangeably with FeO_2^-. The electron transfers from the reductase are simplifications in that the course of electron flow is probably from $FMNH_2/FADH^•$ to $FMNH^•/FADH^•$ in the first reduction (step 2) and (assuming that the reductase contributes the second electron to the P450) from $FMNH^•/FAD^•$ to $FMNH^•/FAD$ in the second reduction step 4.

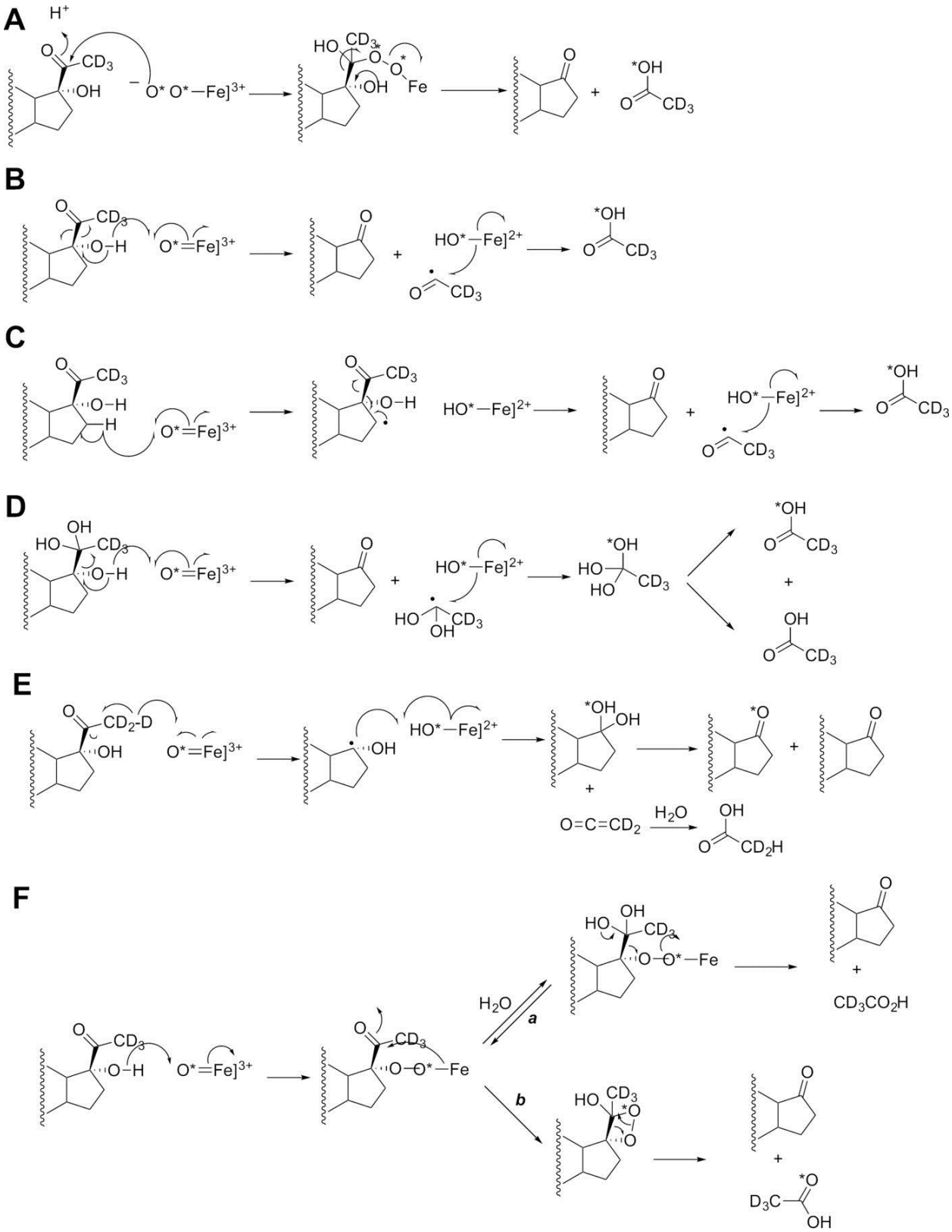

Figure 2.2 Possible mechanisms of P450 17A1-catalyzed 17α,20-lyase reaction and expected ^{18}O labeling [100].

The course of ^{18}O (from $^{18}O_2$) and deuterium (D) labels are indicated with an *asterisk. A*, ferric peroxide mechanism [94,117-120]; *B*, compound I mechanism with hydrogen atom abstraction from the 17α alcohol followed by C17-C20 bond scission to yield an acetyl radical; *C*, compound I mechanism with hydrogen atom abstraction from the C16 carbon; *D*, compound I mechanism with hydrogen atom abstraction from the 17*α* alcohol followed by C17-C20 bond scission to yield a hydrated acetyl radical (*gem*-diol); *E*, compound I mechanism with hydrogen atom abstraction from the C21 methyl group followed by C17-C20 bond scission to yield a C17 radical; *F*, addition of the 17α-hydroxyl group to compound I to yield an iron peroxide-C17 complex, which can decompose via either (*a*) a C20 *gem*-diol or (*b*) a C17-C20 dioxetane. See text for discussion and also Figure 2.18. Mechanisms *B*–*D* result in an acetyl radical that undergoes oxygen rebound with Fe-*OH (compound II), with an oxygen atom from molecular oxygen ($*O_2$) into the acetic acid product.

2.2 Results

2.2.1 Experimental Design for ^{18}O Experiments

The P450 17A1 17,20-lyase reaction produces DHEA from 17α-OHpreg (Figure. 1.4). The product acetic acid is of particular interest in determining the mechanism of P450 17A1 catalysis (Figure 2.2). To unambiguously distinguish the acetic acid formed as a product of the P450 17A1 reaction, the 17α-hydroxy substrate was d_3-labeled at position C21 because of concerns about the level of endogenous acetic acid interfering with that formed in the enzyme reaction, based on our experience with 1- and 2-C carboxylic acids [126-129]. Based on possible mechanisms shown in Figure 2.2, the acetic acid products of $^{18}O_2$ incubations with the 17α-hydroxy steroids are as follows: $CD_3CO^{18}OH$ (mechanisms A, B, C, and Fb), a 1:2 molar ratio of CD_3COOH and $CD_3CO^{18}OH$ (mechanism D), only CD_2HCOOH (mechanism E), or only CD_3COOH (mechanism Fa). Because of the small amounts of acetic acid produced (1:1 stoichiometry with steroid, $\sim$ 25 μmol) during incubations, the acetic acid was converted into an ester using diazoethylpyridine to facilitate characterization. In addition to the increase in mass, the ester is designed for efficient ionization attributable to the nitrogen in the pyridine ring, i.e. 2-(pyridin-2-yl)ethyl acetate [45] (*m/z* 166.1, "MH+") with one ^{16}O incorporated (d_2-labeled,"MH+ + 2") or one ^{16}O incorporated (d_3-labeled,"MH+ + 3"), and one ^{18}O incorporated (d_3-labeled, "MH+ + 5"). A similar approach was used for 17α-OH-[2,2,4,6,6,21,21,21-$^2H_8$]prog.

2.2.2 17α-OHpreg and 17α-OHprog ^{18}O Experiments

One ^{18}O atom was incorporated into acetic acid without deuterium loss (Figure 2.3, B–D) when 17α-OH-[21,21,21-$^2H_3$]preg was used as the substrate, ruling out the mechanism in Figure 2.2 E.

In the case of 17α-OH-[2,2,4,6,6,21,21,21-$^2H_8$]prog as the substrate (Figure 2.4), the signal-to-noise ratio of ^{18}O-incorporated acetate was three times greater than when the 17α-OH-[21,21,21-$^2H_3$]preg substrate was used. This improvement in sensitivity is attributed to the extra centrifugation step to remove the emulsion when extracting the acetic acid product (*cf.* Section 2.4.4). Additionally, a

trideutero-pyridine acetate product with no ^{18}O incorporation at 6 ppm mass tolerance was observed; however, the intensity was small compared with the ^{18}O-incorporated acetate product (~0.1% of ^{18}O-incorporated product), and this isotopologue is likely derived from the residual $^{16}O_2$ in the $^{18}O_2$ cylinder (99% ^{18}O abundance).

2.2.3 Reactions with Oxygen Surrogates, Background and Previous Studies

If the ferric hydroperoxide mechanism is operative, then one might expect the reaction to be supported by the direct addition of H_2O_2 to ferric P450 (Figure 2.1). However, Auchus and Miller [130] reported that no 17,20-lyase activity was observed with recombinant human P450 17A1 plus H_2O_2 in yeast microsomes. Iodosylbenzene is a single oxygen donor and cannot support a reaction that requires two oxygens, i.e. a ferric peroxide complex [131]. Iodosylbenzene also did not support the 17α,20-lyase reaction in a P450 17A1 yeast microsomal system [130].

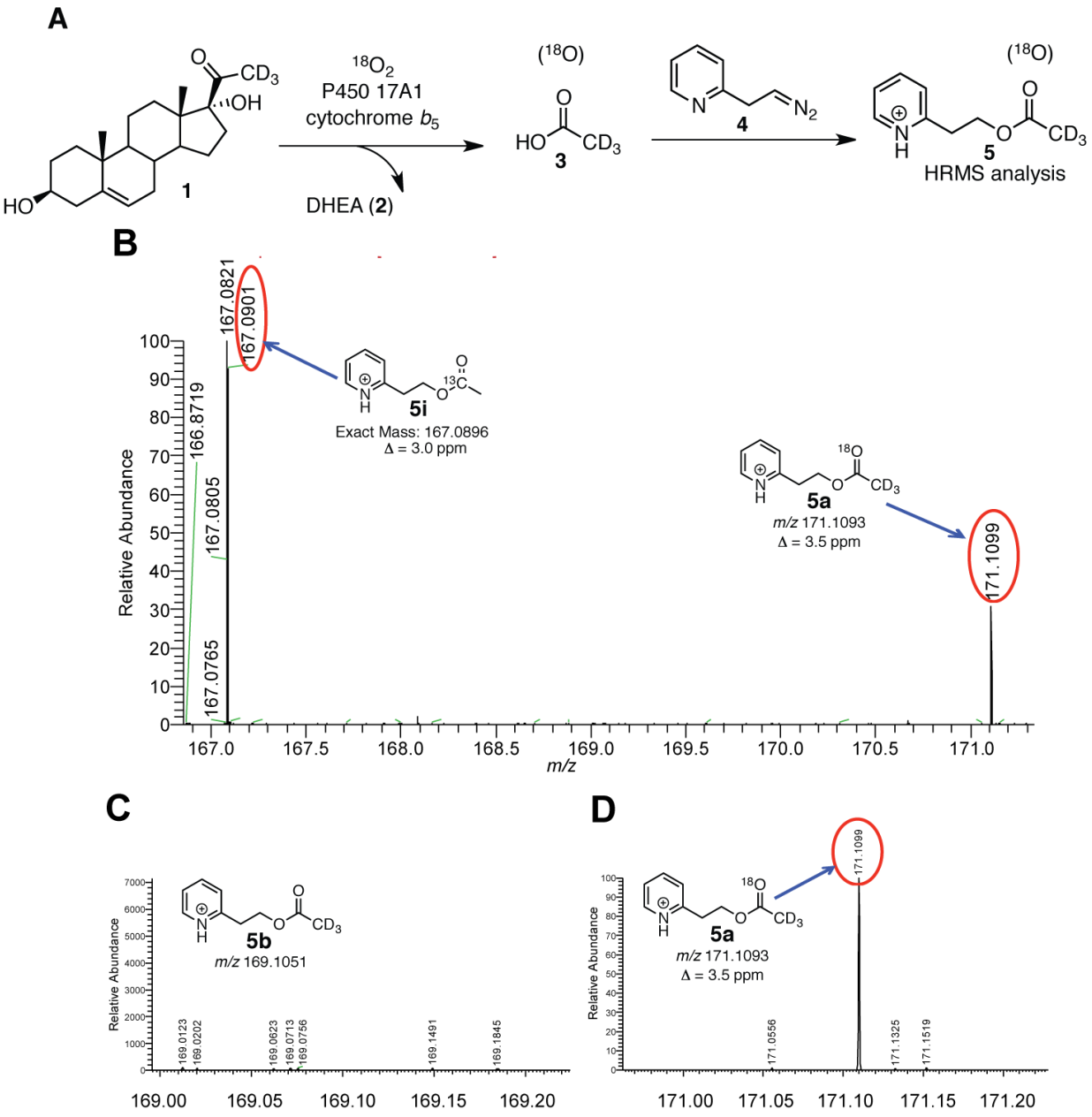

Figure 2.3 P450 17A1 incubation with [21,21,21-$^{2}H_3$]17α-OHpreg (1) in the presence of $^{18}O_2$ followed by derivatization and analysis by HRMS.

A, scheme showing the incubation of deuterated lyase substrate (*1*) with P450 17A1 and b_5 in the presence of $^{18}O_2$. The acetic acid product (*3*) was derivatized with the diazoethylpyridine reagent (*4*) and analyzed by LC-HRMS. *B*, mass spectrum of the *m/z* 166.5–171.3 range by selecting the t_R 3.01–3.12-min time interval in the ion chromatogram corresponding to the pyridine ester retention time. Shown at *m/z* 167.0901 is the peak corresponding to the acetate from background acetic acid from the natural abundance of ^{13}C isotope (*5i*, expected mass, *m/z* 167.0896, Δ 3.0 ppm). The peak at *m/z* 171.1099 corresponds to the acetate derived from the enzymatic product (*5a*, expected mass, *m/z* 171.1093, Δ 3.5 ppm). *C*, expansion of the mass spectrum (*m/z* 168.95–169.22) from *B* showing the absence of d_3-

labeled acetate with no ^{18}O incorporation (*5b*, expected mass, *m/z* 169.1051). *D*, expansion of the mass spectrum (*m/z* 170.95–171.22) from *B* showing the presence of d_3-labeled acetate with ^{18}O incorporation (*5a*, expected mass, *m/z* 171.1093). *p,* profile (peaks are shown in profile mode and not "centroid"). *ESI,* electrospray ionization; *RT,* retention time; *NL,* normalized level. More information about the meaning of the settings can be obtained from the Xcalibur Qual Browser User Guide (Thermo Scientific).

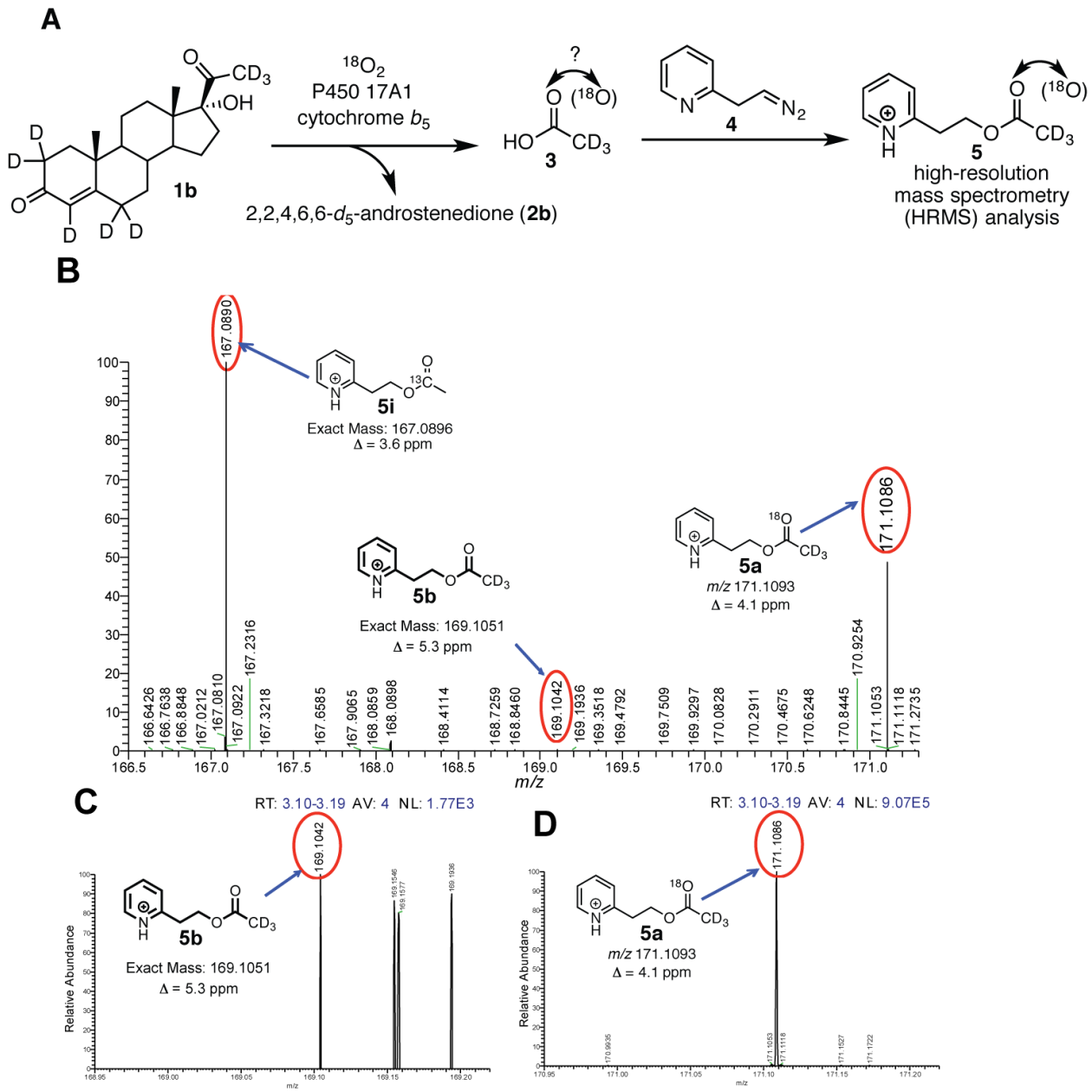

Figure 2.4 P450 17A1 incubation with 17α-OH-[2,2,4,6,6,21,21,21-$^{2}H_8$]prog (1b) in the presence of $^{18}O_2$ followed by derivatization and analysis by HRMS.

A, scheme showing the incubation of deuterated lyase substrate (*1b*) with P450 17A1 and b_5 in the presence of $^{18}O_2$. The acetic acid product (*3*) was derivatized with the diazoethylpyridine reagent (*4*) and analyzed by liquid chromatography-HRMS. *B*, mass spectrum of the *m/z* 166.5–171.3 range by selecting the t_R 3.10–3.19-min time interval in the ion chromatogram corresponding to the pyridine ester retention time. Shown at *m/z* 167.0890 is the peak corresponding to the acetate from background acetic acid from the natural abundance of ^{13}C isotope (*5i*, expected mass, *m/z* 167.0896, Δ 3.6 ppm). The peak at *m/z* 171.1099 corresponds to the acetate derived from the enzymatic product (*5a*, expected mass, *m/z* 171.1093, Δ 4.1 ppm). *C*, expansion of the mass spectrum (*m/z* 168.95–169.22) (from *B*) showing

the detection of d_3-labeled acetate with no ^{18}O incorporation (*5b*, expected mass, *m/z* 169.1051, Δ 5.3 ppm). *D*, expansion of the mass spectrum (*m/z* 170.95–171.22) from *B* showing the presence of d_3-labeled acetate with ^{18}O incorporation (*5a*, expected mass, *m*/*z* 171.1093). *p,* profile (peaks are shown in profile mode and not "centroid"). *ESI,* electrospray ionization. *RT,* retention time. *NL,* normalized level. More information about the meaning of the settings can be obtained from the Xcalibur Qual Browser User Guide (Thermo Scientific).

2.2.4 P450 17A1 Reactions with Iodosylbenzene

Preliminary experiments indicated that the most effective concentration to use was 300 μM (results not presented).

Two products were formed from 17α-OHprog in both the iodosylbenzene and NADPH-based systems (Figure 2.5). The expected product Andro (Figure 1.4) was characterized by co-elution with a standard and by both LC-UV and LC-MS comparisons with a standard (data not shown). The other product, which eluted just before Andro, was identified as 16,17α-di(OH)prog by co-elution with a standard and by both LC-UV and LC-MS comparisons with a reference standard (Figure 2.6). Although the dihydroxy product co-eluted with the 16α,17α-diastereomer, the presence of the 16β-stereoisomer cannot be excluded.

The products formed from 17α-OHpreg were converted to Δ^4 steroids by the action of cholesterol oxidase. These were identified as 16,17α-di(OH)prog and Andro, thus indicating that the products formed from 17α-OHpreg were 16,17α-di(OH)preg and DHEA.

The rates of formation of 16,17α-di(OH)prog and Andro from 17α-OHprog in the NADPH- and iodosylbenzene-based systems were comparable in the absence of b_5 (Figure 2.7 A). The iodosylbenzene-dependent reaction was stimulated 2-fold by b_5, but the stimulation of the reaction that used POR was much greater (10-fold), so that the iodosylbenzene versus POR comparison (with b_5 present) is more disparate (Figure 2.7 A).

With 17α-OHpreg as substrate, a similar conclusion was reached regarding comparisons of the rates of the POR- and iodosylbenzene-supported reactions (Figure 2.7 B). When the 16-hydroxylation of the 17α-hydroxy steroids was considered, the iodosylbenzene-supported reactions were faster (Figure 2.8). It is also notable that these reactions were stimulated by b_5.

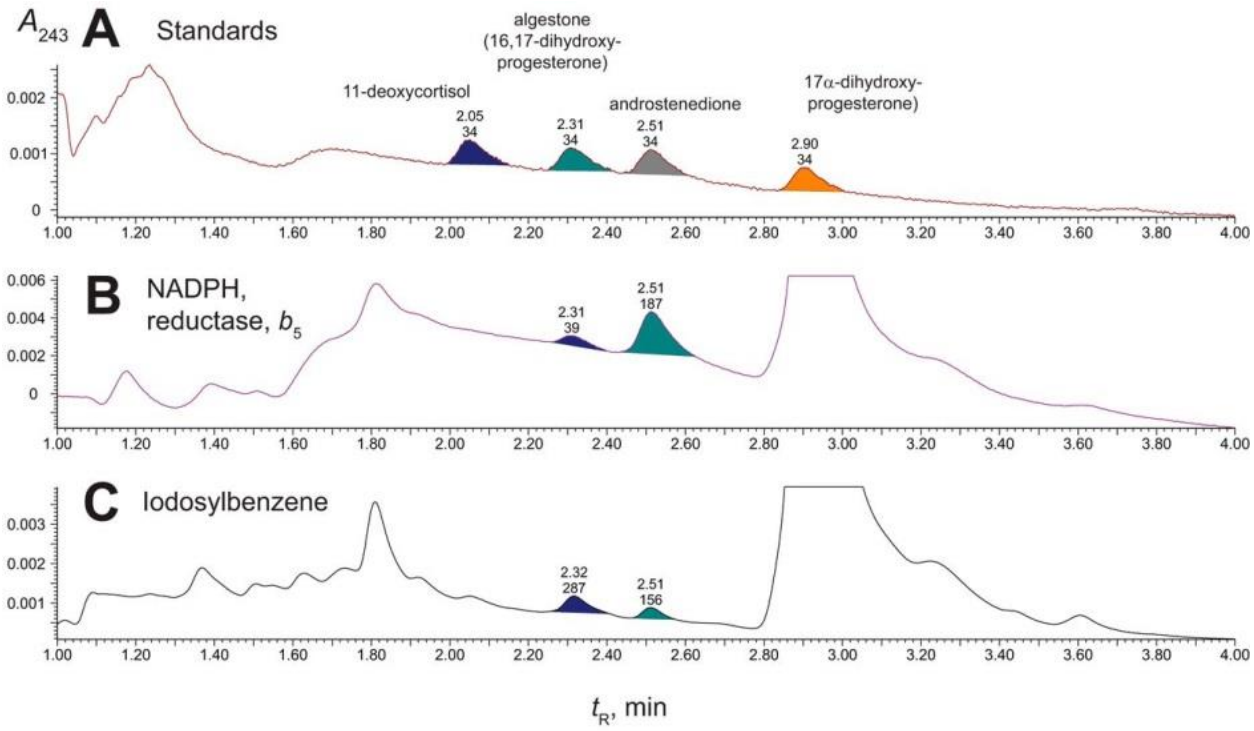

Figure 2.5 Formation of 16,17α-di(OH)prog and Andro from 17α-OHprog by P450 supported by the oxygen surrogate iodosylbenzene.

Retention times (t_R) and integration units are indicated on the chromatograms. *A*, standard compounds. *B*, reaction (0.5 µM P450 17A1) supported by POR (2.0 μM), b_5 (0.5 μM), and NADPH (30 s incubation). *C*, reaction (0.5 μm P450 17A1 and b_5 (0.5 μM)) with 0.30 mM iodosylbenzene (30 s incubation). In control experiments with only b_5 and iodosylbenzene (2 mM) mixed with the 17α-hydroxysteroids, the amounts of Andro detected were <15% of the amounts observed in this and similar studies with both 17α-hydroxysteroids.

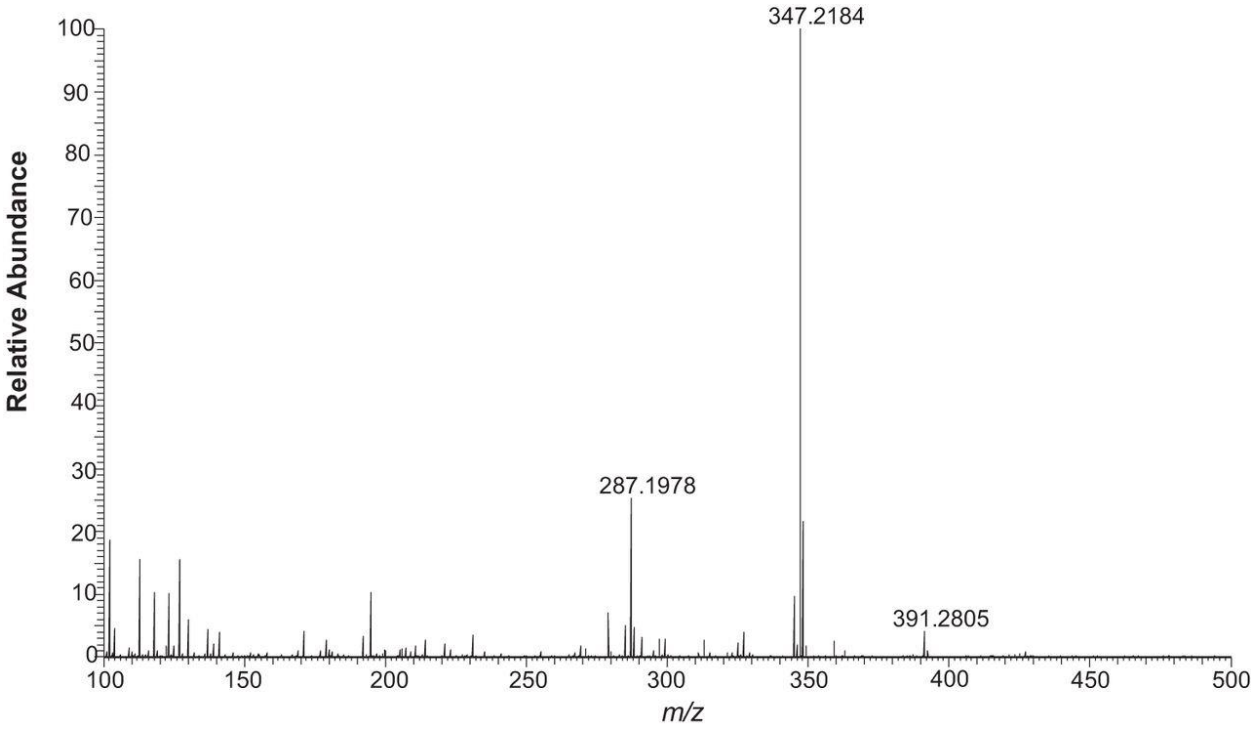

Figure 2.6 Identification of 16,17α-di(OH)prog as a product of 17α-OHprog.

HRMS spectrum of 16,17-di(OH)prog formed in a reaction with POR, b_5, and NADPH. Exact mass 346.2217 (protonated species): observed for MH^+, *m/z* 347.2184 (Δ 9.5 ppm).

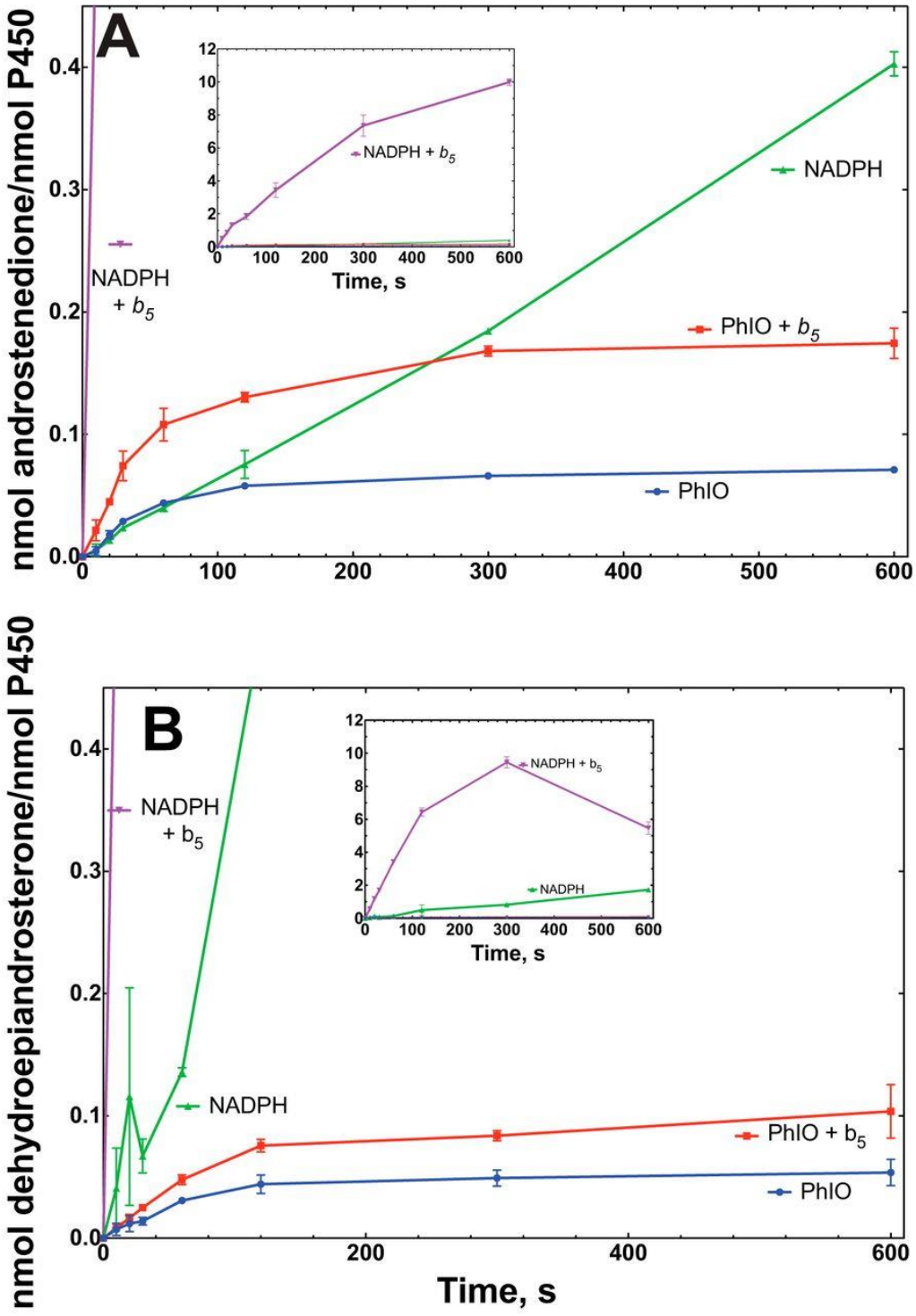

Figure 2.7 Time course and effect of b_5 on 19-carbon steroid formation in the presence of iodosylbenzene (PhIO) or the typical NADPH-supported reaction.

A, oxidation of 17α-OHprog. *B*, oxidation of 17α-OHpreg. The *insets* show the NADPH-supported reactions in the presence of b_5. The *points* are means of duplicate assays, shown as means ± range.

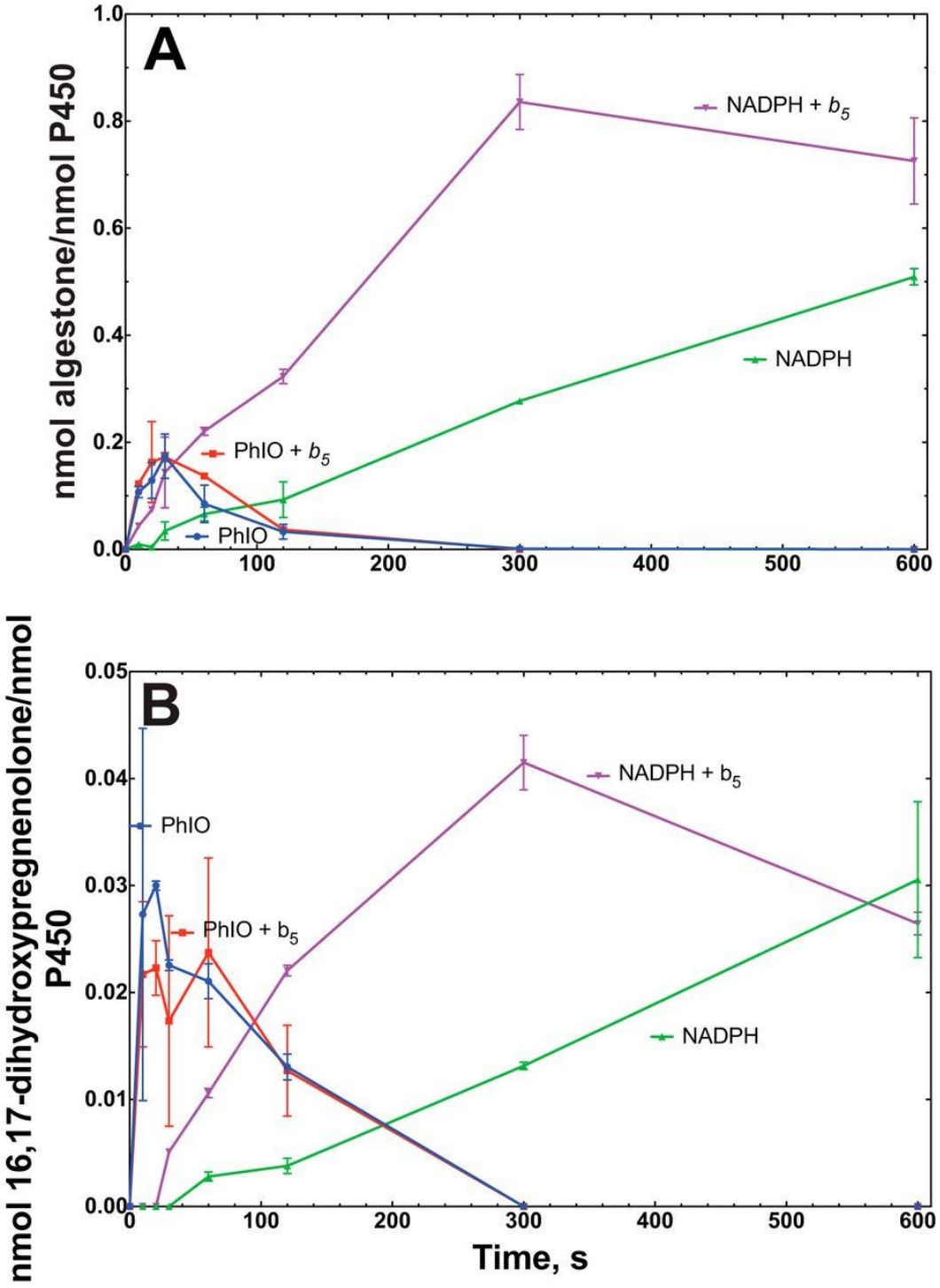

Figure 2.8 Time course and effect of b_5 on steroid 16-hydroxylation in the presence of iodosylbenzene (PhIO) or the typical NADPH-supported reaction.

A, oxidation of 17*α*-OHprog. *B*, oxidation of 17*α*-OHpreg. The *points* are means of duplicate assays, shown as means ± range.

2.2.5 Reactions with H_2O_2

H_2O_2 was added to purified P450 17A1 (with b_5 present), and no detectable 17,20-lyase activity was found toward 17α-OHpreg or 17α-OHprog, using varying concentrations of H_2O_2 (up to 10 mM) (Figure 2.8). Under these conditions, the usual reconstituted P450 17A1/POR/b_5 system yielded the expected products (Figure 2.9, B and E).

2.2.6 Additional Oxidation Products

With both 17α-OHprog and 17α-OHpreg, the rates of formation of the lyase products (Andro and DHEA) were no longer linear after 5 min (300 s) (Figure 2.7). The change was more obvious in the latter case, with the amount of accumulated product decreasing (Figure 2.7 B). The phenomenon was found to be the result of further 16-hydroxylation of the lyase products, in that these products (t_R, UV spectra, and mass spectra) were also identified in the longer term reactions with both substrates (with 16-OH-DHEA being converted to 16-OHandro by cholesterol oxidase in the assays with 17α-OHpreg) (Figure 2.10). The time course of formation of these products from Andro and DHEA is shown in Figure 2.11.

Also noted was a decrease in the level of 16,17α-dihydroxy steroids with extended time (in the NADPH-supported reactions, Figure 2.8). The products formed from (commercial) 16α,17α-di(OH)prog were analyzed. One product was 16α-OHandro, identified above (Figure 2.12). The major product formed from 16α,17α-di(OH)preg was 16α-OH-DHEA, identified by its mass and NMR spectra (Figure 2.13).

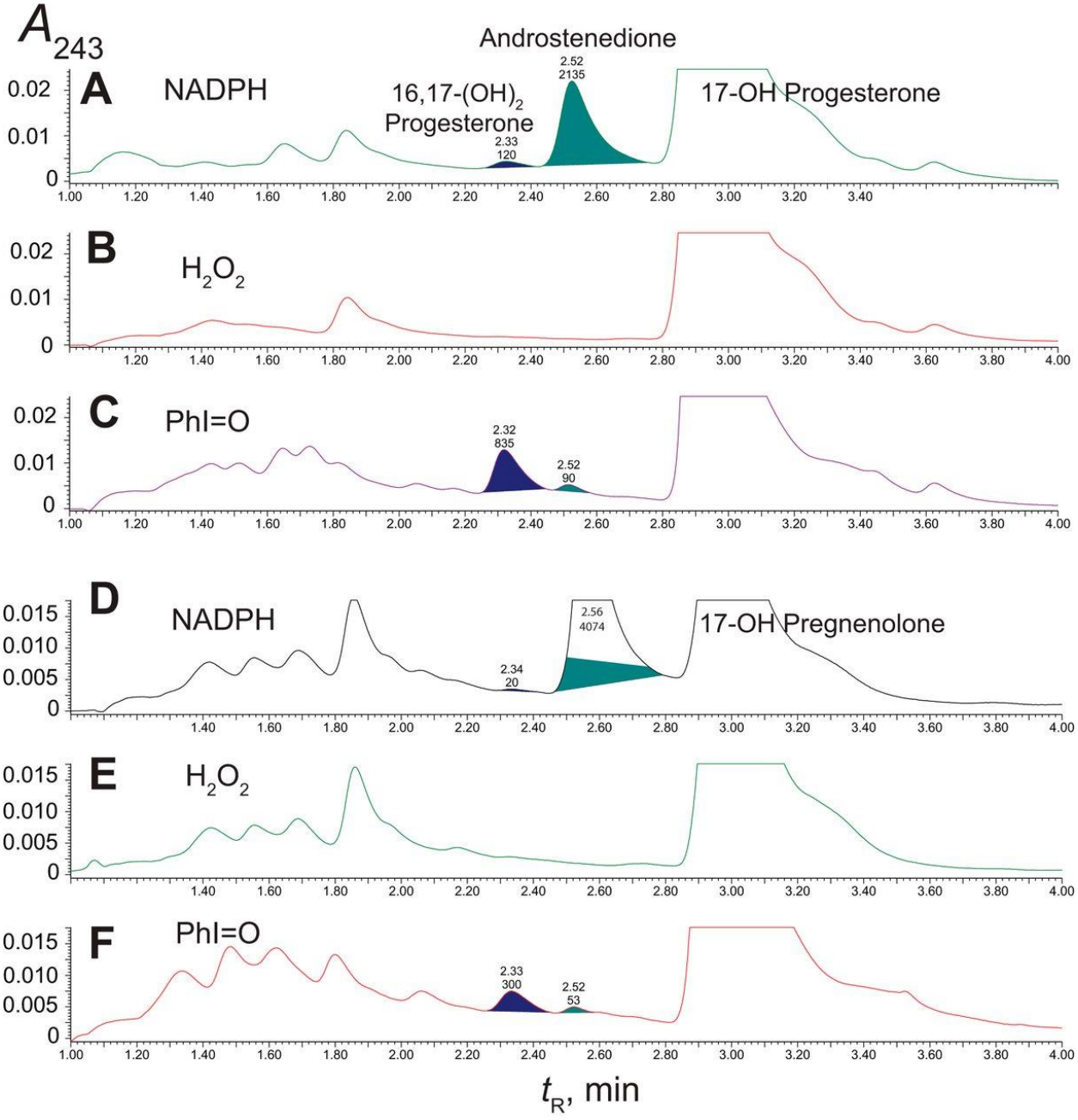

Figure 2.9 Reaction products formed from 17α-OHprog and 17α-OHpreg in P450 17A1 reactions supported by various factors.

Retention times (t_R) and integration units are indicated on the chromatograms. *A–C*, 17α-OHprog; *D–F*, 17α-OHpreg. *A* and *D*, POR, b_5, and NADPH; *B* and *E*, H_2O_2 (10 mM) (with b_5); *C* and *F*, iodosylbenzene (*PhI=O*, 300 μM) (with b_5). In these studies the Δ^5 products (formed from 17α-OHpreg) were oxidized to Δ^4 products to facilitate LC-UV analysis.

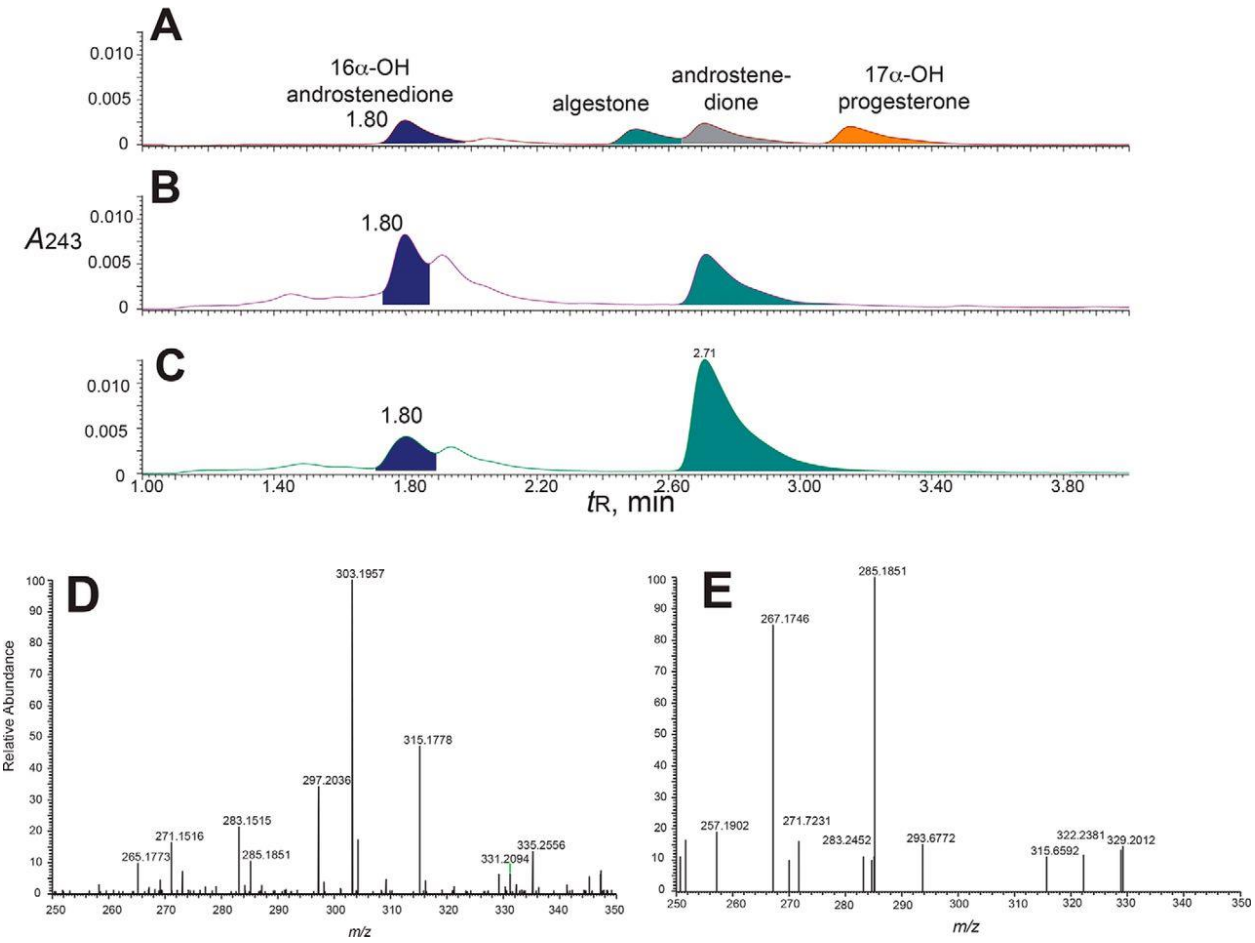

Figure 2.10 Identification of 16-hydroxy steroids as reaction products formed from DHEA and Andro.

A, authentic steroid standards: 16α-OHandro, algestone (16α,17α-di(OH)prog), Andro, and 17α-OHprog; *B*, 10-min DHEA incubation (with products treated with cholesterol oxidase); *C*, 10-min Andro incubation; *D*, mass spectrum of peak identified as 16-OHandro (formed from Andro); *E*, MS/MS analysis of *m/z* 303.2 peak of *D*.

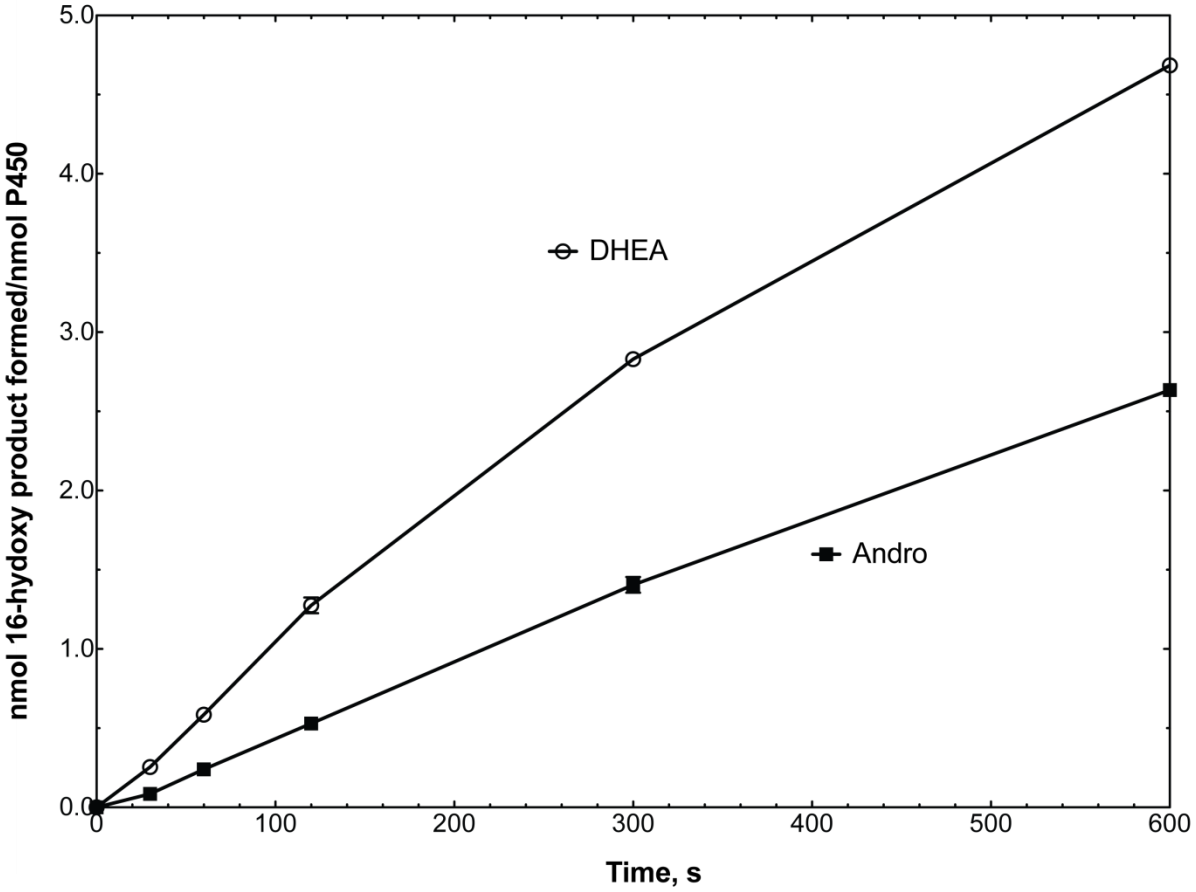

Figure 2.11 Time course of 16-hydroxylation of Andro and DHEA by P450 17A1.

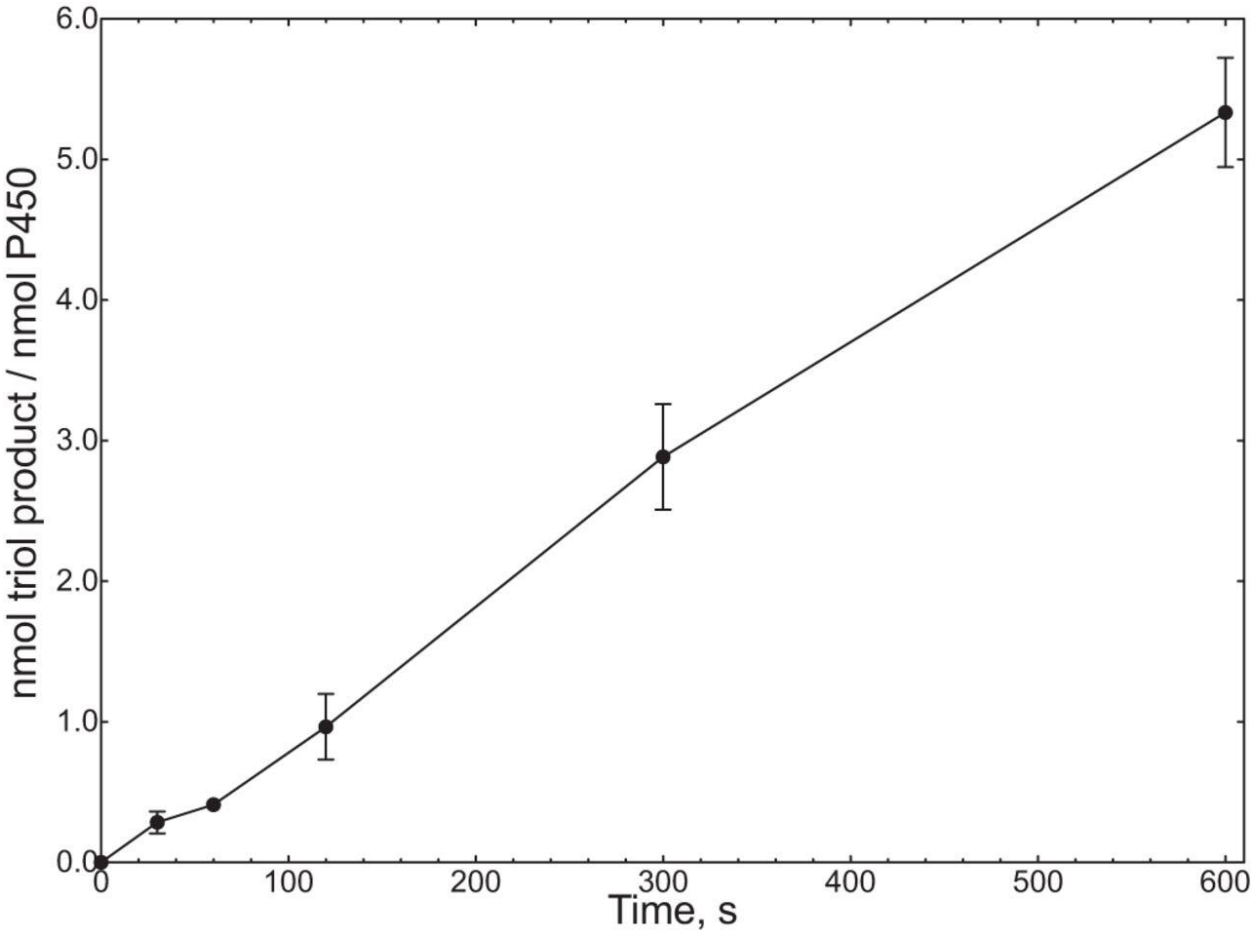

Figure 2.12 Rate of conversion of 16*α*,17*α*-di(OH)prog to 6*β*,16*α*,17*α*-tri(OH)prog (Figure 2.14) by P450 17A1.

The points are means of duplicate assays, shown as means ± range.

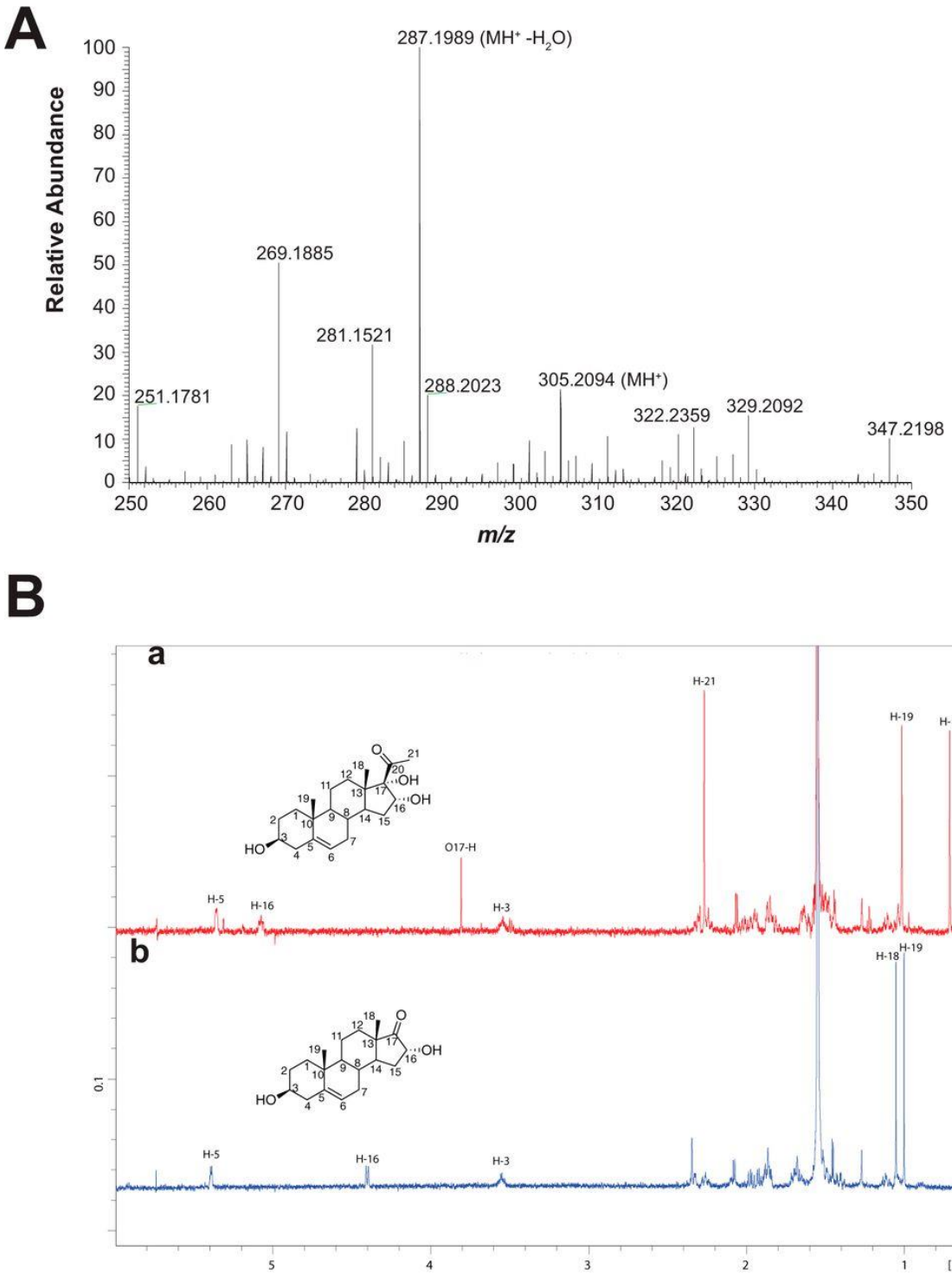

Figure 2.13 Characterization of 16*α*-OH-DHEA.

The product was formed in an incubation of an NADPH-reconstituted P450 17A1 system with 16*α*,17*α*-di(OH)preg and isolated by preparative HPLC. *A*, HRMS spectrum of $[DHEA + 16]^+$ peak, 16*α*-OH-DHEA (theoretical *m/z* for MH^+ 305.2111, found *m/z* 305.2094 (Δ 5.6 ppm)). *B*, NMR spectra of 16*α*,17*α*-di(OH)preg (*a*) and product (*b*) in $CDCl_3$ (600 MHz). See text for discussion.

2.2.7 Identification of Steroid B Ring Hydroxylation Product

The other major product in the incubation of 16*α*,17*α*-di(OH)prog with P450 17A1 was a triol, as judged by HRMS (*m/z* 363.2160, calculated MH+ *m/z* 363.2166, Δ 1.7 ppm) (Figure 2.14 A) [132]. The UV spectrum was similar to those of other Δ^4 3-keto steroids except blue-shifted ~5 nm (Figure 2.14 B), consistent with an intact Δ^4 3-keto steroid having some modification near the chromophore. The site of hydroxylation was identified as C-6 by ^{1}H NMR (Figure 2.14 C and appendix Table 6-1), i.e. 6*β*,16*α*,17*α*-tri(OH)prog [28,133]. The 18, 19, and 21 methyl groups were intact (*δ* 0.79, 1.40, and 2.28 ppm), but there was a new multiplet at δ 4.38 ppm. The NOESY spectrum (appendix Figure 6.1) showed a spatial correlation between the new hydroxymethine proton (*δ* 4.38 ppm) and the Δ^4-proton (*δ* 5.70 ppm). Moreover, the HMBC spectrum (heteronuclear multiple-bond correlation (NMR) spectroscopy) (appendix Figure 6.2) indicated a 3-bond coupling interaction between the C4-carbon (*δ* 125 ppm) and the hydroxymethine proton (*δ* 4.38 ppm) suggesting either the C2-position or the C6-position for the newly identified hydroxymethine proton (*δ* 4.38 ppm). The C6-position for the hydroxymethine proton (*δ* 4.38 ppm) was established because the C2-methylene protons (*δ* 2.53 and 2.42 ppm), which had a 2-bond correlation to the C3-keto carbon atom (*δ* 205.1 ppm) in the HMBC spectrum, were present. Moreover, the COSY spectrum (appendix Figure 6.3) indicated a 3-bond coupling between the C6-proton (*δ* 4.38 ppm) and the C7-protons (*δ* 1.98 and 1.34 ppm) (see also HSQC spectrum, appendix Figure 6.4).

The stereochemistry of the C6-hydroxyl group was assigned as *β*, based on the chemical shifts of the 7-protons of the steroid. In considering the chemical shifts of literature compounds (see Refs. 134 and 135 and see Table 2C in Ref. 132 and references therein), corresponding to 6α- and 6β-OHprog), the chemical shifts of the 7*α*- and 7*β*-protons are very informative. In the isolated P450 17A1 product, the chemical shifts of the 7*α*- and 7*β*-protons were (*δ*) 1.34 and 1.98 ppm, respectively, and in Ref. 132, the 7*α*- and 7*β*-protons were at (*δ*) 1.28 and 2.02 for 6*β*-OHprog, whereas the protons had chemical shifts of (*δ*) 1.11 and 2.19 for 6*α*-OHprog. Thus, 6*β*-hydroxy is the most likely stereochemistry of the new

product. The NOESY spectrum showed spatial correlation between the C6-proton (δ 4.38 ppm) and both of the 7α- and 7β-protons (δ 1.34 and 1.98 ppm). Considering a Newman projection down the C6–C7 bond axis, this NOESY interaction is supported by the 6β-hydroxy configuration (appendix Figure 6.1).

The products formed from 16α,17α-di(OH)preg were also analyzed. One product was 16α-OH-DHEA. The other product was either a tetraol or an epoxytriol (5,6-epoxy-3β,16α,17α-trihydroxypregnan-20-one), as judged by HRMS (*m/z* 365.2305, calculated mass, *m/z* 365.2323, Δ 4.9 ppm). The site of oxygen incorporation was not identified. The major product isolated from this reaction was 16α-OH-DHEA, as can be seen from the ^{1}H NMR spectrum of the purified product (Figure 2.13 B). There is a loss of the C21-methyl protons (δ 2.25 ppm) and an upfield shift of the 16β-proton (5.1 ppm to 4.4 ppm) (Figure 2.13 B). The proton NMR spectrum of the isolated P450 17A1 product also matched a previously reported NMR spectrum of synthetic 16α-OH-DHEA [136].

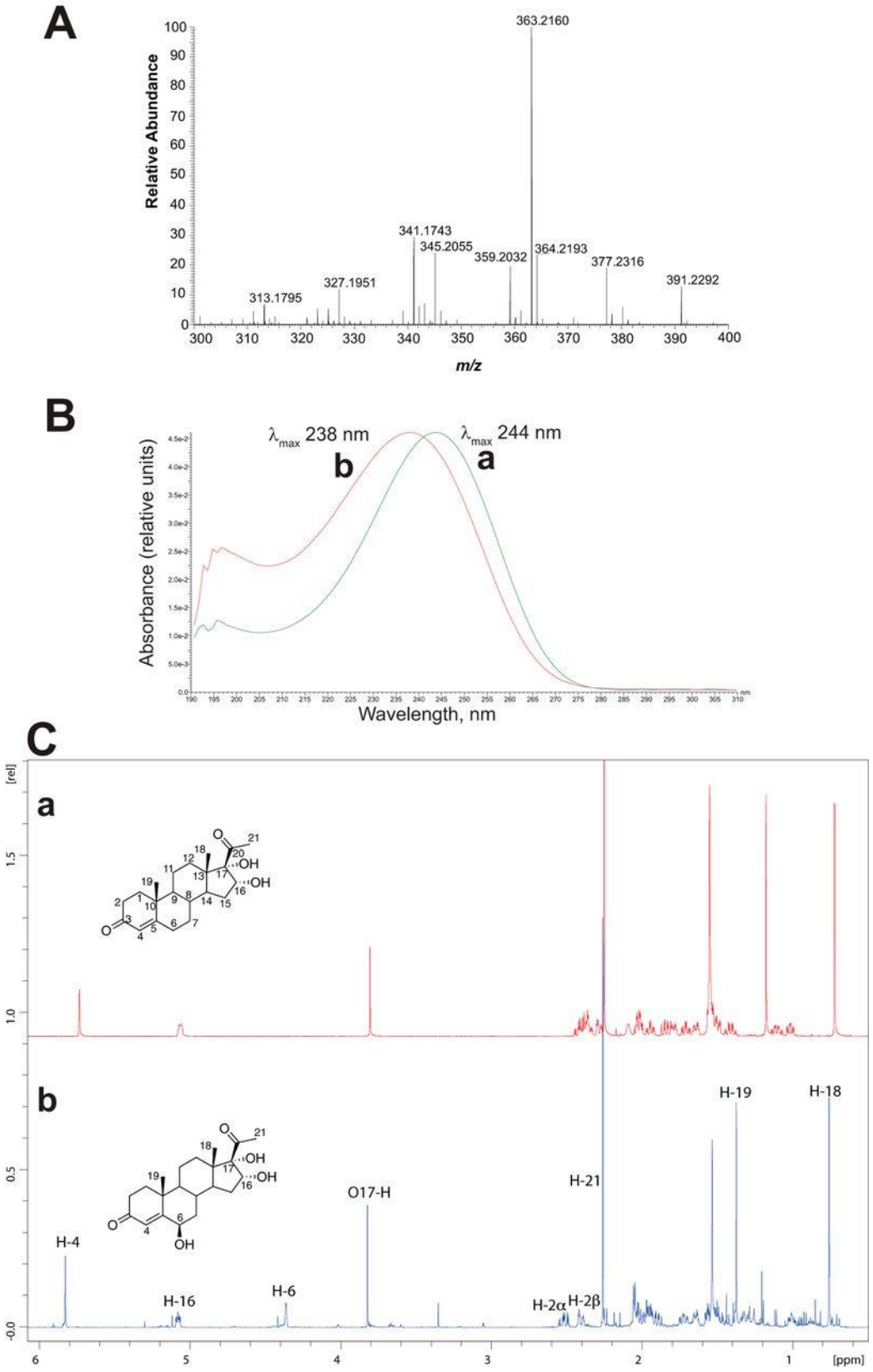

Figure 2.14 Characterization of 6*β*,16*α*,17*α*-tri(OH)prog.

The product was formed in an incubation of an NADPH-reconstituted P450 17A1 system with 16*α*,17*α*-di(OH)prog and isolated by preparative HPLC. *A*, HRMS spectrum (theoretical *m/z* for MH^+ 363.2166, found *m/z* 363.2160 (Δ 1.7 ppm)). *B*, UV spectra of product (*b*) compared with 16*α*,17*α*- di(OH)prog (*a*). *C*, ^{1}H NMR spectra of product (*b*) and 16*α*,17*α*-di(OH)prog (*a*) in $CDCl_3$ (600 MHz). Note that the C-18, C-19, and C-21 methyl signals are intact and the chemical shifts of the H-7 protons appear to be moved upfield, as predicted (appendix Table 6-1). See text and Ref. 132 for discussion, and see appendix Figures 6.1-6.4 for two-dimensional NMR spectra.

2.2.8 Solvent Kinetic Isotope Effects on 17,20-Lyase Reactions

No C–H bond-breaking steps are involved in any steps proposed in Figure 2.2 except for panel D, which is not supported by the ^{18}O work. Thus, no C-H kinetic deuterium isotope effect studies can be applied, but solvent kinetic isotope effect experiments can be informative.

No solvent kinetic isotope effect was found for the 17,20-lyase reaction with 17α-OHprog (measured rates of 1.47 ± 0.03 min^{-1} in H_2O and 1.40 ± 0.03 min^{-1} in 95% D_2O (v/v), n = 4, calculated isotope effect of 1.05 ± 0.09 (S.D.)). In contrast, a small but repeatable inverse isotope effect (0.83 ± 0.05 (S.D.), n = 4) was observed for the 17,20-lyase reaction with 17α-OHpreg under the usual conditions with b_5, POR, and a substrate concentration of 30 μM (measured rates of 4.10 ± 0.22 min^{-1} in H_2O, 4.94 ± 0.13 min^{-1} in 95% D_2O (v/v), calculated from four independent experiments (± S.D.)) (Figures 2.15 and 2.16). The solvent kinetic deuterium isotope effects for the 16-hydroxylation reactions were 1.35 ± 0.15 for 17α-OHprog and 1.34 ± 0.23 for 17α-OHpreg (n = 4, ± S.D., data not shown).

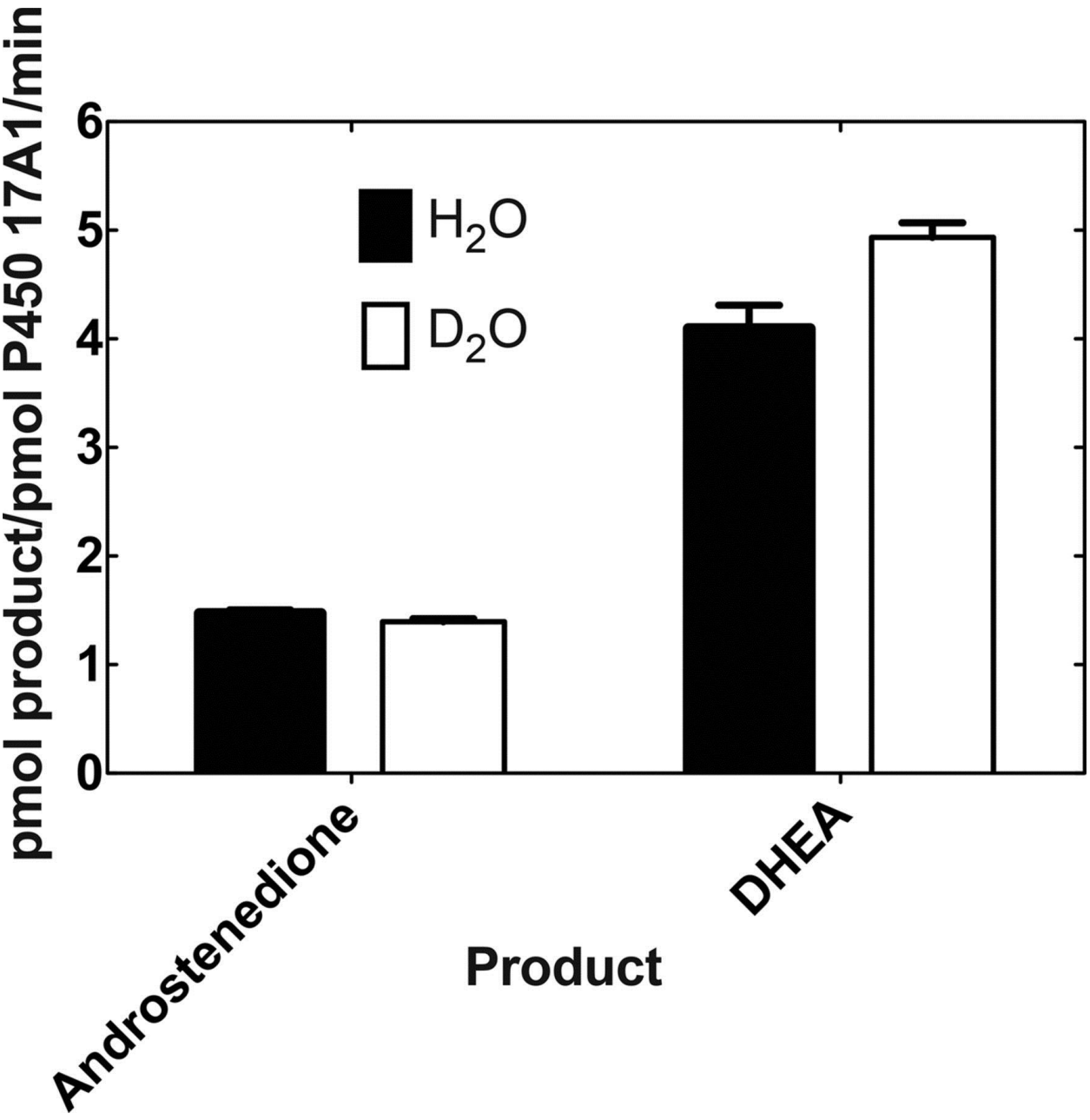

Figure 2.15 Kinetic solvent isotope effects on 17α-OHprog and 17α-OHpreg 17,20-lyase reactions catalyzed by P450 17A1 (in the presence of POR, NADPH, and b_5).

Results are shown as means of four individual experiments ± S.D.

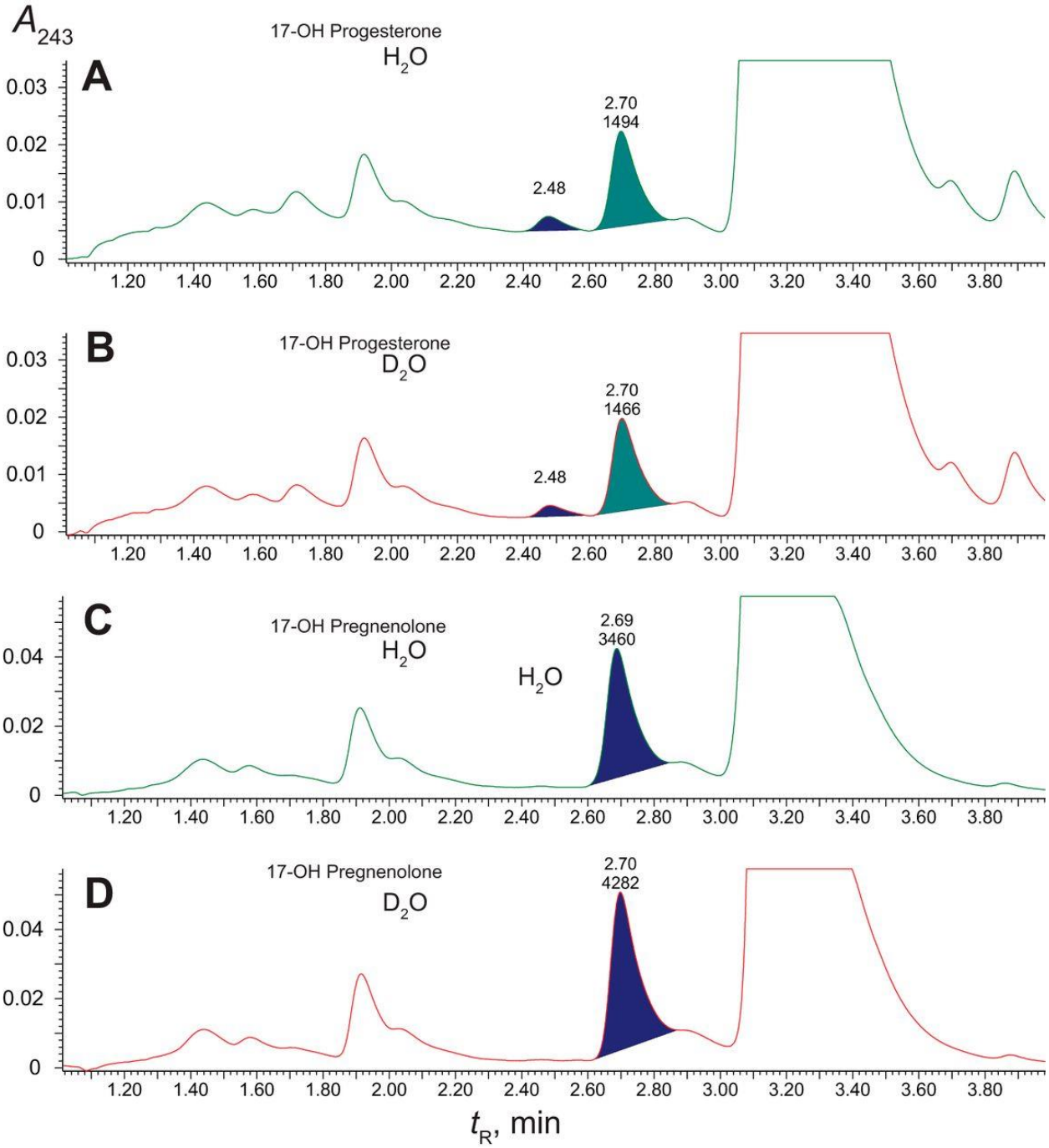

Figure 2.16 Solvent kinetic deuterium isotope effects on 17α-OHprog and 17α-OHpreg reactions catalyzed by P450 17A1 (in the presence of POR and b_5).

Retention times (t_R) and integration units are indicated on the chromatograms. The substrate concentration was 30 μm in all cases, and the reactions were done in either H_2O or 95% D_2O (v/v) at pH or pD 7.4. *A* and *B*, 17α-OHprog; *C* and *D*, 17α-OHpreg. *A* and *C*, H_2O; *B* and *D*, 95% D_2O (v/v).

2.3 Discussion

The results indicate that acetic acid recovered in the human P450 17A1 reactions with either 17α-OHprog or 17α-OHpreg contained an ^{18}O atom derived from molecular oxygen. These results are consonant with the original analysis of Akhtar and co-workers on P450 17A1 [94,117] and, on their own, are consistent with the FeO_2^- mechanism presented in Figure 2.2 A [130,137]. Alternative mechanisms that are still consistent with the ^{18}O labeling results, but involving FeO^{3+}, are presented in Figure 2.2 B, C, and F, arrow b [100,130,138]. The mechanisms in Figure 2.2 B and C involve formation of an acetyl radical, which has adequate chemical precedent [121,139-141]. The dioxetane mechanism is similar to one that has been proposed for tryptophan and indole dioxygenases [142]. One of these two FeO^{3+} mechanisms is proposed to contribute to the lyase reaction in that (i) iodosylbenzene can support the lyase reaction, and (ii) P450 17A1-17α-hydroxysteroid complexes are poised for multiple hydroxylation reactions in addition to lyase reactions.

2.3.1 Incubations with $^{18}O_2$

Previous studies of $^{18}O_2$ incubations with P450 17A1 concluded that ^{18}O incorporation into the acetic acid product was the major isotopologue detected, leading to the conclusion that the ferric peroxide was the iron-active species for C–C bond cleavage [43,116]. However, these studies (i) used low resolution mass spectrometry and (ii) used microsomes from porcine testes as the source of enzyme (i.e. non-purified enzyme); and (iii) the report that used the direct lyase substrate 17α-OH-[21,21,21-$^2H_3$]preg did not present raw data [116], whereas a subsequent report used [16α,17α,21,21,21-$^2H_5$]preg as the substrate and not the direct substrate that results in the formation of DHEA, i.e. 17α-OHpreg [43]. Furthermore, the low resolution mass spectrometry used in these studies yielded an ambiguous determination of ^{18}O-, ^2H-, and ^{13}C-labeled content of the acetate products [43], which resulted in the interpretation of multiple possible mechanisms for the lyase step of P450 17A1 (Figure 2.2). In this work,

the incubations included purified P450 17A1 and labeled lyase substrates (17α-OH-[21,21,21-$^{2}H_3$]preg and 17α-OH-[2,2,4,6,6,21,21,21-$^{2}H_8$]prog) in the presence of $^{18}O_2$ and analyzed the acetate product by HRMS after derivatization with the new diazo reagent. The results unambiguously established that the acetate produced from the enzymatic incubation incorporated one oxygen atom from molecular oxygen in both cases, with the C-21 deuteriums retained (Figures 2.3 and 2.4). Moreover, no significant amounts of any other acetate isotopologues from the enzyme incubation were detected (i.e. loss of one deuterium or lack of ^{18}O incorporation). These experiments agree with the observation of oxygen incorporation from the reports of Akhtar and co-workers [43,116]. However, although these data can support a ferric peroxide mechanism for C–C bond cleavage (Figure 2.2 A), they do not rule out a Compound I mechanism (Figure 2.2 B, C, and F, arrow b).

2.3.2 Oxygen Surrogate Studies, Iodosylbenzene

The use of iodosylbenzene and POR to form Compound I with P450 17A1 resulted in two different activities when the 17α-hydroxysteroid was used as the substrate. In both conditions, 16α-hydroxylation and C–C bond cleavage activities toward 17α-OHprog yielded 16,17α-di(OH)prog and androstenedione, respectively (Figures 2.5, 2.7 A, and 2.8 A). However, the product distributions were different; iodosylbenzene yielded more 16-hydroxylation relative to C–C bond cleavage (~9:1, Figure 2.5 C) compared when POR was used (~0.1:1, Figure 2.5 B). The switch in reactivities depending on the oxidation system used (iodosylbenzene versus POR) suggests a conformational change in the enzyme-substrate complex when the reductase binds to the P450 enzyme. Moreover, when 17α-OHpreg was used as the substrate, the 16-hydroxylation activity was diminished (Figure 2.9, D and F) relative to when 17α-OHprog was used as the substrate. Similarly, this substrate-dependent switch in reactivity is reminiscent of the different 16- versus 17-hydroxylation regioselectivities observed when two different substrates, Prog and Preg, are used for P450 17A1 [40], which is explained by the 3-keto-Δ^4 versus 3β-hydroxy-Δ^5 moieties in the AB-ring systems of these steroid substrates.

Moreover, the fact that P450 17A1 is catalyzing a C-H hydroxylation with its lyase substrate, 17α-OHpreg, supports the presence of a Compound I species, which either hydroxylates the C16-position or cleaves the C17,C20-bond as shown in Figure 2.2. This observation may contradict the conclusions about the active iron hydroperoxo species observed by resonance Raman spectroscopy [115,125]. However, it is possible that the iron peroxohemiketal species reported in the resonance Raman study [125], i.e. Figure 2.2 A, tetrahedral intermediate, was a structural misassignment and that the actual observed species was indeed an iron peroxo intermediate attached through the C17-position of the steroid (Figure 2.2 F). This iron peroxo intermediate can be formed from a nucleophilic attack of the C17-hydroxy group of the lyase substrate (i.e. 17α-OHpreg or 17α-OHprog, Figure 2.2 F) onto Compound I.

It should be pointed out that the iodosylbenzene mechanism may be more complex than just a direct oxygen transfer, as pointed out by Ortiz de Montellano [137]. A possible intermediate is shown in Figure 2.17, which may even have oxidant capacity of its own.

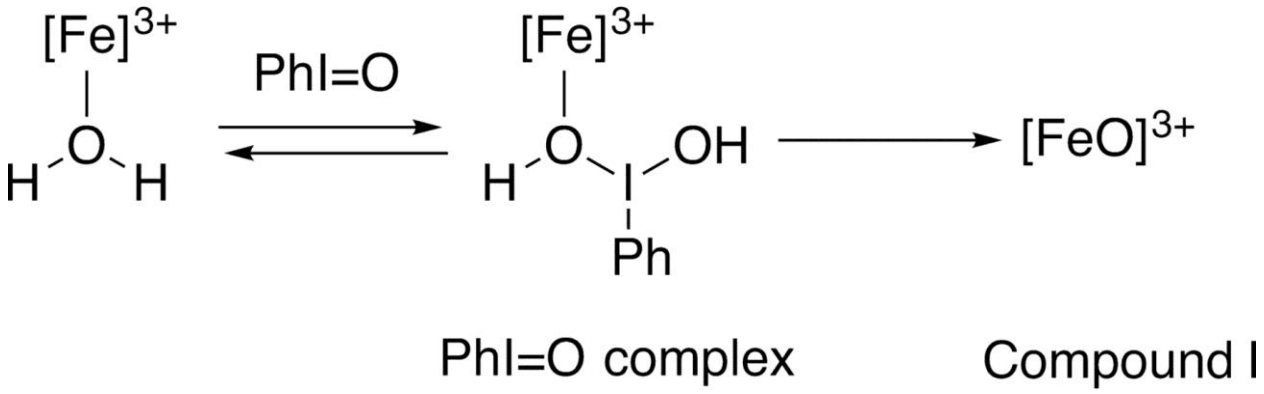

Figure 2.17 Possible oxidizing alternative to Compound I in the iodosylbenzene (PhI=O)-supported reactions [137].

2.3.3 Oxygen Surrogate Studies, Hydrogen Peroxide

Many studies in the literature involve the use of alkyl hydroperoxides as oxygen surrogates for P450 reactions, beginning with Kadlubar et al. [143]. However, although peracids can be used as reagents to generate P450 Compound I [21], studies with alkyl hydroperoxides are problematic due to the production of radicals and their ensuing chemistry [137,144]. Some bacterial Family 152 P450s use H_2O_2 as a physiological cofactor [145-147], and bacterial P450 101A1 ($P450_{cam}$) was mutated to a species that could efficiently utilize H_2O_2 in reactions [148]. H_2O_2 can support some mammalian P450 reactions after direct addition [134,135,149-152] (although generally not as well as alkyl hydroperoxides [143]), but the role of a ferric peroxide in each oxygenation reaction can only be postulated, in that the ferric peroxide can subsequently convert to Compound I.

In principle, the FeO_2^- complex could proceed to compound I (FeO^{3+}) through appropriate acid-base catalysis, but there are also side reactions that may diminish the progress of a putative Fe^{3+}-H_2O_2 complex on to FeO^{3+} (Figure 2.1). Attempts were made to generate and observe Compound I or other intermediates by mixing P450 17A1 with H_2O_2 (10 mM) or iodosylbenzene (300 μM) in a stopped-flow spectrophotometer (dead time ~2 ms, rapid scanning) but were unsuccessful in seeing any distinct complexes (data not presented). However, given the difficulties encountered by others in observing these transient species even with bacterial P450s [21], negative results are inconclusive.

2.3.4 b_5 Effects

Another issue that is still not resolved is the stimulatory effect of b_5, which is known to promote the 17,20-lyase reaction of P450 17A1. Results with apo-b_5, devoid of heme, have shown that b_5 does not donate the second electron in the catalytic cycle of this P450 [57]. The stimulation of 17,20-lyase activity by b_5 in the iodosylbenzene-supported reaction (Figure 2.7) is consistent with this view. b_5 stimulation of the 16-hydroxylation reactions with both 17α-OHprog and 17α-OHpreg was also noted

(Figure 2.7). Discussed in Chapter 3,the stimulation of the 17α-hydroxylation of both Prog and Preg by b_5 (see Chapter 3) has also been observed. The conclusion about the stimulatory role of b_5 in the iodosylbenzene reactions is that it is acting in an allosteric manner to facilitate these reactions (e.g. due to more ideal juxtaposition in reaction intermediates), which is the reason proposed for the normal physiological reaction [32,57,100].

2.3.5 Hydroxylations Catalyzed by P450 17A1

The 16α-hydroxylation of DHEA has previously been reported to be catalyzed by P450 3A4 [153,154]. Upon monitoring the production of DHEA from 17α-OHpreg by P450 17A1 over time (Figure 2.7 B, inset), there was a decrease in DHEA formation in the time points greater than 5 min. This observation suggested that DHEA was further being oxidized to another product. As such, it was hypothesized that this new product would correspond to 16-OH-DHEA based on the other activities of P450 17A1 (16-hydroxylation of Prog [40] and 16-hydroxylation of its 17α-hydroxylated products). The new product, which was converted to its 3-keto-Δ^4 counterpart by cholesterol oxidase, co-chromatographed with standard 16α-OHandro (Figure 2.9). The 16-hydroxylation product of P450 17A1 was also observed when Andro was used as the substrate (Figure 2.10). The ability of P450 17A1 to form 16-hydroxylated androgens is physiologically relevant in that estriol, an abundant and characteristic estrogen during human pregnancies, arises from the aromatization of 16α-hydroxy androgens [155,156].

The current favored working hypotheses are shown in some detail in Figure 2.18. Two involve an acetyl radical and one a steroid dioxetane intermediate, which are both considered viable entities.

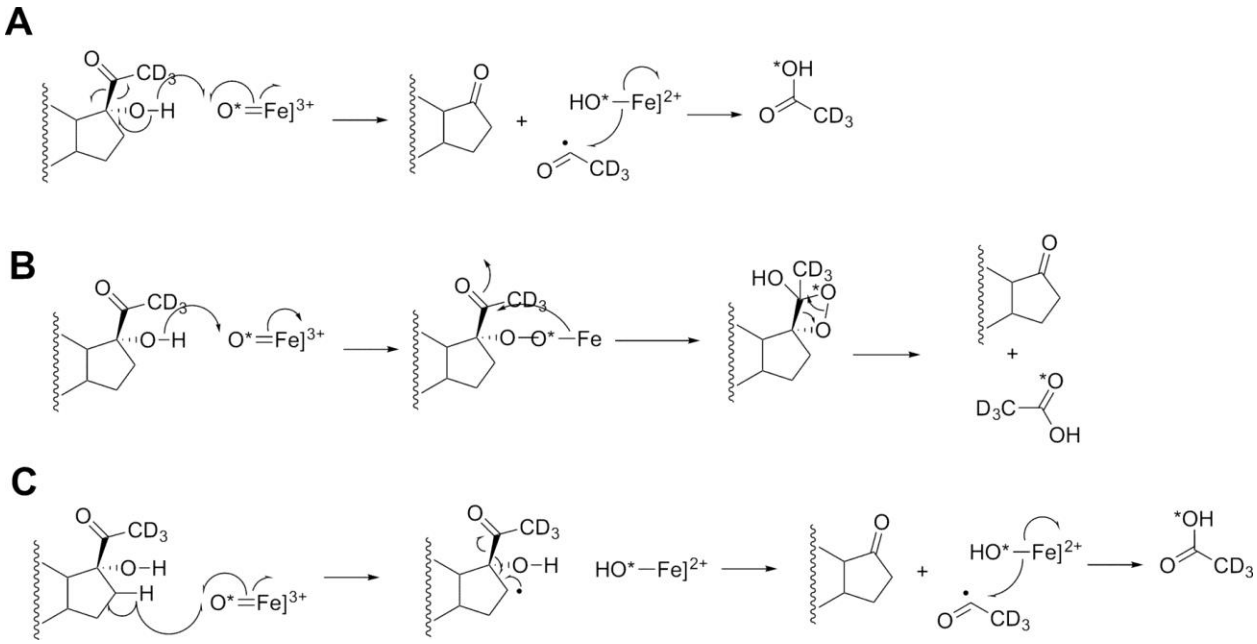

Figure 2.18 Mechanisms of P450 17A1-catalyzed 17,20-lyase reaction consistent with ^{18}O labeling [100], oxygen surrogate results, and solvent kinetic isotope results.

The course of an ^{18}O label (from $^{18}O_2$) is indicated with an *asterisk* [100,130]. *A*, compound I mechanism with hydrogen atom abstraction from the 17α alcohol followed by C17-C20 bond scission to yield an acetyl radical; *B*, addition of the 17*α*-hydroxyl group to compound I to yield an iron peroxide-C17 complex, followed by decomposition via a C17-C20 dioxetane; *C*, Compound I mechanism with hydrogen atom abstraction from the C16 carbon. See text for discussion and also Figure 2.2.

2.3.6 B Ring Hydroxylation of 16α,17α-Di(OH)prog by P450 17A1

Surprisingly the 6*β*-position was hydroxylated when 16*α*,17*α*-di(OH)prog was used as a substrate for P450 17A1 (Figure 2.14). This shift in regioselectively from the D-ring to the B-ring of the steroid by P450 17A1 was due to the presence of two hydroxyl groups on the 16*α*- and 17*α*-positions. Interestingly, regioselectivity was switched from the B-ring to the C–D-ring of the steroid in another P450 system when the Δ^4-double bond was reduced. P450 3A4 hydroxylates the 6*β*-position of testosterone (B-ring of the steroid); however, with 5*α*-dihydrotestosterone as the substrate, P450 3A4 oxygenated the 18*β*-methyl group (between the C–D-ring of the steroid) [29]. The causes for the switch in regioselectivities of the different P450 systems are probably not the same. Moreover, P450 17A1, which normally hydroxylates the *α*-face of (the D-ring of) its steroid substrates (Preg and Prog), introduced a hydroxyl group on the *β*-face of 16*α*,17*α*-di(OH)prog. The hydroxylation of the opposite face can be rationalized from overlaying 17*α*-OHprog and 16*α*,17*α*-di(OH)prog (Figure 2.19). When the C10, C14, and O16 atoms from 16*α*,17*α*-di(OH)prog were aligned with the C14, C10, and O3 atoms of 17*α*-OHprog, the O17 atom of 17*α*-OHprog was positioned 1.4 Å away from the C6 atom of 16*α*,17*α*-di(OH)prog, the site where the new oxygen atom is introduced. Additionally, the 17-oxygen of 17*α*-OHprog was directed at the *β*-face of 16*α*,17*α*-di(OH)prog. The 3-oxo group of 17*α*-OHprog has been shown to hydrogen bond to Asn-202 of P450 17A1 in the crystal structure [63]. Based on the observations with 6*β*-hydroxylation of 16*α*,17*α*-di(OH)prog by P450 17A1 and the overlay of the two different substrates, it is reasonable that the 16*α*-hydroxy group of 16*α*,17*α*-di(OH)prog hydrogen bonds to Asn-202 of P450 17A1, which in turn directs the 6*β*-hydrogen to the active iron center of the enzyme. Interestingly, the 17*α*,20-lyase product for the 16*α*,17*α*-di(OH)prog substrate (i.e. 16*α*-OHandro) was detected by LC-MS analysis and co-elution with the standard, but this lyase product seems to be a minor product in comparison with the 6*β*-hydroxylation product.

2.3.7 17,20-Lyase Reaction of 16α,17α-Di(OH)preg by P450 17A1

Conversely, when 16*α*,17*α*-di(OH)preg was used as the substrate for P450 17A1, the major product isolated from the incubation was 16*α*-OH-DHEA, which is formed from the 17,20-carbon–carbon bond cleavage.

2.3.8 Oxygen Incorporation into 16α,17α-Di(OH)preg by P450 17A1

An additional oxygenation product (M + 16 of substrate) was detected by LC-HRMS when 16*α*,17*α*-di(OH)preg was used as the substrate. However, there was not enough purified material recovered to determine the location of the oxygen on the steroid ring by ^{1}H NMR. A possible site of oxidation may be the C21-position. Alternatively, from the knowledge of 6*β*-hydroxylation reactivity of P450 17A1 with 16*α*,17*α*-di(OH)prog as the substrate, the oxygen may be incorporated in two other possible sites as follows: (i) the $\Delta^{5,6}$-double bond of the substrate to form the 5,6-epoxide or (ii) the C7-position may be hydroxylated. Epoxidation activity of P450 17A1 has been previously reported with a $\Delta^{16,17}$-steroid substrate [157]. Nevertheless, the shift in favoring C–C bond cleavage reactivity over hydroxylation when using the 3*β*-hydroxy-Δ^5 substrate (16*α*,17*α*-di(OH)preg) instead of the 3-keto-Δ^4 substrate (16*α*,17*α*-di(OH)prog) is similar to what occurs with Preg and Prog (i.e. 17,20-carbon-carbon bond cleavage versus 16*α*-hydroxylation). This observation may be related to the hydrogen bonding that occurs between the 3*β*-hydroxy group of the 3*β*-hydroxy-Δ^5 substrate and Asn-202 of the enzyme.

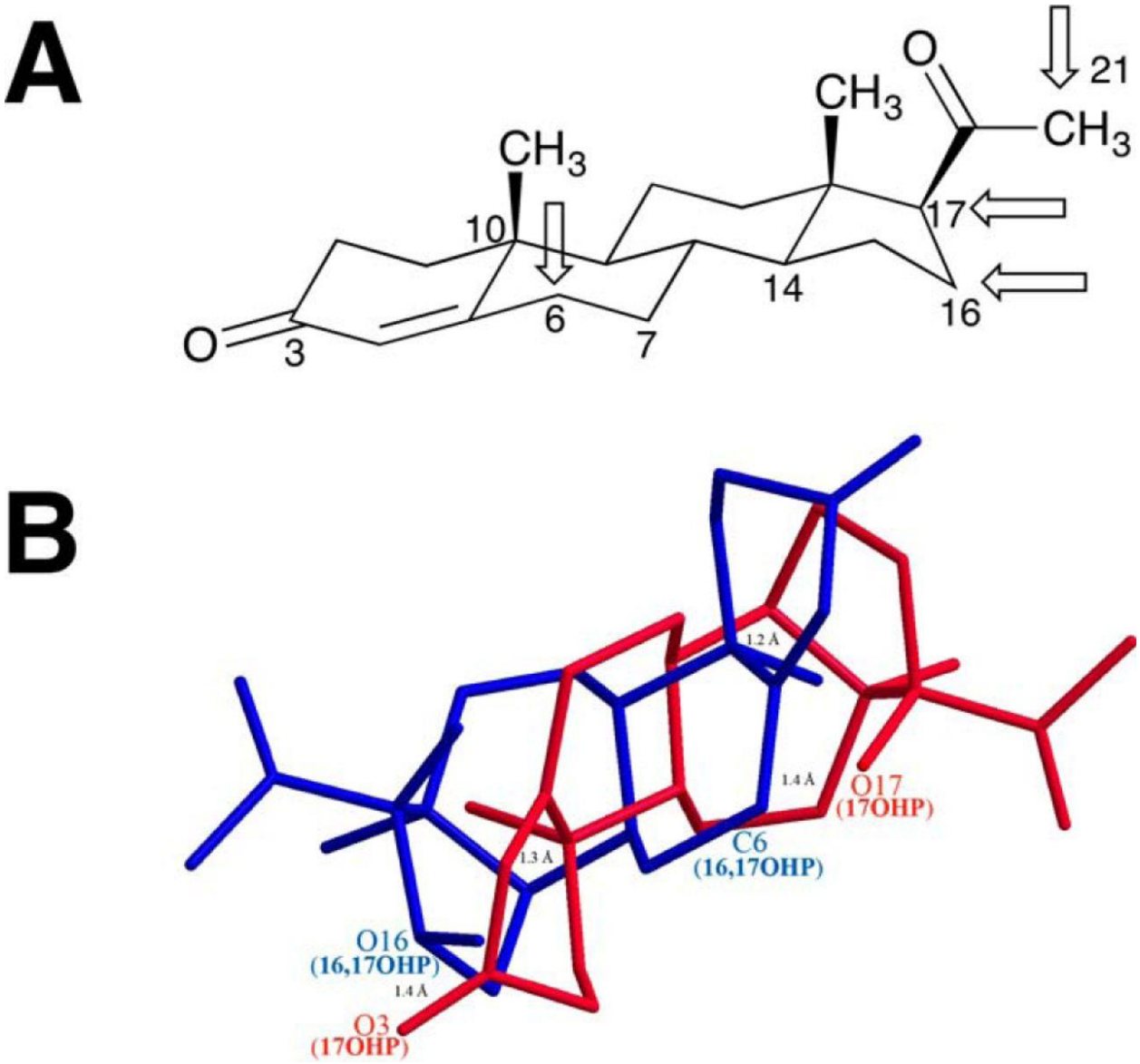

Figure 2.19 Sites of hydroxylation of Prog by P450 17A1.

A, chair configuration of Prog, with the four sites of attack indicated by *arrows. B*, wire diagram of 17*α*-OHprog (*17OHP*, *red*) and 16*α*,17*α*-di(OH)prog (*16,17OHP*, *blue*) overlaid, with the latter in an alternative configuration to show the proximity of the C-6 atom of 16*α*,17*α*-di(OH)prog with the 17-hydroxy group of 17*α*-OHprog. The model was made using Chem3D, with a minimum root mean square error of 0.1 and minimum root mean square gradient of 0.01. The C14, C10, and O3 atoms of 17*α*-OHprog were aligned with the C10, C14, and O16 atoms of 16*α*,17*α*-di(OH)prog, respectively, by displaying the distance measurements of each pair of atoms and then running an overlay minimization calculation. The *green lines* indicate the pair of atoms that were aligned (after overlay minimization, the distances between C14 of 17-OHP and C10 of 16,17-OHP; C10 of 17-OHP and C14 of 16,17-OHP; and O3 of 17-OHP and O17 of 16,17-OHP were 1.2, 1.3, and 1.4 Å, respectively, and are shown as *green lines*). The distance between the O17 atom of 17*α*-OHprog and C6 atom of 16*α*,17*α*-di(OH)prog was 1.4 Å.

2.3.9 Kinetic Solvent Isotope Effects Do Not Support a Ferric Peroxide Mechanism

One argument against the proposed acetyl radical mechanism (Figure 2.2 B) is a reported inverse kinetic solvent deuterium isotope effect (0.39) reported by Sligar and co-workers [113]. If the mechanism in Figure 2.2 B, C, or F, arrow b, were valid, the abstraction of a hydrogen atom from the 17-hydroxyl group (Figure 2.2 B) or the heterolytic cleavage of an O–H bond (Figure 2.2 D) might be expected to be a (partially) rate-limiting step, and an inhibitory effect of hydroxyl deuteration might be expected. In contrast, a similar study by Swinney and Mak [123] reported that (30%) D_2O attenuated androgen formation from Prog using microsomes from pig testes as the enzyme source ($k_H/k_D \sim 1.25$ at pH 7), suggesting that the 17,20-lyase reaction is dependent on Compound I formation either through the protonation of the distal oxygen of ferric peroxide (cf. P450 catalytic cycle) or deuterium atom abstraction from the 17-hydroxyl group of the substrate (Figure 2.2 B).

Because of the discrepancy, the results were reanalyzed in this system (Figure 2.15). Running the normal P450 17A1 reaction (with POR and b_5) in 95% D_2O showed no significant change in the rate of conversion of 17α-OHprog to Andro and a small but statistically significant change in the rate of oxidation of 17α-OHpreg to DHEA, with an apparent isotope effect of 0.83 (Figure 2.16), which is much less than the effect (0.39) reported by Gregory et al. [113]. Interpretation of solvent kinetic deuterium isotope effects is complex [158], in that protonation and deprotonation can occur throughout the amino acid side chains of an enzyme, not only on an iron-oxygen complex. The reason for the small inverse isotope effect with one lyase substrate but not another (Figures 2.15 and 2.16) is unclear. The opposite pattern between the solvent isotope effects for the 17α-OHpreg lyase and the 16-hydroxylation reactions is qualitatively consistent with the report of Gregory et al. [113]. One possibility is that the Δ^5 substrate (17α-OHpreg) 3-hydroxyl group exchanges with deuterium and that this has an effect on the juxtaposition of the substrate in the active site. The hydroxyl moiety has been shown by Scott and co-workers [62,63] to be in hydrogen bonding distance to Asn-202 of human P450 17A1. A substitution of

the 3-hydroxyl group by deuteration (i.e. −OD) could shift the substrate to favor the lyase reaction versus 16-hydroxylation. However, the lack of solvent isotope effects does not allow any definite conclusions about the rate-limiting nature of the abstraction of a proton or hydrogen atom from the 17-OH group, due to the multiple complex influences from solvent deuterium on enzyme function.

Although resonance Raman spectra of what is reported to be the human P450 17A1 FeO_2^-complex have recently been published [115,125], two caveats are as follows: (i) no b_5 (for which the 17,20-lyase reaction is very dependent, e.g. Figure 2.7 B) was present, and (ii) the observed complex was not tested for its catalytic competence, i.e. to form product(s). Even if the FeO_2^- complex did form the normal products (Andro and DHEA, plus the 16-hydroxylation products, which is unlikely) in these experiments, the simultaneous or subsequent intermediacy of an FeO^{3+} species as well could not be ruled out.

2.3.10 Conclusions

The ability of iodosylbenzene, but not H_2O_2, to support the lyase reaction provides what may be the strongest evidence in favor of a Compound I mechanism, in that iodosylbenzene cannot possibly form a peroxy intermediate. The apparent rate of the lyase reaction was similar to that of the NADPH-supported reaction (without b_5) in the case of the 17α-OHprog reaction and was somewhat less than that of the NADPH-supported reaction (without b_5) in the case of the 17α-OHpreg lyase reaction (Figures 2.7 and 2.8). Ideally, the Compound I form of P450 17A1 could be prepared using the approaches that Green and co-workers [21,124,150,159] have used with two bacterial P450s [150], and the reaction could be investigated directly. Nevertheless, in considering all of the literature in this field and that presented here in this article, the iodosylbenzene and H_2O_2 results (Figure 2.11) are difficult to dismiss, even if they are not physiological, and are interpreted as evidence for a Compound I reaction (Figure 2.18).

The multiple hydroxylations are probably catalyzed by FeO^{3+} intermediates, formed with P450 17A1-17α-hydroxy steroid complexes. It is possible that individual reactions (i.e. hydroxylation, lyase) proceed from different FeO complexes, although it is simpler to explain all as emanating from a single iron-oxygen intermediate. The myriad of reactions is depicted in Figure 2.20 and reveals a surprising flexibility in the P450 17A1 enzymes. As indicated, P450 17A1 has been shown to catalyze 21-hydroxylation of Prog [40]. The observed rates are indicated in the figure. Lyase reactions are not overly dominant. The biological activities of most of the products are, still unknown.

In summary, the investigation has produced evidence that a Compound I-type mechanism (Figure 2.18) can be involved in the 17,20-lyase reactions. The results do not rule out a ferric peroxide mechanism, nor do they define the fraction of the normal reaction that is catalyzed by each of the two mechanisms, if both are operative. If further research implicates Compound I in this reaction, then few strong cases for P450 ferric peroxide chemistry will remain, at least in the field of steroid metabolism [45,150,160].

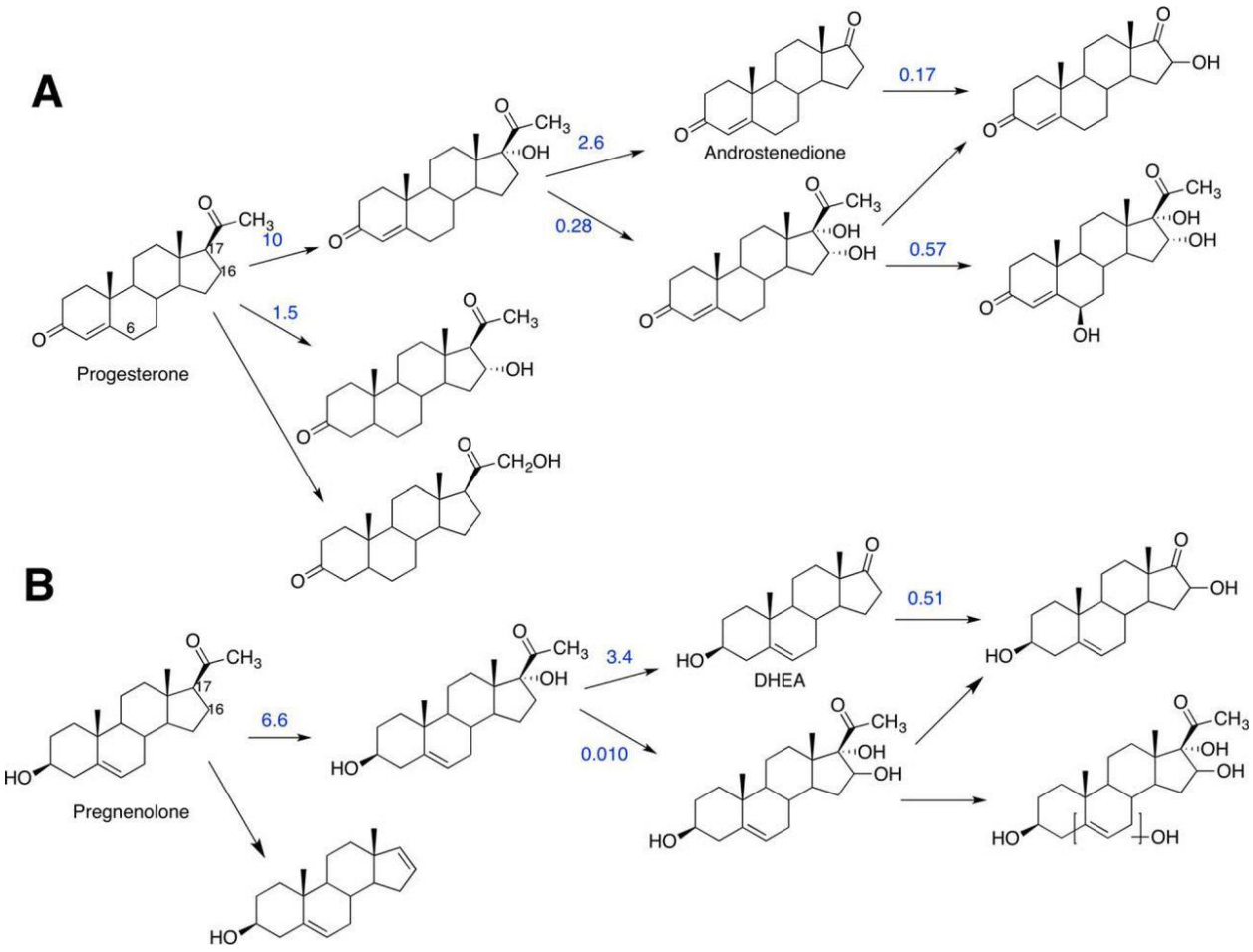

Figure 2.20 Summary of current known reactions of human P450 17A1.

See also Refs. 40,100,116. Rates determined at high substrate concentrations (approximating k_{cat} conditions) in this study are indicated, in units of nanomoles of product formed/min/nmol P450 17A1, when available. *A*, products formed from Prog; *B*, products formed from Preg.

2.4 Material and Methods

2.4.1 General

Bruker instruments (400 and 600 MHz) were used to acquire NMR spectra in the Vanderbilt facility. CD_3CN and $CDCl_3$ residual proton peaks were referenced to δ 1.94 and 7.26 ppm, respectively, and the $CDCl_3$ triplet in the carbon spectrum was referenced to δ 77.16 ppm and CD_3CN was referenced to 118.26 ppm [161]. Unless specified otherwise, all chemicals were purchased from Sigma-Aldrich. A modified version of the nitrosourea reagent was synthesized according to Ref. 45 using 2-(2-pyridyl)ethylamine (instead of 3-(3-pyridyl)propylamine) as the starting material, as described in detail here.

2.4.2 Reagents

17α-OH-[21,21,21-$^2H_3$]prog (96.5% atomic excess as judged by ^{1}H NMR, 97.9% atomic excess as judged by LC-MS) was synthesized and characterized as described previously [40]. 17α-OH-[21,21,21-$^2H_3$]preg (nominal 98.4% atomic excess) and 17α-OH-[2,2,4,6,6,21,21,21-$^2H_8$]prog (nominal 98.7% atomic excess) were purchased from C/D/N Isotopes (Pointe-Claire, Quebec, Canada). 16α,17α-Di(OH)prog (algestone) was purchased from Toronto Research Chemicals (Toronto, Ontario, Canada). 16α-OHAndro was obtained from Steraloids (Newport, RI). Chemical synthesis of (2-(pyridin-2-yl)ethyl)urea [45], 1-nitroso-1-(2-(pyridin-2-yl)ethyl)urea [45], 2-(pyridin-2-yl)ethyl acetate, and 16α,17α-di(OH)preg [157,162] was performed by Francis Yoshimoto as described[163]. Iodosylbenzene was freshly prepared by F. Peter Guengerich [163] per the protocol described in Ref. 164.

2.4.3 Enzymes

Recombinant human P450 3A4 with a C-terminal His_5 tag was expressed in *Escherichia coli* and purified as described previously [165,166]. *E. coli* recombinant rat POR and human liver b_5 were prepared as described by Hanna et al. [167] and Guengerich [168], respectively.

Recombinant human P450 17A1 (with a C-terminal His4 tag) was expressed in *E. coli* and purified by metal-affinity chromatography using a protocol adapted from those previously reported [62,95,169]. Briefly, an *E. coli* codon-optimized cDNA, corresponding to the amino acid sequence reported by DeVore and Scott [62], was purchased (Genewiz, South Plainfield, NJ) and inserted into the pCW-Ori(+) expression vector. The construct was used to transform competent *E. coli* JM109 cells (Agilent), and an isolated colony was used to inoculate 100 ml of Luria-Bertani medium (containing 100 μg/ml ampicillin), which was then incubated at 37 °C with shaking at 250 rpm overnight (12–14 h). Expression ensued by inoculating 1 liter of Terrific Broth medium, containing 100 mg/liter ampicillin and 250 μl/liter of trace elements [170], with 10 ml of the overnight culture and incubating at 37 °C (250 rpm) for ~4 h (OD_{600} ~0.32). The expression culture was then supplemented with 1 mm isopropyl *β-D*-1-thiogalactopyranoside and 1 mM *δ*-aminolevulinic acid, and the incubation conditions were changed to 30 °C and 200 rpm. After ~40 h, the culture was centrifuged at 5000 × g for 10 min, and the bacterial pellet was resuspended in 300 ml of 100 mM Tris-HCl buffer (pH 7.6) containing 500 mM sucrose and 0.5 mM EDTA and placed on ice. The suspension was then treated with 60 μl of a 50 mg/ml lysozyme solution/g of bacterial pellet and incubated on ice for 30 min, with gentle mixing every 10 min. All subsequent steps were conducted on ice or at 4 °C. Next, a spheroplast pellet was obtained by centrifugation at 5000 × g for 10 min and resuspended in 25 ml of 300 mM potassium phosphate buffer (pH 7.4; KPhos) containing 20% glycerol (v/v), 6 mM $Mg(CH_3CO_2)_2$, 0.1 mM dithiothreitol (DTT), 0.1 mM phenylmethylsulfonyl fluoride, and a protease inhibitor mixture (cOmpleteTM, EDTA-free, Roche Applied Science). The spheroplasts were lysed by sonication, and debris and unbroken cells were removed by centrifugation at 9000 × g for 20 min. The cytosol was cleared of the membrane fraction by centrifugation at 100,000 × g for 60 min and was supplemented with 300 mM NaCl and 20 mM imidazole prior to loading onto a nickel-nitrilotriacetic acid (NTA) resin (Qiagen) bed that had been equilibrated with 300 mm KPhos (pH 7.4) containing 300 mM NaCl, 20% glycerol (v/v), 20 mM imidazole,

and 0.1 mM DTT. The bound protein was washed with 10 bed volumes of the same buffer and eluted with the same buffer containing 250 mM imidazole. The purified enzyme was then dialyzed four times against 100-fold volumes of 200 mM KPhos (pH 7.4) containing 20% glycerol (v/v), 0.1 mM EDTA, and 0.1 mM DTT and stored at −70 °C until use.

2.4.4 Assays

2.4.4.1 $^{18}O_2$ Incubations

The standard reconstituted P450 17A1 system contained P450 17A1 (8.4 μM), POR (13 μM), b_5 (14 μM), 130 μM 17α-OH-[21,21,21-$^2H_3$]pre or 100 μM 17α-OH-[2,2,4,6,6,21,21,21-$^2H_8$]prog, and L-α-1,2-dilauroyl-*sn*-glycero-3-phosphocholine (80 μM; DLPC) in 2.2-ml incubation mixtures containing 50 mM KPhos (pH 7.4). Reaction mixtures were placed in Thunberg tubes, and air was removed on a gas train equipped with a manifold [171,172] (three exchanges of argon/vacuum, 5 min each cycle). After introduction of $^{18}O_2$ (Sigma-Aldrich, 99% atomic excess, pressurized cylinder) into a Thunberg tube under vacuum, each reaction was initiated by adding an NADPH-generating system (10 mM glucose 6-phosphate, 0.5 mM $NADP^+$, and 2 μg/ml yeast glucose-6-phosphate dehydrogenase (91); 8% of total reaction volume) tipped from the stopper reservoir, with mixing. Incubations were conducted in a water bath at 37 °C for 30 min for 17α-OH-[21,21,21-$^2H_3$]preg substrate or 60 min for 17α-OH-[2,2,4,6,6,21,21,21-$^2H_8$]prog substrate with shaking at 100 rpm.

The reactions were quenched with CH_2Cl_2 (5 ml), and 500 μl of 3 M HCl (chilled to 0 °C) for the 17α-OH-[21,21,21-$^2H_3$]preg substrate or 1 ml of 3 M HCl (chilled to 0 °C) for the 17α-OH-[2,2,4,6,6,21,21,21-$^2H_8$]prog substrate was added to decrease the pH to ∼1 and facilitate extraction of acetic acid into the organic layer. For cases with 17α-OH-[2,2,4,6,6,21,21,21-$^2H_8$]prog as the substrate, the mixture (after addition of HCl) was mixed with a vortex device and centrifuged at 1500 × g for 1 min to remove the emulsion. Before the reaction of the product acetic acid with the diazo reagent, the

organic extracts were collected, and residual water was removed using anhydrous $MgSO_4$ (~50 mg for each extraction).

2.4.4.2 Derivatization of Acetic Acid

Diazoethylpyridine was prepared *ex tempore* from 1-nitroso-1-(2-(pyridin-2-yl)ethyl)urea (5 mg) in diethyl ether (2 ml), after treatment with KOH (1 ml of a 30% (w/v) solution in H_2O) (33). The organic layer (containing the diazo reagent) was dried with anhydrous $MgSO_4$ (~50 mg), filtered with a cotton-plugged Pasteur pipette, and reacted with an organic extract of each P450 17A1-steroid-$^{18}O_2$ incubation. The solvent was evaporated under a stream of nitrogen, and residues were dissolved in CH_3CN (70 μl).

2.4.4.3 LC-MS Analysis

LC-MS analysis of deuterium-labeled 2-(pyridin-2-yl)ethyl acetate from $^{18}O_2$ incubations was performed using an Acquity UPLC system connected to a Thermo LTQ XL Orbitrap mass spectrometer operating in the electrospray ionization (ESI) positive ion mode. A Phenomenex Kinetex® 2.6-μm C8 100 Å, LC column (100 mm × 2.1 mm) was used for separation of the acetic acid derivative at a flow rate of 0.3 ml/min with the following gradient: 0–1.0 min, 100% A (v/v); 4.0–5.2 min, 100% B (v/v); 5.3–8.0 min, 100% A (v/v); mobile phase A was 10 mM NH_4HCO_2 in H_2O (v/v); and mobile phase B was 10 mM NH_4HCO_2 in 95:5 CH_3CN/H_2O (v/v).

For the $^{18}O_2$ incubation assays, the LTQ mass spectrometer was tuned in the electrospray ionization positive mode using synthetic 2-(pyridin-2-yl)ethyl acetate (see above). The tune settings were as follows: sheath gas flow rate, 15 (arbitrary units); auxiliary gas flow rate, 5 (arbitrary units); sweep gas flow rate, 0 (arbitrary units); spray voltage, 4 kV; capillary temperature, 300 °C; capillary voltage, 16 V; tube lens, 30 V.

The LTQ Orbitrap XL high resolution mass spectrometer was calibrated with the ESI-positive ion calibration solution by direct infusion (10 μl/min with a 500-μl Hamilton syringe) as done previously [45]. The mass spectrometer was first tuned to the standard solution with *m/z* 524.3

(methionine/arginine/phenylalanine/alanine acetate), and the tube lens voltage was set to 145 V to fragment caffeine (*m/z* 195 to 138).

2.4.4.4 17α-Hydroxysteroid Reactions with Oxygen Surrogates

The standard reconstituted system used for comparison included P450 17A1 (0.5 μM for iodosylbenzene, 0.1 μM for H_2O_2), POR (2.0 μM), b_5 (0.5 μM), and DLPC (10 μM) in 0.5-ml incubation mixtures containing 50 mM KPhos (pH 7.4) and the NADPH-generating system. Assays were done as in the case of the ^{18}O-labeling work (see above) except that the incubations were aerobic, as described previously [127], using 10 μM 17α-OHprog or 17α-OHpreg with P450 17A1 (0.5 μM) and no POR, in the absence or presence of b_5 (0.5 μM). H_2O_2 (to 10 mM) or iodosylbenzene (to 2 mM) was added at varying concentrations (from aqueous stocks). The incubations were done for 5 min with H_2O_2 and for 30 s with iodosylbenzene (41, 92), with extraction into CH_2Cl_2 and analysis of the conversion of 17α-OHprog to Andro and of 17α-OHpreg to DHEA by UPLC. The Δ^5 steroids were converted to Δ^4 steroids by treatment with cholesterol oxidase prior to LC-UV analysis [127]. Iodosylbenzene reactions were conducted for a short time period because the reagent is very destructive to P450 heme [131].

Product analysis was done on a Waters Acquity UPLC system with a Waters Acquity UPLC Ethylene Bridged Hybrid (BEH) octadecylsilane (C_{18}) column (2.1 mm × 100 mm, 1.7 μm). LC conditions were as follows: solvent A consisted of 70% CH_3OH and 30% H_2O (v/v), and solvent B was 100% CH_3CN. The products were resolved by a 0.2 ml min^{-1} gradient with the following steps: 0–1 min, hold at 5% B (v/v), 1–4 min, linear gradient from 5 to 30% B (v/v); 4–4.5 min, linear gradient from 30 to 40% B (v/v); 4.5–4.55 min, 40 to 95% B (v/v); 4.55–6.75 min, hold at 95% B (v/v); 6.75–7 min, 95 to 5% B (v/v); and 7–10 min, hold at 95% B (v/v). The column temperature was maintained at 40 °C, and the Δ^4 steroids were quantified by their absorbance at 243 nm.

2.4.4.5 LC-UV-MS Analysis of New Steroid Products

An LTQ Orbitrap XL mass spectrometer was tuned in the atmospheric pressure chemical ionization-positive mode with commercially available steroid solutions in a 1:1 mixture (v/v) of H_2O and CH_3CN (16α-OHandro and 16α,17α-di(OH)prog). The tune settings were as follows: vaporizer temperature, 350 °C; sheath gas flow rate, 50 (arbitrary units); auxiliary gas flow rate, 5 (arbitrary units); sweep gas flow rate, 0 (arbitrary units); discharge current, 10 μA; capillary temperature, 275 °C; capillary voltage, 10 V; tube lens, 25 V. The same LC method used for UV analysis (see above) was employed for the Δ^4 steroid products. The LC conditions for the Δ^5 steroids were as follows: solvent A consisted of 95% H_2O and 5% CH_3OH (v/v), and solvent B was 95% CH_3OH and 5% H_2O (v/v). The gradient steps were as follows: 0–1.5 min, hold at 60% B (v/v); 1.5–7.5 min, linear gradient from 60 to 85% B (v/v); 7.5–7.75 min, hold at 85% B (v/v); 7.75–8.25 min, 85 to 60% B (v/v); and 8.25–10 min, hold at 60% B (v/v). The column was kept at ambient temperature.

2.4.4.6 Solvent Kinetic Isotope Effect Assays

These assays were also done as in the case of the oxygen surrogate experiments (see above), with the incubations done aerobically as described previously [127], using 30 μM 17α-OHprog or 17α-OHpreg with P450 17A1 (0.5 μM)/b_5 (0.5 μM), POR (2 μM), and DLPC (10 μM) in 0.5 ml incubation mixtures containing 50 mM KPhos (pH 7.4), with 1 mM NADPH. In the D_2O experiments, the content of D_2O was 95% (v/v), with the pD adjusted (pH = pD + 0.4) (75, 93). Incubations were for 60 s at 37 °C, and the products were analyzed as for the oxygen surrogate experiments (see above).

2.4.5 Isolation of 6β,16α,17α-Tri(OH)prog as a Product

A 20-ml reaction mixture consisting of the same components described in the oxygen surrogate experiments (see above), using 280 units/ml of catalase and 40 μM 16α,17α-di(OH)prog, was run overnight (~20 h). The product was extracted from the aqueous mixture with 200 ml of CH_2Cl_2, and the solvent was evaporated. The dried product was purified using the same system outlined for the 16,17-

di(OH)preg purification (see above) using an isocratic HPLC method (63.5% CH_3OH) and peak detection at 243 nm.

2.4.6 Isolation of 16α-OH-DHEA as a Product

The same procedure described for the isolation of the 6*β*,16*α*,17*α*-tri(OH)prog product (see above) was used, with the following exceptions. The enzyme concentrations were increased to 1 μM P450 17A1, 4 μM POR, 1 μM b_5, and 3700 units/ml catalase, with 50 μM 16*α*,17*α*-di(OH)preg and the NADPH-generating system. The incubation was run for 4 h. Purification was conducted using the same procedure detailed in the LC-UV purification of 16*α*,17*α*-di(OH)prog (see above), except that the wavelength used to detect the Δ^5 product was 215 nm.

Chapter 3

3. The Kinetic Model

3.1 Introduction

Human steroid biosynthesis is comprised of a series of redox reactions on the sterol nucleus, the majority of which are catalyzed by P450 enzymes [32,173]. Interestingly, several of the steroid-oxidizing P450s catalyze multistep reactions, some of which are carbon-carbon bond cleavage reactions [22,32,45,121]. Early in the steroid synthesis pathway, 17α-hydroxylation of the 21-carbon steroids Preg and Prog produces essential precursors, 17-OHpreg and 17-OHprog, that lead to cortisol production. Alternatively, the 17α-hydroxy steroids are also converted to 19-carbon androgens, DHEA and Andro, through a subsequent desmolase reaction (17,20-lyase) in which the C17-C20 bond is broken. The two functions are catalyzed by human P450 17A1, which is primarily expressed in the adrenal gland and gonads [173], the tissues where glucocorticoids and androgen-derived sex hormones are produced, respectively.

The divergence of the pathways of steroid production at the sites of P450 17A1 expression has been attributed to the presence of b_5 in these tissues [173]. *In vitro* studies with b_5 have shown that that it stimulates the catalytic activities of human P450 17A1, predominantly the 17,20-lyase versus 17α-hydroxylation reaction [53,174]. In some reactions with other P450 enzymes, b_5 participates in electron transfer, but this role was dismissed for the stimulation of P450 17A1 based on the observation that apo-b_5, a form devoid of the heme cofactor, retained the desmolase stimulation activity [57]. Akhtar and associates proposed that b_5 stabilizes an enzyme-substrate conformation in which the ferric peroxide (FeO_2^-) form of P450 17A1 mediates the cleavage reaction [174]. The theory was supported by the b_5 selectivity to enhance primarily the 17,20-lyase reaction, whereas P450 hydroxylation reactions typically follow Compound I (FeO^{3+}) chemistry. However, the results presented in Chapter 2 suggest that the P450 17A1 iron-oxygen species in the desmolase reaction is Compound I, although contribution from the

ferric peroxide has not been ruled out, and the b_5 effect was observed when the corresponding oxygen surrogate, iodosylbenzene, was used. b_5 is currently considered as an allosteric activator of the P450 17A1 17,20-lyase activity, although the exact mechanism of action remains unclear.

Androgen deprivation is the standard form of therapy for advanced prostate cancer patients, many of which undergo surgical orchiectomy to eliminate the primary androgen producing tissue. The procedure yields an initial positive response, but the majority of patients progress to develop castration-resistant prostate cancer (CRPC). While androgen receptor mutations are known factors that contribute to some of the cases of cancer resurgence, the adrenal gland and tumors have been identified as alternative androgen sources that potentiate the disease [68,72,175]. Therefore, inhibition of human P450 17A1 has become a therapeutic goal for prostate cancer, leading to FDA approval of abiraterone as a treatment for CRPC. Abiraterone is a steroid-based P450 17A1 inhibitor that blocks both the 17α-hydroxylation and 17,20-lyase reactions, which is problematic in that it diminishes both androgen and glucocorticoid levels. Orteronel (TAK-700) is another small molecule inhibitor that is selective for the desmolase reaction, but in the clinic, the compound generated adverse effects stemming from cortisol deficiency and development was stopped after failing to exhibit improved efficacy [83].

One issue with reaction-selective inhibition of human P450 17A1 is the processivity of the two reactions. Enzymes that catalyze multistep reactions are characterized as processive when the intermediate product remains enzyme bound in the transition from the first reaction to the second, whereas with a distributive enzyme the intermediate product dissociates and must rebind prior to further reaction. Therefore, reaction-selective inhibition of human P450 17A1 by a competitive inhibitor can only be possible if the catalytic mechanism is distributive. Bovine and zebrafish P450 17A1 have been characterized as distributive, while the guinea pig enzyme was described as processive [90,91,127].

The processivity of human P450 17A1 is the primary focus of this chapter, which was evaluated by kinetic analysis of the recombinant enzyme. Steady-state and pre-steady-state methods were

employed in binding and catalytic assays to measure the kinetic parameters that would differentiate between a processive and a distributive mechanism. Furthermore, b_5 was incorporated in the analyses to test the hypothesis that it stimulates the 17,20-lyase activity by promoting a more processive mechanism. Inhibition studies with TAK-700 enantiomers were conducted to investigate the level of potency required to selectively inhibit the desmolase reaction. Finally, the results from the kinetic analyses were used to develop a minimal kinetic model for human P450 17A1 catalysis of the two reactions.

3.2 Results

3.2.1 Substrate and Product Binding

Initial binding studies indicated that human P450 17A1 bound all the major substrates and products with very high affinity. Dissociation constants (K_d) <0.5 μM were obtained in assays involving sequential, incremental ligand titrations of dilute enzyme in a 10-cm cell (data not shown). However, the validity of these results was questionable due to the subsequent observation of protein instability over long time periods, in that the individual experiments surpassed 60 minutes in length. Alternatively, ligand binding was assessed using fresh enzyme solutions for each steroid concentration. All of the substrates and products evaluated generated the typical Type I difference spectrum. Plots of maximum absorbance difference versus ligand concentrations, fit with a quadratic formula, are shown in Figure 3.1. Human P450 17A1 bound the Δ^5 (pregnenolone series) steroids with higher affinity than the Δ^4 (progesterone) counterparts (Table 3-1). The binding affinity was the highest for the hydroxylase substrates and less for the respective 17-hydroxy steroids, but the differences are not drastic. The enzyme exhibited two-fold greater affinity for 17-OHpreg (K_d 0.52 μM) versus 17-OHprog (K_d 0.95 μM). The desmolase products had the least affinity, and although the K_d for Andro is not reliable (out of range), the apparent lack of enzyme saturation at 10 μM shows that the affinity is considerably lower for this steroid (Figure 3.1 F).

3.2.2 Steady-State Kinetics of Human P450 17A1 Activity

One of the conundrums with b_5 modulation of human P450 17A1 catalytic activity is the distinction between the 17,20-lyase reaction and the 17α-hydroxylation. In these analyses, the steady-state kinetic parameters obtained, using a reconstituted enzyme system, indicate that the b_5 effect on catalytic efficiency is not limited to a single reaction (see Figure 3.2 and Table 3-2). The Michaelis-Menten constants (K_m) for Prog and 17α-OHprog reactions were higher than those for Preg and 17α-OHpreg. The K_m values increased approximately two-fold when b_5 was included, whereas the value for 16α-hydroxylation of Prog increased nearly five-fold. The K_m for 17α-hydroxylation of Prog was the only value that decreased in the presence of b_5. The exact meaning of K_m in these reactions is not clear. The b_5 effect was far more apparent in the k_{cat} parameters, increasing the values by as much as 60-fold for the 17,20-lyase reaction with 17α-OHprog. The differences culminated in enhanced catalytic efficiencies for the 17α-hydroxylation reactions, in addition to the expected 17,20-lyase reactions, with both steroid series, but not for Prog 16α-hydroxylation. Notably, the addition of b_5 to the incubations with Preg resulted in significant catalysis of the 17,20-lyase reaction, even though substrate turnover was maintained below 20%, which was not observed in Prog assays.

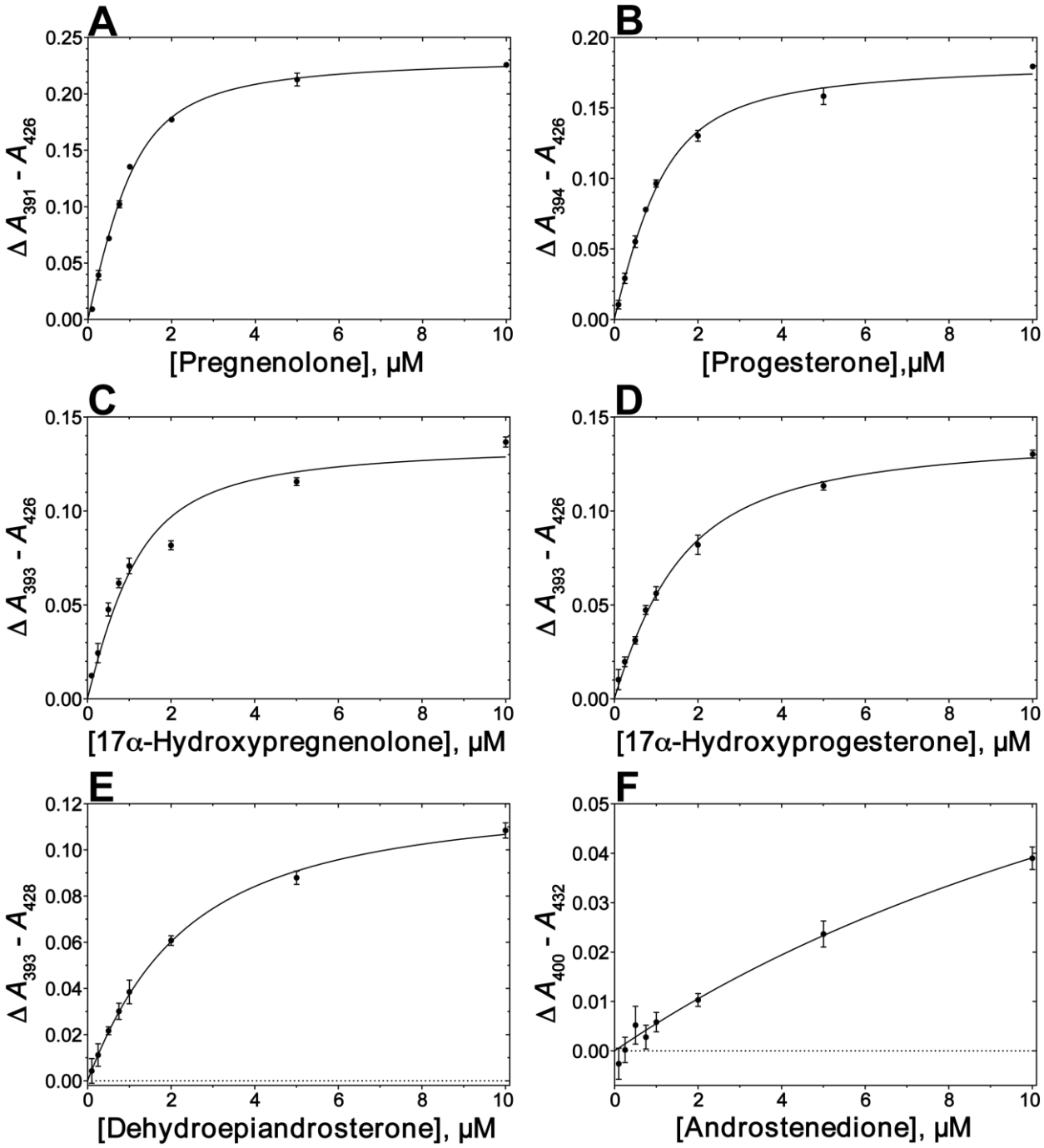

Figure 3.1 Substrate and product binding of human P450 17A1

Production of the Type I spectrum (low-spin to high-spin iron) was monitored from 0.1 to 10 μM ligand concentration. The observed spectral change was fit to a uni-molecular binding model (with quadratic equation, see Section 3.4.5.1). Each data point corresponds to the mean and standard deviation of three replicate shots. See Table 3-1 for estimated K_d values.

Table 3-1 K_d values for P450 17A1 with substrates and products

	K_d, μM
Preg	0.37 ± 0.03
17α-OHpreg	0.52 ± 0.10
DHEA	1.7 ± 0.2
Prog	0.47 ± 0.04
17α-OHprog	0.95 ± 0.08
Andro	19 ± 9

± indicates the standard error of the K_d from analysis of 3 replicates per ligand concentration.

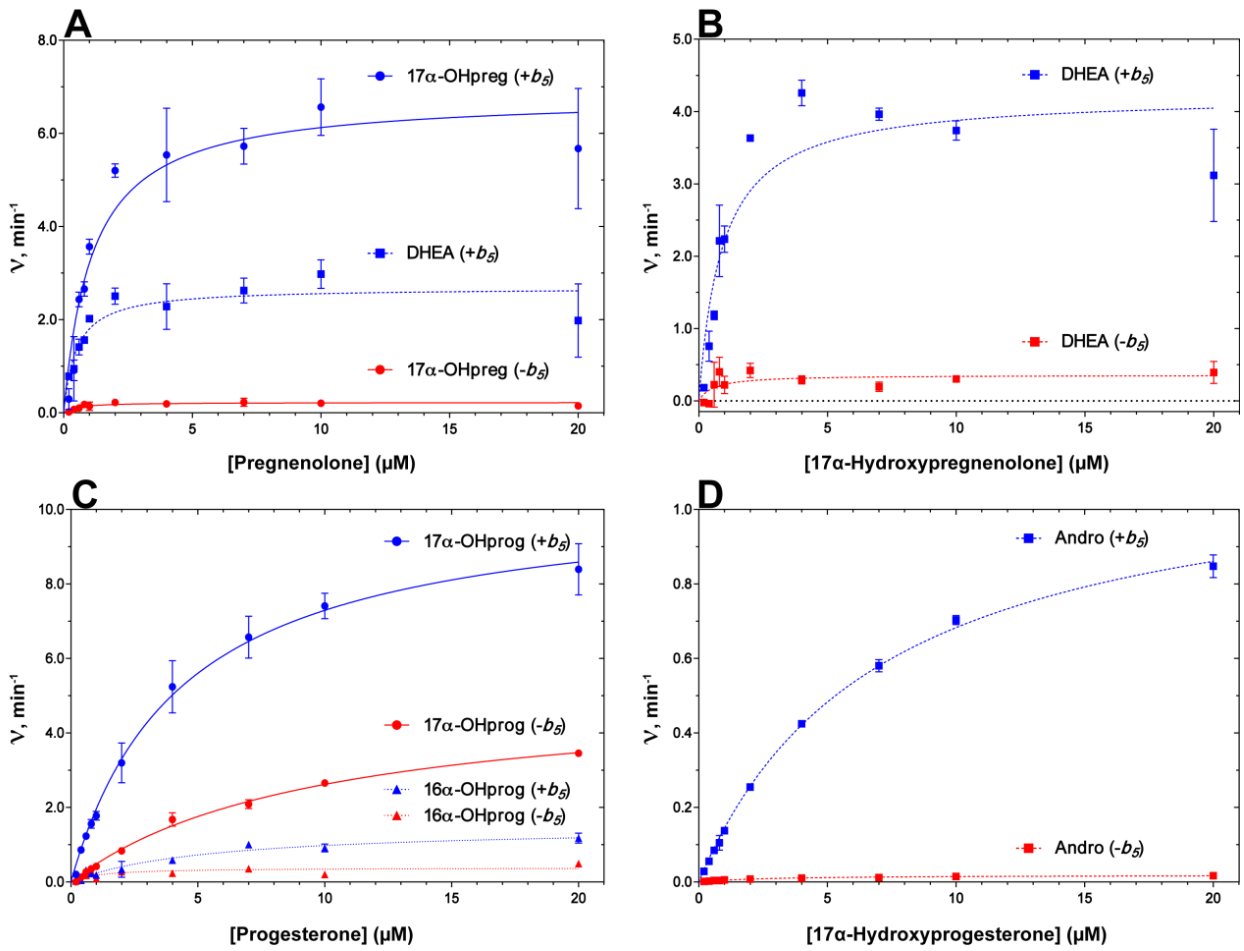

Figure 3.2 Steady-state kinetics of the primary reactions catalyzed by human P450 17A1

Hyperbolic fitting of the product formation rate at from 0.2 to 20 μM substrate concentration. Each data point corresponds to an average rate from two replicate incubation samples and the error bars denote the standard deviation. See Section 3.4.4.1 for experimental details and Table 3-2 for estimated K_m and k_{cat} parameters.

Table 3-2 Steady-state parameters for human P450 17A1 reactions

		k_{cat}, s^{-1}		K_m, μM		k_{cat}/K_m, $\mu M^{-1} s^{-1}$		
Substrate	Reaction	$-b_5$	$+b_5$	$-b_5$	$+b_5$	$-b_5$	$+b_5$	$+/-b_5$ ratio
Preg	*17α-hydroxylation*	**0.0037** (0.0005)	**0.11** (0.01)	**0.5** (0.3)	**1.1** (0.2)	**0.0074** (0.0044)	**0.10** (0.02)	**14**
	Lyase		**0.045** (0.003)		**0.49** (0.14)		**0.092** (0.027)	
17α-OHpreg	*Lyase*	**0.0059** (0.0012)	**0.071** (0.005)	**0.57** (0.46)	**0.91** (0.24)	**0.010** (0.009)	**0.078** (0.021)	**8**
Prog	*17α-hydroxylation*	**0.086** (0.004)	**0.17** (0.01)	**9.7** (0.8)	**4.3** (0.4)	**0.0089** (0.0009)	**0.040** (0.004)	**4**
	16α-hydroxylation	**0.0064** (0.0009)	**0.025** (0.003)	**1.1** (0.6)	**5.3** (1.3)	**0.0058** (0.0030)	**0.0047** (0.0012)	**0.8**
17α-OHprog	*Lyase*	**0.00031** (0.00001)	**0.019** (0.000)	**2.9** (0.3)	**7.1** (0.3)	**0.00011** (0.00001)	**0.0027** (0.0001)	**25**

The values in parenthesis correspond to the standard error of the K_m and k_{cat} from analysis of two replicate incubation samples per substrate concentration.

3.2.3 Pre-Steady-State Experiments

The b_5 stimulatory effect was evident in the steady-state catalysis of all the major human P450 17A1 reactions, but steady-state analyses are insufficient to clarify how the protein expedites the reaction cycle. In order to elucidate the mechanism of action, pre-steady-state studies were used to isolate individual steps in the reaction cycle.

3.2.3.1 Estimating k_{off} Rates

Enzyme-inhibitor trapping assays were employed to evaluate the human P450 17A1 substrate and product dissociation rates, in the presence and absence of b_5. The technique applied exploits the differing spectral changes that occur from perturbations to the heme moiety of the enzyme. The natural steroid ligands generate a Type I difference spectrum, corresponding to a blue shift in the Soret band, which is produced without interaction with the heme and simple displacement of a heme-coordinated water molecule. Conversely, the drug TAK-700 (Orteronel) generates a Type II difference spectrum (blue shift of the Soret band), which is typical of azole-containing P450 inhibitors coordinating nitrogen atoms directly with the heme iron. The k_{off} rate can then be estimated from the spectral conversion of an enzyme-substrate complex to enzyme-inhibitor, with the requirement that substrate does not rebind and inhibitor binding is much faster than steroid dissociation. Accordingly, TAK-700 binding was measured at 6.2 ± 0.5 s^{-1} under the experimental conditions, determined by SVD analysis of the spectral change using a two species model composed of 1) free enzyme and 2) enzyme-inhibitor complex (Figure 3.3 A-E). The same analysis method was used to estimate the steroid k_{off} rates, in experiments starting with P450 17A1-steroid complexes (example of 17α-OHpreg in Figure 3.3 F-J). The results indicate that b_5 does not affect the dissociation rates of the 17,20-lyase substrates (17α-OHpreg and 17α-OHprog), because the parameters changed very little when b_5 was included (Table 3-3).

3.2.3.2 Single-Turnover Kinetics

The b_5 effect on individual chemistry steps was studied using single-turnover catalytic assays. The method relies on the ability to stop the reaction at very short time periods, thereby resolving the time frame for an initial chemical reaction from that of a subsequent step (i.e. intermediate product release and rebinding and/or further chemistry). Furthermore, the incubations are followed to complete conversion of the initial substrate to the final products. These studies illustrated the significant effect b_5 mediates on the ability of human P450 17A1 to catalyze the reactions (Figure 3.4). The rate of Preg turnover was increased by ~ 60% when b_5 was included, while the conversion of Prog remained the same in both conditions (Table 3-4). As expected, b_5 greatly enhanced the oxidation of the 17α-hydroxy steroids, augmenting the conversion rates of 17α-OHpreg and 17α-OHprog by 10- and 4-fold, respectively (Table 3-4). Notably, incubations starting with either Preg or Prog showed a clear lag in production of the corresponding 17,20-lyase product, supporting a distributive mechanism for catalysis of the two reactions. These pre-steady-state catalytic studies also yielded a time course that includes the production of the recently identified human P450 17A1 products (see Chapter 2).

3.2.4 Pulse-Chase Experiments

In contrast to defining enzyme processivity by comparing parameters estimated in separate experiments, pulse-chase studies offer a simple approach to directly probe the dissociation of an intermediate product from the enzyme. These experiments begin with a pulse of labeled starting substrate, and after a given amount of time the reactions are “chased” with an excess of a non-labeled intermediate substrate. The production of labeled 17,20-lyase products is then indicative of the enzyme processivity. A distributive enzyme would hence yield less labeled desmolase products, considering that the released labeled intermediate is unable to rebind in the presence of excess chase substrate. Conversely, the production of labelled 17,20-lyase products by a processive enzyme would be unaffected by the chase, because the intermediate remains in the enzyme between the two reactions.

In light of the weak capacity of human P450 17A1 to catalyze the 17,20-lyase reaction in the absence of b_5, as shown in the catalytic studies discussed above, b_5 was included in all the pulse-chase studies. Furthermore, these analyses were focused on Preg turnover, given that 17,20-lyase catalysis is more prominent in that substrate class. Pulse-chase studies were conducted at steady-state and pre-steady-state conditions, where the conversion of ^{3}H-Preg to ^{3}H-DHEA was followed after the addition of unlabeled 17-OHpreg. At steady-state conditions the reaction pulse length was 1 min, followed by a 10 min chase period. A range of 17α-OHpreg concentrations were used (5 – 75 μM), which all caused some degree of decreased DHEA synthesis. The yield was decreased by only 9% at the lowest 17α-OHpreg concentration used, while the chase with 15-fold higher concentration, 75 μM, attenuated the reaction to 43% of activity observed in the control incubation (Figure 3.5 A). It is possible to interpret these results as evidence for a distributive mechanism. However, the pulse-chase assay under steady-state conditions does not distinguish whether the reduced production of ^{3}H-DHEA is caused by chase-mediated blockade of binding the initial ^{3}H-Preg substrate or rebinding the ^{3}H-17α-OHpreg which was dissociated (in a distributive mechanism). To this end, pulse-chase assays were carried out under single-turnover (rapid-quench) conditions, which allow the introduction of the chase steroid prior to the completion of the initial reaction cycle. The results are therefore more straightforward than those from steady-conditions, considering that only the rebinding of ^{3}H-17α-OHpreg is obstructed and any ^{3}H-DHEA generated must derive from an intermediate that did not dissociate from the substrate pocket. Initial experiments revealed that 17,20-lyase catalysis was unencumbered with a pulse length as short as 0.5 s (data not shown). These results contradicted the conclusion of a distributive mechanism, which was founded on the observation of an approximately 1 s lag phase in the single turnover experiments (Figure 3.4 A). Further investigation indicates that the majority of human P450 17A1 in these incubations (that include b_5) commits to catalyzing the 17,20-lyase reaction when ^{3}H-Preg is bound, based on the observation that ^{3}H-DHEA production continued even when the chase is added early in the lag phase

(0.05 s, Figure 3.5 B). In combination with the failure to segregate the 17α-hydroxylation and 17,20-lyase reactions at steady state conditions, the single-turnover pulse-chase results favor a relatively processive mechanism for the human P450 17A1-b_5 complex.

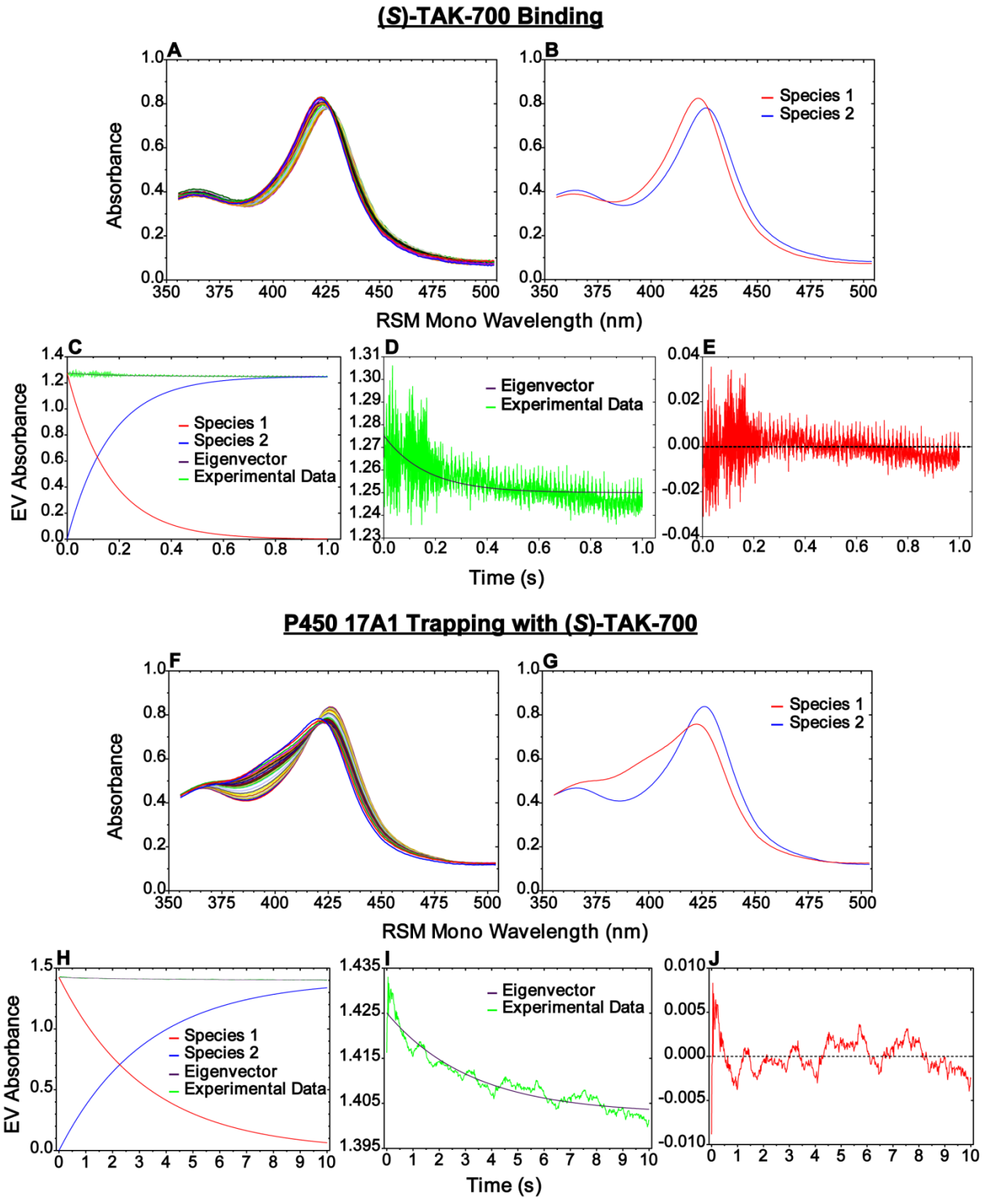

Figure 3.3 Estimating k_{off} parameters with enzyme inhibitor trapping

Example singular value decomposition (SVD) analyses of individual stopped-flow absorbance measurements of mixing 10 μM(S)-TAK-700 with 2 μM human P450 17A1, A-E, or a 2 μM human P450 17A1-17α-OHpreg complex, F-J (final concentration, see Section 3.4.5.2 for details). A sequential two-species model was applied in the SVD analyses, which generated a rate and corresponding standard deviation of the fit. A,F-absolute absorbance, B,G-SVD eigenvector spectra for species 1 and species 2, C,H-SVD eigenvector kinetics of species 1, species 2, the total calculated eigenvector contribution, and the experimental data, D,I-zoomed panel of the total calculated eigenvector contribution and experimental data, E,J-residuals plot (difference between total calculated eigenvector and experimental data)

Table 3-3 k_{off} rates estimated by singular value decomposition (SVD) analysis

	k_{off} (s^{-1})					
	$-b_5$			$+b_5$		
Preg	0.23	±	0.02	0.29	±	0.03
17α-OHpreg	0.32	±	0.02	0.41	±	0.03
DHEA	0.80	±	0.05	0.77	±	0.05
Prog	0.46	±	0.02	0.42	±	0.03
17α-OHprog	0.81	±	0.08	0.92	±	0.04
Andro	1.8	±	0.2	1.4	±	0.1

The k_{off} values correspond to the average rate from three replicate analyses. The ± denotes the propagated error of the standard deviations from the three replicates.

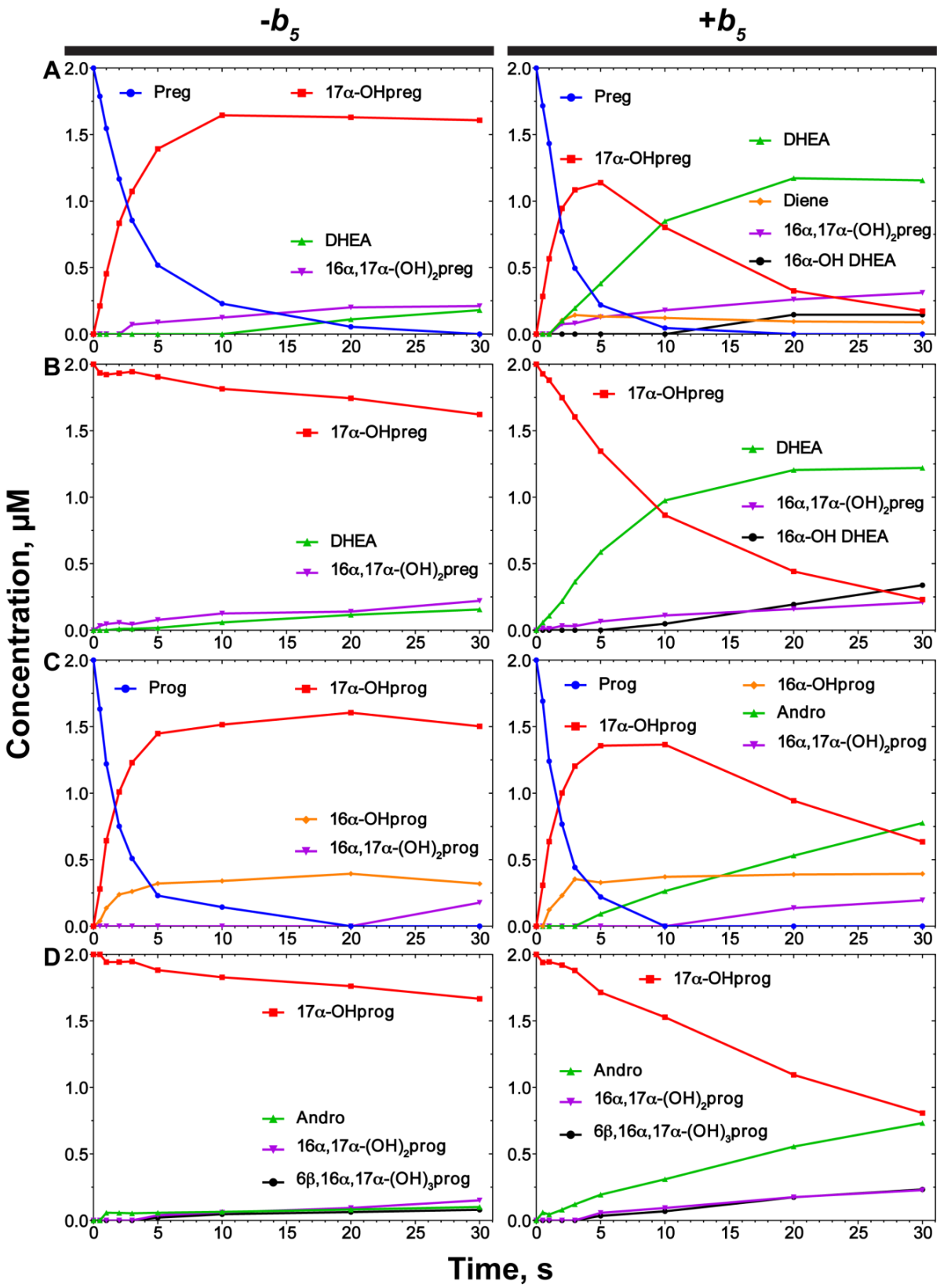

Figure 3.4 Single-turnover kinetics of human P450 17A1

Single-turnover plots for human P450 17A1-mediated oxidation of Preg (A), 17α-OHpreg (B), Prog (C), and 17α-OHprog (D) in incubations lacking and including b_5 (left and right panels, respectively). Each data point corresponds to an individual analysis of four combined replicate incubation samples. See section 3.4.4.2 for experimental details and Table 3-4 for estimated substrate consumption rates.

Table 3-4 Single-turnover substrate oxidation rates

	k, s^{-1}	
Substrate	$-b_5$	$+b_5$
Preg	0.27 ± 0.01	0.43 ± 0.02
17α-OHpreg	0.0074 ± 0.0006	0.077 ± 0.002
Prog	0.46 ± 0.02	0.47 ± 0.02
17α-OHprog	0.0066 ± 0.0005	0.029 ± 0.001

The estimated rates, and corresponding standard error (±), were obtained by fitting the substrate consumption plot (Figure 3.4) to a single-exponential decay model in Prism.

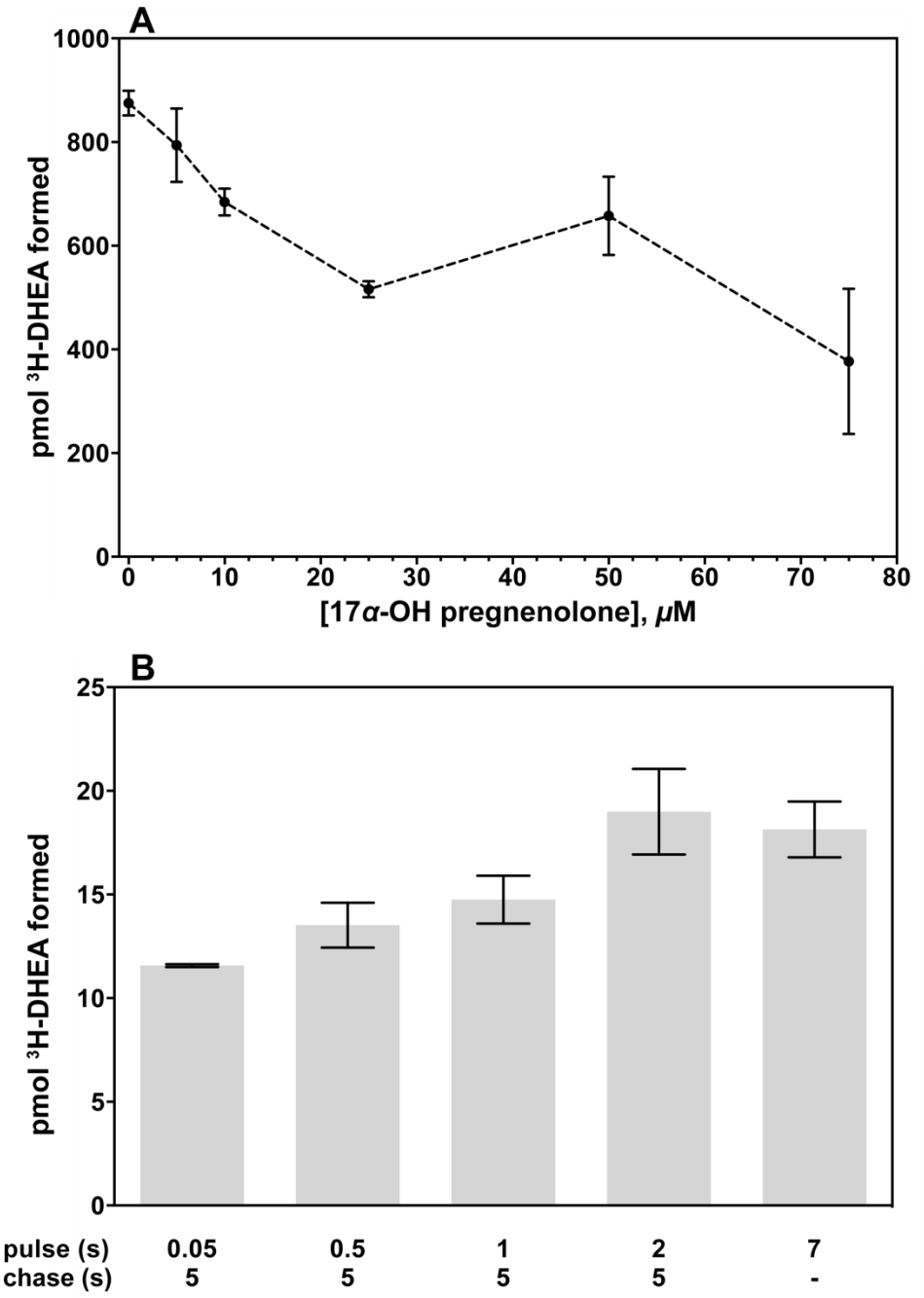

Figure 3.5 Pulse-chase assays under steady-state and single-turnover conditions

A, Production of ^{3}H-DHEA in steady-state incubations pulsed for 1 min with ^{3}H-Preg and chased with 17α-OHpreg (concentrations indicated on x-axis, see Section 3.4.4.3 for experimental details).The results are presented as means ± SD of duplicate experiments. B, Production of ^{3}H-DHEA under single-turnover conditions with variable pulse lengths and chased with 17α-OHpreg for 5 s (where indicated, see Section 3.4.4.3 for experimental details). The results presented in A and B correspond to the means ± SD of duplicate experiments.

3.2.5 Reaction Selective Inhibition by TAK-700 Enantiomers

Defining the processivity of human P450 17A1 is critical for the development of reaction specific inhibitors of the 17,20-lyase reaction but not 17α-hydroxylation. The enzyme should function in a distributive manner in order for a competitive inhibitor to selectively inhibit the desmolase reaction, whereas the likelihood is low that such a compound is able to distinguish between the two substrates/steps in a processive mechanism. In support of a distributive mechanism, TAK-700 was developed by the Takeda company as a selective 17,20-lyase inhibitor. (*S*)-TAK-700 was the enantiomer selected for development and subsequent clinical trials, due to higher potency in comparison with (*R*)-TAK-700 [78,79]. The inhibition profiles of the two enantiomers have been evaluated, and the results are presented in Figure 3.6 and Table 3-5. (*S*)-TAK-700 was the more potent enantiomer based on lower IC_{50} values for all the reactions assessed. Greater reaction selectivity was also observed for (*S*)-TAK-700, with a three-fold lower IC_{50} value for the 17,20-lyase versus 17α-hydroxylation reactions with 17-OHpreg and Preg, respectively, while the difference was approximately two-fold for (*R*)-TAK-700. The reaction selectivity with the progesterone series substrates was the same for both enantiomers, with hydroxylase-lyase IC_{50} ratios of 1.4, although the (*S*)-TAK-700 values were 6.5 times lower. The reactions with the progesterone series substrates exhibited greater susceptibility to the inhibitors, with lower IC_{50} values for both reactions versus those for the 17α-OHpreg cleavage reaction. Notably, both enantiomers were unable to inhibit the 17,20-lyase reaction with greater potency than the 17α-hydroxylation reaction in incubations with Preg as the substrate, considering that the IC_{50} values for both reactions were nearly identical. These results support a processive enzyme mechanism for the human P450 17A1-b_5 system. Although a lower IC_{50} was obtained for the desmolase reaction, the increased potency is dependent on the reaction starting with the 17α-hydroxy steroid. Thus, these inhibitors are unable to selectively inhibit the 17,20-lyase reaction in a processive enzyme system, assuming that the conversion of Preg to DHEA observed in these studies proceeded through such a mechanism.

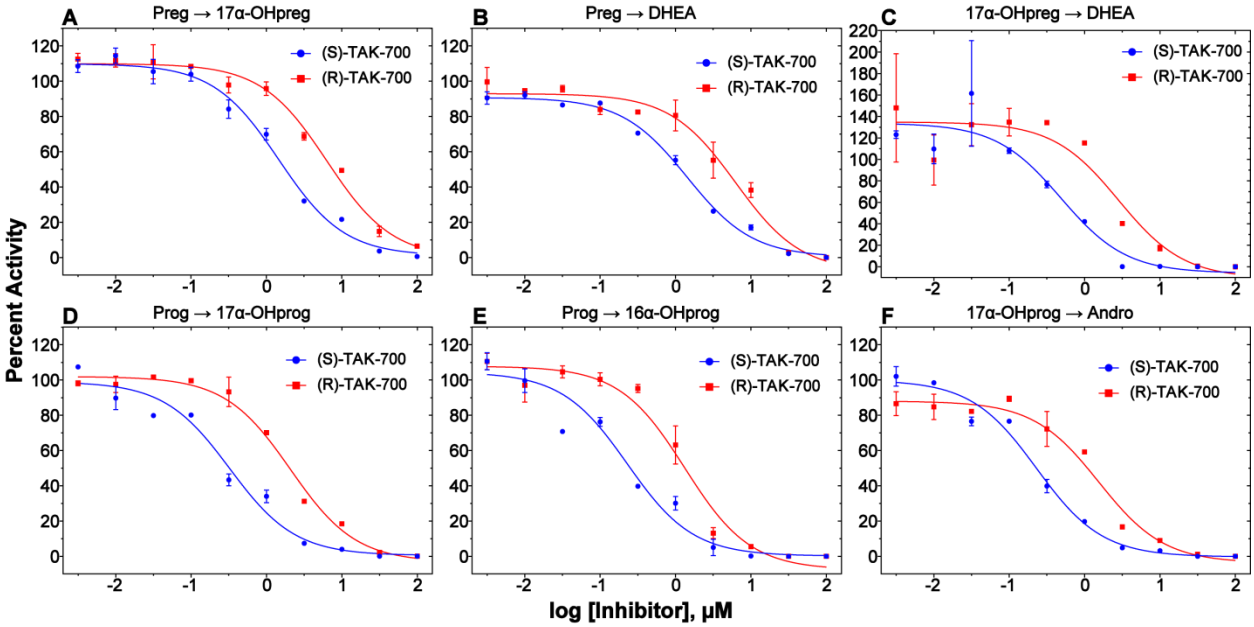

Figure 3.6 Inhibition of human P450 17A1 by TAK-700 enantiomers

(S)- and (R)-TAK-700-mediated inhibition of human P450 17A1 reactions was assessed as residual activity normalized to non-challenged incubation samples. Each data point corresponds to an average residual activity from two replicate samples and the error bars denote the standard deviation. The data was fit with the log(inhibitor) vs response (three parameters) equation in Prism to obtain the IC_{50} values (listed in Table 3-5). See Section 3.4.4.4 for experimental details.

Table 3-5 IC_{50} values for inhibition of steroid oxidation by TAK-700 enantiomers

		IC_{50} (95% CI), μM	
Substrate	Product	(*S*)-TAK-700	(*R*)-TAK-700
Preg	17*α*-OHpreg	**1.5** (1.1 – 1.9)	**6.4** (4.7 – 8.6)
	DHEA	**1.4** (1.2 – 1.8)	**6.3** (4 – 9.7)
17*α*-OHpreg	DHEA	**0.49** (0.22 – 1.1)	**2.8** (1.1 – 7)
Prog	17*α*-OHprog	**0.32** (0.22 – 0.48)	**2.1** (1.6 – 2.8)
	16*α*-OHprog	**0.23** (0.15 – 0.35)	**1.3** (0.86 – 2)
17*α*-OHprog	Andro	**0.23** (0.17 – 0.31)	**1.5** (1 – 2.3)

3.2.6 Kinetic Model

The estimated dissociation rates of the 17α-hydroxy steroids were faster than the respective oxidation rates, while the rates of both steps were comparable for the hydroxylase substrates (Figure 3.7). The k_{off} rates also showed correlation with the experimental K_d parameters, and they were used to calculate the steroid association rates (k_{on}). With the exception of Andro, due to an unreliable dissociation constant, the k_{on} values were similar, ranging from 0.47 - 0.98 μM^{-1} s^{-1} (Table 3-6). Notably, the k_{on} rates were all below the typical diffusion-limited range for enzyme-substrate association (10 - 100 μM^{-1} s^{-1}) [176].

The KinTek Explorer® program was used to fit the experimental data from the steroid titrations and catalytic assays (with b_5 included) to a minimal kinetic model. The model was structured so that all redox steps were grouped in order to generate a single "oxidation" rate, and a simple binding mechanism was assumed. Using the estimated and calculated parameters as starting values, the software produced rates that fit the Δ^5 steroid catalytic data reasonably well, but not the binding data (Figure 3.8 and appendix Figure 6.5). The estimated K_d for 17α-OHpreg (3.5 μM) was greater than the prior value (0.52 μM), while they decreased for Preg (0.37 to 0.066 μM) and DHEA (1.7 to 0.068 μM). Still, the updated 17α-OHpreg dissociation rate (1.0 s^{-1}) remained approximately two times faster than the 17,20-lyase rate (0.42 s^{-1}). The changes to the binding kinetics, and the relationship between the 17α-OHpreg k_{off} and oxidation rates, were consistent when the binding experiments were excluded from the global fit (Figure 3.9 and appendix Figure 6.6). Constraining the binding equilibria to the experimentally derived K_d values exhibited a minor effect to the 17α-OHpreg k_{off}:17,20-lyase reaction ratio (2.7) and the simulated rates described the experimental data sets well (Figure 3.10 and appendix Figure 6.7). However, the estimated k_{on} rate for DHEA was drastically lower than from prior simulations and the calculated value, while those for Preg and 17α-OHpreg were comparable. Additional variations to the parameter restrictions were tested to give similar results (Appendix Figures 6.8-6.11). The

collective global fit results suggest that the 17α-OHpreg dissociation rate is faster than the rate of the desmolase reaction, although the inverse variation to the binding equilibria for 17α-OHpreg and DHEA indicate an apparent disconnect between the binding and catalytic data when a simple kinetic model is applied. The kinetic model for the Δ^4 steroids was less reliable, considering that the simulations did not describe all the data sets as well as achieved for the Δ^5 steroids model (data not shown).

The single-turnover pulse-chase assay data was fit to a minimized kinetic model that had been used to assess the processivity of bovine and guinea pig P450 17A1 [90,91]. Interestingly, the estimated 17,20-lyase rate (0.82 s^{-1}) was faster than the 17α-hydroxylation reaction (0.37 s^{-1}) when none of the parameters were constrained, but the fit was unreliable due to an exceedingly fast k_{off} (4.5 s^{-1}) for 17α-OHpreg (Appendix Figures 6.12-6.13) in comparison to what was observed experimentally (0.41 s^{-1},Table 3-3). The most convincing fit was generated when the 17α-OHpreg K_d was maintained as a constant (0.52 μM), producing a k_{off} rate (0.27 s^{-1}) that was approximately two-fold faster than the 17,20-lyase rate (0.13 s^{-1}, Appendix Figures 6.14-6.15). The similarity of the parameter ratio to that from the global fit using the same constraints (see above) implies that the disproportion of the individually-derived experimental rates is invalid and establishes precedent for the extent of ^{3}H-DHEA production under these assay conditions.

Steroid binding was further evaluated by applying different models to the kinetic binding data from the Δ^5 steroid titrations. A good fit of the kinetic binding data was ultimately achieved in a model that included two conformations of the free enzyme and the enzyme-substrate complex (Figure 3.10 and appendix Figure 6.16). The estimated parameters indicate that only a portion of the free enzyme exists in a steroid-binding state (K_{eq} 0.91), and they conform to diffusion-limited standards as the initial binding step for each steroid was near 10 μM^{-1} s^{-1}. At the present time the binding model and estimated parameters cannot be regarded as definite, considering that further analysis is necessary to confirm the

existence of the individual binding steps. However, the inability to describe the kinetic binding data using simpler models suggests that the steroid binding process of human P450 17A1 is complex.

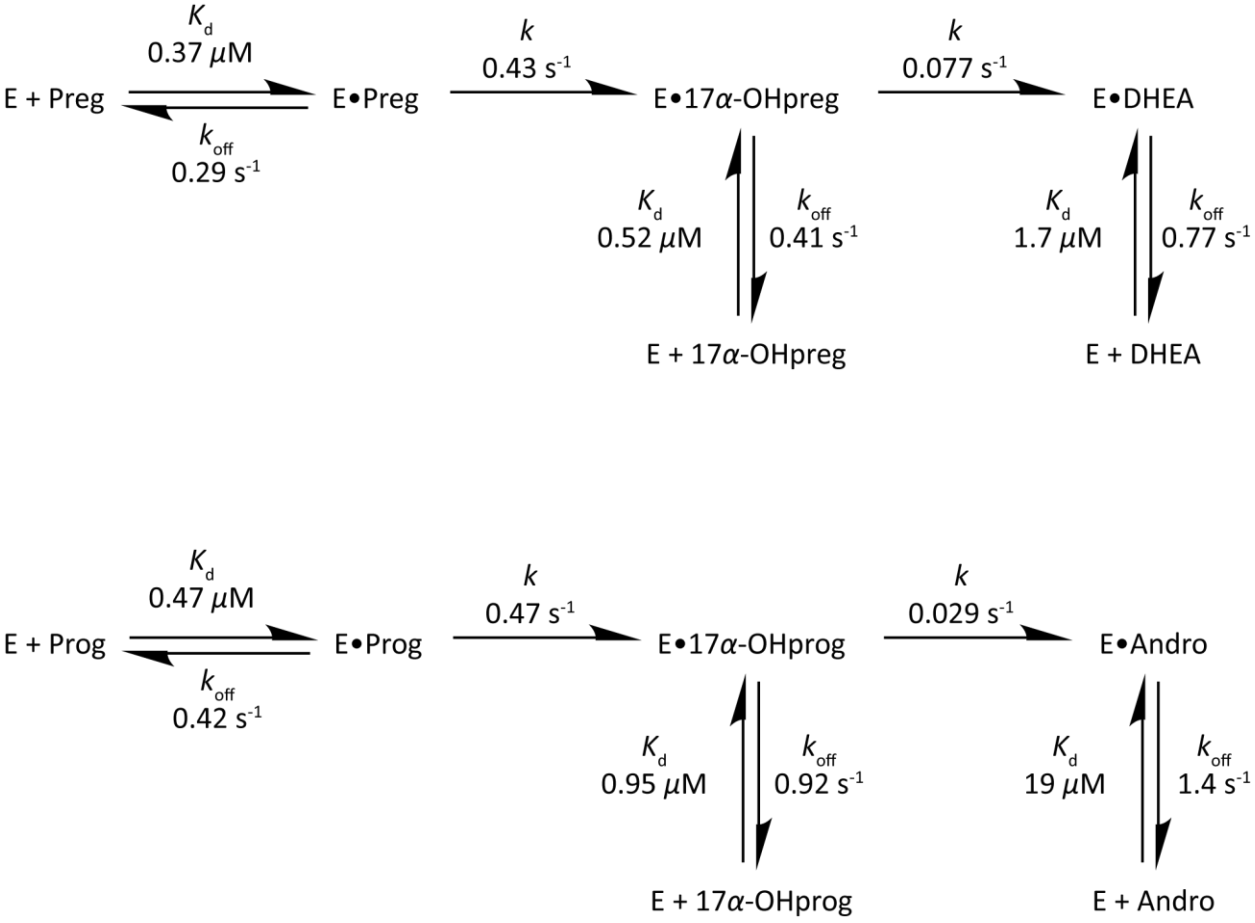

Figure 3.7 Human P450 17A1 binding parameters and substrate oxidation rates

The K_d, k_{off}, and reaction rates (k) correspond to the estimated parameters obtained from ligand binding (Section 3.2.1), enzyme-trapping (Section 3.2.3.1), and single-turnover oxidation experiments (Section 3.2.3.2), respectively.

Table 3-6 k_{on} rates calculated from K_d and k_{off}

	k_{on}, μM^{-1} s^{-1}	
	$-b_5$	$+b_5$
Preg	0.62	0.78
17α-OHpreg	0.62	0.79
DHEA	0.47	0.45
Prog	0.98	0.89
17α-OHprog	0.85	0.97
Andro	0.095	0.074

Preg - Single-Turnover

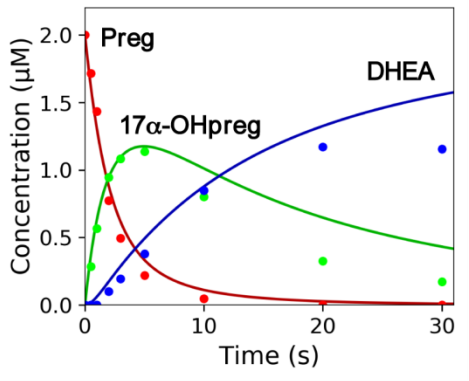

17α-OHpreg - Single-Turnover

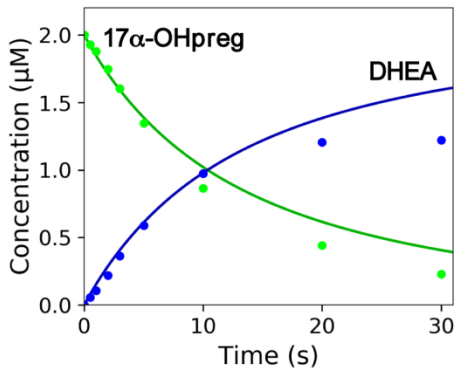

Preg - Steady-State

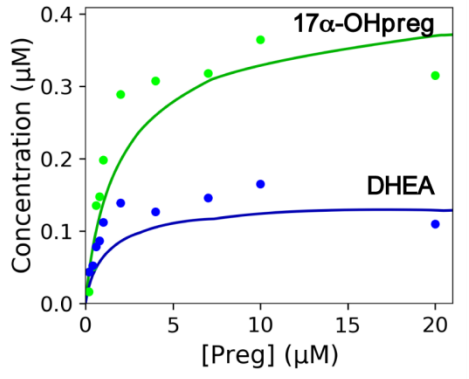

17α-OHpreg - Steady-State

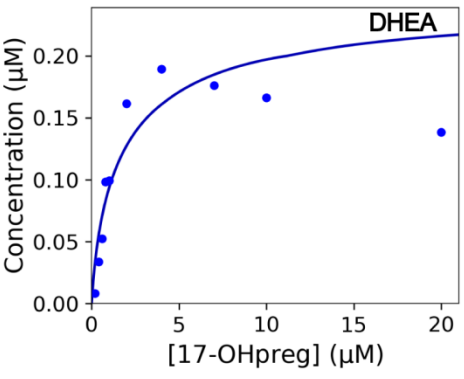

Preg - Binding

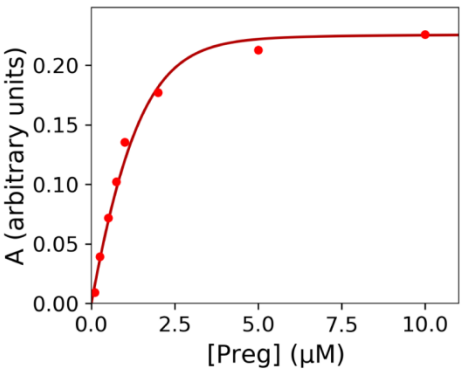

17α-OHpreg - Binding

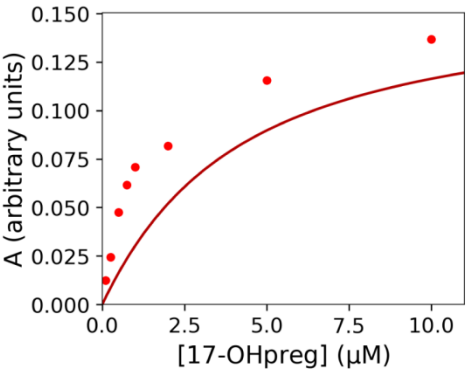

DHEA - Binding

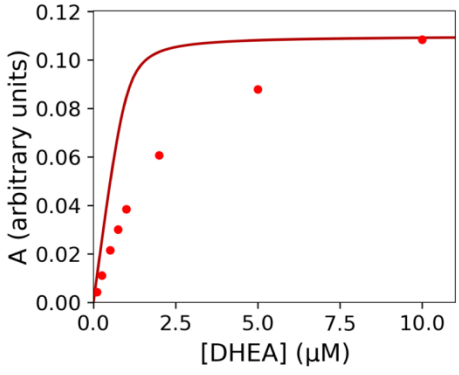

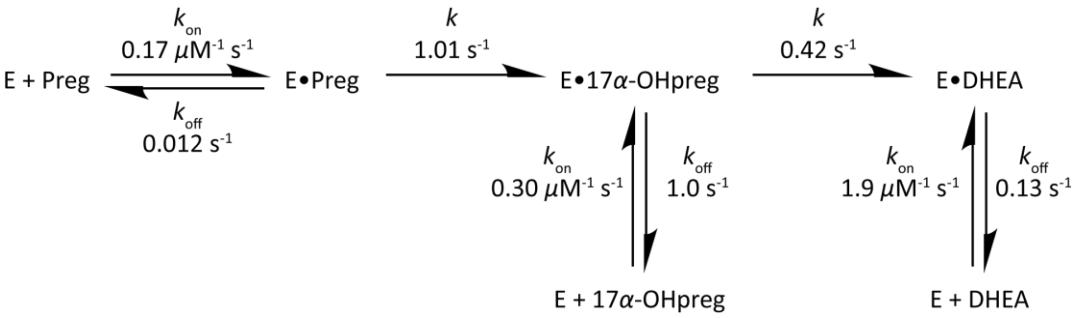

Figure 3.8 Fit results from global data analysis of binding and catalytic assays

Global fitting of experimental data from human P450 17A1 catalytic assays under single-turnover and steady-state conditions and steroid binding titrations to a simple mechanistic model in Kintek Explorer. None of the parameters were fixed and all experiments were included in the global fitting. See Appendix Figure 6.5 for detailed fit iteration results.

Preg - Single-Turnover

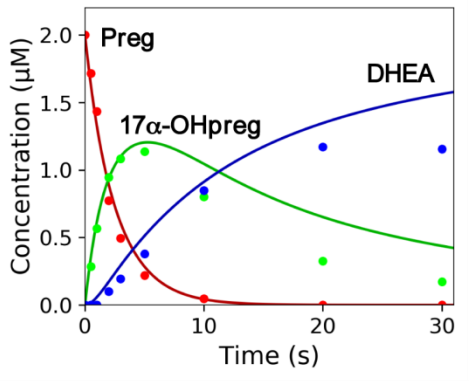

17α-OHpreg - Single-Turnover

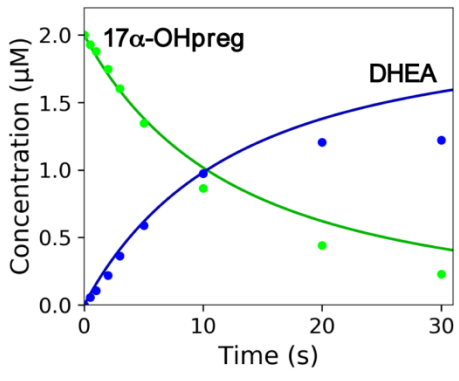

Preg - Steady-State

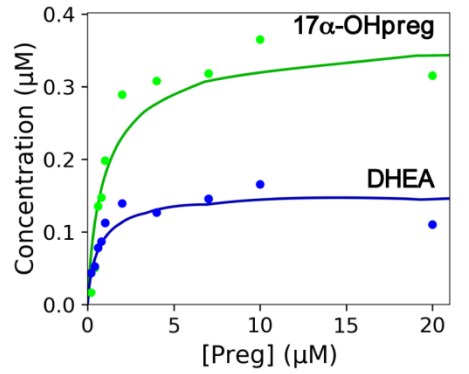

17α-OHpreg - Steady-State

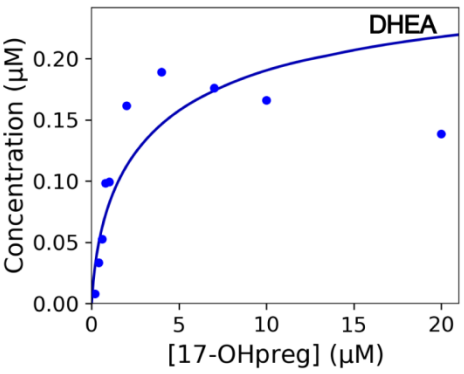

Preg - Binding

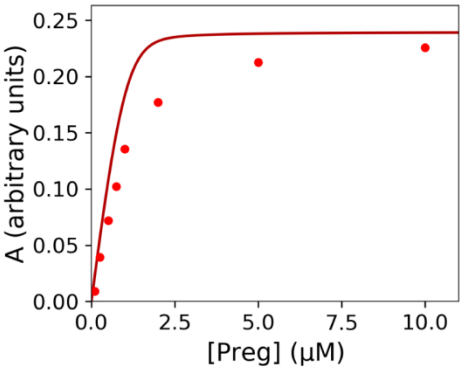

17α-OHpreg - Binding

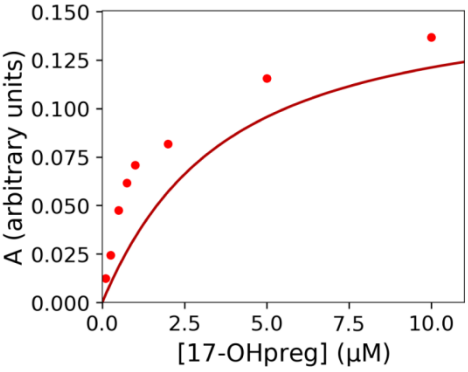

DHEA - Binding

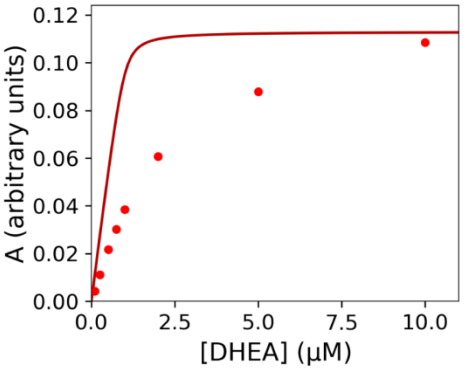

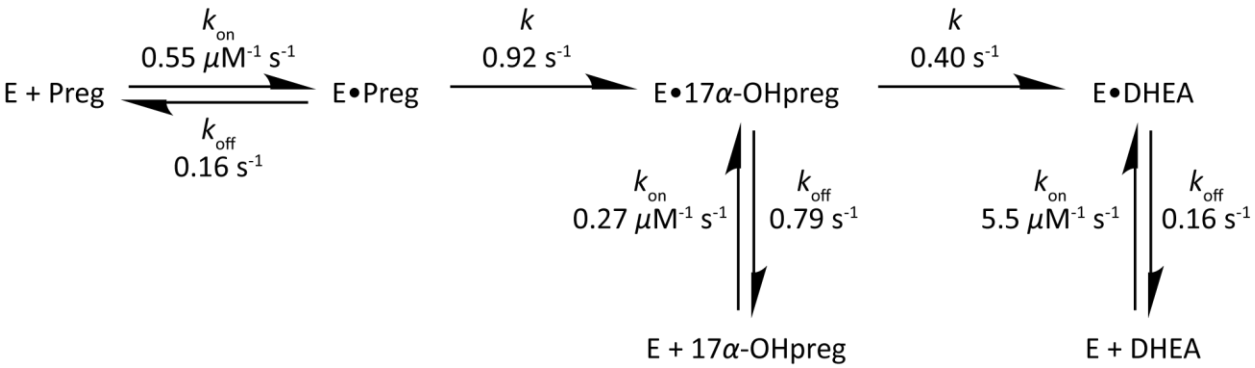

Figure 3.9 Fit results from global data analysis with binding assays excluded

Global fitting of experimental data from human P450 17A1 catalytic assays under single-turnover and steady-state conditions to a simple mechanistic model in Kintek Explorer. The steroid binding experiments were excluded from global fitting. None of the parameters were fixed. See Appendix Figure 6.6 for detailed fit iteration results.

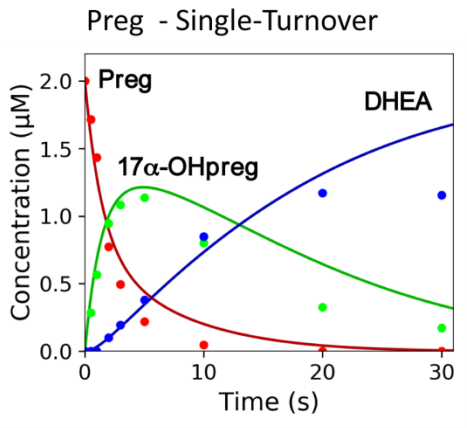
Preg - Single-Turnover
Preg
DHEA
17α-OHpreg
Concentration (μM)
Time (s)

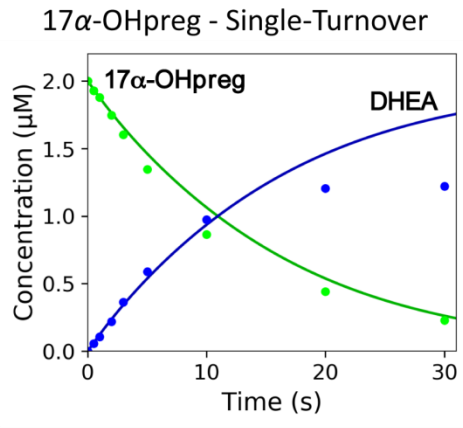
17α-OHpreg - Single-Turnover
17α-OHpreg
DHEA
Concentration (μM)
Time (s)

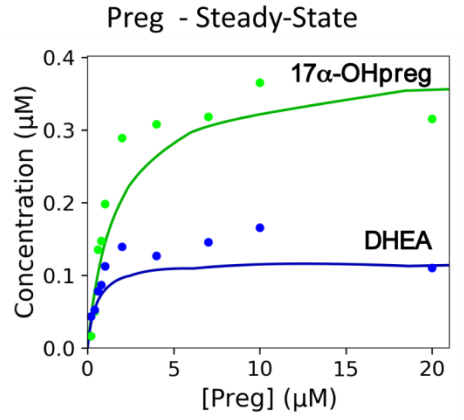
Preg - Steady-State
17α-OHpreg
DHEA
Concentration (μM)
[Preg] (μM)

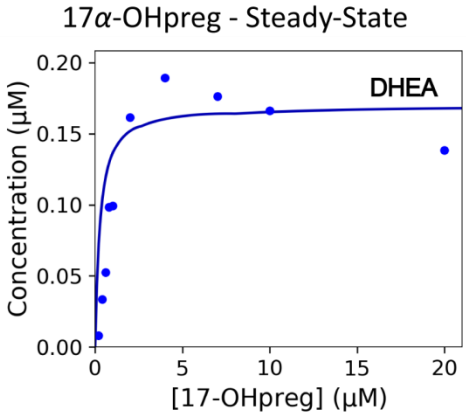
17α-OHpreg - Steady-State
DHEA
Concentration (μM)
[17-OHpreg] (μM)

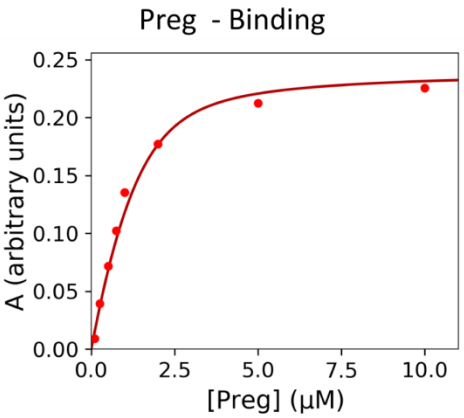
Preg - Binding
A (arbitrary units)
[Preg] (μM)

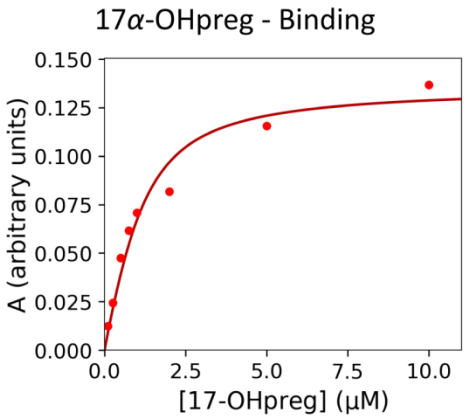
17α-OHpreg - Binding
A (arbitrary units)
[17-OHpreg] (μM)

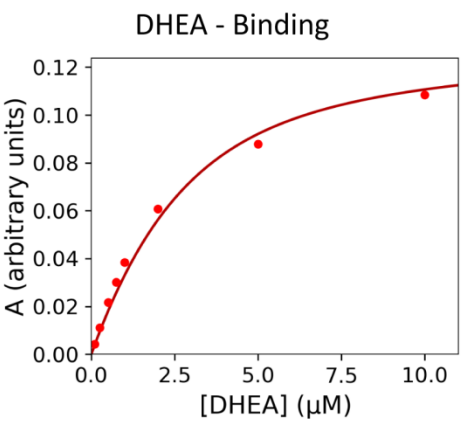
DHEA - Binding
A (arbitrary units)
[DHEA] (μM)

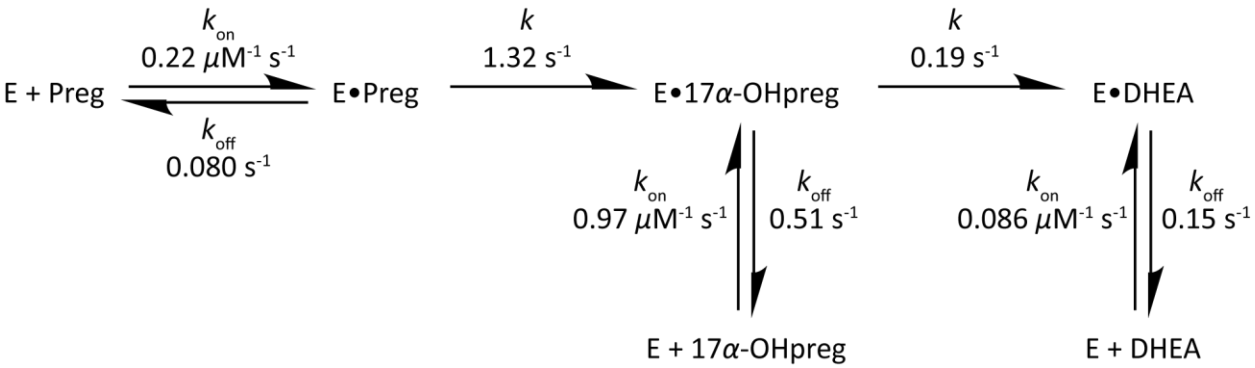

Figure 3.10 Fit results from global data analysis with experimental K_d values as constants

Global fitting of experimental data from human P450 17A1 catalytic assays, under single-turnover and steady-state conditions, and steroid binding titrations to a simple mechanistic model in Kintek Explorer. The steroid binding equilibria were fixed to the experimental K_d values and all experiments were included in the global fitting. See Appendix Figure 6.7 for detailed fit iteration results.

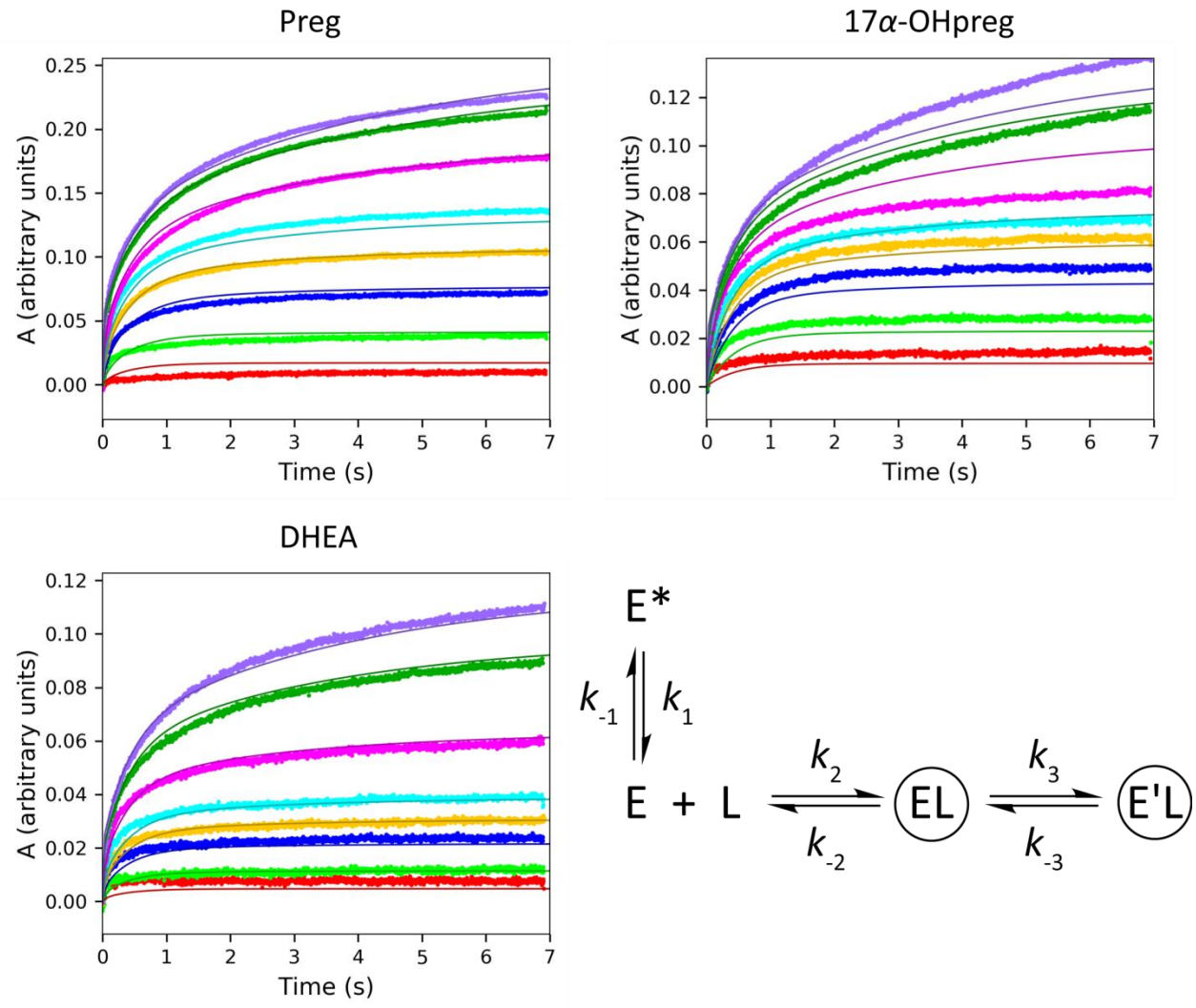

Figure 3.11 Analysis of human P450 17A1 steroid binding kinetics with KinTek Explorer

Stopped-flow absorbance changes from Preg, 17α-OHpreg and DHEA binding. Raw data are presented as scatter plots, and overlaid lines represent the fits from KinTek Explorer software using the model displayed. The species causing an absorbance change in the heme Soret spectra are circled. k_1=0.23 s^{-1}, k_{-1}=0.21 s^{-1}; Preg (ΔA_{391}-A_{426}) k_2=12 μM^{-1} s^{-1}, k_{-2}=4.4 s^{-1}, k_3=0.50 s^{-1}, k_{-3}=1.9 s^{-1}; 17α-OHpreg (ΔA_{393}-A_{426}) k_2=8.4 μM^{-1} s^{-1}, k_{-2}=2.2 s^{-1}, k_3=0.093 s^{-1}, k_{-3}=2.31 s^{-1}; DHEA (ΔA_{393}-A_{428}) k_2=12 μM^{-1} s^{-1}, k_{-2}=12 s^{-1}, k_3=0.10 s^{-1}, k_{-3}=2.3 s^{-1}. See Appendix Figure 6.16 for detailed fit iteration results.

3.3 Discussion

The results indicate that human P450 17A1 is not an inherently processive enzyme when it catalyzes the sequential 17α-hydroxylation and 17,20-lyase reactions. However, when b_5 is present, the catalytic efficiencies of both functions are significantly enhanced, and the conversion of Preg to DHEA becomes more concerted. Observations from the binding studies suggest that human P450 17A1 steroid association is a complex process that cannot be explained with a simple binding mechanism. TAK-700 did exhibit a higher potency for the 17,20-lyase reaction, but the selective capacity of the compound was insufficient to prevent ^{3}H-Preg to ^{3}H-DHEA conversion. The kinetic model developed from global analysis of the experimental data indicates that the 17α-OHpreg k_{off}-17,20-lyase rate ratio is approximately two when bound by the human P450 17A1-b_5 complex.

3.3.1 Steroid Binding

Substrate binding is an enzymatic step that can regulate the processivity of an enzyme. In theory, high affinity for an intermediate product/substrate supports a mechanism where that compound remains bound, while intermediate release is faster when the affinity is low. Recombinant human P450 17A1 exhibited the greatest affinity for Preg (K_d 0.37 μM), Prog (K_d 0.47 μM), and 17α-OHpreg (K_d 0.52 μM) (Table 3-1). Interestingly, these three steroids are considered the physiologically relevant substrates for human P450 17A1, while 17α-OHprog (K_d 0.95 μM) is considered a poor substrate [41]. The disparity in binding affinity between 17α-OHprog and the other steroids (see above) has also been reported by other groups [63,93,177]. It is plausible that greater affinity for 17α-OHpreg versus 17α-OHprog supports a mechanism where the former is a substrate in a processive system, while the mechanism for the latter is more distributive, but such a conclusion requires more compelling evidence than the marginal two-fold difference observed in this work. These studies were extended to the 17,20-lyase products, DHEA and Andro, which had the highest K_d values at 1.7 and 19 μM, respectively. Until recently, DHEA and Andro were considered the catalytic end products of human P450 17A1, but further

oxidation of both steroids (16-hydroxylation) has now been observed in enzyme incubations (see Chapter 2). Although Andro can be used as a substrate, it is likely that the substantial difference in binding affinity renders it a poor substrate in comparison to DHEA, which was demonstrated in single-turnover experiments through production of 16-OH-DHEA and not 16-OHandro (Figure 3.4).

The stimulatory effect of b_5 on the 17,20-lyase reaction by human P450 17A1 could, in theory, derive from alterations to the binding mechanism. Studies on P450 17A1 from other species suggest that their ability to catalyze the scission reaction is determined by the 17α-hydroxy steroid dissociation rate, based on values estimated from pulse-chase assays [90,91]. However, the influence of b_5 on the parameter was not addressed previously, as the protein was not included in the studies. In this work, an enzyme-trapping assay was used for direct analysis of the human P450 17A1 steroid dissociation step in the presence and absence of b_5. In general, the k_{off} rates of the Preg series steroids were two-fold lower than those of the corresponding Prog molecules. Although the difference is not great, these results further support the dominance of the Preg pathway (over Prog) in human P450 17A1 catalysis of the cleavage reaction. It was not surprising that the fastest k_{off} rates were estimated for the 17,20-lyase products, but interestingly, the rates observed for DHEA were similar to those for 17-OHprog. The estimated k_{off} values were only slightly altered when b_5 was included, suggesting that b_5 does not impact the step (Table 3-3). Nevertheless, the absence of a b_5 effect under these conditions does not rule out that interactions with POR may be required to affect substrate binding. Estrada et al. used NMR to perform competition assays with human P450 17A1 and b_5 and rat POR, which showed that substrate binding decreased the ability of rat POR to disrupt the interaction between P450 17A1 and b_5 [67]. However, their analysis did not investigate any of the kinetic parameters for these interactions.

3.3.2 b_5 Enhanced Catalytic Activities

The mechanism by which human b_5 enhances human P450 17A1 catalytic activity has been debated, but the selectivity for the 17,20-lyase reaction is a well-accepted phenomenon. b_5 has been

reported to enhance the 17,20-lyase reaction by up to ten-fold, while the 17α-hydroxylation reactions were augmented two- to three-fold [53,56,65,169,174]. The steady-state catalytic analyses in this investigation suggest that b_5 stimulation is less discriminating between the two reactions and varies based on the substrate type. Most of the K_m values for the primary P450 17A1 reactions were increased approximately two-fold with the addition of b_5, with the exception of Prog 16α-hydroxylation and 17α-hydroxylation reactions, which increased approximately five-fold and decreased two-fold, respectively. The more pronounced b_5 effect was observed in the turnover number (k_{cat}) for all reactions assessed, some of which were drastic. Unexpectedly, the b_5-mediated stimulation of the 17α-hydroxylation reaction with Preg increased the k_{cat} value 30-fold, which was greater than the 12-fold increase of the 17α-OHpreg cleavage rate. The largest increase in turnover number was ~60-fold for 17α-OHProg cleavage, while the rate for the Prog 17α-hydroxylation and 16α-hydroxylation reactions increased two- and four-fold, respectively. In combination, the altered kinetic constants yield significantly improved catalytic efficiencies for reactions with Preg, 17α-OHpreg, and 17α-OHprog. These results provide further evidence that b_5 functions as a sentry between the androgen and glucocorticoid synthesis pathways. Without b_5 stimulation, Preg is a poor substrate for human P450 17A1, which thereby facilitates the conversion of the steroid to Prog by 3β-hydroxysteroid dehydrogenase. In turn, the Prog 17α-hydroxylation reaction does not rely on b_5 stimulation, providing an unencumbered pathway for Preg to glucocorticoid synthesis. On the other hand, human P450 17A1-mediated conversion of Preg and 17α-OHpreg is significantly boosted when b_5 is present, leading to DHEA production. Additionally, the b_5-mediated stimulation of the desmolase reaction with 17α-OHprog increases the androgen pool further.

One apparent caveat with the steady-state catalytic results is the failure to separate the 17α-hydroxylation and 17,20-lyase reactions when b_5 was included in Preg assays. Although the result is informative regarding the processivity of the enzyme, the Michaelis-Menten function used in the analysis does not account for the 17α-OHpreg that was further oxidized to DHEA. As such, the actual k_{cat}

value for Preg 17α-hydroxylation is probably higher than the reported parameter, as was shown by the Preg oxidation rate from single-turnover assays.

The steady-state turnover assays provided an overall view of the human P450 17A1 catalytic ability, but they do not provide insight on specific reaction steps considering that the experiments progress through multiple reaction cycles. In order to eliminate turnover rate limitations derived from steroid binding steps, single-turnover assays were employed to assess the rates for the individual hydroxylation and 17,20-lyase steps. The results show that b_5 stimulated the chemical reaction steps with Preg, 17α-OHpreg, and 17α-OHpreg by ~1.6-, 10-, and 4.4-fold, respectively, but did not affect Prog conversion. This trend correlates with the b_5 effects on the k_{cat} parameters from steady-state assays, in which Prog reactions exhibited the least stimulation. Most of the oxidation rates estimated from the single-turnover assays were greater than the steady-state k_{cat} values, indicating that steady-state catalysis is influenced by other reaction steps. Interestingly, the 17α-OHpreg reaction rates (with and without b_5) were comparable to the respective k_{cat} values, and similarity was also observed for 17α-OHprog with b_5 included. This suggests that the 17,20-lyase itself is a relatively rate-limiting step in the reaction, which b_5 is able to accelerate.

The single-turnover experiments also provided insight towards the processivity of human P450 17A1 and the effect by b_5. The reaction rates derived from the single-turnover assays with 17α-OHpreg and 17α-OHprog were slower than the estimated k_{off} rates for the respective substrate. Additionally, a lag phase was observed in the production of the lyase products. These results indicate a distributive mechanism where the 17α-hydroxy steroid intermediates are more likely to dissociate from the substrate pocket than proceed through the 17,20-lyase reaction. Nonetheless, b_5 was able to stimulate the processivity of the enzyme by decreasing the k_{off}:chemistry rate quotient from ~40 to ~5 for 17α-OHpreg and ~120 to ~30 for 17α-OHprog. In contrast, the parameters for Prog were nearly identical

regardless of the presence of b_5, while the k_{off} rates for Preg were comparable to the chemistry rate without b_5 included.

3.3.3 Pulse-Chase

Pulse-chase assays have been a useful tool to investigate the enzyme processivity of several multistep P450s (e.g. 2A6, 11B2, and 19A1), and this and other laboratories have shown variability in this characteristic [22,89,129]. The technique has also been applied to assess the processivity of P450 17A1 enzymes from other species, which classified guinea pig P450 17A1 as a processive catalyst in Prog to Andro conversion, while 80% of the bovine enzyme was distributive in Preg to DHEA turnover [90,91].

The kinetics discussed above suggest that human P450 17A1 is primarily a distributive enzyme in catalyzing the sequential 17α-hydroxylation and 17,20-lyase reactions, and interactions with b_5 enhances the Preg to DHEA processivity. In this investigation, pulse-chase experiments were conducted under steady-state and single-turnover conditions, with b_5 included as it was critical for the desmolase function. These assays were also focused on Preg to DHEA conversion, in light of the prominence of DHEA production (versus Andro) in the previous experiments. In steady-state pulse-chase studies, a modest effect was observed in reactions initiated with ^{3}H-Preg and challenged with several concentrations of non-labeled 17α-OHpreg. Although the 17,20-lyase reaction was hindered, only the addition of 75 μM 17α-OHpreg decreased the average DHEA production by > 50%. The results parallel prior investigations with zebrafish P450 17A1, which exhibited a distributive mechanism but greater processivity when Preg was the substrate [127]. Single-turnover conditions were then applied to examine the conversion of ^{3}H-Preg to ^{3}H-DHEA through individual reaction cycles. Remarkably, there was only a nominal difference in ^{3}H-DHEA production between the control and experimental chase with a saturating concentration of intermediate steroid (40 μM 17α-OHpreg). Given that the scission reaction was not obstructed to a greater extent, the pulse-chase assays provide evidence that in the presence of b_5 human P450 17A1 catalyzes Preg turnover to DHEA in a processive fashion.

3.3.4 Inhibition

Several human P450 17A1 inhibitors have been developed for the purpose of treating prostate cancer. The only compound to gain FDA approval thus far has been abiraterone, but the capacity of the drug to inhibit both reactions consequently triggers adverse effects due to cortisol deficiency. In this regard, TAK-700 was developed as a lyase-selective inhibitor, although development was discontinued after clinical trials determined the compound lacked greater efficacy versus abiraterone [77,81,82]. Nonetheless, there is utility in TAK-700 to investigate the human P450 17A1 mechanism for catalyzing the 17α-hydroxylation and 17,20-lyase reactions. Chemical synthesis of TAK-700 yields the (*S*)- and (*R*)-enantiomers, of which (*S*)-TAK-700 was chosen for development based on better selectivity versus P450 3A4 inhibition and greater efficacy at reducing DHEA and testosterone levels in cynomolgus monkeys [79]. However, the developers did not present a comprehensive comparison of the enantiomers for all major human P450 17A1 reactions. The catalytic inhibition analyses in this work extended the 17,20-lyase reaction selectivity to both substrate series by both TAK-700 enantiomers and recapitulated the superior potency of the (*S*)- over the (*R*)- conformer. The results also revealed the inability of the compounds to selectively inhibit the 17,20-lyase reaction when Preg is the substrate. Although the (*S*)-TAK-700 IC_{50} value for 17α-OHpreg cleavage was three-fold lower than the IC_{50} for Preg 17α-hydroxylation, the compound failed to inhibit Preg to DHEA conversion with greater sensitivity than the antecedent reaction. The comparable IC_{50} values for both reactions with Preg as the substrate suggest that the inhibition of DHEA synthesis occurs primarily by preventing 17α-OHpreg production. Moreover, this observation provides further support for a mechanism in which the 17α-hydroxylation and 17,20-lyase reactions are concerted when b_5 mediates the human P450 17A1 conversion of Preg.

3.3.5 Global Kinetic Model

Taking into account the estimated k_{off} and 17α-hydroxy steroid consumption rates derived from individual experiments, human P450 17A1 catalysis of the 17α-hydroxylation and 17,20-lyase reactions

can be characterized as distributive, especially when b_5 is not present. Paradoxically, selective inhibition of the 17,20-lyase reaction was lacking when Preg was used as the substrate in the pulse-chase and TAK-700 assays with b_5 included. The contradictory results most likely stem from the specificity of the experimental design. The purpose of the enzyme-inhibitor trapping assay was to evaluate only the rate of steroid release, but the design fails to investigate whether it will be affected by interactions with POR or the P450 oxidation state. Additionally, the single-turnover oxidation rates were assessed under the assumption that the reactions were initiated with all of the substrate being enzyme bound, considering that the estimated K_d values were below the substrate concentration used. In this regard, KinTek Explorer was used to eliminate the simplifying assumptions in the data analysis and permitted the simultaneous application of a mechanistic model to the collective datasets.

The calculated k_{on} values that were used as starting parameters were all below 1 $\mu M^{-1}\,s^{-1}$, which is too slow for a diffusion-limited interaction [176], but they were fast enough based on the estimated k_{cat} and oxidation rates from the single-turnover reactions. However, the rates generated from the global fitting indicate a clear disconnect between the catalytic and equilibrium binding data, in which the affinity of 17-OHpreg was diminished (0.52 μM, estimated to 3.0-3.5 μM from fit) while Preg and DHEA both increased (0.37 μM, estimated to 0.028-0.066 μM from fit, and 1.7 μM, estimated to 0.029-0.068 μM from fit, respectively). This issue was resolved only when the estimated K_d values were set as constants, but even then, the k_{on} for DHEA was unrealistically slow (0.086 $\mu M^{-1}\,s^{-1}$). Although the rates changed based on the various constraints and exclusions applied to the model, the consensus among the global fit results is that the k_{off} of 17α-OHpreg is two to three times faster than the 17,20-lyase reaction. This result was reaffirmed by rates generated from fitting the single-turnover pulse chase data, where the k_{off} was estimated at 0.27 s^{-1} and the scission reaction rate was 0.13 s^{-1} when the experimentally-derived 17α-OHpreg K_d held constant.

The inconsistency in the binding parameters estimated from direct analysis of the equilibrium binding data and the rates derived from the global fit indicated that the simple binding mechanism used in the analyses was likely inaccurate. This reasoning is supported by the complex ligand binding mechanisms of other human P450s. P450 19A1, which also oxides steroids in a multistep process, exhibited a two-phase binding mechanism, with the first step being spectroscopically silent [22]. Additionally, the binding mechanism for the substrate promiscuous P450 3A4 was more complex, involving three steps [98]. The model which best fit the kinetic steroid binding data for human P450 17A1 involved two conformations of the free enzyme as well as the enzyme-substrate complex. The model suggests that the enzyme binds substrate in only one conformation, which is reasonable considering the existence of P450s in open and closed forms [178]. An additional enzyme-substrate conformation is also supported by the observation of multiple conformations in NMR analyses [179]. In contrast to P450s 3A4 and 19A1, the model fits when all the enzyme-substrate complexes induce a spectral change. Although further analysis is required to validate this binding model, the rates leading to the final and possibly "active" conformation (k_3, Preg = 0.50 s^{-1} and 17α-OHpreg = 0.093 s^{-1}) are comparable to the estimated rates of oxidation.

3.3.6 Conclusions

The results from this study extend the range of P450 17A1 catalytic reactions that are significantly enhanced by b_5 to include 17α-hydroxylation of Preg, but not Prog. The phenomenon correlates with the physiological use of Prog and 17α-OHprog as precursors for other essential steroid hormones (aldosterone and cortisol), while the role b_5 is then to "shunt" steroid synthesis towards androgen production starting with Preg. In principle, channeling steroid production towards DHEA synthesis would be most efficient if the 17α-hydroxy steroid intermediate did not dissociate from the enzyme active site, ergo a processive mechanism. Although the 17α-hydroxy steroid k_{off} rates were relatively unaffected when b_5 was included in the enzyme-inhibitor trapping assays, it is possible the

enzyme-substrate complex stabilization mechanism is only operative when P450 17A1 is in a different oxidation state and was therefore missed under the conditions used. This theory is supported by b_5-mediated coupling of P450 17A1 reduction and catalysis [180], given that the protein does not directly participate in electron transfer [57]. The maintenance of a reactive enzyme conformation by b_5 has historically been attributed to the 17,20-lyase reaction [56,174], but the results from this work clarified that it also occurs with a hydroxylase substrate bound. The reason for selective stimulation of the reaction with Preg over Prog is unclear.

The results from the various catalytic assays provide considerable evidence that b_5 may well induce the catenation of the 17,20-lyase and 17α-hydroxylation reactions with Preg as the substrate. First, the two reactions were inseparable in steady-state incubations when b_5 was incubated with Preg, but not Prog. Furthermore, TAK-700, a reaction-selective inhibitor, was unable to dissect the desmolase reaction from the 17α-hydroxylation reaction at a higher potency in reactions that began with Preg, even though the 17,20-lyase IC_{50} with 17α-OHpreg was lower than for Preg oxidation. This result indicates that the DHEA produced in the Preg incubation was generated through a processive mechanism in which the 17α-OHpreg did not dissociate from the enzyme. The single-turnover reactions exhibited a lag phase, which supports a distributive mechanism, and was more pronounced with Prog as the substrate than when Preg was used. However, the pulse-chase assays with Preg indicated that 17α-OHpreg does not dissociate from the enzyme during the lag phase given DHEA production was not diminished when a saturating amount of competitive substrate was introduced during that period.

The rates generated form global fitting of the individual data sets with a minimal kinetic model indicate that human P450 17A1 is at least partially processive with Preg as the substrate, in that the 17,20-lyase rate was generally two-fold slower than the k_{off} for 17α-OHpreg. Based on the evaluation of bovine P450 17A1 (without b_5) which was characterized as 20% processive [91], the rates for the human enzyme would describe it as a more processive enzyme (50% based on their method of calculation). One

critical caveat however, was the inconsistency observed with steroid binding parameters. Further analysis of the binding kinetics showed that steroid binding is complex and possibly includes a conformation of the free enzyme which is unable to bind substrate and two forms of the enzyme-substrate complex. Presumably one of the two enzyme-substrate complexes could be the more active form, which catalyzes the oxidations at a faster rate. The concept of multiple conformations of the enzyme-substrate complex is substantiated by the observation of additional backbone conformations in NMR analyses [179] and the fact that human P450 17A1 can catalyze various oxidations of the same steroid, one of which occurs when the substrate is flipped around in substrate pocket (6*β*-hydroxylation, see Chapter 2). While further investigation is necessary to verify its validity, a mechanistic model is proposed in which the E´ pathway constitutes an alternative conformation, which is stabilized by b_5, that facilitates the reactions at a faster rate (Figure 3.12). Global data fitting to this model was unsuccessful due to unresolved issues with the software crashing.

In summary, the observations from this investigation indicate that the mechanism for P450 17A1 catalysis of the two reactions is primarily distributive in the absence of b_5 and becomes more processive with the Δ^5 series steroids when b_5 is present. The processivity of human P450 17A1 becomes an issue when attempting to selectively inhibit the 17,20-lyase reaction as a treatment for prostate cancer, considering that such a mechanism does not provide an opportunity to parse out the intended function through an competitive inhibitor. In this regard, selective inhibition of androgen production will only be possible if the interactions between human P450 17A1 and b_5 as disrupted.

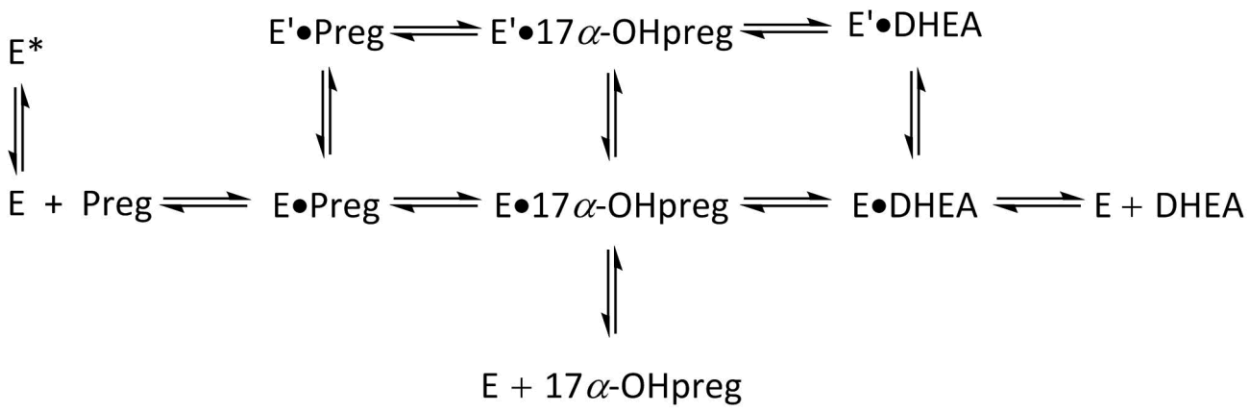

Figure 3.12 Hypothetical human P450 17A1 reaction scheme with additional conformations

The Δ^5 steroids are presented but also represent the Δ^4 steroids.

3.4 Material and Methods

3.4.1 Reagents

Most of the steroids were obtained from either Sigma-Aldrich or Steraloids (Wilton, NH). DHEA was purchased from Waterstonetech (Carmel, IN). [7-^{3}H(N)]-Preg was purchased from PerkinElmer (NET039001MC). [4-^{14}C]-Prog (ARC1398) and [1,2,6,7-^{3}H]-17α-OHprog (ART 0638) were purchased from American Radiolabeled Chemicals (St. Louis, MO. The (*S*)-TAK-700 enantiomer was a generous gift of Millennium Pharmaceuticals.

3.4.2 Purification of (R)-TAK-700

A racemic mixture of TAK-700 was purchased from ApexBio (catalog number A4326), and the compound was dissolved in CH_3OH for purification of the enantiomers. The (*S*)- and (*R*)- enantiomers were resolved on a Chiralcel® OJ-RH 4.6 x 150 mm column with an isocratic 63.5% CH_3OH – 36.5% H_2O mobile phase. The two enantiomeric fractions with absorbance peaks at 238 nm were collected. The (*S*)- and (*R*)- fractions were differentiated using a standard (*S*)-TAK-700 sample (see General section). The (*S*)-TAK-700 was extracted from the aqueous solution with CH_2Cl_2 and the solvent was evaporated *in vacuo*. The dried solid was stored at -20 °C until further use.

3.4.3 Enzymes

E. coli recombinant rat POR and human liver b_5 were prepared as described by Hanna et al. [167] and Guengerich [168], respectively. *E. coli* recombinant human P450 17A1 was prepared as described in Chapter 2. Cholesterol oxidase from Streptomyces sp. was purchased from Sigma-Aldrich (C8649).

3.4.4 Catalytic Assays

3.4.4.1 Steady-state Incubations

The steady-state catalytic assays were conducted using a reconstituted enzyme system in a final reaction volume of 0.5 ml. The reaction mixtures typically contained 0.01-0.5 μM human P450 17A1, 2 μM rat POR, 0.5 μM human b_5 (when included), and 16 μM L-α-1,2-dilauroyl-*sn*-glycero-3-

phosphocholine (added as lipid vesicles after sonication of 1 mg/ml stock; DLPC) in 50 mM potassium phosphate buffer (pH 7.4; KPhos). The P450 17A1 enzyme concentrations used were: 0.01 μM for incubations with Preg and 17-OHpreg, 0.01 μM and 0.5 μM for Prog 17α-hydroxylation and 16α-hydroxylation (respectively), and 0.5 μM in 17-OHprog desmolase assays. Substrate was added at concentrations ranging from 0.2 to 20 μM. Duplicate samples were pre-warmed at 37 °C for 5 min (water bath with gentle shaking) and reactions initiated with the addition of an NADPH-generating system (10 mM glucose 6-phosphate, 0.5 mM $NADP^+$, and 2 μg/ml yeast glucose 6-phosphate dehydrogenase) [181]. The mixtures were incubated for 5 min at 37 °C. Reactions were quenched with the 2 ml CH_2Cl_2, mixed with a vortex device, and placed on ice. The samples were centrifuged to separate the organic and aqueous layers, and 90% of the organic phase was transferred to a new vessel and evaporated under a nitrogen stream. The extracts from Prog and 17-OHprog incubations were resuspended in 100 μl of a CH_3CN-H_2O (1:1) mixture and 10 μl of this was analyzed by UPLC-UV. The Preg and 17-OHpreg extracts were dissolved in 100 μl CH_3OH, mixed with 400 μl of cholesterol oxidase (0.5 units/reaction), and incubated at 30 °C (with shaking at 200 rpm) for 6-12 hours. The extraction procedure was then repeated, and the samples were resuspended and analyzed as Prog and 17-OHprog. The reaction products were resolved on an Acquity BEH C18 UPLC octadecylsilane column (2.1 mm x 100 mm, 1.7 μm) with mobile phases A, 70% CH_3OH/30% H_2O, and B, CH_3CN, at a 0.2 ml/min flow rate. The mobile phase linear gradient proceeded as follows: 0-1 min, 95% A; 4 min, 70% A; 4.5 min, 60% A; 4.55-6.75 min, 5% A; 7-10 min, 95% A (all v/v). The column temperature was maintained at 40 °C, and the sample chamber was held at 4 °C. The reaction products were identified by co-elution with commercial standards and quantified by the A_{243} peak area. k_{cat} and K_m values were estimated from hyperbolic fits in Prism software (GraphPad, San Diego, CA).

3.4.4.2 Single-Turnover Conditions

Single-turnover incubations were performed using an RQF-3 quench-flow instrument (KinTek Corp, Snow Show, PA). The instrument operates through a series of rapid mixing steps through two in-line incubation chambers, where each step dilutes the samples two-fold. The instrument temperature was conditioned at 37 °C. The enzyme substrate mixture in these reactions included 4 μM steroid, 4 μM human P450 17A1, 8 μM rat POR, 4 μM human b_5 (when added), and 32 μM DLPC (lipid vesicles) in 100 mM KPhos (pH 7.4). The following radiolabeled substrates were used in these studies: ^{3}H-Preg (1 mCi/μmol), ^{3}H-17-OHpreg (0.7 mCi/μmol), ^{14}C-Prog (0.06 mCi/μmol), and ^{3}H-17-OHprog (1 mCi/μmol). The reactions were initiated through rapid mixing with 1 mM NADPH in 50 mM KPhos (7.4) in the first reaction chamber. The samples were incubated from 0.5 to 30 s, at which point, the reactions were quenched with HCl (1 M) as they were pushed through the second reaction into the collection vessel. Four time point replicates were collected into the same vessel for analysis to compensate for the low specific activity of ^{14}C-Prog, and the procedure was applied for the other substrates. The samples were centrifuged at 2,000 x g for 5 min to eliminate precipitated protein and the supernatant directly subjected to analysis by HPLC-UV-on-line liquid scintillation counting methods. The reaction products were resolved on a Zorbax RX-C8 octylsilane (4.6 mm x 250 mm, 5 μm) column with mobile phases A, 95% H_2O/5% CH_3OH, and B, 95% CH_3OH/5% H_2O (v/v). With the column at ambient temperature, the following linear gradients (1 ml/min) were used: ^{3}H-Preg, ^{14}C-Prog, and ^{3}H-17-OHprog assays: 0-10 min, 70% B, 15-18 min, 100% B, 20-30 min, 70% B; ^{3}H-17-OHpreg assays: 0-15 min, 65% B, 20-23 min, 100% B, 25-35 min, 65% B (all v/v). The scintillation fluid (Liquiscint™, National Diagnostics, Atlanta, GA) flow rate was 3 ml/min. The reaction products were identified by co-elution with commercial standards (monitored at A_{216} (Preg, 17-OHpreg, and DHEA) and A_{243} (Prog, 17-OHprog, 16-OHprog and Andro)) and quantified by the radiochromatogram peak area using *β*-RAM software.

Radiolabeled 17-OHpreg was prepared through enzyme-mediated conversion of [7-^{3}H(N)]-Preg. [7-^{3}H(N)]-17-OHpreg was obtained from a 30 s incubation with the enzyme system described above, devoid of b_5. The radiolabeled steroid was purified by the chromatographic method applied for ^{3}H-17-OHpreg assays, and fractions were collected (without the *β*-RAM system). The steroid was extracted from the mobile phase with CH_2Cl_2, the organic (lower) layer transferred to a new vessel, and the solvent evaporated under a nitrogen stream. The dried extract was dissolved in C_3H_5OH, and co-elution with commercial 17-OHpreg was used to validate the identity of the radiolabeled compound.

3.4.4.3 Pulse-Chase Assays

Pulse-chase experiments were performed to follow the conversion of ^{3}H-Preg to ^{3}H-DHEA at steady-state and single-turnover conditions.

The reconstituted enzyme-substrate mixture in the steady-state pulse-chase assays is consistent with the protocol described for steady-state incubations, with the following alterations: 1) 0.5 μM human P450 17A1, and 2) 50 μM ^{3}H-Preg (0.013 mCi/μmol). One minute after the reactions were started with the NADPH-generating system, the mixtures were mixed with unlabeled 17-OHpreg, at varying concentrations (5 – 75 μM and vehicle), and the incubations continued for ten minutes before quenching with HCl (0.67 M, final). The mixtures were centrifuged to clear precipitated protein and the steroid products were resolved and quantified by the HPLC methods employed in the single-turnover experiments (*vide supra*) with the following linear gradient: 0-9 min, 75% B; 13.4 min, 86% B; 13.5-15 min, 90% B; 16-25 min, 75% B (all v/v).

The pulse-chase assays done at single-turnover conditions followed a protocol similar to that outlined above, with some distinctions. The standard single-turnover procedure includes one reaction phase, while a pulse-chase experiment requires two incubation periods. This was achieved in the rapid quench instrument by utilizing the second reaction chamber and incubating with a chase compound, while the quenching agent is placed in the collection vial. The reagent concentrations were increased so

that, after two dilutions, the working concentrations in the chase step (second phase) matched those from the single-turnover incubations. The specific activity of ^{3}H-Preg was adjusted to 0.83 mCi/μmol, and 80 μM unlabeled 17-OHpreg was used as the chase compound. The pulse length was varied between 0.05 and 2 s and the chase continued for 5 s before the reaction was quenched in the collection vessel with HCl (0.6 M final). The mixtures were centrifuged to clear precipitated protein, and the steroid products were resolved and quantitated by the method described for the steady-state pulse-chase assays.

3.4.4.4 TAK-700 Inhibition

Competitive inhibition studies with the TAK-700 enantiomers were performed and analyzed by the methods described for steady-state assays. The inhibitors were added to the enzyme substrate mixture with the final composition as: 0.005-100 μM (*S*)- or (*R*)-TAK-700, 5 μM substrate, 0.01 μM human P450 17A1 (0.1 μM in assays with 17-OHprog) , 0.5 μM human b_5, 2 μM POR, 16 μM DLPC (lipid vesicles) in 50 mM KPhos (7.4). The remaining steps, including cholesterol oxidase conversion in Preg and 17-OHpreg assays, were done as described for the steady-state experiments, with the exception of the mobile phase. In order to resolve an inconsistent TAK-700 migration profile, the mobile phase was changed to 5 mM $NH_4CH_3CO_2$-70% CH_3OH/30% H_2O for A and 5 mM $NH_4CH_3CO_2$-90% CH_3CN/10% H_2O for B (all v/v). IC_{50} values were calculated in GraphPad Prism using the formula: Y=bottom+(top-bottom)/(1+10^(X-logIC_{50})).

3.4.5 Binding Studies

3.4.5.1 Ligand Binding

Initial binding studies were performed using previously reported methods [127]. In a 10 cm cell (Starna Cells, Atascadero, CA, catalogue no. 34Q-100, 25 ml), the steroid ligands were incrementally added to 0.1 μM human P450 17A1 in 50 mM KPhos (7.4). The experiment was conducted as a series of additions, and the enzyme samples were exposed to ambient temperature, recurrent mixing, and a

strong light beam for periods > 60 min. Subsequent control experiments, where ligand was not added, exhibited spectral instability in the enzyme over the same period of time. Specifically, a time-dependent decrease in the Soret band was observed, which is problematic considering that the change in the Soret band (upon ligand binding) is the outcome analyzed in the assays (note: no obvious precipitation occurred).

Steroid binding was reanalyzed, with untreated enzyme samples for each steroid concentration, using a stopped-flow instrument equipped with a 20 mm cell and a rapid scanning monochrometer (OLIS RSM-1000, On-Line Instrument Systems, Bogart, GA). The stopped-flow sample syringes were conditioned at 37 °C and filled with either 2 μM human P450 17A1 or 0.2-20 μM steroid in 100 mM KPhos (7.4) with 120 μM DLPC (lipid vesicles). After mixing, the instrument recorded the absorbance spectrum from 350-500 nm at one millisecond intervals for up to 7 s. The differential absorbance maxima and minima were determined by subtracting the final and initial (0 s) spectra. The composite absorbance changes, Δ ($A_{max} - A_{min}$), from three replicates were averaged and plot against the ligand concentrations. The data were fit with a quadratic binding formula to estimate binding constants (K_d) using GraphPad Prism.

$$Y=B+(A/2)(1/E)((K_d+E+X)-((K_d+E+X)^2-(4EX)))^{1/2}$$

3.4.5.2 Inhibitor Trapping

Spectral enzyme-inhibitor trapping assays were implemented to measure dissociation rates for the steroid ligands. The analysis is dependent upon a faster inhibitor binding rate versus the dissociation rates for the steroids. The experiments were performed at ambient temperature using the stopped-flow apparatus described above and (*S*)-TAK-700 as the trapping inhibitor. The on rate for (*S*)-TAK-700 was first measured by mixing 4 μM human P450 17A1 in 100 mM KPhos (7.4) (with 120 μM DLPC (lipid vesicles)) and 20 μM (*S*)-TAK-700 (in the same buffer). The rate was estimated by singular value decomposition (SVD) analysis of the experimental data matrix with the following parameters:

absorbance: measured value, wavelength; 350-500 nm (200 points), and time: 0-1 s (one scan per millisecond). The data was fit with a two-species sequential model (simple first-order) and the calculated rates from at least three replicates were averaged. To assess the dissociation rates, the steroid ligands (4 μM) and human b_5 (4 μM, when included) were added to the enzyme solution. The time component was 0-10 s (averaged mode, 62 scans per second) and data were analyzed as stated.

3.4.6 Kinetic Analysis

Steroid association rate (k_{on}) parameters were calculated using the corresponding dissociation rates (k_{off}), estimated from the inhibitor trapping assays, and the dissociation constants (K_d), derived from the steroid binding experiments, based on the following equation:

$$K_d = k_{off} / k_{on}$$

The experimental data from the catalytic assays, under single-turnover and steady-state conditions, and steroid titrations were concurrently fit to a minimal kinetic model in the KinTek software. The predetermined rates parameters (k_{on}, k_{off}, K_d, and single-turnover substrate conversion rates) were used as starting values in the model, and in some cases, the values were fixed. The limits for the molar extinction coefficients that were applied to the spectral binding experiments were derived from the prior fit with a quadratic formula in prism (see above). The details for each of the model variations are presented in the fit results (Appendix). The imported data sets included the averaged data point with standard deviation (when applicable).

In order to accurately fit the ligand titration and catalytic experiments in a single model, a "kinetically silent" second order activation step was added to prevent the software from regarding the binding assay as a catalytic experiment. The activation step corresponds to the combined P450 17A1 reaction steps that lead to the chemically competent iron-oxygen species (i.e. reduction by POR, binding of molecular oxygen, protonation, and loss of water), which were not evaluated. The concentration of the "activating reagent" was fixed at 1 μM and a K_{eq} of 1 μM was set with $k_{forward}$ = 100 $\mu M^{-1} s^{-1}$ and $k_{reverse}$

= 100 s^{-1}, with the intention of forcing the step to be rapidly reversible in order to prevent any kinetic influence on the other parameters. Additionally, the reversibility accounted for uncoupling (loss of iron-oxygen species that results in the Fe^{3+}) that can occur during Compound I (or ferric peroxide) formation. Any rate limitations derived from uncoupling were considered to be factored into the rate of the chemical reaction step. Simulations without the activation step produced similar results at the same constraints.

The kinetic model was reduced for analysis of the single-turnover pulse-chase data to conform to single-turnover conditions, and paralleled the model applied for analysis of P450 17A1 from other species [90,91].

Steroid binding kinetics was evaluated by applying different enzyme-ligand binding models to the kinetic data obtained in stopped-flow binding assays (see Section 3.4.5.1) using the KinTek Explorer software. The data was reduced by taking the difference of the kinetic traces (~7 s trace, 1 scan per millisecond) at the wavelengths previously designated for A_{max} and A_{min} (e.g. A_{391} and A_{426} kinetic traces were subtracted for Preg assays; see Section 3.4.5.1 and Figure 3.1). Three replicate difference traces for each steroid concentration were averaged and then normalized to t= 0 s. The kinetic traces were then reduced once more by boxed average (n=5) with standard deviation, before import into the KinTek software. The binding models tested included 2-ligand binding and alternative conformations of the enzyme and enzyme-substrate complex. In some models, the visibility of the substrate-enzyme complexes was also varied.

Chapter 4

4. Concluding Remarks

4.1 New Products, New Pathways

P450 17A1 is an indispensable enzyme that functions at the center of the human steroid biosynthetic pathway. Through interactions with b_5, P450 17A1 mediates diverging pathways that lead to the production of glucocorticoids and sex hormones by oxidation of Preg and Prog to 17α-hydroxy steroids and subsequently to DHEA and Andro, respectively. The physiological relevance of these steroid end products is well understood. Glucocorticoids (primarily cortisol in humans) are important for a variety of functions, including stress response, immune system suppression, gluconeogenesis, and lipid metabolism. The sex steroids are divided into two classes: androgens, which are responsible for masculinization and male reproductive function, and estrogens, which mediate the female reproductive system and feminization. Additionally, 16α-OHprog is another well-known end product generated by human P450 17A1 but does not have a defined function, although agonistic activity of the progesterone receptor has been reported and regulation of electrolyte balance was speculated [182]. Interestingly, human P450 17A1 does not catalyze 16α-hydroxylation of Preg.

The scope of P450 17A1 oxidation reactions has been redefined in this investigation. In contrast to the selectivity observed with Preg and Prog, human P450 17A1 converted both 17α-OHpreg and 17α-OHprog into 16(α),17α-dihydroxy steroids. The physiological relevance for the biosynthesis of these novel products is unknown; however, patents for the synthetic preparation of these molecules were obtained as early as 1955 [183,184]. The more studied of the two, 16α,17α-$(OH)_2$prog (also known as algestone) is currently used as the nucleus for the contraceptive drug dihydroxyprogesterone acetophenide. Additionally, human P450 17A1-mediated 16(α)-hydroxylation of DHEA and Andro was also observed, whereas 16α-OH-DHEA production has previously been attributed to P450 3A4 [153,154].

These 16(α)-hydroxy androgens are quite relevant to human biology as they are precursors to estriol (155,156), an estrogen that is found in high levels during pregnancy.

Although unexpected, the identification of additional 16-hydroxylation products is conceivable based on the established reaction with Prog. However, it was unprecedented that human P450 17A1 would be able catalyze a third oxidation reaction with the dihydroxy steroids. The initial hypothesis proposed that the third hydroxylation would be located on carbon-21, considering that trace levels of 21-hydroxylation activity had been reported for the enzyme [40]. Remarkably, NMR analysis of the new products revealed that the oxidation occurred on the steroid B-ring, whereas all the typical P450 17A1 oxidations are localized to the D-ring of the molecule. The new Δ^4 steroid was characterized as 6*β*,16*α*,17*α*-$(OH)_3$prog. A putative B-ring oxidized product was also detected in 16*α*,17*α*-$(OH)_2$preg incubations, but not enough was obtained for adequate NMR analysis. Additionally, human P450 17A1 utilized the dihydroxy steroids as substrates for the 17,20-lyase reaction, which was the primary product observed with 16*α*,17*α*-$(OH)_2$preg as the substrate, yielding an alternative pathway to 16-hydroxy androgen synthesis. The physiological relevance of the trihydroxy steroids is unknown, and their identification has not been reported in prior studies. However, the same oxidation sites were recognized on tetrahydroxy steroids that were identified in urine from neonates with 21-hydroxylase deficiency [185].

The identification of these new steroids poses several new questions, with the first being what are their biological functions? Do they activate, or antagonize, the steroid receptors and signaling pathways in the same fashion as their precursors? Are these steroids found in the body, or is their production simply a phenomenon of the *in vitro* conditions used? These results also challenge the general concept that P450s that oxidize endogenous substrates are constrained to specified catalytic functions based on smaller active sites but xenobiotic metabolizing P450s have larger substrate pockets that facilitate their promiscuity. Is it possible that the other steroid metabolizing P450s also have

unrestrained catalytic abilities, and can they use these new steroids as substrates? These questions can be answered through biochemical analyses, and although it is mere speculation at this point, it would not be surprising if new steroid pathways were identified.

4.2 The b_5 Effect

The b_5-mediated stimulation of human P450 17A1 catalytic activities is a well-known phenomenon. The effect has mainly been recognized with the 17,20-lyase reaction in comparison with 17α-hydroxylation, considering that the reaction rates were augmented by up to ten-fold and two-fold, respectively [53,56,65,169,174]. In reactions with some other P450 enzymes, b_5 acts as a redox partner by facilitating electron transfer to the P450 [54,55]. This role has been precluded for interactions with human P450 17A1 following the observation that redox-deficient apo-b_5 and a Mn-substituted form were able to stimulate the activity [56,57]. The most popular theory has been that b_5 enhances the 17,20-lyase activity by allosterically promoting an enzyme-substrate conformation that facilitates ferric peroxide chemistry [56,174]. However, the analyses discussed in Chapter 2 provide considerable evidence that the cleavage reaction can be arbitrated by the Compound I form of human P450 17A1. Furthermore, b_5 enhanced the 17,20-lyase activity when an oxygen surrogate for Compound I (iodosylbenzene) was employed. Presumably, this result suggests that the allosteric activity of b_5 may occur after the formation of the Compound I iron-oxygen species. Another indication that b_5 is not selective for the ferric peroxide form of human P450 17A1 is that the protein also enhanced 17α- and 16(α)-hydroxylation of Preg and 17α-hydroxy steroids, respectively.

This investigation has produced the first account that b_5 significantly augments the 17α-hydroxylation of Preg, in addition to the 17,20-lyase reaction with the 17α-hydroxy steroids. However, it is still unclear why the same effect was not observed in Prog oxidation. The analyses discussed in Chapter 3 suggest that b_5 stimulates the steps involved in the chemical reaction, which take place after substrate binding and before product release. These observations are consistent with a report that b_5-

mediates the coupling of NADPH consumption and product formation, although the authors indicated the effect was primarily observed for the 17,20-lyase reaction [180]. However, close inspection of the results show that Preg 17α-hydroxylation also exhibited a modest stimulation by b_5, but not in the case with Prog. Based on the results from this investigation, it is likely that a greater effect would have been observed with Preg if the incubation conditions used were more similar to those employed in this work. Still perplexing, however, is the observation that b_5 would affect this reaction phase considering that is when reduction occurs, but it is not active in electron transfer with human P450 17A1. The enigma is further complicated by the characterization that the b_5 and POR both interface with the same site on human P450 17A1 [67]. It is possible that POR is replaced by b_5 following the reduction steps to stabilize the Compound I intermediate, which is conceivable given that b_5 stimulated the reactions supported by iodosylbenzene (which does not involve electron transfer). However, such an exchange is impractical if the end result is a faster reaction rate.

4.3 Processivity and Human P450 17A1 Inhibition

"Studies on Prostatic Cancer… may be the first translational research study of a molecularly targeted therapy in the history of cancer," commented William G. Nelson about the 1941 *Cancer Research* article authored by Charles Huggins and Clarence V. Hodges [186,187]. The 1966 Nobel Prize in Physiology or Medicine was awarded to Huggins "for his discoveries concerning hormonal treatment of prostatic cancer." To date, androgen deprivation remains the primary form of therapy for prostate cancer, which is accomplished by removing the androgen producing tissues (castration) in advanced cases. Although the initial response is positive, cancer progression typically ensues as CRPC. Development of CRPC can be caused by mutations in the androgen receptor, but it is common that androgen production from the adrenals and tumors is the driving factor. In this regard, the only way to impede CRPC progression is to stop androgen production at the enzyme level. However, targeting human P450 17A1 is problematic in that complete inhibition results in the concomitant loss of

glucocorticoid levels. Currently the only FDA approved human P450 17A1 inhibitor, abiraterone, requires adjuvant prednisone therapy to alleviate the adverse effects caused by the hindered cortisol production.

Reaction-selective inhibition of human P450 17A1 has become a "Holy Grail" in drug development for prostate cancer. TAK-700 is one 17,20-lyase selective inhibitor that went through clinical trials, but the drug incited the same adverse effects produced by abiraterone [77,81,82]. Presumably, the reaction selectivity of the drug was insufficient to obtain a dose that stopped androgen production and allowed sufficient cortisol synthesis. One explanation for this failure is that the 17α-hydroxylation and 17,20-lyase reactions cannot be distinguished if the reactions proceed through a processive mechanism in human. The analyses discussed in Chapter 3 suggest that this may actually be the case. Neither of the TAK-700 enantiomers was able to impede the 17,20-lyase reaction in incubations that included Preg and b_5. Additionally, the pulse-chase assays, which included b_5, indicated that at least a fraction of the 17α-OHpreg did not dissociate from human P450 17A1. This result is confounded by the observation that b_5 did not affect the dissocation rates of the 17α-hydroxy steroids, which were estimated to be faster than the rate of the 17,20-lyase reaction. However, the enzyme-inhibitor trapping assays did not take into account the possible b_5-P450 17A1-substrate complex(es) that exist(s) throughout the entire reaction cycle, which may be the one(s) stabilized by b_5 and establish the processive mechanism.

Another perspective was gained from applying a kinetic model to the experimental binding data and the results from catalytic assays with b_5 included. The rate parameters generated from global fitting suggest that approximately half of the 17α-OHpreg that is bound by human P450 17A1 may proceed through the 17,20-lyase processively when stimulated by b_5. Furthermore, analysis of the kinetic binding data revealed that the human P450 17A1 steroid binding process does not fit to a simple model, and multiple conformations were needed to accurately describe the data. These results require further

validation, but they do provide the basis to propose two conformations of the enzyme-substrate complex, in which one may dissociate the substrate readily, while the other proceeds to catalyze the 17,20-lyase reaction through a processive mechanism and is possibly stabilized by b_5. Confirmation of this model would complicate the development of a reaction-selective competitive inhibitor, unless the human P450 17A1-b_5 interaction can be disrupted.

In summary, the catalytic repertoire of human P450 17A1 has been expanded to include a series of novel 16-hydroxy products, in addition to an unprecedented 6β,16α,17α-trihydroxy steroid. The chemical mechanism for the 17,20-lyase reaction was reevaluated, generating strong evidence for a Compound I-mediated reaction. Analysis of the b_5 effect towards human P450 17A1 catalytic activities revealed that 17α-hydroxylation of Preg is also enhanced at a significant level. Lastly, a kinetic model is proposed that includes two conformations of the enzyme-substrate complex, where one is a b_5-stabilized processive form leading to androgen production.

LITERATURE CITED

1. Magid E, Turbeck BO. The rates of the spontaneous hydration of CO_2 and the reciprocal reaction in neutral aqueous solutions between 0 degrees and 38 degrees. *Biochim Biophys Acta*. 1968;165(3):515-24.
2. Steiner H, Jonsson BH, Lindskog S. The catalytic mechanism of carbonic anhydrase. Hydrogen-isotope effects on the kinetic parameters of the human C isoenzyme. *Eur J Biochem*. 1975;59(1):253-9.
3. Lindskog S. Structure and mechanism of carbonic anhydrase. *Pharmacol Ther*. 1997;74(1):1-20.
4. Copeland RA. Enzymes a Practical Introduction to Structure, Mechanism, and Data Analysis. New York: Wiley; 2000.
5. Fischer E. Einfluss der configuration auf die wirkung der enzyme. *Ber Dtsch Chem Ges*. 1894;27(3):2985-93.
6. Lichtenthaler FW. 100 years “schlüssel-schloss-prinzip”: what made Emil Fischer use this analogy? *Angew Chem Int Ed*. 1995;33(23-24):2364-74.
7. Brown AJ. XXXVI.-Enzyme action. *J Chem Soc*. 1902;81(0):373-88.
8. Michaelis L, Menten ML. Die kinetik der invertinwirkung. *Biochem Z*. 1913;49:333-69.
9. Johnson KA, Goody RS. The original Michaelis constant: translation of the 1913 Michaelis-Menten paper. *Biochemistry*. 2011;50(39):8264-9.
10. Briggs GE, Haldane JB. A note on the kinetics of enzyme action. *Biochem J*. 1925;19(2):338-9.
11. Lineweaver H, Burk D. The determination of enzyme dissociation constants. *J Am Chem Soc*. 1934;56(3):658-66.
12. Hofstee BH. Non-inverted versus inverted plots in enzyme kinetics. *Nature*. 1959;184:1296-8.
13. Johnson KA. Fitting enzyme kinetic data with KinTek Global Kinetic Explorer. *Methods Enzymol*. 2009;467:601-26.
14. Johnson KA, Simpson ZB, Blom T. FitSpace explorer: an algorithm to evaluate multidimensional parameter space in fitting kinetic data. *Anal Biochem*. 2009;387(1):30-41.
15. Nelson DR. The cytochrome P450 homepage. *Hum Genomics*. 2009;4(1):59.
16. Rupasinghe S, Schuler MA, Kagawa N, Yuan H, Lei L, Zhao B, Kelly SL, Waterman MR, Lamb DC. The cytochrome P450 gene family CYP157 does not contain EXXR in the K-helix reducing the absolute conserved P450 residues to a single cysteine. *FEBS Lett*. 2006;580(27):6338-42.
17. Omura T, Sato R. A new cytochrome in liver microsomes. *J Biol Chem*. 1962;237:1375-6.
18. Omura T, Sato R. The carbon monoxide-binding pigment of liver microsomes. Ii. solubilization, purification, and properties. *J Biol Chem*. 1964;239:2379-85.
19. Omura T, Sato R. The carbon monoxide-binding pigment of liver microsomes. I. evidence for its hemoprotein nature. *J Biol Chem*. 1964;239:2370-8.
20. Guengerich FP, Munro AW. Unusual cytochrome P450 enzymes and reactions. *J Biol Chem*. 2013;288(24):17065-73.
21. Rittle J, Green MT. Cytochrome P450 Compound I: capture, characterization, and C-H bond activation kinetics. *Science*. 2010;330(6006):933-7.
22. Sohl CD, Guengerich FP. Kinetic analysis of the three-step steroid aromatase reaction of human cytochrome P450 19A1. *J Biol Chem*. 2010;285(23):17734-43.
23. Nelson DR, Koymans L, Kamataki T, Stegeman JJ, Feyereisen R, Waxman DJ, Waterman MR, Gotoh O, Coon MJ, Estabrook RW, Gunsalus IC, Nebert DW. P450 superfamily: update on new sequences, gene mapping, accession numbers and nomenclature. *Pharmacogenetics*. 1996;6(1):1-42.

24. Poulos TL, Finzel BC, Gunsalus IC, Wagner GC, Kraut J. The 2.6-A crystal structure of Pseudomonas putida cytochrome P-450. *J Biol Chem*. 1985;260(30):16122-30.
25. Poulos TL, Finzel BC, Howard AJ. High-resolution crystal structure of cytochrome P450cam. *J Mol Biol*. 1987;195(3):687-700.
26. Berman HM, Westbrook J, Feng Z, Gilliland G, Bhat TN, Weissig H, Shindyalov IN, Bourne PE. The protein data bank. *Nucleic Acids Res*. 2000;28(1):235-42.
27. Hasemann CA, Kurumbail RG, Boddupalli SS, Peterson JA, Deisenhofer J. Structure and function of cytochromes P450:a comparative analysis of three crystal structures. *Structure*. 1995;3(1):41-62.
28. Krauser JA, Voehler M, Tseng LH, Schefer AB, Godejohann M, Guengerich FP. Testosterone 1 β-hydroxylation by human cytochrome P450 3A4. *Eur J Biochem*. 2004;271(19):3962-9.
29. Cheng Q, Sohl CD, Yoshimoto FK, Guengerich FP. Oxidation of dihydrotestosterone by human cytochromes P450 19A1 and 3A4. *J Biol Chem*. 2012;287(35):29554-67.
30. Guengerich FP, Cheng Q. Orphans in the human cytochrome P450 superfamily: approaches to discovering functions and relevance in pharmacology. *Pharmacol Rev*. 2011;63(3):684-99.
31. Nebert DW, Russell DW. Clinical importance of the cytochromes P450. *Lancet*. 2002;360(9340):1155-62.
32. Guengerich FP. Human cytochrome P450 enzymes. In: Ortiz de Montellano PR, editor. Cytochrome P450: Structure, Mechanism, and Biochemistry. NY: Springer International Publishing; 2015. p. 523-785.
33. Wienkers LC, Heath TG. Predicting in vivo drug interactions from in vitro drug discovery data. *Nat Rev Drug Discov*. 2005;4(10):825-33.
34. Häggström M, Stannered, Hoffmeier, Settersr, Richfield D. Diagram of the pathways of human steroidogenesis. *WikiJournal of Medicine*. 2014;1(1):1-5.
35. Pruitt KD, Brown GR, Hiatt SM, Thibaud-Nissen F, Astashyn A, Ermolaeva O, Farrell CM, Hart J, Landrum MJ, McGarvey KM, Murphy MR, O'Leary NA, Pujar S, Rajput B, Rangwala SH, Riddick LD, Shkeda A, Sun H, Tamez P, Tully RE, Wallin C, Webb D, Weber J, Wu W, DiCuccio M, Kitts P, Maglott DR, Murphy TD, Ostell JM. RefSeq: an update on mammalian reference sequences. *Nucleic Acids Res*. 2014;42(D1):D756-D63.
36. Schonemann MD, Muench MO, Tee MK, Miller WL, Mellon SH. Expression of P450c17 in the human fetal nervous system. *Endocrinology*. 2012;153(5):2494-505.
37. Puche C, Jose M, Cabero A, Meseguer A. Expression and enzymatic activity of the P450c17 gene in human adipose tissue. *Eur J Endocrinol*. 2002;146(2):223-9.
38. Casey ML, MacDonald PC. Demonstration of steroid 17α-hydroxylase activity in human fetal kidney, thymus, and spleen. *Steroids*. 1982;40(1):91-7.
39. Swart P, Swart AC, Waterman MR, Estabrook RW, Mason JI. Progesterone 16 alpha-hydroxylase activity is catalyzed by human cytochrome P450 17 alpha-hydroxylase. *J Clin Endocrinol Metab*. 1993;77(1):98-102.
40. Yoshimoto FK, Zhou Y, Peng H-M, Stidd D, Yoshimoto JA, Sharma KK, Matthew S, Auchus RJ. Minor activities and transition state properties of the human steroid hydroxylases cytochromes P450c17 and P450c21, from reactions observed with deuterium-labeled substrates. *Biochemistry*. 2012;51(36):7064-77.
41. Flück CE, Miller WL, Auchus RJ. The 17, 20-lyase activity of cytochrome P450c17 from human fetal testis favors the Δ^5 steroidogenic pathway. *J Clin Endocrinol Metab*. 2003;88(8):3762-6.
42. Soucy P, Lacoste L, Luu-The V. Assessment of porcine and human 16-ene-synthase, a third activity of P450c17, in the formation of an androstenol precursor. *Eur J Biochem*. 2003;270(6):1349-55.

43. Akhtar M, Corina D, Miller S, Shyadehi AZ, Wright JN. Mechanism of the acyl-carbon cleavage and related reactions catalyzed by multifunctional P-450s: studies on cytochrome P-$450_{17\alpha}$. *Biochemistry*. 1994;33(14):4410-8.
44. Akhtar M, Calder MR, Corina DL, Wright JN. Mechanistic studies on C-19 demethylation in oestrogen biosynthesis. *Biochem J*. 1982;201(3):569-80.
45. Yoshimoto FK, Guengerich FP. Mechanism of the third oxidative step in the conversion of androgens to estrogens by cytochrome P450 19A1 steroid aromatase. *J Am Chem Soc*. 2014;136(42):15016-25.
46. Sanghvi A, Grassi E, Warty V, Diven W, Wight C, Lester R. Reversible activation-inactivation of cholesterol 7α-hydroxylase possibly due to phosphorylation-dephosphorylation. *Biochem Biophys Res Commun*. 1981;103(3):886-92.
47. Sanghvi A, Grassi E, Diven W. Loss of cholesterol 7α-hydroxylase activity in vitro in the presence of bivalent metal ions and by dialysis of rat liver microsomes. *Proc Natl Acad Sci U S A*. 1983;80(8):2175-8.
48. Redlich G, Zanger UM, Riedmaier S, Bache N, Giessing ABM, Eisenacher M, Stephan C, Meyer HE, Jensen ON, Marcus K. Distinction between human cytochrome P450 (CYP) isoforms and identification of new phosphorylation sites by mass spectrometry. *J Proteome Res*. 2008;7(11):4678-88.
49. Zhang LH, Rodriguez H, Ohno S, Miller WL. Serine phosphorylation of human P450c17 increases 17,20-lyase activity: implications for adrenarche and the polycystic ovary syndrome. *Proc Natl Acad Sci U S A*. 1995;92(23):10619-23.
50. Tee MK, Miller WL. Phosphorylation of human cytochrome P450c17 by p38α selectively increases 17,20 lyase activity and androgen biosynthesis. *J Biol Chem*. 2013;288(33):23903-13.
51. Pandey AV, Mellon SH, Miller WL. Protein phosphatase 2A and phosphoprotein SET regulate androgen production by P450c17. *J Biol Chem*. 2003;278(5):2837-44.
52. Pandey AV, Miller WL. Regulation of 17,20-lyase activity by cytochrome b_5 and by serine phosphorylation of P450c17. *J Biol Chem*. 2005;280(14):13265-71.
53. Katagiri M, Kagawa N, Waterman MR. The role of cytochrome b_5 in the biosynthesis of androgens by human P450c17. *Arch Biochem Biophys*. 1995;317(2):343-7.
54. Hildebrandt A, Estabrook RW. Evidence for the participation of cytochrome b_5 in hepatic microsomal mixed-function oxidation reactions. *Arch Biochem Biophys*. 1971;143(1):66-79.
55. Yamazaki H, Nakano M, Imai Y, Ueng Y-F, Guengerich FP, Shimada T. Roles of cytochrome b_5 in the oxidation of testosterone and nifedipine by recombinant cytochrome P450 3A4 and by human liver microsomes. *Arch Biochem Biophys*. 1996;325(2):174-82.
56. Lee-Robichaud P, Akhtar ME, Akhtar M. Control of androgen biosynthesis in the human through the interaction of Arg347 and Arg358 of CYP17 with cytochrome b_5. *Biochem J*. 1998;332(2):293-6.
57. Auchus RJ, Lee TC, Miller WL. Cytochrome b_5 augments the 17,20-lyase activity of human P450c17 without direct electron transfer. *J Biol Chem*. 1998;273(6):3158-65.
58. Morgan ET, Coon MJ. Effects of cytochrome b_5 on cytochrome P-450-catalyzed reactions. Studies with manganese-substituted cytochrome b_5. *Drug Metab Dispos*. 1984;12(3):358-64.
59. Guryev OL, Gilep AA, Usanov SA, Estabrook RW. Interaction of apo-cytochrome b_5 with cytochromes P4503A4 and P45017A: relevance of heme transfer reactions. *Biochemistry*. 2001;40(16):5018-31.
60. Yamazaki H, Shimada T, Martin MV, Guengerich FP. Stimulation of cytochrome P450 reactions by apo-cytochrome b_5 : evidence against transfer of heme from cytochrome p450 3A4 to apo-cytochrome b_5 or heme oxygenase. *J Biol Chem*. 2001;276(33):30885-91.

61. Simonov AN, Holien JK, Yeung JCI, Nguyen AD, Corbin CJ, Zheng J, Kuznetsov VL, Auchus RJ, Conley AJ, Bond AM, Parker MW, Rodgers RJ, Martin LL. Mechanistic scrutiny identifies a kinetic role for cytochrome b_5 regulation of human cytochrome P450c17 (CYP17A1, P450 17A1). *PLOS ONE*. 2015;10(11):e0141252.
62. DeVore NM, Scott EE. Structures of cytochrome P450 17A1 with prostate cancer drugs abiraterone and TOK-001. *Nature*. 2012;482(7383):116-9.
63. Petrunak EM, DeVore NM, Porubsky PR, Scott EE. Structures of human steroidogenic cytochrome P450 17A1 with substrates. *J Biol Chem*. 2014;289(47):32952-64.
64. Geller DH, Auchus RJ, Mendonca BB, Miller WL. The genetic and functional basis of isolated 17,20-lyase deficiency. *Nat Genet*. 1997;17(2):201-5.
65. Lee-Robichaud P, Akhtar ME, Wright JN, Sheikh QI, Akhtar M. The cationic charges on Arg347, Arg358 and Arg449 of human cytochrome P450c17 (CYP17) are essential for the enzyme's cytochrome b_5-dependent acyl-carbon cleavage activities. *J Steroid Biochem Mol Biol*. 2004;92(3):119-30.
66. Peng H-M, Liu J, Forsberg SE, Tran HT, Anderson SM, Auchus RJ. Catalytically relevant electrostatic interactions of cytochrome P450c17 (CYP17A1) and cytochrome b_5. *J Biol Chem*. 2014;289(49):33838-49.
67. Estrada DF, Laurence JS, Scott EE. Substrate-modulated cytochrome P450 17A1 and cytochrome b_5 interactions revealed by NMR. *J Biol Chem*. 2013.
68. Miller WL, Auchus RJ. The molecular biology, biochemistry, and physiology of human steroidogenesis and its disorders. *Endocr Rev*. 2011;32(1):81-151.
69. Scaroni C, Opocher G, Mantero F. Renin-angiotensin-aldosterone system: A long-term follow-up study in 17α-hydroxylase deficiency syndrome (17OHDS). *Clin Exp Hypertens A*. 1986;8(4-5):773-80.
70. Sherbet DP, Tiosano D, Kwist KM, Hochberg Z, Auchus RJ. CYP17 mutation E305G causes isolated 17,20-lyase deficiency by selectively altering substrate binding. *J Biol Chem*. 2003;278(49):48563-9.
71. Geller DH, Auchus RJ, Miller WL. P450c17 mutations R347H and R358Q selectively disrupt 17,20-lyase activity by disrupting interactions with P450 oxidoreductase and cytochrome b_5. *Mol Endocrinol*. 1999;13(1):167-75.
72. Cai C, Chen S, Ng P, Bubley GJ, Nelson PS, Mostaghel EA, Marck B, Matsumoto AM, Simon NI, Wang H, Chen S, Balk SP. Intratumoral *de novo* steroid synthesis activates androgen receptor in castration-resistant prostate cancer and is upregulated by treatment with CYP17A1 inhibitors. *Cancer Res*. 2011;71(20):6503-13.
73. Kan PB, Hirst MA, Feldman D. Inhibition of steroidogenic cytochrome P-450 enzymes in rat testis by ketoconazole and related imidazole anti-fungal drugs. *Journal of Steroid Biochemistry and Molecular Biology*. 1985;23(6):1023-9.
74. van der Pas R, Hofland LJ, Hofland J, Taylor AE, Arlt W, Steenbergen J, van Koetsveld PM, de Herder WW, de Jong FH, Feelders RA. Fluconazole inhibits human adrenocortical steroidogenesis in vitro. *J Endocrinol*. 2012;215(3):403-12.
75. Gal M, Orly J. Selective inhibition of steroidogenic enzymes by ketoconazole in rat ovary cells. *Clin Med Insights Reprod Health*. 2014;8(4074-CMRH-Selective-Inhibition-of-Steroidogenic-Enzymes-by-Ketoconazole-in-Rat-O.pdf):15-22.
76. U. S. Food and Drug Administration/Center for Drug Evaluation and Research. Abiraterone acetate. 2015. Silver Spring, MD
77. Bird IM, Abbott DH. The hunt for a selective 17,20 lyase inhibitor; learning lessons from nature. *J Steroid Biochem Mol Biol*. 2016;163:136-46.

78. Kaku T, Matsunaga N, Ojida A, Tanaka T, Hara T, Yamaoka M, Kusaka M, Tasaka A. 17,20-Lyase inhibitors. Part 4: Design, synthesis and structure–activity relationships of naphthylmethylimidazole derivatives as novel 17,20-lyase inhibitors. *Bioorg Med Chem*. 2011;19(5):1751-70.
79. Kaku T, Hitaka T, Ojida A, Matsunaga N, Adachi M, Tanaka T, Hara T, Yamaoka M, Kusaka M, Okuda T, Asahi S, Furuya S, Tasaka A. Discovery of orteronel (TAK-700), a naphthylmethylimidazole derivative, as a highly selective 17,20-lyase inhibitor with potential utility in the treatment of prostate cancer. *Bioorg Med Chem*. 2011;19(21):6383-99.
80. Yamaoka M, Hara T, Hitaka T, Kaku T, Takeuchi T, Takahashi J, Asahi S, Miki H, Tasaka A, Kusaka M. Orteronel (TAK-700), a novel non-steroidal 17,20-lyase inhibitor: Effects on steroid synthesis in human and monkey adrenal cells and serum steroid levels in cynomolgus monkeys. *J Steroid Biochem Mol Biol*. 2012;129(3–5):115-28.
81. Zhu H, Garcia JA. Targeting the adrenal gland in castration-resistant prostate cancer: A Case for Orteronel, a selective CYP-17 17,20-lyase inhibitor. *Curr Oncol Rep*. 2013;15(2):105-12.
82. Gomez L, Kovac JR, Lamb DJ. CYP17A1 inhibitors in castration-resistant prostate cancer. *Steroids*. 2015;95:80-7.
83. Takeda Pharmaceutical Company Limited. Takeda announces termination of orteronel (TAK-700) development for prostate cancer in Japan, U.S.A. and Europe. 2014. June 19 Report No.
84. Njar VCO, Brodie AMH. Discovery and development of galeterone (TOK-001 or VN/124-1) for the treatment of all stages of prostate cancer. *J Med Chem*. 2015;58(5):2077-87.
85. Soifer HS, Souleimanian N, Wu S, Voskresenskiy AM, Kisaayak Collak F, Cinar B, Stein CA. Direct regulation of androgen receptor activity by potent CYP17 inhibitors in prostate cancer cells. *J Biol Chem*. 2012;287(6):3777-87.
86. Rafferty SW, Eisner JR, Moore WR, Schotzinger RJ, Hoekstra WJ. Highly-selective 4-(1,2,3-triazole)-based P450c17a 17,20-lyase inhibitors. *Bioorg Med Chem Lett*. 2014;24(11):2444-7.
87. Yin L, Hu Q. CYP17 inhibitors: abiraterone, 17,20-lyase inhibitors, and multi-targeting agents. *Nat Rev Urol*. 2014;11(1):32-42.
88. Stein M, Patel N, Bershadskiy A, Sokoloff A, Singer E. Androgen synthesis inhibitors in the treatment of castration-resistant prostate cancer. *Asian J Androl*. 2014;16(3):387-400.
89. Imai T, Yamazaki T, Kominami S. Kinetic studies on bovine cytochrome P45011β catalyzing successive reactions from deoxycorticosterone to aldosterone. *Biochemistry*. 1998;37(22):8097-104.
90. Tagashira H, Kominami S, Takemori S. Kinetic studies of cytochrome P-450$_{17\alpha}$,lyase dependent androstenedione formation from progesterone. *Biochemistry*. 1995;34(34):10939-45.
91. Yamazaki T, Ohno T, Sakaki T, Akiyoshi-Shibata M, Yabusaki Y, Imai T, Kominami S. Kinetic analysis of successive reactions catalyzed by bovine cytochrome P450$_{17\alpha}$,lyase. *Biochemistry*. 1998;37(9):2800-6.
92. Zuber M, Simpson E, Waterman M. Expression of bovine 17 alpha-hydroxylase cytochrome P-450 cDNA in nonsteroidogenic (COS 1) cells. *Science*. 1986;234(4781):1258-61.
93. Imai T, Globerman H, Gertner JM, Kagawa N, Waterman MR. Expression and purification of functional human 17α-hydroxylase/17,20-lyase (P450c17) in *Escherichia coli*. use of this system for study of a novel form of combined 17α-hydroxylase/17,20-lyase deficiency. *J Biol Chem*. 1993;268(26):19681-9.
94. Akhtar M, Corina DL, Miller SL, Shyadehi AZ, Wright JN. Incorporation of label from $^{18}O_2$ into acetate during side-chain cleavage catalysed by cytochrome P-450$_{17\alpha}$(17α-hydroxylase-17,20-lyase). *J Chem Soc Perkin 1*. 1994(3):263-7.
95. Pallan PS, Wang C, Lei L, Yoshimoto FK, Auchus RJ, Waterman MR, Guengerich FP, Egli M. Human cytochrome P450 21A2, the major steroid 21-hydroxylase: Structure of the

enzyme·progesterone substrate complex and rate-limiting C-H bond cleavage. *J Biol Chem*. 2015;290(21):13128-43.
96. Rendic S, Guengerich FP. Survey of human oxidoreductases and cytochrome P450 enzymes involved in the metabolism of xenobiotic and natural chemicals. *Chemical Research in Toxicology*. 2015;28(1):38-42.
97. Guengerich FP. Common and uncommon cytochrome P450 reactions related to metabolism and chemical toxicity. *Chemical Research in Toxicology*. 2001;14(6):611-50.
98. Isin EM, Guengerich FP. Complex reactions catalyzed by cytochrome P450 enzymes. *Biochim Biophys Acta*. 2007;1770(3):314-29.
99. Ortiz de Montellano PR. Substrate oxidation by cytochrome P450 enzymes. In: Ortiz de Montellano PR, editor. Cytochrome P450: Structure, Mechanism, and Biochemistry. NY: Springer International Publishing; 2015. p. 111-76.
100. Yoshimoto FK, Auchus RJ. The diverse chemistry of cytochrome P450 17A1 (P450c17, CYP17A1). *J Steroid Biochem Mol Biol*. 2015;151:52-65.
101. Groves JT. High-valent iron in chemical and biological oxidations. *Journal of Inorganic Biochemistry*. 2006;100(4):434-47.
102. Bell SR, Groves JT. A highly reactive P450 model Compound I. *J Am Chem Soc*. 2009;131(28):9640-1.
103. Morand P, Williamson DGT, Layne DS, Lompakrzymien L, Salvador J. Conversion of an androgen epoxide into 17-β-estradiol by human placental microsomes. *Biochemistry*. 1975;14(3):635-8.
104. Fishman J. Biochemical-mechanism of aromatization. *Cancer Res*. 1982;42(8):3277-80.
105. Akhtar M, Corina D, Pratt J, Smith T. Studies on the removal of C-19 in oesterogen biosynthesis using $^{18}O_2$. *J Chem Soc Chem Commun*. 1976(21):854-6.
106. Goto J, Fishman J. Participation of a Nonenzymatic Transformation in Biosynthesis of Estrogens from Androgens. *Science*. 1977;195(4273):80-1.
107. Hahn EF, Fishman J. Immunological probe of estrogen biosynthesis - evidence for the 2-β-Hydroxylative pathway in aromatization of androgens. *J Biol Chem*. 1984;259(3):1689-94.
108. Caspi E, Wicha J, Arunachalam T, Nelson P, Spiteller G. Estrogen biosynthesis - concerning the obligatory intermediacy of 2-β-hydroxy-10-β-formylandrost-4-ene-3,17-dione. *J Am Chem Soc*. 1984;106(23):7282-3.
109. Hackett JC, Brueggemeier RW, Hadad CM. The final catalytic step of cytochrome P450 aromatase: A density functional theory study. *J Am Chem Soc*. 2005;127(14):5224-37.
110. Sen K, Hackett JC. Coupled electron transfer and proton hopping in the final step of CYP19-catalyzed androgen aromatization. *Biochemistry*. 2012;51(14):3039-49.
111. Mak PJ, Luthra A, Sligar SG, Kincaid JR. Resonance raman spectroscopy of the oxygenated intermediates of human CYP19A1 implicates a Compound I intermediate in the final lyase step. *J Am Chem Soc*. 2014;136(13):4825-8.
112. Cole PA, Robinson CH. Mechanism and inhibition of cytochrome-P-450 aromatase. *J Med Chem*. 1990;33(11):2933-42.
113. Gregory MC, Denisov IG, Grinkova YV, Khatri Y, Sligar SG. Kinetic solvent isotope effect in human P450 CYP17A1-mediated androgen formation: Evidence for a reactive peroxoanion intermediate. *J Am Chem Soc*. 2013;135(44):16245-7.
114. Khatri Y, Gregory MC, Grinkova YV, Denisov IG, Sligar SG. Active site proton delivery and the lyase activity of human CYP17A1. *Biochem Biophys Res Commun*. 2014;443(1):179-84.
115. Gregory M, Mak PJ, Sligar SG, Kincaid JR. Differential hydrogen bonding in human CYP17 dictates hydroxylation versus lyase chemistry. *Angew Chem Int Ed*. 2013;52(20):5342-5.
116. Miller SL, Wright JN, Corina DL, Akhtar M. Mechanistic studies on pregnene side-chain cleavage enzyme (17-α-hydroxylase-17,20-lyase) using O-18. *J Chem Soc Chem Commun*. 1991(3):157-9.

117. Lee-Robichaud P, Shyadehi AZ, Wright JN, Akhtar ME, Akhtar M. Mechanistic kinship between hydroxylation and desaturation reactions - acyl-carbon bond-cleavage promoted by pig and human CYP17 (P-450(17-α)17-α-Hydroxylase-17,20-Lyase). *Biochemistry*. 1995;34(43):14104-13.
118. Akhtar M, Lee-Robichaud P, Akhtar ME, Wright JN. The impact of aromatase mechanism on other P450s. *J Steroid Biochem Mol Biol*. 1997;61(3-6):127-32.
119. Akhtar M, Wright JN, Lee-Robichaud P. A review of mechanistic studies on aromatase (CYP19) and 17α-hydroxylase-17,20-lyase (CYP17). *J Steroid Biochem Mol Biol*. 2011;125(1-2):2-12.
120. Akhtar M, Wright JN. Acyl-carbon bond cleaving cytochrome P450 enzymes: CYP17A1, CYP19A1 and CYP51A1. *Monooxygenase, Peroxidase and Peroxygenase Properties and Mechanisms of Cytochrome P450*. 2015;851:107-30.
121. Guengerich FP, Sohl CD, Chowdhury G. Multi-step oxidations catalyzed by cytochrome P450 enzymes: Processive vs. distributive kinetics and the issue of carbonyl oxidation in chemical mechanisms. *Arch Biochem Biophys*. 2011;507(1):126-34.
122. Caspi E, Arunachalam T, Nelson PA. Biosynthesis of estrogens - aromatization of (19*R*)-[19-H-3,H-2,H-1]-3-β-hydroxyandrost-5-en-17-ones, (19*S*)-[19-H-3,H-2,H-1]-3-β-hydroxyandrost-5-en-17-ones, and (19*RS*)-[19-H-3,H-2,H-1]-3-β-hydroxyandrost-5-en-17-ones by human placental aromatase. *J Am Chem Soc*. 1986;108(8):1847-52.
123. Swinney DC, Mak AY. Androgen formation by cytochrome-P450 CYP17 - solvent isotope effect and pl studies suggest a role for protons in the regulation of oxene versus peroxide chemistry. *Biochemistry*. 1994;33(8):2185-90.
124. Krest CM, Onderko EL, Yosca TH, Calixto JC, Karp RF, Livada J, Rittle J, Green MT. Reactive intermediates in cytochrome P450 catalysis. *J Biol Chem*. 2013;288(24):17074-81.
125. Mak PJ, Gregory MC, Denisov IG, Sligar SG, Kincaid JR. Unveiling the crucial intermediates in androgen production. *Proc Natl Acad Sci U S A*. 2015;112(52):15856-61.
126. Cai HL, Guengerich FP. Mechanism of aqueous decomposition of trichloroethylene oxide. *J Am Chem Soc*. 1999;121(50):11656-63.
127. Pallan PS, Nagy LD, Lei L, Gonzalez E, Kramlinger VM, Azumaya CM, Wawrzak Z, Waterman MR, Guengerich FP, Egli M. Structural and kinetic basis of steroid 17α,20-lyase activity in teleost fish cytochrome P450 17A1 and its absence in cytochrome P450 17A2. *J Biol Chem*. 2015;290(6):3248-68.
128. Chowdhury G, Calcutt MW, Nagy LD, Guengerich FP. Oxidation of methyl and ethyl nitrosamines by cytochrome P450 2E1 and 2B1. *Biochemistry*. 2012;51(50):9995-10007.
129. Chowdhury G, Calcutt MW, Guengerich FP. Oxidation of N-nitrosoalkylamines by human cytochrome P450 2A6 sequential oxidation to aldehydes and carboxylic acids and analysis of reaction steps. *J Biol Chem*. 2010;285(11):8031-44.
130. Auchus RJ, Miller WL. Molecular modeling of human P450c17 (17α-hydroxylase/17,20-lyase): Insights into reaction mechanisms and effects of mutations. *Mol Endocrinol*. 1999;13(7):1169-82.
131. Lichtenberger F, Ullrich V. Cytochrome-P-450 catalyzed oxene transfer from various donors. *Hoppe Seylers Z Physiol Chem*. 1976;357(8):1037-.
132. Kirk DN, Toms HC, Douglas C, White KA, Smith KE, Latif S, Hubbard RWP. A survey of the high-Field H-1-NMR spectra of the steroid-hormones, their hydroxylated derivatives, and related-compounds. *J Chem Soc Perkin 2*. 1990(9):1567-94.
133. Hayamizu K, Ishii T, Yanagisawa M, Kamo O. Complete assignments of the H-1 and C-13 NMR-spectra of testosterone and 17-α-methyltestosterone and the H-1 parameters obtained from 600 Mhz spectra. *Magnetic Resonance in Chemistry*. 1990;28(3):250-6.

134. Renneberg R, Scheller F, Ruckpaul K, Pirrwitz J, Mohr P. NADPH and H_2O_2-dependent reactions of cytochrome P-450_{lm} compared with peroxidase catalysis. *FEBS Lett*. 1978;96(2):349-53.
135. Renneberg R, Damerau W, Jung C, Ebert B, Scheller F. Study of H_2O_2-supported N-demethylations catalyzed by cytochrome-P-450 and horseradish-peroxidase. *Biochem Biophys Res Commun*. 1983;113(1):332-9.
136. Hamilton NM, Dawson M, Fairweather EE, Hamilton NS, Hitchin JR, James DI, Jones SD, Jordan AM, Lyons AJ, Small HF, Thomson GJ, Waddell ID, Ogilvie DJ. Novel steroid inhibitors of glucose 6-phosphate dehydrogenase. *J Med Chem*. 2012;55(9):4431-45.
137. Ortiz de Montellano PR. Oxygen activation and transfer. In: Ortiz de Montellano PR, editor. Cytochrome P-450: Structure, Mechanism, and Biochemistry. Boston, MA: Springer US; 1986. p. 217-71.
138. Betancor C, Francisco CG, Freire R, Suarez E. The reaction of enols with superoxide anion radicals - preparation of tertiary alpha-ketols. *J Chem Soc Chem Commun*. 1988(14):947-8.
139. Pestovsky O, Bakac A. Reactivity of aqueous Fe(IV) in hydride and hydrogen atom transfer reactions. *J Am Chem Soc*. 2004;126(42):13757-64.
140. Bakac A. Reactions of superoxo and oxo metal complexes with aldehydes. Radical-specific pathways for cross-disproportionation of superoxometal ions and acylperoxyl radicals. *J Am Chem Soc*. 2002;124(31):9136-44.
141. Paraskevas PD, Sabbe MK, Reyniers MF, Papayannakos NG, Marin GB. Kinetic modeling of alpha-hydrogen abstractions from unsaturated and saturated oxygenate compounds by hydrogen atoms. *J Phys Chem A*. 2014;118(40):9296-309.
142. Basran J, Efimov I, Chauhan N, Thackray SJ, Krupa JL, Eaton G, Griffith GA, Mowat CG, Handa S, Raven EL. The mechanism of formation of N-formylkynurenine by heme dioxygenases. *J Am Chem Soc*. 2011;133(40):16251-7.
143. Kadlubar FF, Morton KC, Ziegler DM. Microsomal-catalyzed hydroperoxide-dependent C-oxidation of amines. *Biochem Biophys Res Commun*. 1973;54(4):1255-61.
144. Mansuy D, Bartoli JF, Momenteau M. Alkane hydroxylation catalyzed by metalloporphyrins - evidence for different active oxygen species with alkylhydroperoxides and iodosobenzene as oxidants. *Tetrahedron Letters*. 1982;23(27):2781-4.
145. Lee DS, Yamada A, Sugimoto H, Matsunaga I, Ogura H, Ichihara K, Adachi S, Park SY, Shiro Y. Substrate recognition and molecular mechanism of fatty acid hydroxylation by cytochrome P450 from *Bacillus subtilis* - crystallographic, spectroscopic, and mutational studies. *J Biol Chem*. 2003;278(11):9761-7.
146. Rude MA, Baron TS, Brubaker S, Alibhai M, Del Cardayre SB, Schirmer A. Terminal olefin (1-alkene) biosynthesis by a novel P450 fatty acid decarboxylase from jeotgalicoccus species. *Applied and Environmental Microbiology*. 2011;77(5):1718-27.
147. Fujishiro T, Shoji O, Nagano S, Sugimoto H, Shiro Y, Watanabe Y. Crystal structure of H_2O_2-dependent cytochrome P450(SPα) with its bound fatty acid substrate insight into the regioselective hydroxylation of fatty acids at the α position. *J Biol Chem*. 2011;286(34):29941-50.
148. Joo H, Lin ZL, Arnold FH. Laboratory evolution of peroxide-mediated cytochrome P450 hydroxylation. *Nature*. 1999;399(6737):670-3.
149. Nordblom GD, Coon MJ. Hydrogen-peroxide formation and stoichiometry of hydroxylation reactions catalyzed by highly purified liver microsomal cytochrome-P-450. *Arch Biochem Biophys*. 1977;180(2):343-7.
150. Renneberg R, Capdevila J, Chacos N, Estabrook RW, Prough RA. Hydrogen-peroxide supported oxidation of benzo [*a*]pyrene by rat-liver microsomal fractions. *Biochemical Pharmacology*. 1981;30(8):843-8.

151. Holm KA, Engell RJ, Kupfer D. Regioselectivity of hydroxylation of prostaglandins by liver-microsomes supported by nadph versus H_2O_2 in methylcholanthrene-treated and control rats - formation of novel prostaglandin metabolites. *Arch Biochem Biophys*. 1985;237(2):477-89.
152. Guengerich FP, Vaz ADN, Raner GN, Pernecky SJ, Coon MJ. Evidence for a role of a perferryl-oxygen complex, FeO^{3+}, in the *N*-oxygenation of amines by cytochrome P450 enzymes. *Molecular Pharmacology*. 1997;51(1):147-51.
153. Lacroix D, Sonnier M, Moncion A, Cheron G, Cresteil T. Expression of CYP3A in the human liver - Evidence that the shift between CYP3A7 and CYP3A4 occurs immediately after birth. *Eur J Biochem*. 1997;247(2):625-34.
154. Niwa T, Yabusaki Y, Honma K, Matsuo N, Tatsuta K, Ishibashi F, Katagiri M. Contribution of human hepatic cytochrome P450 isoforms to regioselective hydroxylation of steroid hormones. *Xenobiotica*. 1998;28(6):539-47.
155. Kirschner MA, Wiqvist N, Diczfalusy E. Studies on oestriol synthesis from dehydroepiandrosterone sulphate in human pregnancy. *Acta Endocrinol (Copenh)*. 1966;53(4):584-97.
156. Stevenson DE, Wright JN, Akhtar M. Mechanistic consideration of P-450 dependent enzymic reactions - studies on estriol biosynthesis. *J Chem Soc Perkin 1*. 1988(7):2043-52.
157. Yoshimoto FK, Peng HM, Zhang HM, Anderson SM, Auchus RJ. Epoxidation activities of human cytochromes P450c17 and P450c21. *Biochemistry*. 2014;53(48):7531-40.
158. Walsh C. Enzymatic Reaction Mechanisms: W. H. Freeman; 1979.
159. Yosca TH, Rittle J, Krest CM, Onderko EL, Silakov A, Calixto JC, Behan RK, Green MT. Iron(IV)hydroxide pK(a) and the role of thiolate ligation in C-H bond activation by cytochrome P450. *Science*. 2013;342(6160):825-9.
160. Davydov R, Strushkevich N, Smil D, Yantsevich A, Gilep A, Usanov S, Hoffman BM. Evidence that Compound I is the active species in both the hydroxylase and lyase steps by which P450scc converts cholesterol to pregnenolone: EPR/ENDOR/cryoreduction/annealing studies. *Biochemistry*. 2015;54(48):7089-97.
161. Gottlieb HE, Kotlyar V, Nudelman A. NMR chemical shifts of common laboratory solvents as trace impurities. *Journal of Organic Chemistry*. 1997;62(21):7512-5.
162. Vijaykumar D, Mao W, Kirschbaum KS, Katzenellenbogen JA. An efficient route for the preparation of a 21-fluoro progestin-16 alpha,17 alpha-dioxolane, a high-affinity ligand for PET imaging of the progesterone receptor. *Journal of Organic Chemistry*. 2002;67(14):4904-10.
163. Yoshimoto FK, Gonzalez E, Auchus RJ, Guengerich FP. Mechanism of 17,20-Lyase and new hydroxylation reactions of human cytochrome P450 17A1: O-18 labeling and oxygen surrogate evidence for a role of a perferryl oxygen. *J Biol Chem*. 2016;291(33):17143-64.
164. Saltzman H, Sharefkin JG. Iodosobenzene. *Org Synth*. 1963;43:60-1.
165. Gillam EMJ, Baba T, Kim BR, Ohmori S, Guengerich FP. Expression of modified human cytochrome-P450 3A4 in Escherichia-coli and purification and reconstitution of the enzyme. *Arch Biochem Biophys*. 1993;305(1):123-31.
166. Hosea NA, Miller GP, Guengerich FP. Elucidation of distinct ligand binding sites for cytochrome P450 3A4. *Biochemistry*. 2000;39(20):5929-39.
167. Hanna IH, Teiber JF, Kokones KL, Hollenberg PF. Role of the alanine at position 363 of cytochrome P450 2B2 in influencing the NADPH- and hydroperoxide-supported activities. *Arch Biochem Biophys*. 1998;350(2):324-32.
168. Guengerich FP. Reduction of cytochrome b_5 by NADPH-cytochrome P450 reductase. *Arch Biochem Biophys*. 2005;440(2):204-11.

169. Pechurskaya TA, Lukashevich OP, Gilep AA, Usanov SA. Engineering, expression, and purification of "soluble" human cytochrome $P450_{17\alpha}$ and its functional characterization. *Biochemistry-Moscow*. 2008;73(7):806-11.
170. Sandhu P, Baba T, Guengerich FP. Expression of modified cytochrome-P450-2C10-(2C9) in *Escherichia coli*, purification, and reconstitution of catalytic activity. *Arch Biochem Biophys*. 1993;306(2):443-50.
171. Foust GP, Burleigh BD, Mayhew SG, Williams CH, Massey V. An anaerobic titration assembly for spectrophotometric use. *Anal Biochem*. 1969;27(3):530-&.
172. Guengerich FP, Krauser JA, Johnson WW. Rate-limiting steps in oxidations catalyzed by rabbit cytochrome P450 1A2. *Biochemistry*. 2004;43(33):10775-88.
173. Auchus RJ, Miller WL. P450 enzymes in steroid processing. In: Ortiz de Montellano PR, editor. Cytochrome P450: Structure, Mechanism, and Biochemistry. NY: Springer International Publishing; 2015. p. 851-79.
174. Lee-Robichaud P, Wright JN, Akhtar ME, Akhtar M. Modulation of the activity of human 17α-hydroxylase-17,20-lyase (CYP17) by cytochrome b_5: endocrinological and mechanistic implications. *Biochem J*. 1995;308(3):901-8.
175. Montgomery RB, Mostaghel EA, Vessella R, Hess DL, Kalhorn TF, Higano CS, True LD, Nelson PS. Maintenance of intratumoral androgens in metastatic prostate cancer: A mechanism for castration-resistant tumor growth. *Cancer Res*. 2008;68(11):4447-54.
176. Fersht A. Structure and Mechanism in Protein Science. Freeman, New York; 1999.
177. Sagara Y, Barnes HJ, Waterman MR. Expression in Escherichia-coli of functional cytochrome-P450c17 lacking its hydrophobic amino-terminal signal anchor. *Arch Biochem Biophys*. 1993;304(1):272-8.
178. Poulos TL, Johnson EF. Structures of cytochrome P450 enzymes. In: Ortiz de Montellano PR, editor. Cytochrome P450: Structure, Mechanism, and Biochemistry. NY: Springer International Publishing; 2015. p. 3-32.
179. Estrada DF, Skinner AL, Laurence JS, Scott EE. Human cytochrome P450 17A1 conformational selection. *J Biol Chem*. 2014;289(20):14310-20.
180. Peng H-M, Im S-C, Pearl NM, Turcu AF, Rege J, Waskell L, Auchus RJ. Cytochrome b_5 Activates the 17,20-lyase activity of human cytochrome P450 17A1 by increasing the coupling of NADPH consumption to androgen production. *Biochemistry*. 2016;55(31):4356-65.
181. Guengerich F. Analysis and characterization of enzymes and nucleic acids relevant to toxicology. Hayes' Principles and Methods of Toxicology. 6 ed: CRC Press; 2014. p. 1905-64.
182. Storbeck K-H, Swart P, Africander D, Conradie R, Louw R, Swart AC. 16α-Hydroxyprogesterone: Origin, biosynthesis and receptor interaction. *Mol Cell Endocrinol*. 2011;336(1–2):92-101.
183. Julian PL, Magnani A, inventors; Smith Kline & French Laboratories, assignee. Methods for preparing 16alpha-hydroxypregnenes and intermediates obtained therein. United States of America1966.
184. Colton FB, inventor; G. D. Searle & Co., assignee. 16alpha,17alpha-Dihydroxypregnen-20-one derivatives. United States of America1955.
185. Christakoudi S, Cowan DA, Taylor NF. Steroids excreted in urine by neonates with 21-hydroxylase deficiency. 2. Characterization, using GC–MS and GC–MS/MS, of pregnanes and pregnenes with an oxo- group on the A- or B-ring. *Steroids*. 2012;77(5):382-93.
186. Nelson WG. Commentary on Huggins and Hodges: “Studies on Prostatic Cancer”. *Cancer Res*. 2016;76(2):186-7.
187. Huggins C, Hodges CV. Studies on prostatic cancer. I. The effect of castration, of estrogen and of androgen injection on serum phosphatases in metastatic carcinoma of the prostate. *Cancer Res*. 1941;1(4):293-7.

PUBLICATIONS

Yoshimoto FK, Jung I, Goyal S, Gonzalez E, Guengerich FP. Isotope-Labeling Studies Support an Electrophilic Compound I Iron Active Species (FeO^{3+}) for the Carbon-Carbon Bond Cleavage Reaction of the Cholesterol Side Chain Cleavage Enzyme, Cytochrome P450 11A1 (P450scc). *J. Am. Chem. Soc.* 2016 Aug 29. 138(37): 12124-12141

Yoshimoto FK*, Gonzalez E*, Auchus RJ, Guengerich FP. Mechanism of 17α,20-Lyase and New Hydroxylation Reactions of Human Cytochrome P450 17A1. ^{18}O Labelling and Oxygen Surrogate Evidence for a Role of a Perferryl Oxygen. *J. Biol. Chem.* 2016 Aug 12. 291(33): 17143-17164. *Co-first Author

Pallan PS, Nagy LD, Lei L, Gonzalez E, Kramlinger VM, Azumaya CM, Wawrzak Z, Waterman MR, Guengerich FP, Egli M. Structural and Kinetic Basis of Steroid 17α,20-Lyase Activity in Teleost Fish Cytochrome P450 17A1 and Its Absence in Cytochrome P450 17A2. *J. Biol. Chem*. 2015 Feb 6. 290(6): 3248-3268

Gonzalez E, Granados JC, Short JD, Ammons DR, Rampersad J. Parasporins from a Caribbean Island: Evidence for a Globally Dispersed *Bacillus thuringiensis* Strain. *Curr Microbiol*. 2011 May 1. 62(5):1643-1648.

APPENDIX

LIST OF FIGURES

Figures Page

LIST OF TABLES

Tables Page

Table 6-1 NMR shift assignments for 6*β*,16*α*,17*α*-tri(OH)prog

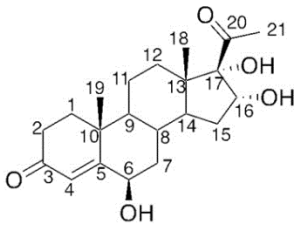

Carbon atom	δ_C	δ_H
1	36	2.06, 1.74 (COSY δ 2.53)
2	34.3	2.53, 2.42
3	205.1 (HMBC-2CH_2)	
4	127.7	5.84 (broad s)
5	167.5	
6	73.0	4.38 (broad s) (NOESY to δ 5.84)
7	38.5	1.98, 1.34 (COSY δ 4.38)
8	29.5 (43, 44)	1.99
9	52.9 (HMBC 19-CH_3, 1-H)	1.02
10	42.7 (HMBC – C19-CH_3/C6-CH/C2-CH_2)	
11	20 (43)	1.66 (COSY δ 1.08, 1.94), δ 1.48
12	30.8	1.97, 1.53
13	35.4 (HMBC 18-CH_3)	
14	48.9 (43, 44)	2.03 (W-coupling to δ 5.09, four bonds away)
15	33.6	1.59, 1.92 (COSY δ 5.09)
16	72.3	5.09
17	88.6	
18	15.1	0.79
19	19.5	1.40
20	211.4	
21	27.4	2.28

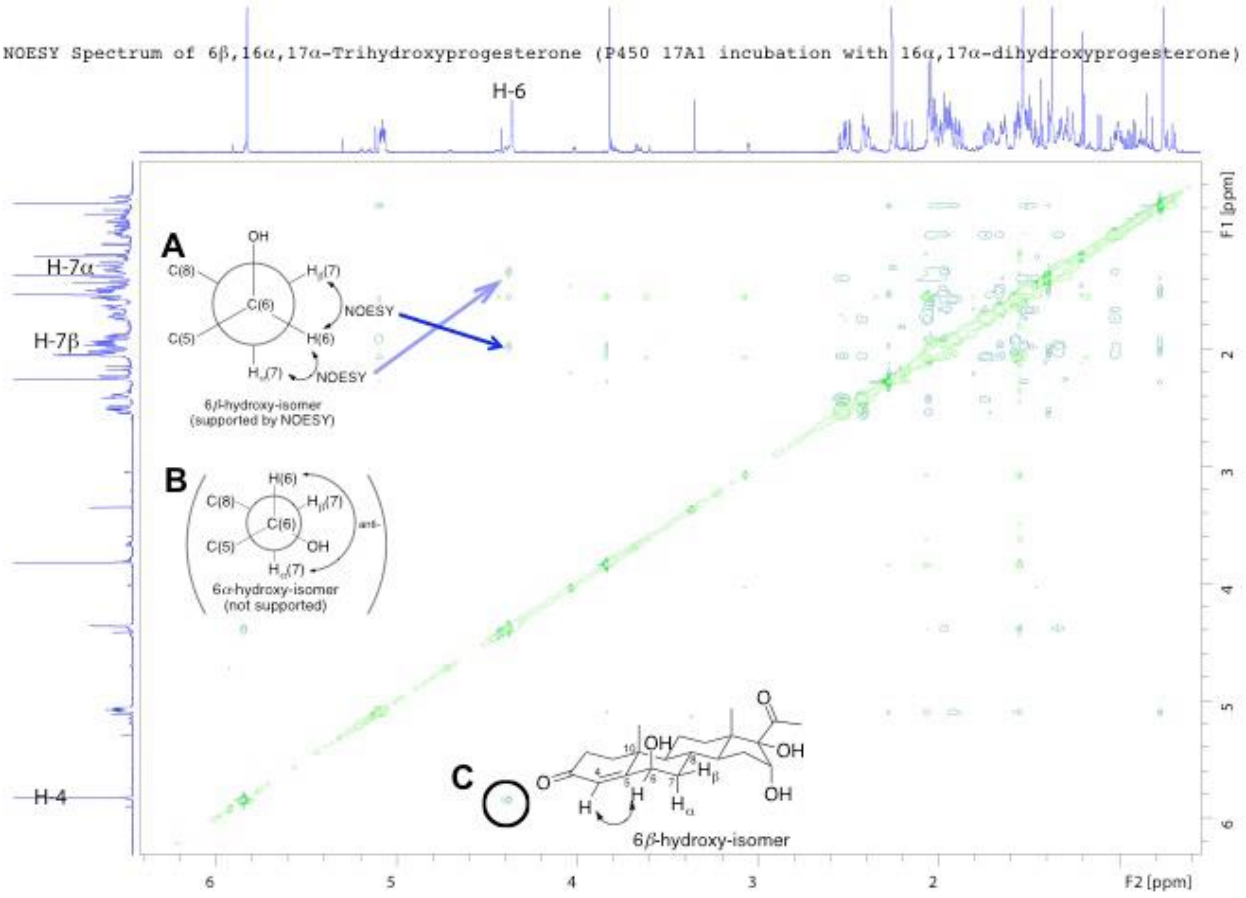

Figure 6.1 NOESY NMR spectrum of *6β*,16*α*,17*α*-tri(OH)prog derived from 16*α*,17*α*-di(OH)prog (600 MHz, $CDCl_3$).

(A) Newman projection along C6-C7 bond axis to show the proximity between H-6*α* (*δ* 4.38 ppm) with H-7*α* (*δ* 1.34 ppm) and H-7*β* (*δ* 1.98 ppm) protons that is supported by the NOESY data, and for comparison: (B) a Newman projection along the C6-C7 bond axis of a hypothetical 6*α*-hydroxy epimer (6*α*,16*α*,17*α*-trihydroxyprogesterone) to show anticonfiguration of H-6*β* with H-7*α*. (C) NOESY interaction between H-6 (*δ* 4.38 ppm) and H-4 (*δ* 5.84 ppm) protons.

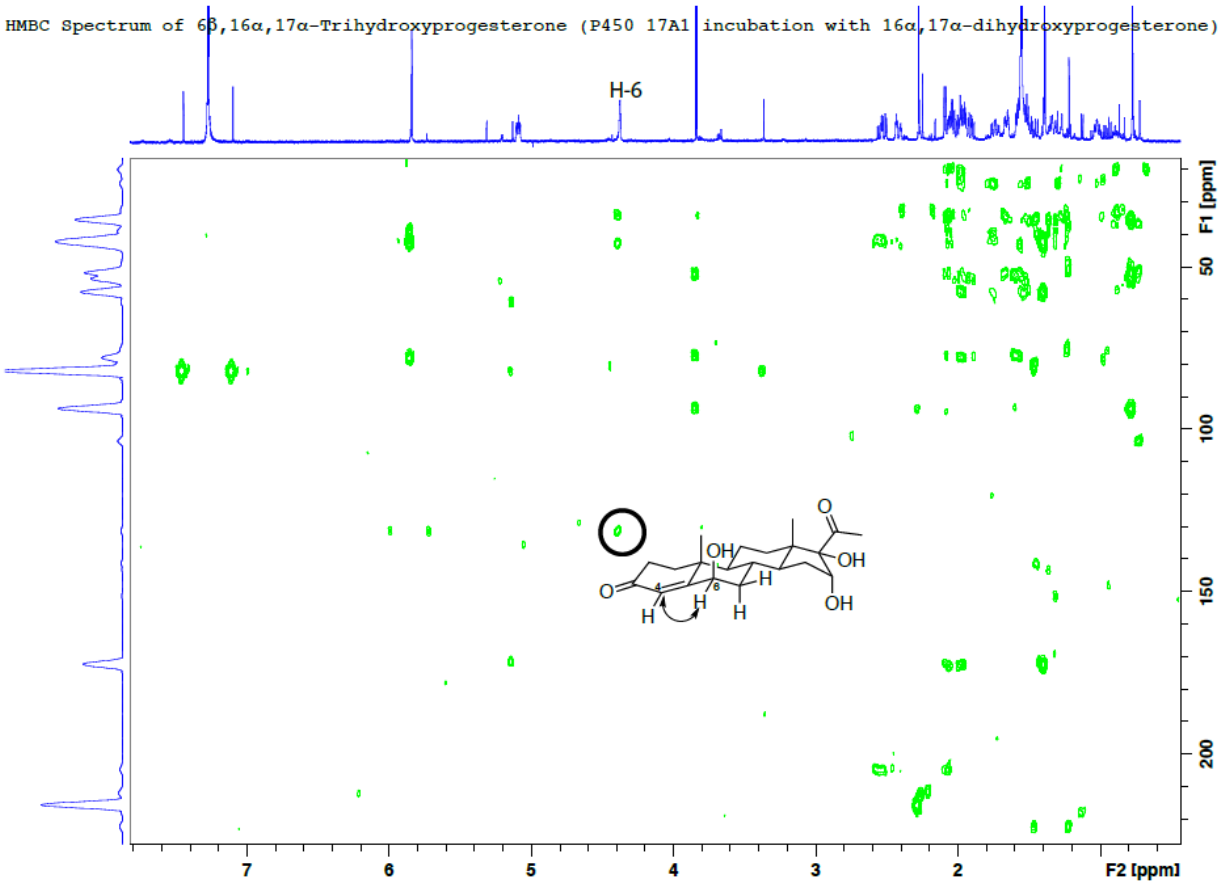

Figure 6.2 HMBC NMR spectrum of 6*β*,16*α*,17*α*-tri(OH)prog derived from 16*α* ,17*α* –di(OH)prog (600 MHz, $CDCl_3$).

The H-6 hydroxymethine proton (*δ* 4.38 ppm) is shown to have a 3-bond coupling to the C4-carbon (*δ* 128 ppm).

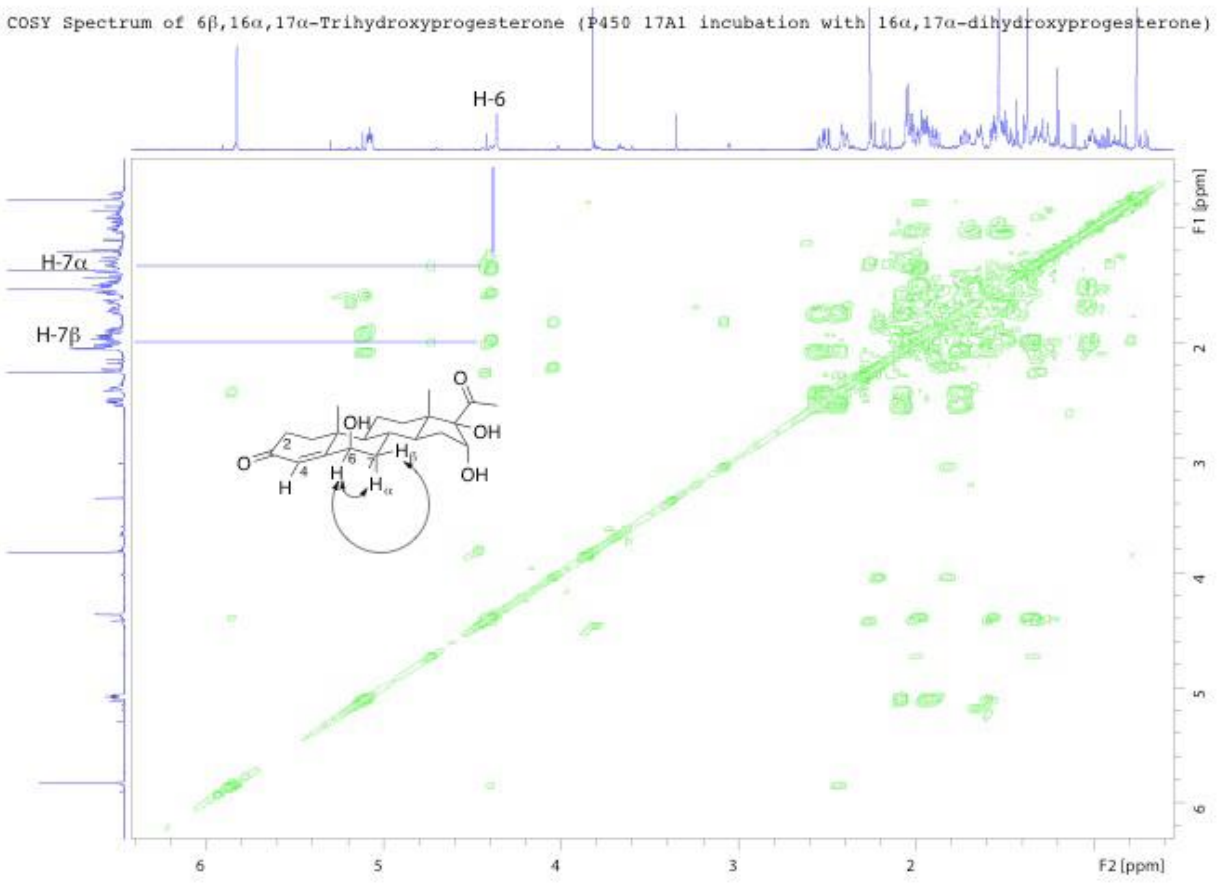

Figure 6.3 COSY NMR spectrum of 6*β*,16*α*,17*α* –tri(OH)prog derived from 16*α*,17*α*-di(OH)prog (600 MHz, $CDCl_3$).

Shown with the lines are the 3-bond coupling interaction between the H-6 proton (*δ* 4.38 ppm) with the H-7protons (*δ* 1.34 and 1.98 ppm).

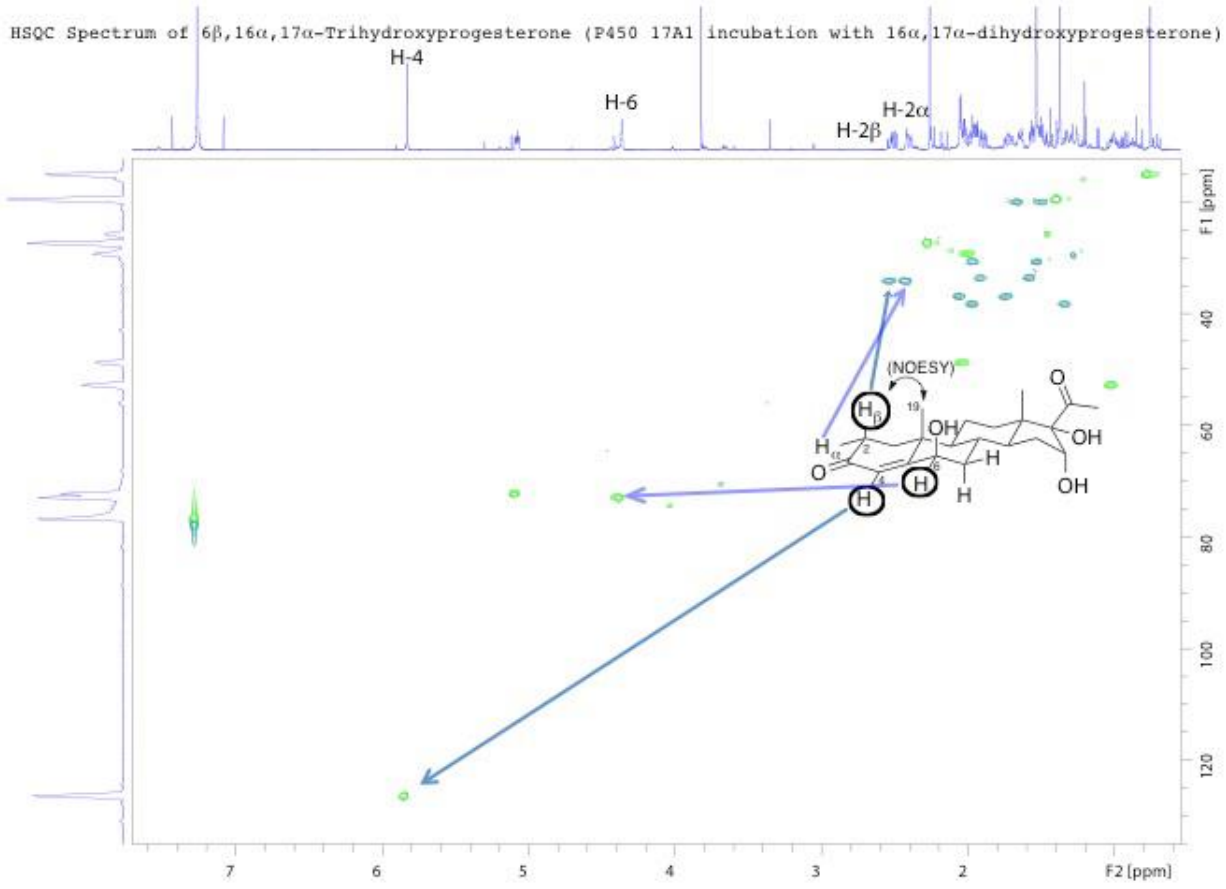

Figure 6.4 HSQC NMR spectrum of 6*β*,16*α*,17*α*-tri(OH)prog derived from 16*α*,17*α*-di(OH)prog (600 MHz, $CDCl_3$).

The arrows show the assignment of C2, C4, and C7 carbons (*δ* 34.2, 127.7, and 38.5 ppm) with their respective one-bond heteronuclear correlations to assign their attached protons.

■

Figure 6.5 KinTek Explorer iterations for Figure 3.8

Version : Professional Version 6.1.170130

Build : PRO
Config : gsl
Fitter : Levmar.
Levmar Box : 1.
Levmar Ln : 0.
Levmar Cycle: 0.
Levmar Linear: 0.
fitLevmarInitialMu: 0.0001.
fitLevmarTol1: 1e-008.
fitLevmarTol2: 1e-008.
fitLevmarTol3: 1e-012.

Fit stop reason: small |Dp|
Fit iterations/calls: iter:1 fn:368 jac:1

Data to fit : Empirical Data.
Fit Function : Fit to Model.
Fit Domain : 11 observable(s) over 12 experiment(s).
Fit Time : 132.413 seconds

Experiments : Exp1 (id=0), Exp2 (id=2), Exp3 (id=3), Exp5 (id=64), Exp4 (id=45), Exp6 (id=65), Exp7 (id=66), Exp8 (id=67), Exp9 (id=68), Exp10 (id=70), Exp11 (id=71), Exp12 (id=73)
Data Points : 99
Params Fit : 11
Deg of Freedom : 88
Chi : 0.91867
Chi2 / DoF : 0.00959
GammaQ : 1.00000
Computed Sigma : 0.09280

Reaction	Constant	Constraint	Value	StdErr	%Error	Keq
E + P = EP	k+1		0.173	0.231	134	15
	k-1		0.0115	0.122	1060	
E + I = EI	k+2		0.296	0.179	60.4	0.288
	k-2		1.03	1.18	114	

E + A = EA k+3 1.89 8.45 447 14.7
k-3 0.129 0.169 131

EP + POR = rEP k+4 X 100 n/a n/a (1)
k-4 X 100 n/a n/a

EI + POR = rEI k+5 X 100 n/a n/a (1)
k-5 X 100 n/a n/a

rEP = EI k+6 1.01 0.374 37 1.01e+007
k-6 X 0 n/a n/a

rEI = EA k+7 0.418 0.289 69.1 4.18e+006
k-7 X 0 n/a n/a

RATE-CONSTANTS
k+1 0.173 0.231
k-1 0.0115 0.122
k+2 0.296 0.179
k-2 1.03 1.18
k+3 1.89 8.45
k-3 0.129 0.169
k+4 100 n/a
k-4 100 n/a
k+5 100 n/a
k-5 100 n/a
k+6 1.01 0.374
k-6 0 n/a
k+7 0.418 0.289
k-7 0 n/a

Experiment	Factor	Constraint	Value	StdErr	%Error
Experiment 5a	a		0.227	0.11	48.4
Experiment 5b	a		0.227	0.11	48.4
Experiment 6a	b		0.16	0.204	128

Experiment 6b	b	0.16	0.204	128
Experiment 7a	c	0.11	0.0948	86.2
Experiment 7b	c	0.11	0.0948	86.2

OUTPUT-FACTORS
a 0.227 0.11
b 0.16 0.204
c 0.11 0.0948

Experiment	Reagent	Constraint	Value	StdErr	%Error
Experiment 1	EP	X	4	n/a	n/a
Experiment 1 mix1	POR	X	1	n/a	n/a
Experiment 2	EI	X	4	n/a	n/a
Experiment 2 mix1	POR	X	1	n/a	n/a
Experiment 3	E	X	0.01	n/a	n/a
Experiment 3 mix1	POR	X	1	n/a	n/a
Experiment 3	E	X	0.01	n/a	n/a
Experiment 3 mix1	POR	X	1	n/a	n/a
Experiment 4	E	X	0.01	n/a	n/a
Experiment 4 mix1	POR	X	1	n/a	n/a
Experiment 4	E	X	0.01	n/a	n/a
Experiment 4 mix1	POR	X	1	n/a	n/a
Experiment 5	E	X	1	n/a	n/a
Experiment 5	E	X	1	n/a	n/a
Experiment 6	E	X	1	n/a	n/a
Experiment 6	E	X	1	n/a	n/a
Experiment 7	E	X	1	n/a	n/a
Experiment 7	E	X	1	n/a	n/a

INITIAL-CONCENTRATIONS
EP-e1m1 4 n/a
POR-e1m2 1 n/a
EI-e2m1 4 n/a
POR-e2m2 1 n/a
E-e3m1 0.01 n/a
POR-e3m2 1 n/a
E-e3m1 0.01 n/a
POR-e3m2 1 n/a
E-e4m1 0.01 n/a
POR-e4m2 1 n/a
E-e4m1 0.01 n/a

POR-e4m2 1 n/a
E-e5 1 n/a
E-e5 1 n/a
E-e6 1 n/a
E-e6 1 n/a
E-e7 1 n/a
E-e7 1 n/a

Covariance Matrix

	k+1	k-1	k+2	k-2	k+3	k-3	k+6	k+7	a	b	c
k+1	+1.55										
k-1	+0.645	+0.431									
k+2	+0.361	+0.199	+0.93								
k-2	+0	+0	+0	+40.1							
k+3	+32.7	+11.9	+25.5	+0	+2070						
k-3	+0.378	+0.0921	+0.257	+0	+32.7	+0.833					
k+6	+1.27	+1.18	+0.434	+0	+19.8	+0.0302	+4.05				
k+7	+0	+0	+0	+9.04	+0	+0	+0	+2.43			
a	+0	+0	+0	+0.54	+0	+0	+0.0654	+0.107	+0.35		
b	+0	+0	+0	+2.76	+0	+0	+0	+0.735	+0.0382	+1.21	
c	+0	+0	+0	+0.361	+0	+0	+0	+0.102	+0.0112	+0.0388	+0.261

■

Figure 6.6 KinTek Explorer iterations for Figure 3.9

Version : Professional Version 6.1.170130

Build : PRO
Config : gsl
Fitter : Levmar.
Levmar Box : 1.
Levmar Ln : 0.
Levmar Cycle: 0.
Levmar Linear: 0.
fitLevmarInitialMu: 0.0001.
fitLevmarTol1: 1e-008.
fitLevmarTol2: 1e-008.
fitLevmarTol3: 1e-012.

Fit stop reason: small |Dp|
Fit iterations/calls: iter:1 fn:165 jac:1

Data to fit : Empirical Data.
Fit Function : Fit to Model.
Fit Domain : 8 observable(s) over 6 experiment(s).
Fit Time : 54.910 seconds

Experiments : Exp1 (id=0), Exp2 (id=2), Exp3 (id=3), Exp5 (id=64), Exp4 (id=45), Exp6 (id=65)
Data Points : 75
Params Fit : 8
Deg of Freedom : 67
Chi : 0.91137
Chi2 / DoF : 0.01240
GammaQ : 1.00000
Computed Sigma : 0.10594

Reaction	Constant	Constraint	Value	StdErr	%Error	Keq
E + P = EP	k+1		0.552	1.33	241	35.1
	k-1		0.0157	0.454	2890	
E + I = EI	k+2		0.266	0.147	55.5	0.337
	k-2		0.788	0.966	123	

E + A = EA k+3 5.46 27.7 508 34
k-3 0.161 0.318 198

EP + POR = rEP k+4 X 100 n/a n/a (1)
k-4 X 100 n/a n/a

EI + POR = rEI k+5 X 100 n/a n/a (1)
k-5 X 100 n/a n/a

rEP = EI k+6 0.92 0.719 78.1 9.2e+006
k-6 X 0 n/a n/a

rEI = EA k+7 0.397 0.278 70.1 3.97e+006
k-7 X 0 n/a n/a

RATE-CONSTANTS
k+1 0.552 1.33
k-1 0.0157 0.454
k+2 0.266 0.147
k-2 0.788 0.966
k+3 5.46 27.7
k-3 0.161 0.318
k+4 100 n/a
k-4 100 n/a
k+5 100 n/a
k-5 100 n/a
k+6 0.92 0.719
k-6 0 n/a
k+7 0.397 0.278
k-7 0 n/a

Experiment Factor Constraint Value StdErr %Error

OUTPUT-FACTORS

Experiment Reagent Constraint Value StdErr %Error

Experiment 1	EP	X	4	n/a	n/a
Experiment 1 mix1	POR	X	1	n/a	n/a
Experiment 2	EI	X	4	n/a	n/a
Experiment 2 mix1	POR	X	1	n/a	n/a
Experiment 3	E	X	0.01	n/a	n/a
Experiment 3 mix1	POR	X	1	n/a	n/a
Experiment 3	E	X	0.01	n/a	n/a
Experiment 3 mix1	POR	X	1	n/a	n/a
Experiment 4	E	X	0.01	n/a	n/a
Experiment 4 mix1	POR	X	1	n/a	n/a
Experiment 4	E	X	0.01	n/a	n/a
Experiment 4 mix1	POR	X	1	n/a	n/a

INITIAL-CONCENTRATIONS

EP-e1m1	4	n/a
POR-e1m2	1	n/a
EI-e2m1	4	n/a
POR-e2m2	1	n/a
E-e3m1	0.01	n/a
POR-e3m2	1	n/a
E-e3m1	0.01	n/a
POR-e3m2	1	n/a
E-e4m1	0.01	n/a
POR-e4m2	1	n/a
E-e4m1	0.01	n/a
POR-e4m2	1	n/a

Covariance Matrix

	k+1	k-1	k+2	k-2	k+3	k-3	k+6	k+7
k+1	+39.3							
k-1	+7.68	+4.59						
k+2	+0.902	+0.452	+0.484					
k-2	+0	+0	+0	+20.8				
k+3	+512	+47.2	+27.1	+0	+17100			
k-3	+3.25	+0	+0.108	+0	+168	+2.26		
k+6	+7.67	+6.98	+0.628	+0	+4.19	+0	+11.5	
k+7	+0	+0	+0	+5.49	+0	+0	+0	+1.72

Figure 6.7 KinTek Explorer iterations for Figure 3.10

Version : Professional Version 6.1.170130

Build : PRO
Config : gsl
Fitter : Levmar.
Levmar Box : 1.
Levmar Ln : 0.
Levmar Cycle: 0.
Levmar Linear: 0.
fitLevmarInitialMu: 0.0001.
fitLevmarTol1: 1e-008.
fitLevmarTol2: 1e-008.
fitLevmarTol3: 1e-012.

Fit stop reason: small |Dp|
Fit iterations/calls: iter:1 fn:118 jac:1

Data to fit : Empirical Data.
Fit Function : Fit to Model.
Fit Domain : 11 observable(s) over 12 experiment(s).
Fit Time : 51.983 seconds

Experiments : Exp1 (id=0), Exp2 (id=2), Exp3 (id=3), Exp5 (id=64), Exp4 (id=45), Exp6 (id=65), Exp7 (id=66), Exp8 (id=67), Exp9 (id=68), Exp10 (id=70), Exp11 (id=71), Exp12 (id=73)
Data Points : 99
Params Fit : 8
Deg of Freedom : 91
Chi : 1.06476
Chi2 / DoF : 0.01246
GammaQ : 1.00000
Computed Sigma : 0.10756

Reaction	Constant	Constraint	Value	StdErr	%Error	Keq
E + P = EP	k+1	3	0.215	0.154	71.6	(2.7)
	k-1	3	0.0796	0	0	
E + I = EI	k+2	2	0.973	0.656	67.4	(1.92)
	k-2	2	0.508	0	0	

E + A = EA k+3 1 0.0857 0.219 256 (0.588)
k-3 1 0.146 0 0

EP + POR = rEP k+4 X 100 n/a n/a (1)
k-4 X 100 n/a n/a

EI + POR = rEI k+5 X 100 n/a n/a (1)
k-5 X 100 n/a n/a

rEP = EI k+6 1.32 0.21 15.9 1.32e+007
k-6 X 0 n/a n/a

rEI = EA k+7 0.185 0.0177 9.62 1.85e+006
k-7 X 0 n/a n/a

RATE-CONSTANTS
k+1 0.215 0.154
k-1 0.0796 0
k+2 0.973 0.656
k-2 0.508 0
k+3 0.0857 0.219
k-3 0.146 0
k+4 100 n/a
k-4 100 n/a
k+5 100 n/a
k-5 100 n/a
k+6 1.32 0.21
k-6 0 n/a
k+7 0.185 0.0177
k-7 0 n/a

Experiment	Factor	Constraint	Value	StdErr	%Error
Experiment 5a	a		0.241	0.129	53.7
Experiment 5b	a		0.241	0.129	53.7
Experiment 6a	b		0.136	0.131	96.1

Experiment 6b	b	0.136	0.131	96.1
Experiment 7a	c	0.131	0.175	133
Experiment 7b	c	0.131	0.175	133

OUTPUT-FACTORS
a 0.241 0.129
b 0.136 0.131
c 0.131 0.175

Experiment	Reagent	Constraint	Value	StdErr	%Error
Experiment 1	EP	X	4	n/a	n/a
Experiment 1 mix1	POR	X	1	n/a	n/a
Experiment 2	EI	X	4	n/a	n/a
Experiment 2 mix1	POR	X	1	n/a	n/a
Experiment 3	E	X	0.01	n/a	n/a
Experiment 3 mix1	POR	X	1	n/a	n/a
Experiment 3	E	X	0.01	n/a	n/a
Experiment 3 mix1	POR	X	1	n/a	n/a
Experiment 4	E	X	0.01	n/a	n/a
Experiment 4 mix1	POR	X	1	n/a	n/a
Experiment 4	E	X	0.01	n/a	n/a
Experiment 4 mix1	POR	X	1	n/a	n/a
Experiment 5	E	X	1	n/a	n/a
Experiment 5	E	X	1	n/a	n/a
Experiment 6	E	X	1	n/a	n/a
Experiment 6	E	X	1	n/a	n/a
Experiment 7	E	X	1	n/a	n/a
Experiment 7	E	X	1	n/a	n/a

INITIAL-CONCENTRATIONS
EP-e1m1 4 n/a
POR-e1m2 1 n/a
EI-e2m1 4 n/a
POR-e2m2 1 n/a
E-e3m1 0.01 n/a
POR-e3m2 1 n/a
E-e3m1 0.01 n/a
POR-e3m2 1 n/a
E-e4m1 0.01 n/a
POR-e4m2 1 n/a
E-e4m1 0.01 n/a

POR-e4m2 1 n/a
E-e5 1 n/a
E-e5 1 n/a
E-e6 1 n/a
E-e6 1 n/a
E-e7 1 n/a
E-e7 1 n/a

Covariance Matrix

	k+1	k+2	k+3	k+6	k+7	a	b	c
k+1	+0.512							
k+2	+0	+9.29						
k+3	+0	+0	+1.04					
k+6	+0	+0	+0.035	+0.957				
k+7	+0.00479	+0.0855	+0	+0	+0.00681			
a	+0	+0.037	+0.0119	+0.021	+0	+0.362		
b	+6.27e-006	+0	+3.14e-005	+1.62e-006	+0	+0	+0.37	
c	+0.00544	+0.0846	+0	+0	+0.00169	+0	+0	+0.664

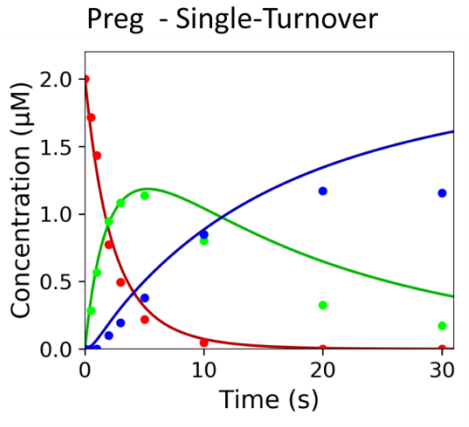
Preg - Single-Turnover
Concentration (μM)
Time (s)

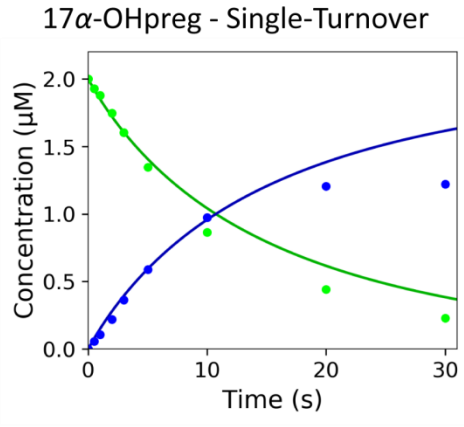
17α-OHpreg - Single-Turnover
Concentration (μM)
Time (s)

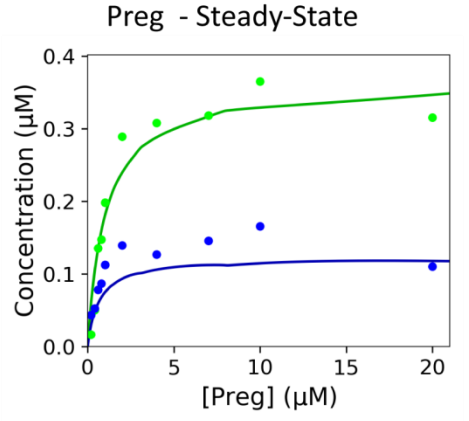
Preg - Steady-State
Concentration (μM)
[Preg] (μM)

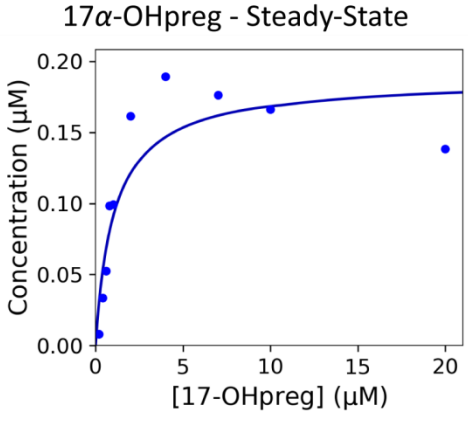
17α-OHpreg - Steady-State
Concentration (μM)
[17-OHpreg] (μM)

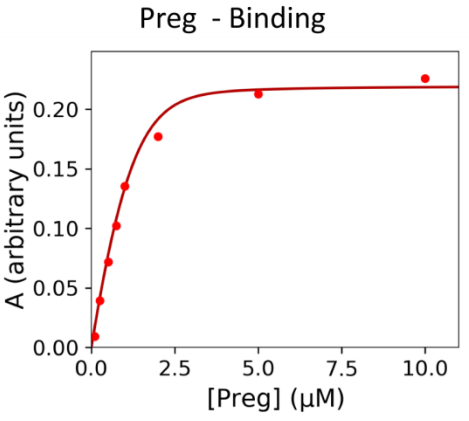
Preg - Binding
A (arbitrary units)
[Preg] (μM)

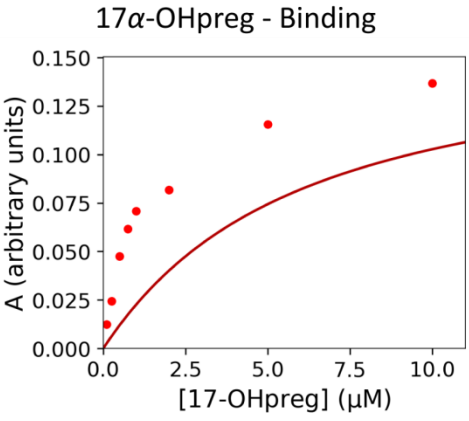
17α-OHpreg - Binding
A (arbitrary units)
[17-OHpreg] (μM)

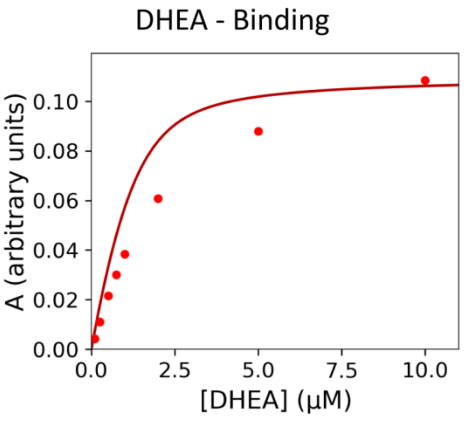
DHEA - Binding
A (arbitrary units)
[DHEA] (μM)

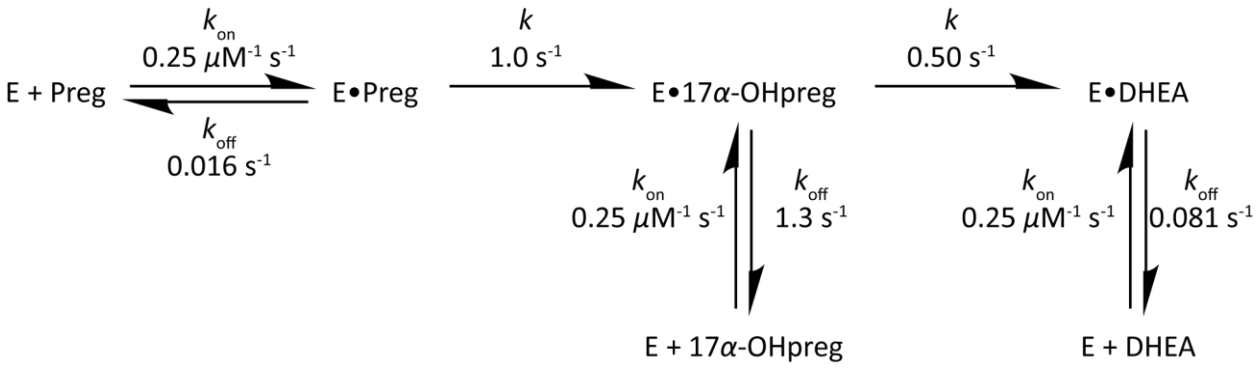

Figure 6.8 Fit results from global data analysis with bound k_{on} rates

Global fitting of experimental data from human P450 17A1 catalytic assays, under single-turnover and steady-state conditions, and steroid binding titrations to a simple mechanistic model in Kintek Explorer. The steroid k_{on} rates were bound as a constant value for all steroids. All experiments were included in the global fitting. See Appendix Figure 6.9 for detailed fit iteration results.

Figure 6.9 Figure 6.12 Kinetic Explorer iteration for Figure 6.8

Version : Professional Version 6.2.170308

Build : PRO
Config : gsl
Fitter : Levmar.
Levmar Box : 1.
Levmar Ln : 0.
Levmar Cycle: 0.
Levmar Linear: 0.
fitLevmarInitialMu: 0.0001.
fitLevmarTol1: 1e-008.
fitLevmarTol2: 1e-008.
fitLevmarTol3: 1e-012.

Fit stop reason: small |Dp|
Fit iterations/calls: iter:1 fn:151 jac:1

Data to fit : Empirical Data.
Fit Function : Fit to Model.
Fit Domain : 11 observable(s) over 12 experiment(s).
Fit Time : 59.393 seconds

Experiments : Exp1 (id=0), Exp2 (id=2), Exp3 (id=3), Exp5 (id=64), Exp4 (id=45), Exp6 (id=65), Exp7 (id=66), Exp8 (id=67), Exp9 (id=68), Exp10 (id=70), Exp11 (id=71), Exp12 (id=73)
Data Points : 99
Params Fit : 9
Deg of Freedom : 90
Chi : 0.93478
Chi2 / DoF : 0.00971
GammaQ : 1.00000
Computed Sigma : 0.09443

Reaction	Constant	Constraint	Value	StdErr	%Error	Keq
E + P = EP	k+1	1	0.25	0.112	45	15.5
	k-1		0.0161	0.149	922	
E + I = EI	k+2	1	0.25	0	0	0.192
	k-2		1.3	1.25	95.9	

E + A = EA k+3 1 0.25 0 0 3.1
k-3 0.0805 0.0865 107

EP + POR = rEP k+4 X 100 n/a n/a (1)
k-4 X 100 n/a n/a

EI + POR = rEI k+5 X 100 n/a n/a (1)
k-5 X 100 n/a n/a

rEP = EI k+6 1 0.437 43.6 1e+007
k-6 X 0 n/a n/a

rEI = EA k+7 0.498 0.35 70.4 4.98e+006
k-7 X 0 n/a n/a

RATE-CONSTANTS
k+1 0.25 0.112
k-1 0.0161 0.149
k+2 0.25 0
k-2 1.3 1.25
k+3 0.25 0
k-3 0.0805 0.0865
k+4 100 n/a
k-4 100 n/a
k+5 100 n/a
k-5 100 n/a
k+6 1 0.437
k-6 0 n/a
k+7 0.498 0.35
k-7 0 n/a

Experiment	Factor	Constraint	Value	StdErr	%Error
Experiment 5a	a		0.22	0.107	48.6
Experiment 5b	a		0.22	0.107	48.6
Experiment 6a	b		0.16	0.237	148

Experiment 6b	b	0.16	0.237	148
Experiment 7a	c	0.11	0.111	101
Experiment 7b	c	0.11	0.111	101

OUTPUT-FACTORS
a 0.22 0.107
b 0.16 0.237
c 0.11 0.111

Experiment	Reagent	Constraint	Value	StdErr	%Error
Experiment 1	EP	X	4	n/a	n/a
Experiment 1 mix1	POR	X	1	n/a	n/a
Experiment 2	EI	X	4	n/a	n/a
Experiment 2 mix1	POR	X	1	n/a	n/a
Experiment 3	E	X	0.01	n/a	n/a
Experiment 3 mix1	POR	X	1	n/a	n/a
Experiment 3	E	X	0.01	n/a	n/a
Experiment 3 mix1	POR	X	1	n/a	n/a
Experiment 4	E	X	0.01	n/a	n/a
Experiment 4 mix1	POR	X	1	n/a	n/a
Experiment 4	E	X	0.01	n/a	n/a
Experiment 4 mix1	POR	X	1	n/a	n/a
Experiment 5	E	X	1	n/a	n/a
Experiment 5	E	X	1	n/a	n/a
Experiment 6	E	X	1	n/a	n/a
Experiment 6	E	X	1	n/a	n/a
Experiment 7	E	X	1	n/a	n/a
Experiment 7	E	X	1	n/a	n/a

INITIAL-CONCENTRATIONS
EP-e1m1 4 n/a
POR-e1m2 1 n/a
EI-e2m1 4 n/a
POR-e2m2 1 n/a
E-e3m1 0.01 n/a
POR-e3m2 1 n/a
E-e3m1 0.01 n/a
POR-e3m2 1 n/a
E-e4m1 0.01 n/a
POR-e4m2 1 n/a
E-e4m1 0.01 n/a

POR-e4m2 1 n/a
E-e5 1 n/a
E-e5 1 n/a
E-e6 1 n/a
E-e6 1 n/a
E-e7 1 n/a
E-e7 1 n/a

Covariance Matrix

	k+1	k-1	k-2	k-3	k+6	k+7	a	b	c
k+1	+0.354								
k-1	+0.243	+0.621							
k-2	+0	+0	+43.7						
k-3	+0	+0	+0	+0.21					
k+6	+0.505	+1.74	+0	+0	+5.34				
k+7	+0	+0	+11.5	+0	+0	+3.44			
a	+0.0182	+0.134	+0	+0	+0.4	+0	+0.32		
b	+0	+0	+2.75	+0	+0	+0.828	+0	+1.57	
c	+0	+0	+0	+0.032	+0	+0.00467	+0	+0.00424	+0.347

Preg - Single-Turnover

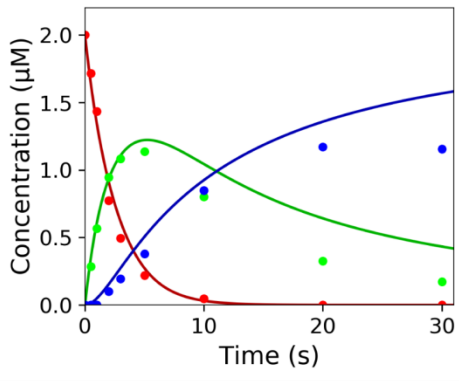

17α-OHpreg - Single-Turnover

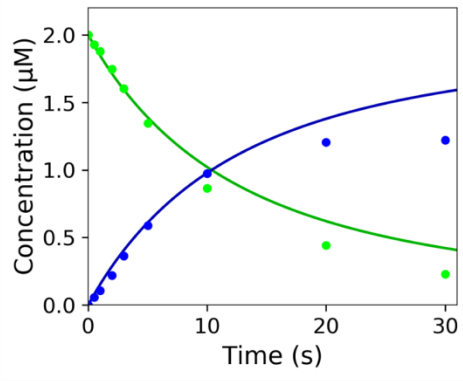

Preg - Steady-State

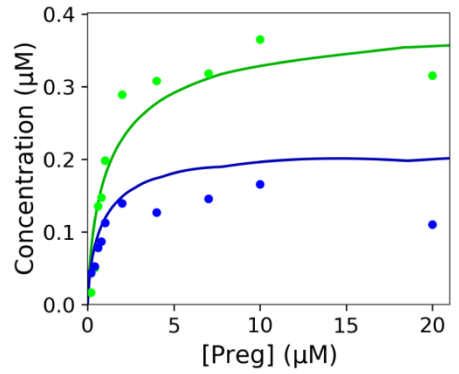

17α-OHpreg - Steady-State

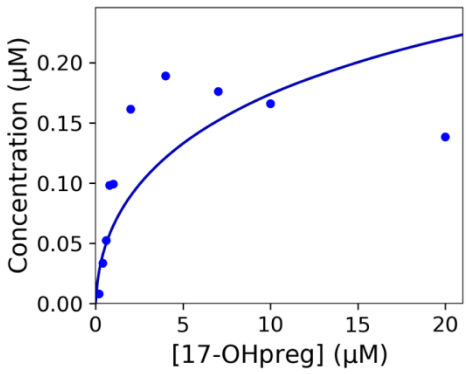

Preg - Binding

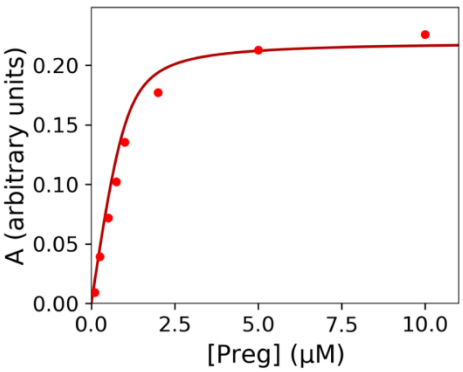

17α-OHpreg - Binding

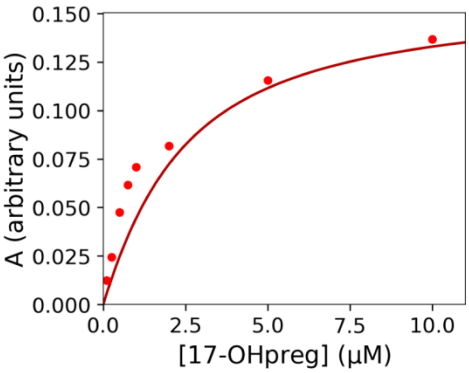

DHEA - Binding

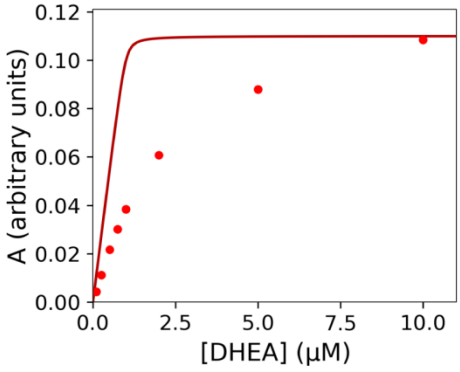

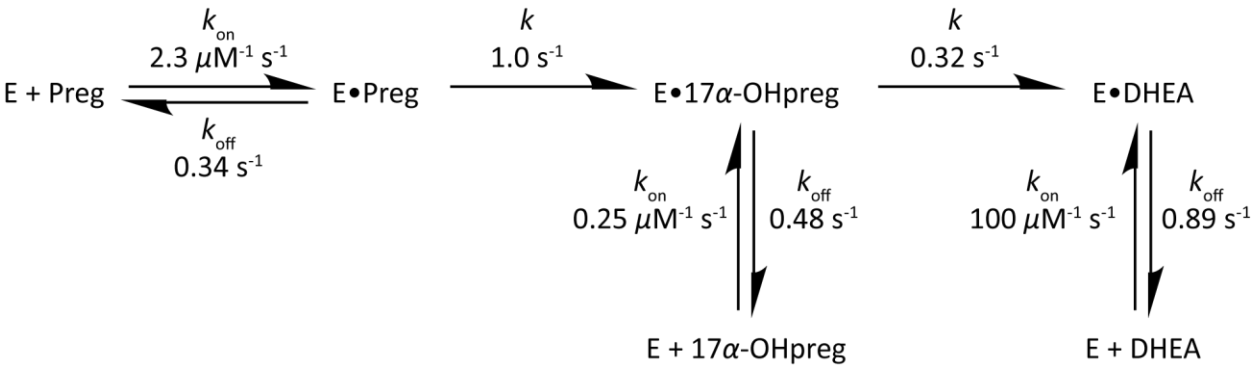

Figure 6.10 Fit results from global data analysis with bound k_{off} rates

Global fitting of experimental data from human P450 17A1 catalytic assays, under single-turnover and steady-state conditions, and steroid binding titrations to a simple mechanistic model in Kintek Explorer. The steroid k_{off} rates were bound per the ratios observed in the enzyme-inhibitor trapping assays. All experiments were included in the global fitting. See Appendix Figure 6.11 for detailed fit iteration results.

Figure 6.11 Kinetic Explorer iteration for Figure 6.10

Version : Professional Version 6.2.170308

Build : PRO
Config : gsl
Fitter : Levmar.
Levmar Box : 1.
Levmar Ln : 0.
Levmar Cycle: 0.
Levmar Linear: 0.
fitLevmarInitialMu: 0.0001.
fitLevmarTol1: 1e-008.
fitLevmarTol2: 1e-008.
fitLevmarTol3: 1e-012.

Fit stop reason: small |Dp|
Fit iterations/calls: iter:10 fn:206 jac:10

Data to fit : Empirical Data.
Fit Function : Fit to Model.
Fit Domain : 11 observable(s) over 12 experiment(s).
Fit Time : 121.899 seconds

Experiments : Exp1 (id=0), Exp2 (id=2), Exp3 (id=3), Exp5 (id=64), Exp4 (id=45), Exp6 (id=65), Exp7 (id=66), Exp8 (id=67), Exp9 (id=68), Exp10 (id=70), Exp11 (id=71), Exp12 (id=73)
Data Points : 99
Params Fit : 9
Deg of Freedom : 90
Chi : 0.92676
Chi2 / DoF : 0.00954
GammaQ : 1.00000
Computed Sigma : 0.09362

Reaction	Constant	Constraint	Value	StdErr	%Error	Keq
E + P = EP	k+1		2.23	3.76	169	6.62
	k-1	1	0.336	0.161	47.8	
E + I = EI	k+2		0.254	0.119	46.7	0.535
	k-2	1	0.475	0	0	

E + A = EA k+3 100 163 163 112
k-3 1 0.893 0 0

EP + POR = rEP k+4 X 100 n/a n/a (1)
k-4 X 100 n/a n/a

EI + POR = rEI k+5 X 100 n/a n/a (1)
k-5 X 100 n/a n/a

rEP = EI k+6 1.01 0.315 31 1.01e+007
k-6 X 0 n/a n/a

rEI = EA k+7 0.324 0.0902 27.9 3.24e+006
k-7 X 0 n/a n/a

RATE-CONSTANTS
k+1 2.23 3.76
k-1 0.336 0.161
k+2 0.254 0.119
k-2 0.475 0
k+3 100 163
k-3 0.893 0
k+4 100 n/a
k-4 100 n/a
k+5 100 n/a
k-5 100 n/a
k+6 1.01 0.315
k-6 0 n/a
k+7 0.324 0.0902
k-7 0 n/a

Experiment	Factor	Constraint	Value	StdErr	%Error
Experiment 5a	a		0.22	0.105	47.7
Experiment 5b	a		0.22	0.105	47.7
Experiment 6a	b		0.16	0.154	96.3

Experiment 6b	b	0.16	0.154	96.3
Experiment 7a	c	0.11	0.087	79.1
Experiment 7b	c	0.11	0.087	79.1

OUTPUT-FACTORS
a 0.22 0.105
b 0.16 0.154
c 0.11 0.087

Experiment	Reagent	Constraint	Value	StdErr	%Error
Experiment 1	EP	X	4	n/a	n/a
Experiment 1 mix1	POR	X	1	n/a	n/a
Experiment 2	EI	X	4	n/a	n/a
Experiment 2 mix1	POR	X	1	n/a	n/a
Experiment 3	E	X	0.01	n/a	n/a
Experiment 3 mix1	POR	X	1	n/a	n/a
Experiment 3	E	X	0.01	n/a	n/a
Experiment 3 mix1	POR	X	1	n/a	n/a
Experiment 4	E	X	0.01	n/a	n/a
Experiment 4 mix1	POR	X	1	n/a	n/a
Experiment 4	E	X	0.01	n/a	n/a
Experiment 4 mix1	POR	X	1	n/a	n/a
Experiment 5	E	X	1	n/a	n/a
Experiment 5	E	X	1	n/a	n/a
Experiment 6	E	X	1	n/a	n/a
Experiment 6	E	X	1	n/a	n/a
Experiment 7	E	X	1	n/a	n/a
Experiment 7	E	X	1	n/a	n/a

INITIAL-CONCENTRATIONS
EP-e1m1 4 n/a
POR-e1m2 1 n/a
EI-e2m1 4 n/a
POR-e2m2 1 n/a
E-e3m1 0.01 n/a
POR-e3m2 1 n/a
E-e3m1 0.01 n/a
POR-e3m2 1 n/a
E-e4m1 0.01 n/a
POR-e4m2 1 n/a
E-e4m1 0.01 n/a

POR-e4m2 1 n/a
E-e5 1 n/a
E-e5 1 n/a
E-e6 1 n/a
E-e6 1 n/a
E-e7 1 n/a
E-e7 1 n/a

Covariance Matrix

	k+1	k-1	k+2	k+3	k+6	k+7	a	b	c
k+1	+403								
k-1	+0	+0.735							
k+2	+0	+0.0501	+0.403						
k+3	+8620	+402	+103	+754000					
k+6	+0	+0.402	+0.0338	+0	+2.82				
k+7	+0	+0.283	+0	+145	+0.086	+0.232			
a	+0	+0.0694	+0.00812	+0	+0.315	+0.0171	+0.314		
b	+0	+0.0946	+0	+37	+0.0505	+0.0749	+0.00828	+0.677	
c	+0	+0	+0	+0	+0.0117	+0	+0.00139	+0	+0.216

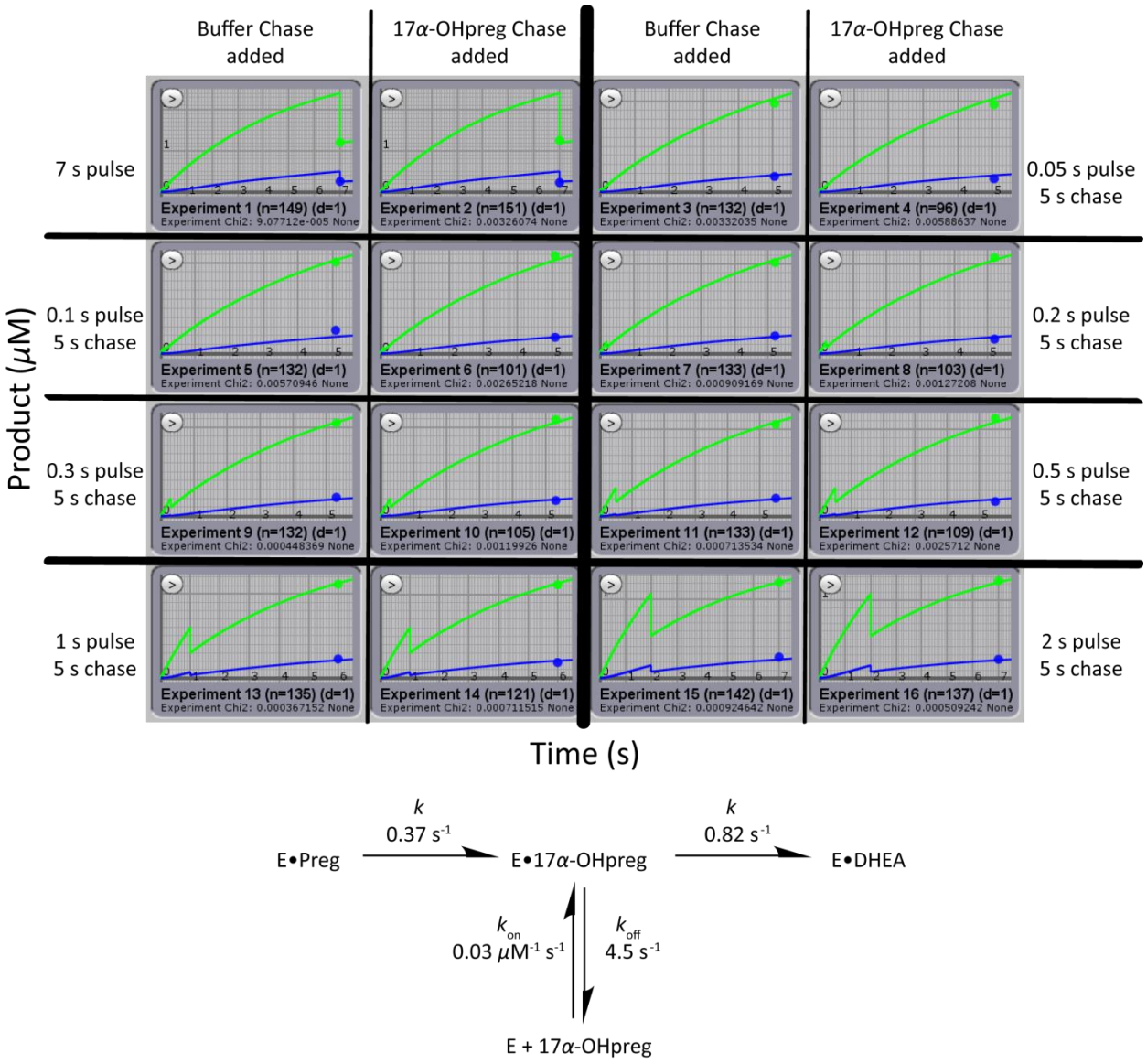

Figure 6.12 Fit results from pulse-chase data analysis

Fitting of ^{3}H-preg pulse-chase experimental data with a minimal kinetic model to estimate the k_{off} and reaction rates in Kintek Explorer. None of the rates were constrained. See Appendix Figure 6.13 for detailed fit iteration results.

Figure 6.13 Kinetic Explorer iteration for Figure 6.12

Version : Professional Version 6.2.170308

Build : PRO
Config : gsl
Fitter : Levmar.
Levmar Box : 1.
Levmar Ln : 0.
Levmar Cycle: 0.
Levmar Linear: 0.
fitLevmarInitialMu: 0.0001.
fitLevmarTol1: 1e-008.
fitLevmarTol2: 1e-008.
fitLevmarTol3: 1e-012.

Fit stop reason: small |Dp|
Fit iterations/calls: iter:1 fn:260 jac:1

Data to fit : Empirical Data.
Fit Function : Fit to Model.
Fit Domain : 32 observable(s) over 16 experiment(s).
Fit Time : 11.772 seconds

Experiments : Exp1 (id=0), Exp2 (id=5), Exp3 (id=7), Exp4 (id=9), Exp5 (id=11), Exp6 (id=12), Exp7 (id=13), Exp8 (id=14), Exp9 (id=15), Exp10 (id=16), Exp11 (id=17), Exp12 (id=18), Exp13 (id=19), Exp14 (id=20), Exp15 (id=21), Exp16 (id=22)
Data Points : 32
Params Fit : 4
Deg of Freedom : 28
Chi : 0.17477
Chi2 / DoF : 0.00109
GammaQ : 1.00000
Computed Sigma : 0.03139

Reaction	Constant	Constraint	Value	StdErr	%Error	Keq
E + I^ = EI^	k+1	“	0.03	0.0521	174	0.00672
	k-1	”	4.46	36.2	812	
EP^ + POR = rEP^	k+2	X	100	n/a	n/a	(1)

k-2 X 100 n/a n/a

EI^ + POR = rEI^ k+3 X 100 n/a n/a (1)
k-3 X 100 n/a n/a

rEP^ = EI^ k+4 • 0.369 0.0107 2.89 3.69e+006
k-4 X 0 n/a n/a

rEI^ = EA^ k+5 – 0.821 6.67 812 8.21e+006
k-5 X 0 n/a n/a

E + I = EI k+6 “ 0.03 0 0 0.00672
k-6 ” 4.46 0 0

EP + POR = rEP k+7 X 100 n/a n/a (1)
k-7 X 100 n/a n/a

EI + POR = rEI k+8 X 100 n/a n/a (1)
k-8 X 100 n/a n/a

rEP = EI k+9 • 0.369 0 0 3.69e+006
k-9 X 0 n/a n/a

rEI = EA k+10 – 0.821 0 0 8.21e+006
k-10 X 0 n/a n/a

RATE-CONSTANTS
k+1 0.03 0.0521
k-1 4.46 36.2
k+2 100 n/a
k-2 100 n/a
k+3 100 n/a
k-3 100 n/a
k+4 0.369 0.0107
k-4 0 n/a
k+5 0.821 6.67
k-5 0 n/a
k+6 0.03 0
k-6 4.46 0
k+7 100 n/a
k-7 100 n/a
k+8 100 n/a
k-8 100 n/a
k+9 0.369 0
k-9 0 n/a
k+10 0.821 0
k-10 0 n/a

Experiment	Factor	Constraint	Value	StdErr	%Error

OUTPUT-FACTORS

Experiment	Reagent	Constraint	Value	StdErr	%Error
Experiment 1	EP^	X	4	n/a	n/a
Experiment 1	POR	X	1	n/a	n/a
Experiment 1 mix1	POR	X	1	n/a	n/a
Experiment 2	EP^	X	4	n/a	n/a
Experiment 2	POR	X	1	n/a	n/a
Experiment 2 mix1	POR	X	1	n/a	n/a
Experiment 2 mix40	I	X	40	n/a	n/a
Experiment 3	EP^	X	4	n/a	n/a
Experiment 3	POR	X	1	n/a	n/a
Experiment 3 mix1	POR	X	1	n/a	n/a
Experiment 4	EP^	X	4	n/a	n/a
Experiment 4	POR	X	1	n/a	n/a
Experiment 4 mix1	POR	X	1	n/a	n/a
Experiment 4 mix40	I	X	40	n/a	n/a
Experiment 5	EP^	X	4	n/a	n/a
Experiment 5	POR	X	1	n/a	n/a
Experiment 5 mix1	POR	X	1	n/a	n/a
Experiment 6	EP^	X	4	n/a	n/a
Experiment 6	POR	X	1	n/a	n/a
Experiment 6 mix1	POR	X	1	n/a	n/a

Experiment 6 mix40 I X 40 n/a n/a
Experiment 7 EP^ X 4 n/a n/a
Experiment 7 POR X 1 n/a n/a
Experiment 7 mix1 POR X 1 n/a n/a
Experiment 8 EP^ X 4 n/a n/a
Experiment 8 POR X 1 n/a n/a
Experiment 8 mix1 POR X 1 n/a n/a
Experiment 8 mix40 I X 40 n/a n/a
Experiment 9 EP^ X 4 n/a n/a
Experiment 9 POR X 1 n/a n/a
Experiment 9 mix1 POR X 1 n/a n/a
Experiment 10 EP^ X 4 n/a n/a
Experiment 10 POR X 1 n/a n/a
Experiment 10 mi1 POR X 1 n/a n/a
Experiment 10 mi40 I X 40 n/a n/a
Experiment 11 EP^ X 4 n/a n/a
Experiment 11 POR X 1 n/a n/a
Experiment 11 mi1 POR X 1 n/a n/a
Experiment 12 EP^ X 4 n/a n/a
Experiment 12 POR X 1 n/a n/a
Experiment 12 mi1 POR X 1 n/a n/a
Experiment 12 mi40 I X 40 n/a n/a
Experiment 13 EP^ X 4 n/a n/a
Experiment 13 POR X 1 n/a n/a
Experiment 13 mi1 POR X 1 n/a n/a
Experiment 14 EP^ X 4 n/a n/a
Experiment 14 POR X 1 n/a n/a
Experiment 14 mi1 POR X 1 n/a n/a
Experiment 14 mi40 I X 40 n/a n/a
Experiment 15 EP^ X 4 n/a n/a
Experiment 15 POR X 1 n/a n/a
Experiment 15 mi1 POR X 1 n/a n/a
Experiment 16 EP^ X 4 n/a n/a
Experiment 16 POR X 1 n/a n/a
Experiment 16 mi1 POR X 1 n/a n/a
Experiment 16 mi40 I X 40 n/a n/a

INITIAL-CONCENTRATIONS
EP^-e1m1 4 n/a
POR-e1m1 1 n/a
POR-e1m2 1 n/a
EP^-e2m1 4 n/a
POR-e2m1 1 n/a
POR-e2m2 1 n/a
I-e2m2 40 n/a
EP^-e3m1 4 n/a
POR-e3m1 1 n/a
POR-e3m2 1 n/a

EP^-e4m1 4 n/a
POR-e4m1 1 n/a
POR-e4m2 1 n/a
I-e4m2 40 n/a
EP^-e5m1 4 n/a
POR-e5m1 1 n/a
POR-e5m2 1 n/a
EP^-e6m1 4 n/a
POR-e6m1 1 n/a
POR-e6m2 1 n/a
I-e6m2 40 n/a
EP^-e7m1 4 n/a
POR-e7m1 1 n/a
POR-e7m2 1 n/a
EP^-e8m1 4 n/a
POR-e8m1 1 n/a
POR-e8m2 1 n/a
I-e8m2 40 n/a
EP^-e9m1 4 n/a
POR-e9m1 1 n/a
POR-e9m2 1 n/a
EP^-e10m1 4 n/a
POR-e10m1 1 n/a
POR-e10m2 1 n/a
I-e10m2 40 n/a
EP^-e11m1 4 n/a
POR-e11m1 1 n/a
POR-e11m2 1 n/a
EP^-e12m1 4 n/a
POR-e12m1 1 n/a
POR-e12m2 1 n/a
I-e12m2 40 n/a
EP^-e13m1 4 n/a
POR-e13m1 1 n/a
POR-e13m2 1 n/a
EP^-e14m1 4 n/a
POR-e14m1 1 n/a
POR-e14m2 1 n/a
I-e14m2 40 n/a
EP^-e15m1 4 n/a
POR-e15m1 1 n/a
POR-e15m2 1 n/a
EP^-e16m1 4 n/a
POR-e16m1 1 n/a
POR-e16m2 1 n/a
I-e16m2 40 n/a

Covariance Matrix

	k+1	k-1	k+4	k+5
k+1	+0.689			
k-1	+0	+333000		
k+4	+0	+4.06	+0.0288	
k+5	+0	+61200	+0.853	+11300

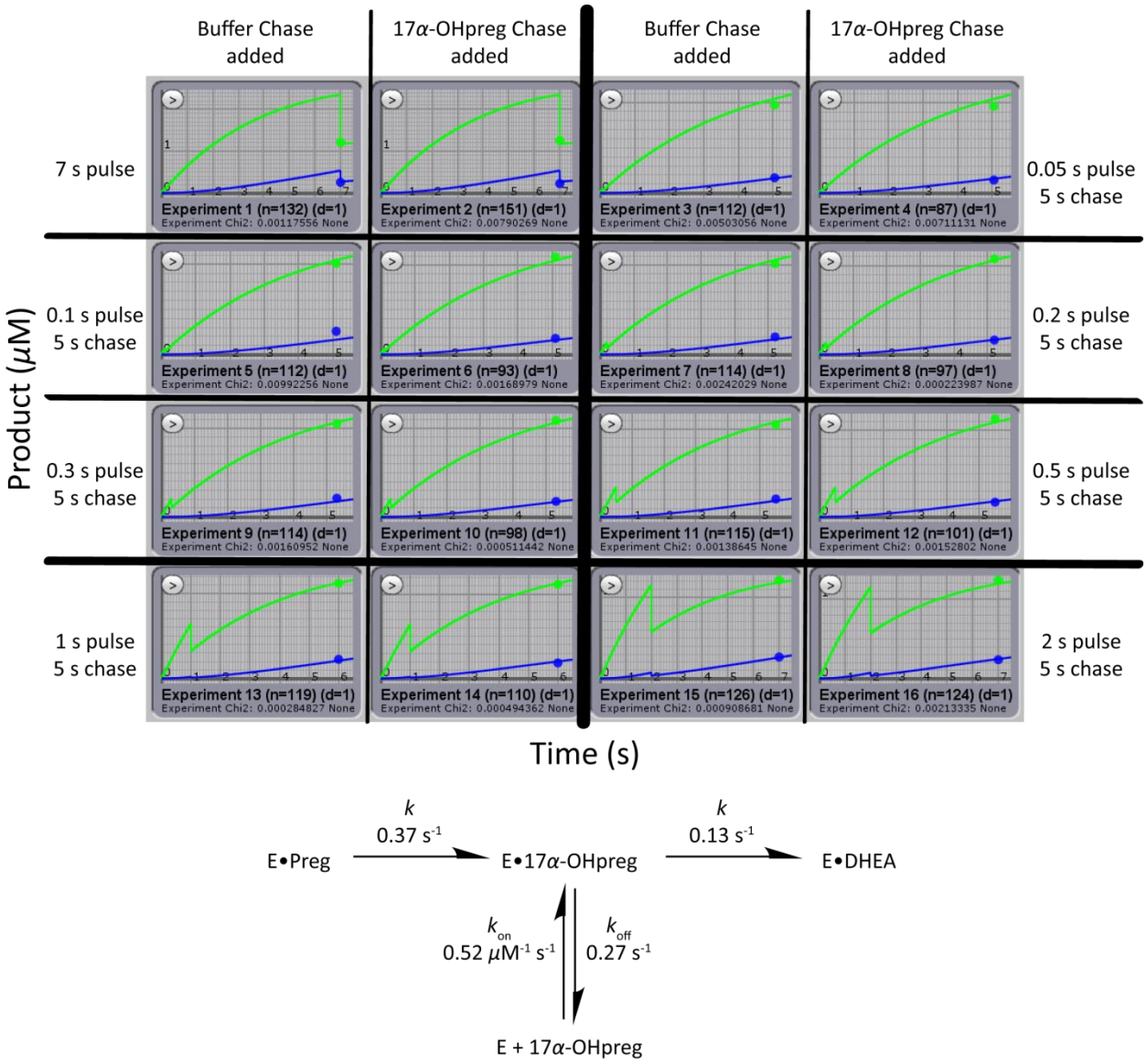

Figure 6.14 Fit results from pulse-chase data analysis with experimental 17α-OHpreg K_d values as constraint

Fitting of ^{3}H-preg pulse-chase experimental data with a minimal kinetic model to estimate the k_{off} and reaction rates in Kintek Explorer. The experimental 17α-OHpreg K_d was applied as a binding equilibrium constraint. See Appendix Figure 6.13 for detailed fit iteration results.

Figure 6.15 Kinetic Explorer iteration for Figure 6.14

Version : Professional Version 6.2.170308

Build : PRO
Config : gsl
Fitter : Levmar.
Levmar Box : 1.
Levmar Ln : 0.
Levmar Cycle: 0.
Levmar Linear: 0.
fitLevmarInitialMu: 0.0001.
fitLevmarTol1: 1e-008.
fitLevmarTol2: 1e-008.
fitLevmarTol3: 1e-012.

Fit stop reason: small |Dp|
Fit iterations/calls: iter:1 fn:221 jac:1

Data to fit : Empirical Data.
Fit Function : Fit to Model.
Fit Domain : 32 observable(s) over 16 experiment(s).
Fit Time : 9.749 seconds

Experiments : Exp1 (id=0), Exp2 (id=5), Exp3 (id=7), Exp4 (id=9), Exp5 (id=11), Exp6 (id=12), Exp7 (id=13), Exp8 (id=14), Exp9 (id=15), Exp10 (id=16), Exp11 (id=17), Exp12 (id=18), Exp13 (id=19), Exp14 (id=20), Exp15 (id=21), Exp16 (id=22)
Data Points : 32
Params Fit : 3
Deg of Freedom : 29
Chi : 0.21056
Chi2 / DoF : 0.00153
GammaQ : 1.00000
Computed Sigma : 0.03782

Reaction	Constant	Constraint	Value	StdErr	%Error	Keq
E + I^ = EI^	k+1	1	0.521	0.672	129	(1.92)
	k-1	1	0.272	0	0	
EP^ + POR = rEP^	k+2	X	100	n/a	n/a	(1)

k-2 X 100 n/a n/a

EI^ + POR = rEI^ k+3 X 100 n/a n/a (1)
k-3 X 100 n/a n/a

rEP^ = EI^ k+4 “ 0.366 0.0126 3.43 3.66e+006
k-4 X 0 n/a n/a

rEI^ = EA^ k+5 ” 0.127 0.0338 26.6 1.27e+006
k-5 X 0 n/a n/a

E + I = EI k+6 1 0.521 0 0 (1.92)
k-6 1 0.272 0 0

EP + POR = rEP k+7 X 100 n/a n/a (1)
k-7 X 100 n/a n/a

EI + POR = rEI k+8 X 100 n/a n/a (1)
k-8 X 100 n/a n/a

rEP = EI k+9 “ 0.366 0 0 3.66e+006
k-9 X 0 n/a n/a

rEI = EA k+10 ” 0.127 0 0 1.27e+006
k-10 X 0 n/a n/a

RATE-CONSTANTS
k+1 0.521 0.672
k-1 0.272 0
k+2 100 n/a
k-2 100 n/a
k+3 100 n/a
k-3 100 n/a
k+4 0.366 0.0126
k-4 0 n/a
k+5 0.127 0.0338
k-5 0 n/a
k+6 0.521 0
k-6 0.272 0
k+7 100 n/a
k-7 100 n/a
k+8 100 n/a
k-8 100 n/a
k+9 0.366 0
k-9 0 n/a
k+10 0.127 0
k-10 0 n/a

Experiment	Factor	Constraint	Value	StdErr	%Error

OUTPUT-FACTORS

Experiment	Reagent	Constraint	Value	StdErr	%Error
Experiment 1	EP^	X	4	n/a	n/a
Experiment 1	POR	X	1	n/a	n/a
Experiment 1 mix1	POR	X	1	n/a	n/a
Experiment 2	EP^	X	4	n/a	n/a
Experiment 2	POR	X	1	n/a	n/a
Experiment 2 mix1	POR	X	1	n/a	n/a
Experiment 2 mix40	I	X	40	n/a	n/a
Experiment 3	EP^	X	4	n/a	n/a
Experiment 3	POR	X	1	n/a	n/a
Experiment 3 mix1	POR	X	1	n/a	n/a
Experiment 4	EP^	X	4	n/a	n/a
Experiment 4	POR	X	1	n/a	n/a
Experiment 4 mix1	POR	X	1	n/a	n/a
Experiment 4 mix40	I	X	40	n/a	n/a
Experiment 5	EP^	X	4	n/a	n/a
Experiment 5	POR	X	1	n/a	n/a
Experiment 5 mix1	POR	X	1	n/a	n/a
Experiment 6	EP^	X	4	n/a	n/a
Experiment 6	POR	X	1	n/a	n/a
Experiment 6 mix1	POR	X	1	n/a	n/a

Experiment 6 mix40 I X 40 n/a n/a
Experiment 7 EP^ X 4 n/a n/a
Experiment 7 POR X 1 n/a n/a
Experiment 7 mix1 POR X 1 n/a n/a
Experiment 8 EP^ X 4 n/a n/a
Experiment 8 POR X 1 n/a n/a
Experiment 8 mix1 POR X 1 n/a n/a
Experiment 8 mix40 I X 40 n/a n/a
Experiment 9 EP^ X 4 n/a n/a
Experiment 9 POR X 1 n/a n/a
Experiment 9 mix1 POR X 1 n/a n/a
Experiment 10 EP^ X 4 n/a n/a
Experiment 10 POR X 1 n/a n/a
Experiment 10 mi1 POR X 1 n/a n/a
Experiment 10 mi40 I X 40 n/a n/a
Experiment 11 EP^ X 4 n/a n/a
Experiment 11 POR X 1 n/a n/a
Experiment 11 mi1 POR X 1 n/a n/a
Experiment 12 EP^ X 4 n/a n/a
Experiment 12 POR X 1 n/a n/a
Experiment 12 mi1 POR X 1 n/a n/a
Experiment 12 mi40 I X 40 n/a n/a
Experiment 13 EP^ X 4 n/a n/a
Experiment 13 POR X 1 n/a n/a
Experiment 13 mi1 POR X 1 n/a n/a
Experiment 14 EP^ X 4 n/a n/a
Experiment 14 POR X 1 n/a n/a
Experiment 14 mi1 POR X 1 n/a n/a
Experiment 14 mi40 I X 40 n/a n/a
Experiment 15 EP^ X 4 n/a n/a
Experiment 15 POR X 1 n/a n/a
Experiment 15 mi1 POR X 1 n/a n/a
Experiment 16 EP^ X 4 n/a n/a
Experiment 16 POR X 1 n/a n/a
Experiment 16 mi1 POR X 1 n/a n/a
Experiment 16 mi40 I X 40 n/a n/a

INITIAL-CONCENTRATIONS
EP^-e1m1 4 n/a
POR-e1m1 1 n/a
POR-e1m2 1 n/a
EP^-e2m1 4 n/a
POR-e2m1 1 n/a
POR-e2m2 1 n/a
I-e2m2 40 n/a
EP^-e3m1 4 n/a
POR-e3m1 1 n/a
POR-e3m2 1 n/a

EP^-e4m1 4 n/a
POR-e4m1 1 n/a
POR-e4m2 1 n/a
I-e4m2 40 n/a
EP^-e5m1 4 n/a
POR-e5m1 1 n/a
POR-e5m2 1 n/a
EP^-e6m1 4 n/a
POR-e6m1 1 n/a
POR-e6m2 1 n/a
I-e6m2 40 n/a
EP^-e7m1 4 n/a
POR-e7m1 1 n/a
POR-e7m2 1 n/a
EP^-e8m1 4 n/a
POR-e8m1 1 n/a
POR-e8m2 1 n/a
I-e8m2 40 n/a
EP^-e9m1 4 n/a
POR-e9m1 1 n/a
POR-e9m2 1 n/a
EP^-e10m1 4 n/a
POR-e10m1 1 n/a
POR-e10m2 1 n/a
I-e10m2 40 n/a
EP^-e11m1 4 n/a
POR-e11m1 1 n/a
POR-e11m2 1 n/a
EP^-e12m1 4 n/a
POR-e12m1 1 n/a
POR-e12m2 1 n/a
I-e12m2 40 n/a
EP^-e13m1 4 n/a
POR-e13m1 1 n/a
POR-e13m2 1 n/a
EP^-e14m1 4 n/a
POR-e14m1 1 n/a
POR-e14m2 1 n/a
I-e14m2 40 n/a
EP^-e15m1 4 n/a
POR-e15m1 1 n/a
POR-e15m2 1 n/a
EP^-e16m1 4 n/a
POR-e16m1 1 n/a
POR-e16m2 1 n/a
I-e16m2 40 n/a

Covariance Matrix

	k+1	k+4	k+5
k+1	+79		
k+4	+0	+0.0276	
k+5	+3.76	+0.00772	+0.2

Figure 6.16 Kinetic Explorer iteration for Figure 3.11

Version : Professional Version 6.1.170130

Build : PRO
Config : gsl
Fitter : Levmar.
Levmar Box : 1.
Levmar Ln : 0.
Levmar Cycle: 0.
Levmar Linear: 0.
fitLevmarInitialMu: 0.0001.
fitLevmarTol1: 1e-008.
fitLevmarTol2: 1e-008.
fitLevmarTol3: 1e-012.

Fit stop reason: small |Dp|
Fit iterations/calls: iter:1 fn:135 jac:1

Data to fit : Empirical Data.
Fit Function : Fit to Model.
Fit Domain : 24 observable(s) over 24 experiment(s).
Fit Time : 8.226 seconds

Experiments : Exp1 (id=1), Exp2 (id=9), Exp3 (id=24), Exp4 (id=46), Exp5 (id=47), Exp6 (id=48), Exp7 (id=49), Exp8 (id=50), Exp9 (id=51), Exp10 (id=52), Exp11 (id=53), Exp12 (id=54), Exp13 (id=55), Exp14 (id=56), Exp15 (id=57), Exp16 (id=58), Exp17 (id=59), Exp18 (id=60), Exp19 (id=61), Exp20 (id=62), Exp21 (id=63), Exp22 (id=64), Exp23 (id=65), Exp24 (id=66)
Data Points : 33304
Params Fit : 20
Deg of Freedom : 33284
Chi : 0.90234
Chi2 / DoF : 0.00002
GammaQ : -0.00000
Computed Sigma : 0.00494

Reaction	Constant	Constraint	Value	StdErr	%Error	Keq
E1 = E2	k+1		0.233	0.0103	4.43	1.1
	k-1		0.212	0.011	5.2	

E2 + P = E2P	k+2	12	1.06	8.85	2.74
	k-2	4.37	0.666	15.2	
E2P = E3P	k+3	0.499	0.208	41.8	0.266
	k-3	1.88	0.0956	5.09	
E2 + I = E2I	k+4	8.43	1.2	14.2	3.92
	k-4	2.15	0.64	29.8	
E2I = E3I	k+5	0.0928	0.268	289	0.0401
	k-5	2.31	0.347	15	
E2 + A = E2A	k+6	11.5	2.99	26	0.943
	k-6	12.2	3.93	32.3	
E2A = E3A	k+7	0.101	0.354	349	0.0435
	k-7	2.33	0.184	7.86	

RATE-CONSTANTS

k+1	0.233 0.0103
k-1	0.212 0.011
k+2	12 1.06
k-2	4.37 0.666
k+3	0.499 0.208
k-3	1.88 0.0956
k+4	8.43 1.2
k-4	2.15 0.64
k+5	0.0928 0.268
k-5	2.31 0.347
k+6	11.5 2.99
k-6	12.2 3.93
k+7	0.101 0.354
k-7	2.33 0.184

Experiment	Factor	Constraint	Value	StdErr	%Error
Experiment 1a	a		0.107	0.00337	3.15
	b		0.888	0.294	33.1
Experiment 2a	c		0.0465	0.00414	8.9
	d		2.56	7.04	275
Experiment 3a	e		0.0472	0.00383	8.1
	f		2.32	7.8	336

Experiment 1b	a	0.107	0.00337	3.15
	b	0.888	0.294	33.1
Experiment 1c	a	0.107	0.00337	3.15
	b	0.888	0.294	33.1
Experiment 1d	a	0.107	0.00337	3.15
	b	0.888	0.294	33.1
Experiment 1e	a	0.107	0.00337	3.15
	b	0.888	0.294	33.1
Experiment 1f	a	0.107	0.00337	3.15
	b	0.888	0.294	33.1
Experiment 1g	a	0.107	0.00337	3.15
	b	0.888	0.294	33.1
Experiment 1h	a	0.107	0.00337	3.15
	b	0.888	0.294	33.1
Experiment 2b	c	0.0465	0.00414	8.9
	d	2.56	7.04	275
Experiment 2c	c	0.0465	0.00414	8.9
	d	2.56	7.04	275
Experiment 2d	c	0.0465	0.00414	8.9
	d	2.56	7.04	275
Experiment 2e	c	0.0465	0.00414	8.9
	d	2.56	7.04	275
Experiment 2f	c	0.0465	0.00414	8.9
	d	2.56	7.04	275
Experiment 2g	c	0.0465	0.00414	8.9
	d	2.56	7.04	275
Experiment 2h	c	0.0465	0.00414	8.9
	d	2.56	7.04	275
Experiment 3b	e	0.0472	0.00383	8.1
	f	2.32	7.8	336
Experiment 3c	e	0.0472	0.00383	8.1
	f	2.32	7.8	336

Experiment 3d	e	0.0472	0.00383	8.1
	f	2.32	7.8	336
Experiment 3e	e	0.0472	0.00383	8.1
	f	2.32	7.8	336
Experiment 3f	e	0.0472	0.00383	8.1
	f	2.32	7.8	336
Experiment 3g	e	0.0472	0.00383	8.1
	f	2.32	7.8	336
Experiment 3h	e	0.0472	0.00383	8.1
	f	2.32	7.8	336

OUTPUT-FACTORS
a 0.107 0.00337
b 0.888 0.294
c 0.0465 0.00414
d 2.56 7.04
e 0.0472 0.00383
f 2.32 7.8

Experiment	Reagent	Constraint	Value	StdErr	%Error
Experiment 1a	E1	X	1	n/a	n/a
Experiment 1a	E2	X	1	n/a	n/a
Experiment 1a mi0.1	P	X	0.1	n/a	n/a
Experiment 1b mi0.25	P	X	0.25	n/a	n/a
Experiment 1c mi0.5	P	X	0.5	n/a	n/a
Experiment 1d mi0.75	P	X	0.75	n/a	n/a
Experiment 1e mi1	P	X	1	n/a	n/a
Experiment 1f mi2	P	X	2	n/a	n/a
Experiment 1g mi5	P	X	5	n/a	n/a
Experiment 1h mi10	P	X	10	n/a	n/a
Experiment 2a	E1	X	1	n/a	n/a
Experiment 2a	E2	X	1	n/a	n/a
Experiment 2a mi0.1	I	X	0.1	n/a	n/a
Experiment 2b mi0.25	I	X	0.25	n/a	n/a
Experiment 2c mi0.5	I	X	0.5	n/a	n/a
Experiment 2d mi0.75	I	X	0.75	n/a	n/a
Experiment 2e mi1	I	X	1	n/a	n/a
Experiment 2f mi2	I	X	2	n/a	n/a
Experiment 2g mi5	I	X	5	n/a	n/a
Experiment 2h mi10	I	X	10	n/a	n/a

Experiment 3a E1 X 1 n/a n/a
Experiment 3a E2 X 1 n/a n/a
Experiment 3a mi0.1 A X 0.1 n/a n/a
Experiment 3b mi0.25 A X 0.25 n/a n/a
Experiment 3c mi0.5 A X 0.5 n/a n/a
Experiment 3d mi0.75 A X 0.75 n/a n/a
Experiment 3e mi1 A X 1 n/a n/a
Experiment 3f mi2 A X 2 n/a n/a
Experiment 3g mi5 A X 5 n/a n/a
Experiment 3h mi10 A X 10 n/a n/a

INITIAL-CONCENTRATIONS
E1-e1.1m1 1 n/a
E2-e1.1m1 1 n/a
P-e1.1m2 0.1 n/a
P-e1.2m2 0.25 n/a
P-e1.3m2 0.5 n/a
P-e1.4m2 0.75 n/a
P-e1.5m2 1 n/a
P-e1.6m2 2 n/a
P-e1.7m2 5 n/a
P-e1.8m2 10 n/a
E1-e2.1m1 1 n/a
E2-e2.1m1 1 n/a
I-e2.1m2 0.1 n/a
I-e2.2m2 0.25 n/a
I-e2.3m2 0.5 n/a
I-e2.4m2 0.75 n/a
I-e2.5m2 1 n/a
I-e2.6m2 2 n/a
I-e2.7m2 5 n/a
I-e2.8m2 10 n/a
E1-e3.1m1 1 n/a
E2-e3.1m1 1 n/a
A-e3.1m2 0.1 n/a
A-e3.2m2 0.25 n/a
A-e3.3m2 0.5 n/a
A-e3.4m2 0.75 n/a
A-e3.5m2 1 n/a
A-e3.6m2 2 n/a
A-e3.7m2 5 n/a
A-e3.8m2 10 n/a

Covariance Matrix

	k+1	k-1	k+2	k-2	k+3	k-3	k+4	k-4	k+5	k-5	k+6	k-6	k+7	k-7	a	b	c	d	e	f
k+1	+1.09																			
k-1	+1.1	+1.24																		
k+2	+0	+4.01	+11500																	
k-2	+7.79	+13.3	+6640	+4530																
k+3	+10.3	+12.8	+1290	+1180	+444															
k-3	+0	+0	+0	+0	+0	+93.5														
k+4	+0	+0	+0	+0	+0	+10.1	+14600													
k-4	+0	+0	+0	+0	+0	+3.27	+7250	+4190												
k+5	+3.15	+3.38	+4.42	+31	+33.5	+0	+2400	+1630	+736											
k-5	+1.08	+2.26	+48.5	+58.4	+32.7	+0	+0	+0	+0	+1230										
k+6	+0	+0	+122	+96.1	+22.1	+4.66	+0	+0	+0	+22.3	+91200									
k-6	+9.11	+15.9	+275	+357	+216	+0	+0	+0	+36.8	+71.1	+113000	+158000								
k+7	+7.22	+8.69	+50.5	+112	+95	+0	+0	+0	+23	+20	+4820	+10200	+1280							
k-7	+0.823	+1.39	+22.9	+30.2	+18.6	+0	+0	+0	+3.25	+6	+0	+0	+0	+344						
a	+0	+0	+0	+0	+0	+0.761	+0.132	+0.0403	+0	+0	+0	+0	+0	+0	+0.116					
b	+0	+0	+0	+0	+0	+241	+172	+52.1	+0	+0	+0	+0	+0	+0	+3.57	+882				
c	+0	+0	+0.171	+0.126	+0.0201	+0.00775	+0	+0	+0	+8.86	+0.101	+0.156	+0.00448	+0.0127	+7.68e-007	+0	+0.175			
d	+0	+0	+0	+0	+0	+89.8	+0	+0	+0	+24200	+174	+0	+0	+0	+0.937	+1190	+202	+507000		
e	+0	+0	+0.0937	+0.0369	+0	+0.00844	+0.0337	+0.0126	+0	+0.0116	+0	+0	+0	+0	+4.33e-005	+0.0474	+9.72e-005	+0.466	+0.15	
f	+0	+0	+0	+0	+0	+166	+1800	+547	+0	+0	+0	+0	+0	+12300	+2.18	+2840	+0	+12600	+49.1	+622000